USGS Research on Mineral Resources—1991 Program and Abstracts

Seventh Annual V.E. McKelvey Forum on
Mineral and Energy Resources

U.S. GEOLOGICAL SURVEY CIRCULAR 1062

Cover: San José tin-silver mine at Oruro, Bolivia, where high-grade ores are hosted by a volcanic complex consisting of quartz latite domes in coeval lavas and breccias of Miocene age. One of the world's largest silver deposits, it has been worked almost continuously since its discovery in the 16th century. Photograph by George E. Ericksen.

USGS Research on Mineral Resources—1991 Program and Abstracts

Edited by ELIZABETH E. GOOD, JOHN F. SLACK, and RAMA K. KOTRA

Seventh Annual V.E. McKelvey Forum on Mineral and Energy Resources, held in Reno, Nevada, February 11–14, 1991

U.S. GEOLOGICAL SURVEY CIRCULAR 1062

U.S. DEPARTMENT OF THE INTERIOR
MANUEL LUJAN, Jr., Secretary

U.S. GEOLOGICAL SURVEY
Dallas L. Peck, Director

ORGANIZING COMMITTEE FOR THE 1991 MCKELVEY FORUM

Rama K. Kotra, Chairman
Robert A. Ayuso
Harvey E. Belkin
James P. Calzia
Richard J. Goldfarb
William F. Hanna
Richard F. Hardyman
Thelma F. Harms
Carroll Ann Hodges
Thomas D. Light
Melvin H. Podwysocki
William I. Ridley
Michael G. Sawlan
John F. Slack
Bruce D. Smith
Holly J. Stein
Gary R. Winkler

UNITED STATES GOVERNMENT PRINTING OFFICE: 1991

Free on application to the
Books and Open-File Reports Section
U.S. Geological Survey
Federal Center, Box 25425
Denver, CO 80225

Library of Congress Cataloging in Publication Data

ISSN 1054–3899

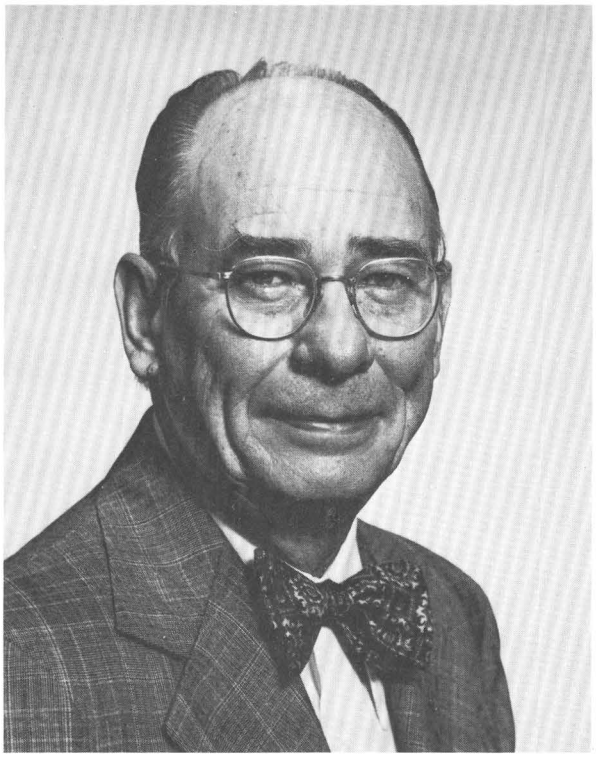

A society's wealth depends on the use it makes of raw materials, energy, and especially ingenuity.
—V.E. McKelvey

The Siberian city of Noril'sk (above the Arctic Circle in the U.S.S.R.) is near one of the world's largest concentrations of magmatically accumulated nickel, copper, cobalt, and platinum-group metals. This east-looking view shows downtown Noril'sk, smelters that process sulfide ores, and the highland (right background) where ores were first mined. As part of a recently established agreement between the U.S. Geological Survey and the Soviet Ministry of Geology, joint U.S.-Soviet research on mineral deposits in the Noril'sk district is underway.

FOREWORD

The V.E. McKelvey Forum is named for Vincent E. McKelvey in recognition of his lifelong contributions in mineral and energy resources as a research scientist, as Chief Geologist of the U.S. Geological Survey (USGS), and as Director of the USGS. The Forum is an annual event, and its purpose is to encourage direct communication between USGS scientists and members of the private sector, academia, and other government agencies. The first six Forums have been well attended and have been very successful in fostering better communication. The subject of the Forum has alternated between mineral and energy resources. This year the focus is again on minerals and has as its general theme domestic and international mineral resource perspectives.

This 1991 V.E. McKelvey Forum presents results from a broad spectrum of mineral-resource studies by USGS scientists that apply new concepts and techniques in the earth sciences. Much of the interdisciplinary research covered at the Forum stresses novel methodologies and approaches that can aid in the discovery of new mineral deposits and the assessment of mineral resources. Once again, we have selected Reno, Nevada, as the site for the Forum, as the city represents an important center for the United States mining industry. Such an environment should enhance the invaluable interchange between USGS and industry personnel that is essential for shaping future USGS program policies and for communication of program results to our intended users.

As in past years, our program emphasizes both basic and applied research activities. The former includes the examination of various geologic characteristics and exploration guides for a variety of mineral deposit types. Topics include discussion of significant mineral deposits from a variety of different tectonic settings, including the anorogenic mid-continent region, the Basin and Range, the continental margin orogenic belts, and mid-oceanic ridges. Results of more applied studies, integrating geological, geochemical, and geophysical investigations, are used to assess the mineral resources of quadrangles in Alaska and the lower 48, National Forest Roadless Areas of Idaho, and Alaska's Tongass National Forest, our Nation's largest National Forest. A number of papers also assess the United States resources of industrial and agricultural minerals, commodities certainly of growing concern in the 1990's.

A significant addition to the 1991 McKelvey Forum is the special daylong program emphasizing international studies. The morning session covers the role of Federal and commercial sectors in international minerals development. The afternoon program of talks, as well as various poster presentations, discusses mineral-resource studies either completed or in progress in Canada, Mexico, Venezuela, Ecuador, Bolivia, Peru, Chile, Argentina, Saudi Arabia, Indonesia, China, and the U.S.S.R. Much of this work has been carried out in collaboration with representatives of academia and government from those countries. The resulting dissemination of new information will hopefully provide industry with additional overseas exploration targets and with new data to refine exploration models in this country.

I am confident that once more the McKelvey Forum will result in productive exchanges between government, academia, and the minerals industry. It is our hope that this unique meeting will continue to provide the USGS with the necessary feedback that will help guide our future policy directions and will help us serve the mineral-resource needs of the Nation.

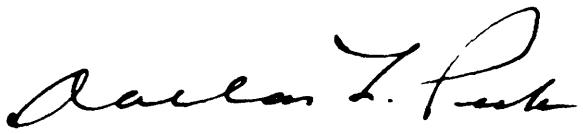

Dallas L. Peck
Director

PROGRAM OF LECTURES AND DISCUSSIONS

MONDAY, FEBRUARY 11, 1991

4:00–9:00 p.m. Registration
7:00–10:00 p.m. POSTER SESSION/Reception

TUESDAY, FEBRUARY 12, 1991

7:30 a.m. Registration
8:30 Welcome and opening remarks
8:40 Introduction to the research programs of the Office of Mineral Resources, U.S. Geological Survey — *Michael P. Foose*
9:00 Preview of U.S. Geological Survey mineral resources research: Seventh Annual V.E. McKelvey Forum — *William C. Bagby*
9:30 Exploration guides for precious-metal deposits in volcanic domes — *Charles G. Cunningham and George E. Ericksen*
10:00 Farah Garan, Saudi Arabia—Bimodal-volcanogenic Zn-Cu-Au mineralization in a Late Proterozoic rift basin, southeastern Arabian Shield—*Jeff L. Doebrich, Arthur A. Bookstrom, and Richard B. Carten*
10:30 COFFEE BREAK AND POSTER SESSION
11:00 KEYNOTE LECTURE: Transitions between epithermal and mesothermal environments — *Richard H. Sillitoe*
12:00 p.m. LUNCH
1:00 Tectonomagmatic settings of Proterozoic metallogenic provinces in the Southwestern United States — *Clay M. Conway*
1:30 Origin of iron, rare-earth elements, copper, and gold in Middle Proterozoic deposits of the midcontinent region, U.S.A. — *W.C. Day, G.B. Sidder, A.E. McCafferty, L.E. Cordell, E.B. Kisvarsanyi, R.O. Rye, and L.M. Nuelle*
2:00 Concentration and zonation of copper and palladium in the Mesozoic Belmont diabase sheet, Culpeper basin, northern Virginia—An exploration guide to enrichment of precious metals in mafic magmatic rocks — *A.J. Froelich, Laurel G. Woodruff, Harvey E. Belkin, and David Gottfried*
2:30 Advances in plumbic prospecting — *Bruce R. Doe*
3:00 COFFEE BREAK AND POSTER SESSION
3:30 The use of lead-isotope geochemistry to evaluate economic potential for gold-silver mineralization —An example from the North Amethyst vein system and the Creede mining district, Colorado — *Nora K. Foley and Robert A. Ayuso*
4:00 The Re-Os isotope system as a tracer in the study of the origin of platinum-group-element and gold deposits — *R.J. Walker, J.W. Morgan, D.D. Lambert, A.J. Naldrett, J.K. Bohlke, and V. Rajamani*
4:30 Synorogenic, auriferous fluids of the Juneau gold belt, southeast Alaska—Stable-isotope evidence for a deep crustal origin — *R.J. Goldfarb and W.J. Pickthorn*
5:00 $^{40}Ar/^{39}Ar$ thermochronology of fracture-controlled mineral deposits of the Idaho batholith—Age, thermal history, and origin — *L.W. Snee, Karen Lund, K.V. Evans, C.H. Gammons, and M.J. Kunk*

TUESDAY EVENING, FEBRUARY 12, 1991

7:30 DIRECTOR'S LECTURE: Tectonic control on the migration of crustal fluids and the formation of regional metallogenic provinces — *David L. Leach*
8:30–10:00 POSTER SESSION/Reception

WEDNESDAY, FEBRUARY 13, 1991

8:30 a.m. Regional structural setting of gold deposits in the Carolina slate belt of North Carolina — *Terry W. Offield and Terry L. Klein*
9:00 Black shales as hosts for unconventional platinum-group-element resources? Examples from southern China and the Yukon, Canada, and implications for U.S. resources — *Richard I. Grauch, Raymond M. Coveney, Jr., James B. Murowchick, and Chen Nansheng*
9:30 Assessment of undiscovered mineral resources, Tongass National Forest, southeastern Alaska — *David A. Brew, Lawrence J. Drew, Jeanine M. Schmidt, David H. Root, and Donald F. Huber*
10:00 Detailed profiles of southeastern Arizona obtained by a truck-mounted magnetometer—A step toward better utilization of the information content of geophysical data — *Mark E. Gettings, Mark W. Bultman, and Frederick S. Fisher*
AND
Geology and mineral-resource assessment of part of the northern Safford basin, southeastern Arizona — *Brenda B. Houser, J.M. Kruger, and Roy A. Johnson*
10:40 COFFEE BREAK AND POSTER SESSION
11:00 Subsurface structure and lithology near the Getchell gold trend, Osgood Mountains, Nevada—Geophysical insights — *V.J.S. Grauch, Donald B. Hoover, and Wayne S. Wojniak*
11:30 Mapping minerals with imaging spectroscopy near Canon City, Colorado — *Roger N. Clark, Andrea J. Gallagher, and Gregg A. Swayze*
12:00 p.m. McKELVEY FORUM LUNCHEON
LUNCHEON ADDRESS: Making high grade — *Stephen E. Kesler*
2:00 Large sulfide-sulfate mounds, hydrothermal fluids, and altered sediment in Escanaba Trough, southern Gorda Ridge—Elements of a mature hydrothermal system at a sediment-covered spreading axis — *Randolph A. Koski, Janet L. Morton, Robert A. Zierenberg, Wayne C. Shanks III, Andrew C. Campbell, and Keith A. Kvenvolden*
2:30 Marine ferromanganese deposits near the Marshall Islands — *James R. Hein, Jung-Keuk Kang, Marjorie S. Schulz, Suk-Hoon Yoon, and Virginia K. Smith*
3:00 COFFEE BREAK AND POSTER SESSION
3:30 U.S. Geological Survey research on agricultural industrial minerals in the United States—Implications for exploration — *James R. Herring, David Z. Piper, Sherilyn Willliams-Stroud, Charles S. Spirakis, and Richard A. Sheppard*

WEDNESDAY, FEBRUARY 13, 1991—Continued

4:00 Mercury-sulfur-gypsum mineralization at Crater, California—A suggestion of gold mineralization at depth — *Sherman P. Marsh, Chester T. Wrucke, and Kevin P. Corbett*

4:30 Geology and mineral potential of Precambrian basement rocks of the Trans-Hudson orogen, U.S.A. — *P.K. Sims, Zell E. Peterman, and T.G. Hildenbrand*

WEDNESDAY EVENING, FEBRUARY 13, 1991

5:30–7:00 OPEN HOUSE — Mackay School of Mines, University of Nevada, Reno, and new USGS field office in the Laxalt Strategic Materials Building

8:00–9:30 DIRECTOR'S SPECIAL BRIEFING: US-USSR cooperative studies in mineral resources

THURSDAY, FEBRUARY 14, 1991

Morning Session: The role of Federal and commercial sectors in international minerals development

Session Chairman: *Dallas L. Peck, Director, U.S. Geological Survey*

Opening remarks and the role of the USGS in international mineral resources — *Dallas L. Peck, Director, USGS*

The role of the Bureau of Mines in international mineral resources — *TS Ary, Director, U.S. Bureau of Mines*

Mellon Bank's role in stimulating international minerals development — *Peter H. Conze, Jr., Senior Vice-President, Mellon Bank*

The Inter-American Development Bank's role in stimulating minerals development — *Juan Proaño, Inter-American Development Bank*

Criteria for investment in international exploration — *Jack Parry, Senior Vice-President, Newmont Mining Corporation and Newmont Gold*

Criteria for investment in international exploration — *John I. Sharpe, Vice-President for Exploration, Battle Mountain Gold Company*

Opportunities for mineral exploration in Bolivia — *Ing. Marcelo Claure Zapata, Director, Servicio Geologico de Bolivia (GEOBOL)*

Opportunities for mineral exploration in Chile — *Juan Carlos Parra Espinosa, Subdirector for Geology, Servicio Nacional de Geologia y Mineria (SERNAGEOMIN), Chile*

Afternoon Session: Examples of selected USGS international mineral resource investigations

Volcanic-hosted epithermal precious-metal desposits in the central Andes—Geology, resources, and exploration strategy — *George E. Ericksen, Charles G. Cunningham, and Barbara A. Eiswerth*

An overview of the mineral resources and USGS activities in Venezuela — *Jeffrey C. Wynn*

Mineral resources of the Bolivian Altiplano — Results of the GEOBOL-USGS-TDP Mineral Resource Evaluation Project — *Keith Long, S. Ludington, and R. Carrasco*

Mineral-resource assessment of Puerto Rico — *Gregory E. McKelvey and Walter J. Bawiec*

Platinum-group-mineral investigations, East and South Kalimantan, Indonesia — *Michael L. Zientek and Bambang Pardiarto*

Mineral-resource investigations in Saudi Arabia by the U.S. Geological Survey — *Paul L. Williams*

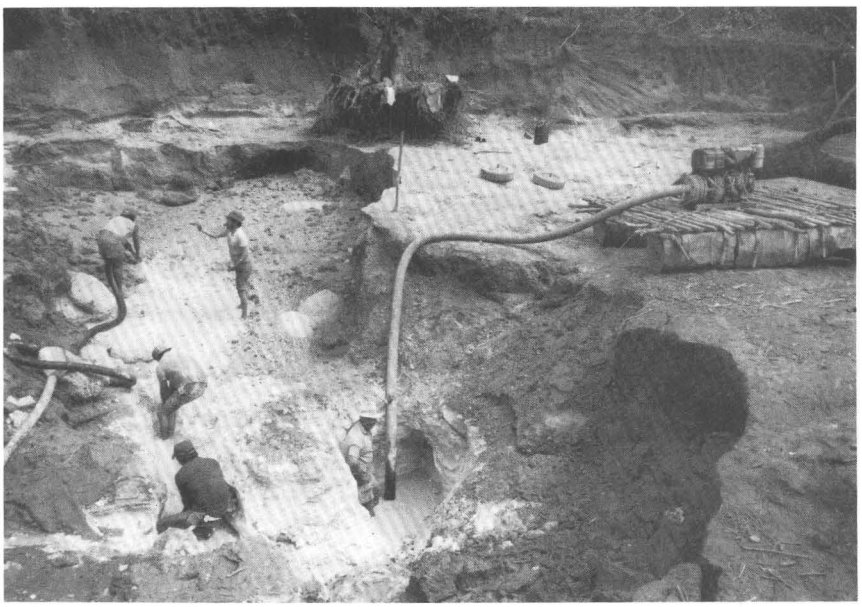

Small-scale hydraulic mining adjacent to the Chicanán River near Kilometer 88, Venezuela. Gold is being extracted from the Uairén Formation of the Roraima Group. Photograph by Jeffrey C. Wynn in January 1989.

LIST OF POSTERS

I. INTERNATIONAL STUDIES

Mineral-resource assessment of Puerto Rico — *by Walter J. Bawiec, Andrew Griscom, Richard D. Krushensky, Sherman P. Marsh, Gregory E. McKelvey, and Kathryn M. Scanlon*

Copper deposits in Tertiary red beds in Bolivia — *by Dennis Cox, Raul Carrasco, Orlando André, Alberto Hinojosa, and Keith Long*

Use of Landsat Thematic Mapper images for studying volcanic-rock-hosted precious-metal deposits in the central Andean region — *by B.A. Eiswerth, T.L. Bowers, Lucia Cuitino, Felipe Diaz, Hugo Gumucio, Aldo Gutarra, Nestor Jimenez, J.L. Lizeca, Ramon Moscoso, Fernando Murillo, Luis Quispesivana, Jaime Rodriguez, L.C. Rowan, Rubén Tejada, and César Vilca*

Comparative metallogeny of the Soviet Far East and Alaska — *by Donald J. Grybeck, Warren J. Nokleberg, and Thomas K. Bundtzen*

Geology and genesis of the Baid Al Jimalah and Silsilah tungsten-tin deposits, Kingdom of Saudi Arabia — *by Robert J. Kamilli*

Mineral-resource assessment of the Altiplano and Cordillera Occidental, Bolivia—A progress report — *by Sherman P. Marsh, Dan H. Knepper, Jr., Keith R. Long, and John W. Cady*

A reconnaissance study of gold mineralization associated with garnet skarn at Nambija, Zamora Province, Ecuador — *by Gregory E. McKelvey and Jane M. Hammarstrom*

Reconnaissance geologic mapping using digital aeromagnetic data and space-shuttle radar data for a heavily forested area of the Guayana Shield, northwestern Brazil — *by Fernando P. Miranda, Anne E. McCafferty, and James V. Taranik*

Latin American mineral-resource data available through the U.S. Geological Survey — *by Frances Wahl Pierce and Karen Sue Bolm*

Early to Middle Proterozoic supracrustal rocks and mineralization of the southern Guayana Shield, Venezuela — *by Gary B. Sidder, William E. Brooks, Yasmin Estanga, Fernando Nuñez, and Andres Garcia*

Evolution of an Early Proterozoic rift basin in the La Esmeralda area, Guayana Shield, Venezuela — *by G.B. Sidder, W.C. Day, R.M. Tosdal, S.D. Olmore, Luis Guzman, and Freddy Prieto*

Gold-bearing quartz veins along the Mojave-Sonora megashear zone, northern Sonora, Mexico — *by Miles L. Silberman, Anita Moore-Nall, and Brian M. Smith*

SOPAC—A decade of research on mineral and hydrocarbon resources in the South Pacific — *by F.L. Wong, B.A. Richmond, H.G. Greene, J.R. Dingler, J.R. Hein, K.A. Kvenvolden, M.S. Marlow, J.L. Morton, D.M. Rubin, D.W. Scholl, and J.G. Vedder*

U.S. Geological Survey mineral-resource and tectonic studies in Venezuela — *by J.C. Wynn, S.D. Olmore, Floyd Gray, W.C. Day, G.B. Sidder, and N.J Page*

II. MINERAL-RESOURCE ASSESSMENTS

Geophysical applications in mineral-resource assessments, Cedar City 1° × 2° quadrangle, southwestern Utah — *by H. Richard Blank*

Preliminary assessment of the mineral resources of the Cedar City 1° × 2° quadrangle, Utah — *by Theresa M. Cookro, Michael A. Shubat, and Janet L. Jones*

Mineral-resource potential of the Sitka 1° × 3° quadrangle, southeastern Alaska — *by S.M. Karl, R.J. Goldfarb, K.D. Kelley, D.M. Sutphin, C.A. Finn, A.B. Ford, and D.A. Brew*

Mineral-resource assessment of the Goodnews 1° × 3° quadrangle and parts of the Hagemeister Island and Nushagak Bay quadrangles, southwestern Alaska — *by J.E. Kilburn, S.E. Box, R.J. Goldfarb, J.E. Gray, and J.L. Jones*

Areas of mineral-resource favorability (with emphasis on gold and chromite) in the Anchorage 1° × 3° quadrangle, southern Alaska — *by D.J. Madden-McGuire and G.R. Winkler*

Resource assessment of the Mount Katmai 1° × 2° quadrangle and adjacent parts of the Naknek and Afognak quadrangles, Alaska Peninsula — *by J.R. Riehle, S.E. Church, and L.B. Magoon*

III. MINERALIZING PROCESSES AND SYSTEMS

Mineral deposits of the Midcontinent Rift, Lake Superior region, United States and Canada — *by William F. Cannon and Teresa A. McGervey*

Geologic map of the Sierrita-Mogollon Corridor (Arizona-New Mexico) and implications for mineral resources — *by Leslie J. Cox, Brenda B. Houser, Eric R. Force, Mark E. Gettings, Alison Burchell, and Frederick S. Fisher*

Anomalous concentrations of fine-grained native gold in stream sediments of east-central Lemhi County, Idaho — *by George A. Desborough, William H. Raymond, and Karl V. Evans*

Element dispersion in alluvium covering gold deposits in the Kelley Creek valley, Getchell gold trend, Humboldt County, Nevada — *by D.E. Detra, S.M. Smith, P.K. Theobald, and P.M. Theodorakos*

Triassic-Jurassic magmatic arc of western Nevada and eastern California—Part III: Mineral deposits — *by J.L. Doebrich, L.J. Garside, D.R. Shawe, J.H. McCarthy, Jr., R.L. Turner, R.F. Hardyman, J.A. Erdman, H.F. Bonham, and J.V. Tingley*

The Bisbee Group of the Tombstone Hills, southeastern Arizona—Stratigraphy, structure, metamorphism, and mineralization — *by Eric R. Force*

Lithologic and tectonic controls on mercury mineralization in the Bethel 1° × 3° quadrangle, southwestern Alaska — *by Thomas P. Frost and Stephen E. Box*

Geochemical investigation of ground water associated with disseminated gold deposits along the Getchell trend, northern Nevada — *by D.J. Grimes, W.H. Ficklin, J.B. McHugh, and A.L. Meier*

The Mogollon mining district, southwestern New Mexico—Classic epithermal silver-gold vein deposits revisited — *by Robert J. Kamilli*

Recognition of distinct terranes in lower Paleozoic host rocks in the Getchell gold trend, Humboldt County, Nevada — *by Dawn J. Madden-McGuire and Sherman P. Marsh*

Tourmalinite and iron-formation in the Yellowjacket Formation, Idaho cobalt belt, Lemhi County, Idaho — *by Peter J. Modreski and Jon J. Connor*

Phosphorite deposits of the northern Blake Plateau as observed from the *NR–1* submarine and *Delta* minisubmersible — *by Peter Popenoe and Frank T. Manheim*

Silt-fraction mineralogy of unconsolidated sediment samples from the continental shelf, slope, and rise off the northeastern United States — *by L.J. Poppe and J.A. Commeau*

Triassic-Jurassic magmatic arc of western Nevada and eastern California—Part IV: A model for the evaluation of Cenozoic basins for concealed mineral systems — *by D.L. Sawatzky, G.L. Raines, J.L. Doebrich, R.L. Turner, L.J. Garside, and J.H. McCarthy, Jr.*

Triassic-Jurassic magmatic arc of western Nevada and eastern California—Part I: Geology — *by R.A. Schweickert, J.H. Stewart, J.H. Dilles, L.J. Garside, R.C. Greene, R.F. Hardyman, D.S. Harwood, and N.J. Silberling*

Triassic-Jurassic magmatic arc of western Nevada and eastern California—Part II: Audio-magnetotelluric survey near Reno and Carson City, Nevada — *by R.M. Senterfit and D.P. Klein*

The Getchell gold trend, northwestern Nevada—Geologic structure delineated by further processing of electromagnetic data collected during a helicopter survey — *by W.S. Wojniak and D.B. Hoover*

IV. GEOCHEMICAL AND GEOPHYSICAL INVESTIGATIONS

Geochemical evidence for near-surface precious- and base-metal disseminated and vein deposits in the west-central Vermilion district, northeastern Minnesota — *by H.V. Alminas, J.B. McHugh, and E.C. Perry, Jr.*

Chemistry of natural waters in the St. Helens mining district, Washington—A test of hydrogeochemical prospecting methods in the Cascade Range — *by Roger P. Ashley, Russell C. Evarts, and William R. Miller*

Geochemistry and metallogeny of granitic rocks from the Appalachian Mountains—Examples from the Northeast Kingdom batholith, Vermont, and the Lucerne and Deblois batholiths, Maine — *by Robert A. Ayuso and Joseph G. Arth*

Applications of gravity data to studies of framework geology, evaluation of mineral deposits, and mineral prospecting in northwestern Alaska — *by David F. Barnes and John S. Kelley*

Synthesis of geophysical and geological data centered on the Idaho batholith and the Challis volcanic field, Idaho — *by John W. Cady, Viki Bankey, Keenan Lee, A.E. McCafferty, James A. Pitkin, and W.D. Stanley*

Can trace and rare-earth elements in fluorite be useful in geochemical exploration? Encouraging evidence from the Sierra Cuchillo area, New Mexico — *by R.G. Eppinger, L.G. Closs, A.L. Meier, and J.M. Motooka*

Biogeochemical and geochemical expression of poorly exposed epithermal mineralization in the southeastern Challis volcanic field, Idaho — *by J.A. Erdman, Falma Moye, and P.K. Theobald*

Geochemical exploration criteria for epithermal cinnabar and stibnite deposits, southwestern Alaska — *by J.E. Gray, D.E. Detra, R.J. Goldfarb, and K.E. Slaughter*

Seasonal variation in the silver concentration in mesquite (*Prosopis juliflora*) collected near Globe, Arizona — *by Thelma F. Harms*

Low-level gold determinations by use of flow injection analysis-atomic absorption spectrophotometry—An application to precious-metal-resource assessment in the Iditarod 1° × 3° quadrangle, southwestern Alaska — *by D.M. Hopkins, J.E. Gray, and K.E. Slaughter*

Geophysical and geological studies of the Roseau 1° × 2° quadrangle, Minnesota and Ontario — *by R.J. Horton, W.C. Day, T.L. Klein, and B.D. Smith*

Interpretation of new geophysical data obtained by airborne instruments for the Effie-Coon Lake area, Minnesota — *by Robert J. Horton, Bruce D. Smith, Victor F. Labson, and Robert J. Bisdorf*

Regional aeromagnetic and gravity data bases for studies centered on the Idaho batholith and Challis volcanic field — *by Anne E. McCafferty and Viki Bankey*

Hydrogeochemical exploration in areas of thin glacial overburden, northeastern Minnesota — *by W.R. Miller, W.H. Ficklin, and J.B. McHugh*

Preliminary results of geochemical investigations of aerial gamma-ray anomalies in the Getchell gold trend, Humboldt County, Nevada — *by James A. Pitkin*

Development and testing of the CHIM electrogeochemical exploration method — *by David B. Smith, Donald B. Hoover, and Richard F. Sanzolone*

V. GENERAL TOPICS AND NEW TECHNIQUES

Geologic settings of barite deposits as indicators of the potential for other types of mineral deposits — *by Sandra H.B. Clark*

Laser-microprobe studies of sulfur isotopes in stockwork and massive sulfide ores, Rua Cove mine, south-central Alaska — *by Douglas E. Crowe, Wayne C. Shanks III, and John W. Valley*

An overview of industrial minerals of the U.S. Atlantic and Gulf of Mexico Coastal Plains — *by John W. Hosterman*

Natural aggregates—Mining challenge of the 1990's — *by William H. Langer*

Heavy-mineral placers at the Fall Zone — *by Curtis E. Larsen*

Application of grade and tonnage models to the development of strategies for mineral deposit exploration — *by Gregory E. McKelvey and James D. Bliss*

Geophysical logs in an oxide copper deposit near Casa Grande, Arizona — *by Philip H. Nelson, David J. Johnston, Henry G. Kreis, and Jon L. Mikesell*

Basin evolution and petroleum studies in the U.S. eastern Great Basin—Relevance to mineral investigations — *by Christopher J. Potter, John A. Grow, Charles H. Thorman, Harry E. Cook, and James A. Peterson*

The origin of evaporite deposits—A model based on a hydrologically open system — *by Warren W. Wood and Ward E. Sanford*

CONVERSION FACTORS

Conversion factors and abbreviations for units used in this report are given below.

Multiply	By	To obtain
	Length	
millimeter (mm)	0.03937	inch (in.)
meter (m)	3.281	foot (ft)
kilometer (km)	0.6214	mile (mi)
inch (in.)	25.4	millimeter (mm)
foot (ft)	0.3048	meter (m)
mile (mi)	1.609	kilometer (km)
	Area	
square centimeter (cm^2)	0.1550	square inch (in^2)
square kilometer (km^2)	0.3861	square mile (mi^2)
	Volume	
liter (L)	1.057	quart (qt)
	Mass	
gram (g)	0.03527	ounce avoirdupois (oz avdp)
kilogram (kg)	2.205	pound avoirdupois (lb avdp)
metric ton (t)	1.102	short ton (2,000 lb)
	Pressure	
bar	100	kilopascal (kPa)
	Temperature	
degree Celsius (°C)	1.8 and add 32	degree Fahrenheit (°F)

Abbreviations

A, ampere
Å, angstrom
Ga, giga-annum (10^9 years ago)
h, hour

Hz, hertz
kHz, kilohertz
Ma, mega-annum (10^6 years ago)
m.y., million years (10^6 years duration)

ng, nanogram
nT, nanotesla
ohm-m, ohm-meter
ppb, parts per billion

ppm, parts per million
μg, microgram
μm, micrometer
V, volt
yr, year

Seventh Annual V.E. McKelvey Forum on Mineral and Energy Resources

USGS Research on Mineral Resources—1991 Program and Abstracts

Edited by Elizabeth E. Good, John F. Slack, *and* Rama K. Kotra

Geochemical Evidence for Near-Surface Precious- and Base-Metal Disseminated and Vein Deposits in the West-Central Vermilion District, Northeastern Minnesota

By H.V. Alminas, J.B. McHugh, *and* E.C. Perry, Jr.

The study area encompasses some 568 km^2 within St. Louis, Lake, and Cook Counties, Minn., and is centered on the Archean greenstone belt of the west-central Vermilion district. This belt is composed predominantly of mafic metavolcanic and associated rocks that were intruded on the north and south by major granitoid bodies (Sims, 1976).

A-horizon soils, developed from glacial till, outwash, and lacustrine deposits of Wisconsin age that cover this area to a depth of 0–17 m, were sampled at 754 sites in cooperation with the Minnesota Geological Survey. These soils were analyzed for 31 elements by spectrographic methods and for gold by atomic-absorption spectroscopy.

This study indicates that two major areas contain anomalous concentrations of gold, silver, and base metals. A third area is characterized by anomalous concentrations of Cr, Mg, Ni, Co, and platinum-group elements. The more intensely mineralized gold-bearing area is approximately 89 km^2 in areal extent and is centered on Lake Vermilion. Here the gold contents of the soils are as high as 1.1 ppm, and the gold is associated with Ag, Cu, Ti, Co, Pb, Zn, Mo, Cr, Ni, La, V, and Y. The mineralization is restricted primarily to the felsic volcaniclastic units, and a pronounced metal zonation is evident. A strong positive aeromagnetic anomaly, apparently related to that of the Lost Lake intrusive bodies, shows a good spatial correlation with the mineralization.

Manuscript approved for publication November 5, 1990.

The second gold-bearing area is in the eastern end of the belt between Fall and Jasper Lakes and encompasses some 77 km^2. Here the soils contain up to 68 ppb gold. The total geochemical association in this area includes Cu, Ti, Mn, Ag, Co, Pb, Mo, Ni, Sc, Zn, and V. Zonation in this anomaly is less evident, and Ag is less abundant. This area has greater Pb, Zn, and Mo concentrations than does the area at Lake Vermilion. Lamprophyric and syenitic intrusions are present in the central part of this area, and a pronounced aeromagnetic anomaly is essentially coextensive with it.

The two geochemical anomalies indicate widespread precious- and base-metal mineralization in the district. This mineralization is apparently related to the buried epizonal granite and syenite in the Lake Vermilion area as well as to lamprophyric rocks intruded into the Lake Vermilion Formation and Ely Greenstone during the Algoman orogeny. Northeast-trending faults, probably associated with the late phase of the Algoman orogeny (Sims and Mudrey, 1972), may have controlled the mineralization. These geochemical anomalies probably indicate the presence of near-surface, gold-bearing disseminated and (or) vein deposits. Striking similarities exist between the geologic, structural, and geochemical features of the Vermilion district and comparable features described by Colvine and others (1988) for the Archean lode gold deposits in Ontario.

A Cr-Mg-Ni-Co soil anomaly centered on Little Long Lake encompasses some 61 km^2. The anomalous area is associated with mafic and ultramafic intrusions and is characterized by the presence of abundant sulfides and narrow, linear, northeast-trending positive aeromagnetic anomalies. Some outcrop samples collected within the area have platinum and palladium concentrations as high as 0.15 and 0.10 ppm, respectively. This area is believed to hold some potential for economic concentrations of the platinum-group elements.

REFERENCES CITED

Colvine, A.C., Fyon, J.A., Heather, K.B., Marmont, Soussan, Smith, P.M., and Troop, D.G., 1988, Archean lode gold deposits in Ontario: Ontario Geological Survey Miscellaneous Paper 139, 136 p.

Sims, P.K., 1976, Early Precambrian tectonic-igneous evolution in the Vermilion district, northeastern Minnesota: Geological Society of America Bulletin, v. 87, no. 3, p. 379–389.

Sims, P.K., and Mudrey, M.G., Jr., 1972, Syenitic plutons and associated lamprophyres, *in* Geology of Minnesota; A centennial volume: St. Paul, Minn., Minnesota Geological Survey, p. 140–152.

Chemistry of Natural Waters in the St. Helens Mining District, Washington—A Test of Hydrogeochemical Prospecting Methods in the Cascade Range

By Roger P. Ashley, Russell C. Evarts, *and* William R. Miller

The main part of the St. Helens mining district, Washington, is defined by a cluster of small mines and prospects that occupy an area about 12 km in diameter, centered about 17 km north-northeast of Mount St. Helens (fig. 1). Most mineral occurrences in the district are small polymetallic veins, but the district also includes an unmined porphyry copper deposit, and several hydrothermally altered areas without known mineral prospects.

Streams, springs, and drill holes throughout the district were sampled in three successive years (1977–79); samples were collected during periods of both high and low surface flow. Constituents determined included copper, zinc, molybdenum, arsenic, uranium, calcium, magnesium, sodium, potassium, sulfate, silica, chloride, and fluoride; alkalinity was also measured. Cation/chloride ratios, which tend to normalize the dilution effects associated with high flow levels, show stronger anomaly contrast than do unadjusted cation values.

The Earl porphyry copper deposit is poorly exposed over an area of about 1 km^2; it is drained mainly by two second-order streams. An adjacent area of mineralization of similar size extends under glacial deposits and alluvium in the Green River, a third-order stream. Drill holes, springs, and surface waters in the vicinity of the Earl deposit show anomalous amounts of copper, zinc, molybdenum, and sulfate.

Five second-order streams drain most of a 5-km^2 hydrothermally altered area on a ridge in the northern part of the district. This area is underlain by intensely leached and pyritized plutonic rock and hornfels. The alteration is mainly advanced argillic; in addition to quartz and pyrite, mineral assemblages include pyrophyllite, diaspore, alunite, kaolinite, corundum, topaz, and rutile. All stream waters contain anomalous concentrations of sulfate, produced by the oxidation of abundant pyrite. Two drainages show anomalous amounts of copper and zinc, two other drainages show anomalous amounts of molybdenum and fluoride, and one drainage shows both these associations.

A hydrothermally altered area covering 8 km^2 spans the lower part of the valley of Quartz Creek at the northeast edge of the district. It is drained by numerous high-gradient, first- and second-order streams that empty into Quartz Creek. The alteration is mainly argillic and is characterized by mineral assemblages dominated by kaolinite or smectite, but advanced argillic assemblages occur locally. All streams sampled in this area show anomalous amounts of one or more of the components sulfate, copper, molybdenum, and arsenic.

Four areas of patchy clay-carbonate alteration associated with dikes and sills occur around the periphery of the St. Helens district. Surface waters from two of these areas lack anomalous components, and surface waters from one area show anomalous concentrations of sulfate only. The fourth area includes zones of carbonate-free argillic alteration and contains abundant pyrite; streams draining this area have anomalous concentrations of sulfate, copper, zinc, and arsenic. In all the hydrothermally altered areas that produce sulfate anomalies, the components magnesium, sodium, potassium, and silica are also enriched in surface waters because of the destruction of feldspars and mafic minerals in adjacent unaltered rocks by acidic waters derived from oxidizing pyrite.

The polymetallic veins in the district are small quartz veins containing pyrite, chalcopyrite, sphalerite, and galena. Some have significant gold and silver contents. Associated propylitic alteration envelopes surround inner phyllic alteration zones and are no more than a few meters wide. Eight of these veins occur within the Spirit Lake pluton in drainages where we saw no other alteration or mineralization. All these drainages show anomalous amounts of zinc, molybdenum, or arsenic, and a few also show copper or sulfate anomalies. Only one of five veins in hornfels around the Spirit Lake pluton, however, produced anomalies (zinc and arsenic) in surface waters.

Our results show that surface-water sampling for base metals and sulfate together can reliably detect significant areas of porphyry copper mineralization and intense hydrothermal alteration in the Cascade Range. Areas of such intense alteration may host shallow precious-metal deposits and deeper base-metal deposits.

Figure 1 (Ashley and others). Location of the St. Helens mining district, Washington.

Geochemistry and Metallogeny of Granitic Rocks from the Appalachian Mountains—Examples from the Northeast Kingdom Batholith, Vermont, and the Lucerne and Deblois Batholiths, Maine

By Robert A. Ayuso *and* Joseph G. Arth

Detailed petrographic and chemical studies of six calc-alkalic Devonian plutons of the Northeast Kingdom, Vermont, and of the Devonian, generally alkali-calcic Lucerne and Deblois batholiths in coastal Maine characterize the metallogenic potential of granitic rocks in the Appalachian Mountains. The Northeast Kingdom batholith is probably underlain by Proterozoic Grenville-type basement; in contrast, the Lucerne and Deblois batholiths may be underlain by Proterozoic Avalonian-type basement.

The Northeast Kingdom batholith ranges from metaluminous to strongly peraluminous and from quartz-biotite-amphibole gabbro and diorite to biotite granodiorite and muscovite-garnet leucogranite; the SiO_2 content of the batholith ranges from 48 to 77 weight percent. The rocks are characterized by euhedral sphene and magnetite. Low molar values of K_2O/Na_2O ratios (<1) are also characteristic, except in leucogranitic rocks that are potassic. The batholith generally has low Rb (<200 ppm) and high Sr (>100 ppm) contents except in the muscovite-bearing, peraluminous leucogranites. Rare-earth-element (REE) contents, light REE fractionation (chondrite-normalized La/Yb ratios = 2–60), and the general depletion of incompatible elements are similar to those in calc-alkalic suites. Leucogranitic rocks that have a high potential to be associated with granitophile ore deposits have low to moderate REE contents (30–131 ppm), large negative Eu anomalies, numerous aplites and pegmatites, obvious hydrothermal alteration and stockworks, relatively high Rb/Sr ratios (up to 20), high F(Li+Rb)/(Sr+Ba) ratios (up to 3,000), high Sn, W, and Mo contents, and abundant sulfide minerals. Initial $^{87}Sr/^{86}Sr$ ratios range from 0.7045 to 0.7071, $^{206}Pb/^{204}Pb$ ratios range from 18.13 to 18.46, and $^{143}Nd/^{144}Nd$ ratios range from 0.51187 to 0.51200. Isotopic results and range of abundance and ratios of incompatible cations (for example, Ta < 1 ppm, Th < 20 ppm, and U < 10 ppm) are consistent with derivation of the batholith from sources that included the lower and mid-continental crust (Grenville-type rocks) in combination with subcontinental mantle.

The Lucerne and Deblois batholiths are metaluminous and have SiO_2 contents ranging from 70 to 76 weight percent. They are mostly biotite bearing, commonly are enriched in alkali feldspar, and contain ilmenite, tourmaline, and minor hornblende. K_2O/Na_2O ratios are >1. Aplites and pegmatites are not abundant, but a fluid phase existed in the porphyritic facies of the Lucerne batholith, which also contains anomalously high concentrations of Sn (up to 45 ppm), W (up to 55 ppm), and As (up to 6,500 ppm) and quartz and greisen veins containing pyrite, arsenopyrite, and fine-grained cassiterite. The batholiths have high Rb contents (>200 ppm) and low Sr contents (<100 ppm). REE contents are generally high (up to 320 ppm), and REE patterns have large negative Eu anomalies, are fractionated in the light REE, and are relatively flat in the heavy REE (chondrite-normalized La/Yb ratios = 4–15). Incompatible cations are more abundant than in the Northeast Kingdom batholith (for example, Ta is >1 ppm, Th is up to 60 ppm; U is up to 30 ppm). Initial $^{87}Sr/^{86}Sr$ ratios in the Lucerne and Deblois batholiths range from 0.7040 to 0.7110 (Andrew and others, 1983), and $^{206}Pb/^{204}Pb$ ratios range from 18.38 to 18.89. Results are consistent with an origin from the middle continental crust by melting of metasedimentary and metavolcanic rocks of the Avalonian basement.

The calc-alkalic Northeast Kingdom batholith is chemically distinct from the more alkalic rocks of the Lucerne and Deblois batholiths. However, granitic rocks in both areas contain specialized plutons likely to be associated with granitophile ore deposits, especially those containing tin, tungsten, and molybdenum.

REFERENCE CITED

Andrew, A.S., Loiselle, M.C., and Wones, D.R., 1983, Granitic plutonism as an indicator of microplates in the Paleozoic of central and eastern Maine: Earth and Planetary Science Letters, v. 66, p. 151–165.

Applications of Gravity Data to Studies of Framework Geology, Evaluation of Mineral Deposits, and Mineral Prospecting in Northwestern Alaska

By David F. Barnes *and* John S. Kelley

More than 5,000 gravity measurements in the western Brooks Range, Alaska, aid in the interpretation of thrust-belt structures, estimation of the mass of two known mineral deposits, and possible identification of other undiscovered mineral deposits. The data set includes reconnaissance measurements that use river gradients and altimetry for elevation control and have an accuracy of about 15 m, very detailed traverses over two ore deposits, where surveyed elevations are accurate to about 0.3 m, and 3,500 measurements with similar surveyed elevation control along seismic lines in the National Petroleum Reserve in Alaska (NPRA).

Geologic structures are reflected in an arcuate band of strongly positive isostatic anomalies that strike northeastward approximately parallel to geologic grain across the western end of the Brooks Range. These anomalies are

Figure 1 (Barnes and Kelley). Oblique aerial photograph of the Nimiuktuk barite deposit, which forms a small hill (10 m high, 50 m wide, and 80 m long) of almost pure barite in the western Brooks Range, Alaska. Nimiuktuk and the giant Red Dog massive sulfide deposit were used to define the gravitational signature searched for among the 3,500 gravity measurements of the National Petroleum Reserve in Alaska. The photograph was taken from the west-northwest by I.L. Tailleur in 1978.

coincident with a belt of mafic volcanic and plutonic rocks, which many workers believe to be klippen of an extensive thrust sheet rooted in the Angayucham terrane along the south flank of the Brooks Range. Magnitudes of the isostatic anomalies are, however, much larger than those associated with rocks of the Angayucham terrane. The sources of positive gravity anomalies are better modeled as inclined stocks or, possibly, stacked slabs of igneous rocks rather than as simple klippen. The postulated stocks are probably still close to their emplacement sites.

Detailed gravity surveys of the Nimiuktuk (fig. 1) and Red Dog mineral deposits are part of the western Brooks Range data set. Two gravity profiles across the Nimiuktuk barite body indicated a 2-mgal anomaly having horizontal dimensions of more than 100 m. The model that best fits the Nimiuktuk deposit is a cylinder having a density contrast of 1.70 g/cm^3; this model implies that the deposit is almost pure barite and has a radius and depth of about 50 m and a total mass of about 1.5 Mt. The Red Dog massive sulfide deposit, nearing production in 1990, causes a gravity anomaly of about 2 mgal with horizontal dimensions of about 200×500 m; an associated barite-rich body has an anomaly of about 4 mgal with horizontal dimensions of about 500×700 m. Preliminary estimates of ore quantities based on densities from surface sampling and possible mathematical models are comparable to those provided by early developmental drilling. The agreement among the estimates probably is partly due to the shallowness of the deposit.

The NPRA investigation within the mountainous part of northwestern Alaska included more than 3,500 gravity measurements with surveyed elevation control and station separations of about 400 m. Anomalies similar to those at Nimiuktuk and Red Dog appear in this data set as single-station spikes having amplitudes of 2–4 mgal; initially, such spikes were deleted from the data set because they were considered either errors or anomalies too narrow to represent deep structures. However, in 1981, the entire data set was reviewed, and 12 single-station anomalies in areas geologically favorable for mineralization and having associated geochemical anomalies were selected for possible verification and reexamination. In the ensuing 9 yr, only one anomaly has been reinvestigated. Here the gravity and elevation data were verified, but an adjacent bedrock outcrop indicated that basement topography beneath Quaternary sediments might explain the anomaly. The remaining promising gravity anomalies are yet to be field checked.

Mineral-Resource Assessment of Puerto Rico

By Walter J. Bawiec, Andrew Griscom, Richard D. Krushensky, Sherman P. Marsh, Gregory E. McKelvey, *and* Kathryn M. Scanlon

The U.S. Geological Survey is currently involved in a mineral-resource assessment of the Commonwealth of Puerto Rico as part of the National Mineral Resources Assessment Program (NAMRAP). The assessment will aid the Government of Puerto Rico and the mining community in land-use planning, revisions of tax codes and commercial law, investment planning, and mineral exploration. This mineral-resource assessment, which will be completed in 1992, will incorporate all available geological information for Puerto Rico in a readily understood format. Much of this information has never been published.

Mineral resources, including metals, nonmetals, and construction materials, were assessed both onshore and offshore. Puerto Rico consists of a core of Early Cretaceous to Tertiary volcanic and volcaniclastic rocks, associated intrusive rocks, and limestone, transgressed by postvolcanic sedimentary rocks. Among these volcanic and intrusive rocks are primitive and calc-alkalic island-arc suites. Such settings host a wide variety of mineral deposits. More than 200 mineral occurrences known in Puerto Rico have been classified by deposit types according to models of Cox and Singer (1986).

Nickel is known in laterite deposits, copper and gold are in porphyry deposits, iron and copper are in skarns, gold is in placers and epithermal deposits, phosphate is derived from guano in caves, and bauxite is present in karst terranes. Clay, limestone, and glass sand are presently being extracted, and past production of gold, manganese, and iron is documented.

For this project, an unpublished geologic map of the island has been digitized at a scale of 1:100,000 as an information base. Individual lithologic units from the geologic map can be displayed as metallogenic terranes of similar or related environments on the digitized map.

The geochemical data available for Puerto Rico have been derived mainly from a regional stream-sediment sampling program. Data from soil and rock samples are also available. The most detailed sampling has been in the central one-third of the island, where porphyry copper systems have been discovered. Regional geophysical data consist of aeromagnetic maps for nearly 60 percent of the island and gravity coverage of the entire island.

Information on offshore areas comes partly from approximately 2,000 sediment samples from the insular shelf. Data from these samples have been used to map surficial sediment types and, in conjunction with seismic-profile data, to estimate offshore sand and gravel resources.

REFERENCE CITED

Cox, D.P., and Singer, D.A., eds., 1986, Mineral deposit models: U.S. Geological Survey Bulletin 1693, 379 p.

Geophysical Applications in Mineral-Resource Assessment, Cedar City 1° × 2° Quadrangle, Southwestern Utah

By H. Richard Blank

The Cedar City 1° × 2° quadrangle in southwestern Utah encompasses the structural transition from Basin and Range to Colorado Plateau and was a locus of extensive late Cenozoic magmatism and mineralization. It contains diverse mineral and energy resources, including precious and base metals, rare earths, uranium, iron, oil, coal, and geothermal deposits, along with various industrial materials. Geophysical data contribute to knowledge of the geologic environment of these deposits and facilitate assessment of the potential for discovery of additional resources in the region.

Geophysical coverage presently available consists mainly of regional aeromagnetic and gravity surveys and NURE (National Uranium Resource Evaluation) aeroradiometric surveys. A detailed aeromagnetic survey has been made of the so-called iron axis of southwestern Utah in support of iron exploration. The principal sources of aeromagnetic anomalies are not iron deposits but rather volcanic rocks, hypabyssal intrusive rocks, and Precambrian crystalline basement.

Aeromagnetic data delineate the subsurface extent of the partly exposed Mineral Mountain, Bull Valley-Big Mountain, Iron Mountain, and Granite Mountain-Three Peaks Miocene monzonitic intrusions, all of which have associated mineral deposits. These data indicate the presence of additional hypabyssal intrusions beneath Sevier Valley, Parowan Valley, and the west flank of the Red Hills. A concealed extension of the Mineral Mountain body may have controlled hydrothermal systems responsible for mineralization in the Goldstrike district.

Buried intrusions revealed by aeromagnetic anomalies in the northwest corner of the quadrangle are probably related to the Indian Peak and Caliente caldera complexes, whose ring structures are delineated by gravity data. The Gold Springs and State Line gold districts are possible manifestations of mineralization controlled by such structures.

Bouguer gravity anomalies, mainly a reflection of contrasts between low-density sedimentary and volcanic rocks and much denser carbonate sequences and Precambrian basement, delineate a basin-range fabric beneath alluvium of the Escalante Valley. Some of the deeper basins in the valley may contain evaporite deposits, and, in at least two places (Newcastle and Zane), concealed basin-and-range faults control the circulation of geothermal fluids. Gravity data are used to distinguish pediment-covered bedrock from valley-fill areas and, thus, to identify areas accessible for mining.

Aeromagnetic and gravity data have been used to address problems related to the regional geologic framework of southwestern Utah, which bear only indirectly on resource assessment yet are important for planning exploration. The Cedar City quadrangle straddles an east-trending gravity discontinuity that passes through the Basin and Range-Colorado Plateau transition and elsewhere appears to mark an abrupt northward deepening of the Precambrian basement accompanied by a drastic increase in volume of silicic igneous rocks. The presence of this discontinuity suggests that pervasive silicic magmatism beneath this part of the Colorado Plateau was responsible for the basement uplifts interpreted from signatures seen on the potential-field maps. The basement highs are closely associated with east-tilted fault blocks and are possible sources of weak hydrothermal systems.

NURE radiometric data are of limited value in the Cedar City quadrangle because of excessive terrain clearances and wide traverse spacing. However, a more tightly controlled survey would have obvious utility in mapping uraniferous zones on the plateau. Spectroradiometric data and Landsat Thematic Mapper data are expected to be valuable in mapping hydrothermally altered zones throughout the region.

Assessment of Undiscovered Mineral Resources, Tongass National Forest, Southeastern Alaska

By David A. Brew, Lawrence J. Drew, Jeanine M. Schmidt, David H. Root, *and* Donald F. Huber

The Tongass National Forest is the Nation's largest national forest; it covers about 70,000 km^2, which is more than 80 percent of southeastern Alaska (fig. 1). The U.S. Forest Service, which is revising the Tongass Land Management Plan, has requested resource information from many sources, has analyzed and interpreted the information, and has prepared a Draft Environmental Impact Statement. It is now reviewing the comments thereon and revising the alternatives prior to releasing the Final Environmental Impact Statement. The Forest Service is attempting to include mineral-resource data in the plan.

The U.S. Geological Survey (USGS) has been continuously active in southeastern Alaska since 1956 and is currently conducting a probabilistic assessment of the undiscovered mineral resources of the region. This regional assessment is based largely on previously completed assessments of individual Wilderness Areas, Wilderness Study Areas, and quadrangles that make up almost all of southeastern Alaska and that have been mapped at the scale of 1:250,000 as part of the Alaska Mineral Resources Assessment Project. These previously completed assessments were based on USGS reconnaissance geologic, geochemical, and geophysical mapping that has been reported in USGS publications. A few assessments were joint USGS-U.S. Bureau of Mines (USBM) efforts, and one is primarily a joint effort by the USBM and the State of Alaska Division of Geological and Geophysical Surveys. Only 4 of the 15 quadrangles in southeastern Alaska are not included in a preexisting assessment; however, 2 of the 4 are already studied.

The available data on regional geology, economic geology, stream-sediment and panned-concentrate geochemistry, bedrock geochemistry, and mineral resources were reviewed at the 1:250,000 scale along with aeromagnetic, gravity, aeroradiometric, and telegeologic information. One hundred twenty-seven mineral-resource tracts, ranging in area from 16 to 2,920 km^2, were identified as likely to contain undiscovered metallic mineral resources in 34 different types of deposits. Each tract was judged to contain one or more different types of mineral deposits. The number of as-yet-undiscovered deposits of each type discoverable by conventional mineral exploration methods was estimated for each tract at the 0.95, 0.90, 0.50, 0.10, and 0.05 probability levels. Many small tracts were combined to allow probabilistic assessment, but, because such assessments were not made of the smallest tracts or of tracts judged to be already well explored, we made final probabilistic assessments of 96 tracts containing 21 different types of deposits. Areas not assigned to tracts are interpreted to lack undiscovered mineral deposits of the types specified.

Estimates of the number of deposits in each tract were used in combination with the worldwide tonnage and grade distributions for each deposit type to calculate a probabilistic undiscovered mineral-resource endowment for each tract by means of the USGS MARK3 mineral-resource-endowment simulator (Root and Scott, 1988). By Monte Carlo simulation, this computer program produces a distribution of tonnages for each metal contained in each deposit type in a given tract. When aggregated over all deposit types, these distributions yield a probabilistic estimate of the undiscovered mineral resources in each tract. The estimates of mineral-resource endowment for all the individual tracts are combined to provide an aggregated estimate of the undiscovered mineral-resource endowment of the Tongass National Forest and adjacent lands in southeastern Alaska.

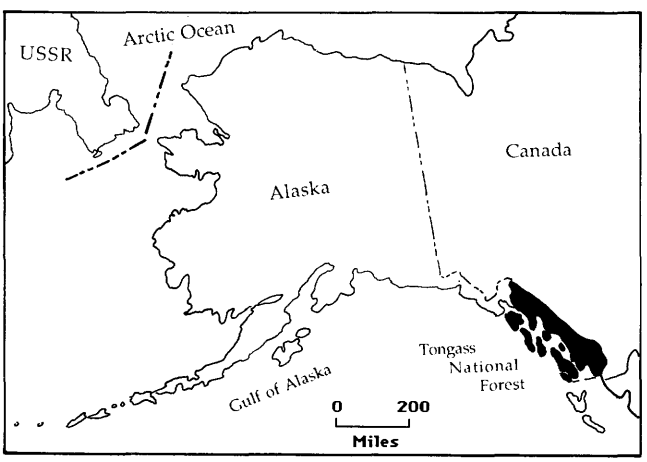

Figure 1 (Brew and others). Location of the Tongass National Forest in southeastern Alaska.

REFERENCE CITED

Root, D.H., and Scott, W.A., 1988, User manual for mineral simulation program: U.S. Geological Survey Open-File Report 88–15, 63 p.

Synthesis of Geophysical and Geological Data Centered on the Idaho Batholith and the Challis Volcanic Field, Idaho

By John W. Cady, Viki Bankey, Keenan Lee, A.E. McCafferty, James A. Pitkin, *and* W.D. Stanley

A digital geophysical data base, assembled for mineral-resource assessments of Wilderness Study Areas in Idaho, can be used for geophysical and geological interpretations beyond the scope of the mineral-resource assessments. The study area is bounded by lats 42° and 47° N. and longs 110° and 118° W.

Maps being prepared at a scale of 1:1,000,000 include topographic, gravity, and aeromagnetic maps and terrace-density and terrace-magnetization maps derived from the gravity and magnetic data (see McCafferty and Bankey, this volume). Data used to create the maps are available on magnetic tape from the EROS (Earth Resources Observation Satellite) Data Center, Sioux Falls, SD 57198. Other maps in preparation as of August 1990 include radioelement maps derived from aerial gamma-ray spectrometry and linear-feature and lineament maps derived from interpretation of Landsat multispectral scanner imagery.

Density, magnetic susceptibility, and remanent magnetization of about 700 rock samples collected from the study area will be included in the regional data base to calibrate geophysical interpretations. Seven thousand mine and prospect records have been obtained from the U.S. Geological Survey's Mineral Resources Data System (MRDS) for evaluating the relations between geophysical anomalies and mineral deposits. Geophysical, rock physical property, and MRDS data and a digital geologic map are being transferred to the GRASS geographic information system developed by the U.S. Army Corps of Engineers. GRASS will be used to determine characteristic geophysical parameters and physical properties of geologic map units to aid geophysical interpretation and correlation with known mineral deposits.

An east-west magnetotelluric (MT) profile was made across the west side of the Idaho batholith and the Idaho suture zone near McCall in 1989. In a separate study, an east-west MT profile was made near Leesburg. MT measurements were made in 1990 across the trans-Challis lineament zone northwest of Ketchum. The MT studies are designed to determine subsurface structure and to evaluate the potential for ore bodies in the contact areas between electrically resistive rocks of the batholith and conductive sedimentary and volcanic rocks.

Preliminary interpretations include the following:

(1) Magnetic highs show that Tertiary intrusive rocks are extensive in the shallow subsurface beneath the Challis Volcanics and the Idaho batholith of Cretaceous age. Gravity lows show that the Tertiary intrusions coalesce at depth into a batholith comparable in size to the Idaho batholith.

(2) A northwest-trending lineament defined by the aeromagnetic, radioelement, and topographic data crosses the Salmon River Mountains midway between Challis and Salmon along the alignment of Big Creek. The lineament is defined by linear magnetic highs caused by magnetic Precambrian quartzite and schist, by Ordovician mafic to ultramafic intrusive rocks, and, possibly, by Tertiary intrusive rocks.

(3) Ovoid belts of magnetic highs 40–70 km in diameter occur in the southwestern Snake River Plain and Owyhee Plateau in association with calderalike structures in felsic volcanic rocks.

Mineral Deposits of the Midcontinent Rift, Lake Superior Region, United States and Canada

By William F. Cannon *and* Teresa A. McGervey

About 450 mineral deposits are known in Middle Proterozoic rocks of the Midcontinent Rift system in Michigan, Wisconsin, Minnesota, and Ontario. Data on these deposits provide clues for further exploration of the rift, both where it is exposed in the Lake Superior region and along its nearly 2,000-km-long extension in the Precambrian basement beneath Paleozoic cover in the midcontinent region. The 1:500,000-scale map (Cannon and McGervey, in press) of the Lake Superior region shows the locations, size classifications, and geologic types for these deposits on a geologic base map.

The principal mineral produced from the rift has been copper. It has been obtained mostly from native copper deposits hosted in basalt flows and interflow sedimentary rocks and from stratabound deposits in lacustrine shales. Lesser copper production has come from sulfide veins in basalt and from breccia pipes. Silver has been produced from epithermal veins in Ontario, which also host polymetallic deposits of lead, zinc, copper, barite, and fluorite.

Very large resources of copper-nickel-cobalt mineralization are proven in the Duluth Complex and other rift-related mafic intrusive bodies. Lesser known but potentially significant resources include uranium in pitchblende veins, uranium and rare-earth elements in alkalic rocks, copper sulfide (chalcocite) deposits in volcanic rocks, titanium and vanadium in mafic intrusive rocks, and platinum-group elements in mafic intrusive rocks.

All the mineral deposits and resources have been discovered along about 15 percent of the strike length of the rift. This part of the rift is well exposed in the Lake Superior region. Subsurface extensions of the rift in the midcontinent region to the south, well known from geophysical studies and a limited number of basement-penetrating wells, constitute a major exploration frontier. If the buried parts of the rift are as thoroughly mineralized as the exposed parts, several thousand mineral deposits should be present at the Precambrian surface beneath Paleozoic cover rocks.

REFERENCE CITED

Cannon, W.F., and McGervey, T.A., in press, Map showing mineral deposits of the Midcontinent Rift, Lake Superior region, United States and Canada: U.S. Geological Survey Miscellaneous Field Studies Map MF–2153, scale 1:500,000.

Mapping Minerals with Imaging Spectroscopy near Canon City, Colorado

By Roger N. Clark, Andrea J. Gallagher, *and* Gregg A. Swayze

Imaging spectroscopy data were obtained in 1989 over Canon City, Colo., by using the U.S. National Aeronautics and Space Administration's Advanced Visual/Infrared Imaging Spectrometer (AVIRIS), which has a ground resolution of 20 m. Spectral analysis of imaging spectroscopy data allows mapping of any material (such as minerals, vegetation, manmade materials, and water) having unique absorption features in the measured spectral region. AVIRIS acquires data in the spectral range from 0.4 to 2.45 μm in 224 spectral channels. The narrow spectral channels of AVIRIS form a continuous reflectance spectrum of the surface, in contrast to the four to seven channels of Landsat data. Landsat data can be used to distinguish general brightness and slope differences in the reflectance spectrum of the surface; imaging spectroscopy provides the same information and also resolves absorption bands in the spectrum that can be used to identify specific minerals.

A new method of spectral analysis has been developed to map minerals in the Canon City test area. First, an absorption feature in the spectrum is isolated by removing the continuum in the reflectance spectrum (which also removes topographic effects from the analysis). Then a least-squares fit is performed on the absorption feature profile by using the reference-library spectrum of a known material. The method can be used to map minerals (and other materials) at very low concentrations as well as to distinguish between minerals traditionally difficult to differentiate in the field.

At Canon City, dolomite, limestone, arkose, sandstone, and shale units form hogbacks dipping gently southwest on the east limb of a broad syncline. These rock units are truncated by northwest-trending faults, which juxtapose them against meta-igneous and gneissic rock units to the northeast. We have distinguished and mapped calcite, dolomite, illite, montmorillonite, hematite, goethite, kaolinite, and other minerals in these units and subtle compositional variations within individual rock units. These mineral-based map images correspond well with the geologic maps of the region, and field checks of the results prove that they are highly accurate.

Clays and other OH-bearing minerals, iron oxides, and carbonates are just some of the many minerals that have diagnostic absorption features that can be used for mapping. Spectral analysis shows that kaolinite can be mapped where its concentration is only a few weight percent and that even crystalline order and disorder in kaolinite can be distinguished. The images for the Canon City area show more detail in some places than do standard geologic maps.

Mineral maps for hundreds of square kilometers can be computed from images in only a few minutes of computer time. Such maps could be used to create geologic maps for petrologic, tectonic, and mineral-exploration studies. Color images produced from combinations of mineral maps yield a pseudogeologic map. Such images could provide valuable information before or during fieldwork and, thus, could greatly enhance the productivity of field studies.

Geologic Settings of Barite Deposits as Indicators of the Potential for Other Types of Mineral Deposits

By Sandra H.B. Clark

Different types of barite deposits that form under different physical and chemical conditions have distinctive mineral associations (Clark and others, 1990). Some sediment-hosted, stratiform barite deposits, such as those of the Nevada barite belt, are predominantly barite, but others are associated with Zn-Pb-Ag deposits, such as those of the Selwyn basin and Kechika trough of western Canada, the Red Dog area of Alaska, and the Meggen deposits of Germany. Barite nodules in shales or mudstones may occur peripheral to stratiform deposits of barite and (or) base-metal sulfides; therefore, occurrences of barite nodules may indicate proximity to undiscovered stratiform base-metal sulfide and (or) barite deposits. However, barite nodules in shales or mudstones are not always indicators of associated stratiform deposits, because they may form by redox precipitation at anoxic-dysoxic interfaces in unconsolidated sediments during diagenesis and do not necessarily indicate the involvement of barium-enriched fluids.

Volcanic-associated stratiform barite deposits may occur with polymetallic (Cu-Pb-Zn±Au±Ag) massive sulfide deposits, such as the Kuroko ore bodies of Japan and the Buchans ore bodies of Newfoundland. Barite also is spatially related to volcanic-associated Au-Ag deposits in the Hemlo area of Ontario and the Barite Hill area of South Carolina. The relations between barite and Au-Ag mineralization in these areas are uncertain; some of the barite may be stratiform, but later hydrothermal barite mineralization is more closely associated spatially with Au-Ag mineralization.

Some stratiform syngenetic to diagenetic barite deposits are associated with economic concentrations of evaporite minerals that formed in supratidal zones. Examples are barite-celestite deposits of northeastern Mexico and western Argentina.

Carbonate-rock-hosted stratabound deposits of barite and residual deposits that overlie them are common in areas that contain deposits or occurrences of sphalerite, galena, and (or) fluorite. In some barite deposits, such as the residual deposits of the Cartersville district of Georgia, barite in the bedrock is not associated with sulfide minerals

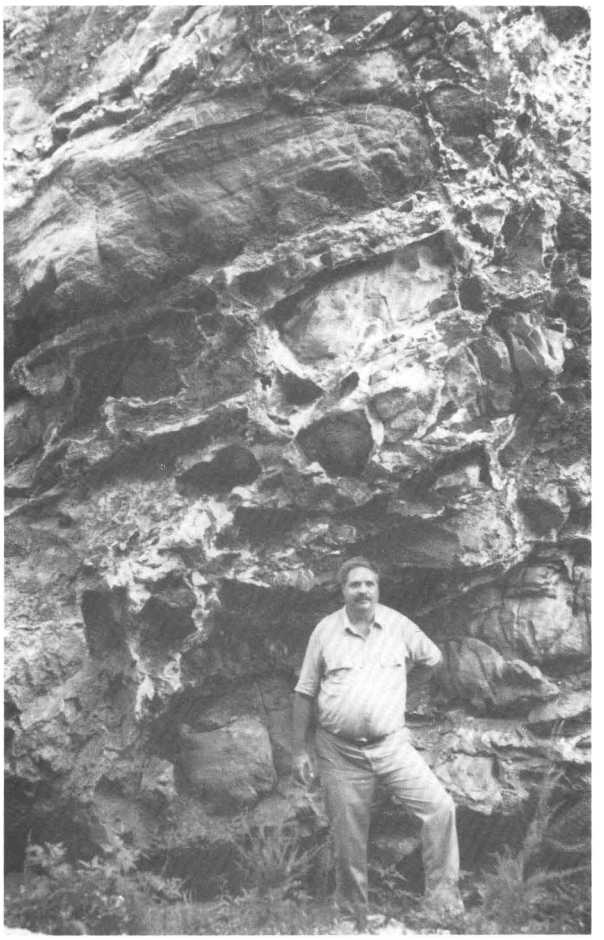

Figure 1 (Sandra Clark). Stratabound barite (white material in fractures above and behind Travis A. Paris) in crackle breccia zone in Lower Ordovician Mascot Dolomite, Thompson mine, Sweetwater district, Tennessee. Photograph by Sandra H.B. Clark, 1988.

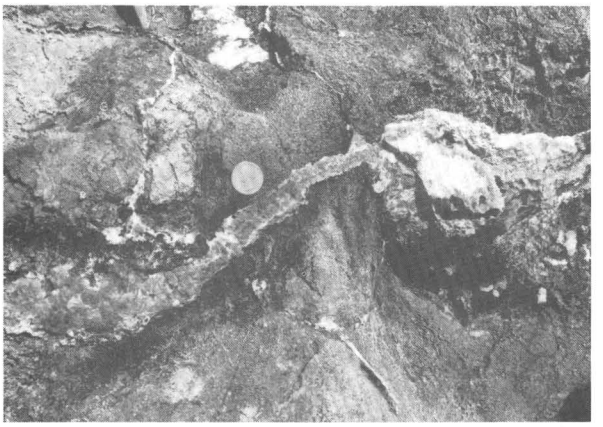

Figure 2 (Sandra Clark). Stratabound fluorite (gray) and barite (white) in fractures in collapse breccia zone in Lower Ordovician Kingsport Formation, Ballard mine, Sweetwater district, Tennessee. Photograph by Sandra H.B. Clark, 1988.

or fluorite, but, in others, stratabound barite in the bedrock is associated with fluorite (Sweetwater district, Tennessee; figs. 1 and 2) and (or) base-metal sulfide minerals (Southeast Missouri district). In the Central Tennessee district, barite occurs both within major stratabound Zn-Pb-F deposits and within veins overlying them.

As the above examples suggest, study of the geologic setting of barite occurrences and deposits can provide information about the potential for spatially associated deposits of other mineral resources, including base-metal sulfides, precious metals, fluorite, and celestite.

REFERENCE CITED

Clark, S.H.B., Gallagher, M.J., and Poole, F.G., 1990, World barite resources—A review of recent production patterns and a genetic classification, *in* Minerals, materials, and industry: London, The Institution of Mining and Metallurgy, p. 175–184.

Tectonomagmatic Settings of Proterozoic Metallogenic Provinces in the Southwestern United States

By Clay M. Conway

Tholeiitic, calc-alkalic, and calcic, bimodal to unimodal, largely marine, subduction-arc assemblages dated at 1,790 to 1,720 Ma are exposed from the Cheyenne belt in southern Wyoming to northern New Mexico and central Arizona. Rocks older than 1,760 Ma are present only near the Cheyenne belt. The arcs were accreted to the North American craton between about 1,750 Ma and 1,700 Ma, probably as numerous tectonostratigraphic terranes. They constitute a metallogenic province characterized primarily by submarine exhalative deposits. Most of the scores of massive sulfide deposits throughout this province are rich in Zn and Cu and contain lesser and variable amounts of Pb, Au, and Ag. Several Au deposits are exhalative, and areas having potential for exhalative Au have been identified. Exhalative W-Cu deposits in Colorado may belong to this province. Precious- and base-metal veins and porphyry-type Cu prospects are locally associated with plutonic rocks of the province. Ultramafic rocks or sheeted dikes known in several localities suggest the presence of oceanic crust. A Co-Ni-Cr-Cu prospect is known at one locality of ultramafic rocks.

By 1,700 Ma, the subduction-arc terrane formed a belt of incompletely stabilized continental crust more than 600 km wide. Strata and intrusions of continental character were emplaced within and marginal to this new crust largely in the interval 1,700 to 1,650 Ma, possibly during a rifting event that resulted in a passive continental margin in Arizona and New Mexico. Paleocurrent data from thick fluvial to tidal mature sandstone sequences in central

Arizona, northern New Mexico, and the Needle Mountains of Colorado indicate transport toward deep basins in southern Arizona and New Mexico. The mature sandstones at most localities overlie and are locally interbedded with high-silica ash-flow rhyolite and minor basalt; rhyolite and associated hypabyssal rocks are products of subaerial caldera magmatism. Deep-seated granites are present in southeastern California, central to northern Arizona, northern New Mexico, and as far north as the Boulder Creek batholith in Colorado. The igneous rocks dated at 1,700 to 1,650 Ma are generally alkalic-calcic and subaluminous to peraluminous; they are similar to anorogenic granites of the region that are dated at 1,480 to 1,400 Ma.

The 1,700- to 1,650-Ma rocks constitute a metallogenic province dominated by elements enriched in evolved granitic magmas. There has been little production of metals from this province, however. The Boriana tungsten deposit of northwestern Arizona, which is genetically related to a 1,690-Ma two-mica granite, is possibly the best-known deposit of this type. Caldera-related hypabyssal rocks in central Arizona are enriched in Sn, Be, Nb, La, and Y; associated sedimentary rocks contain small Be deposits. Early subaqueous volcanic sequences contain a few small massive sulfide deposits. In northern New Mexico, W prospects and Sn anomalies in drainage sediments are associated with felsic volcanic and hypabyssal rocks. One stratiform W deposit and a regionally extensive sediment layer enriched in Mn, Nb, Ta, W, Sn, and Sb are between rhyolite and an overlying quartz sandstone and may be exhalative. Fe-rich beds are also associated with rhyolite and quartzite in this province.

Granites dated at 1,480 to 1,400 Ma occur throughout the regions discussed above and constitute a third distinct metallogenic province. Like the 1,700- to 1,650-Ma igneous rocks, they are not likely to be subduction related, and they have potential for metals characteristically enriched in evolved granite magmas. For example, the granites locally are highly enriched in U and Th; near Bagdad, Ariz., they produced W vein deposits. Petrographically and metallogenically similar plutons dated at 1,370 to 1,360 Ma and 1,060 Ma occur in limited areas in Colorado.

In southeastern California, igneous rocks of the three provinces discussed above are superimposed on crust formed between 2.3 and 2.0 Ga. This region of anomalous crust has apparently unique metallogenic characteristics. It contains 1,720-Ma massive sulfide deposits that have extremely low contents of Au and Ag and 1,400-Ma syenite complexes, one of which hosts the Mountain Pass rare-earth-element deposit.

A region in southern California west of the Mojave-Sonora megashear differs from the provinces discussed above. It contains, for example, the 1.2-Ga anorthosite complex in the San Gabriel Mountains, which has resource potential for Ti, V, and rare-earth elements.

Preliminary Assessment of the Mineral Resources of the Cedar City 1° × 2° Quadrangle, Utah

By Theresa M. Cookro, Michael A. Shubat, *and* Janet L. Jones

Mineral resources of the Cedar City 1° × 2° quadrangle, Utah, were assessed in 1989–90 during a cooperative study by the U.S. Geological Survey (USGS) and the Utah Geological and Mineral Survey (Eppinger and others, 1990). This preliminary study, which was part of the National Mineral Resources Assessment Program, was used to aid Federal land-use planning and to provide data for future mineral-resource studies. During the assessment, the Utah Geological and Mineral Survey added new information to the Mineral Resources Data System (MRDS) of the USGS.

Principal commodities of the 13 metal mining districts in the quadrangle include iron, silver, gold, gallium, germanium, and base metals. Nationally, the Iron Springs and Pinto districts were the greatest producers of iron ore west of the Mississippi until the mines closed in the 1980's; mines have reopened, and the districts currently supply about 550,000 tons of ore per year to the Geneva steel plant in Orem, Utah. The Escalante mine, in the Escalante district, was one of the largest silver mines in Utah until it closed in 1989. Gold has been produced as a byproduct at base-metal and silver mines in the quadrangle, and a new bulk-minable gold deposit is now in production in the Goldstrike district. The Apex mine, in the Tutsagubet district, produced gallium (used for integrated circuits) and germanium (used in infrared optics and fiber optics) from a collapse breccia pipe. The pipe originally was mined for highly oxidized ores of copper, lead, and silver that contained minor gold and zinc. In the Silver Reef district, silver was produced from a roll-front environment, similar to that of the uranium roll-front deposits. Exploration is in progress in the Goldstrike, Tutsagubet, and Antelope Range districts and in the Washington Dome area.

Industrial mineral resources within the quadrangle include volcanic rock products, bentonite clay (produced for the Glen Canyon Dam project), kaolin, petrified wood, agate, dimensional sandstone, limestone, gypsum, marble, and sand and gravel. Oil and coal resources are also abundant within the Cedar City quadrangle. The Virgin oil field, Utah's oldest oil field, produced 25 million barrels. Three coal fields (Kolob, Harmony, and Alton) and part of a fourth (Kaiparowits) lie within the quadrangle and contain approximately 6 billion tons of reserves.

REFERENCE CITED

Eppinger, R.G., Winkler, G.R., Cookro, T.M., Shubat, M.A., Blank, H.R., Crowley, J.K., Kucks, R.P., and Jones, J.L., 1990, Preliminary assessment of the mineral resources of the Cedar City 1° × 2° quadrangle, Utah: U.S. Geological Survey Open-File Report 90–34, 146 p.

Copper Deposits in Tertiary Red Beds in Bolivia

By Dennis Cox, Raul Carrasco, Orlando André, Alberto Hinojosa, *and* Keith Long

Stratabound copper deposits are found in red to brown sandstone, conglomerate, and siltstone of Miocene and Pliocene age in the Altiplano of southwestern Bolivia. Chalcocite and native copper replace carbonate cement and locally replace fossil plant materials. Ore minerals are associated with zones of bleaching and chloritization of the host rocks. More than 70 deposits have been found from Lake Titicaca to near the border with Argentina. More than half of these deposits contain less than 10,000 t of copper, but two larger districts are known: Corocoro and Chacarilla, which together contain more than 1,000,000 t of copper. These large deposits are associated with diapirs of gypsum, and the Corocoro deposit, with a possible salt intrusion. These diapirs originated from evaporites in the lower part of the Tertiary section. The Corocoro fault controlled most of the mineralization at Corocoro and is unique in that strata on both sides dip away from the breccia-filled fault zone. Massive halite was encountered near the fault in a shaft sunk in 1974.

Replacement of carbonate in the sandstone matrix by native copper, formation of native copper pseudomorphs after aragonite, and bleaching and chloritization of host rock near depositional sites can be described by the following two equations:

$$8\ CuCl_3^{2-} + 12\ CaCO_3 + 16\ H^+ + CH_4 = 8\ Cu^0 + 12\ CaCl_2 + 13\ CO_2 + 10\ H_2O$$

and

$$20\ \underset{\text{limonite}}{FeO(OH)} + 4\ \underset{\text{kaolinite}}{Al_2Si_2O_5(OH)_4} + 4\ SiO_2 + 5\ C = 4\ \underset{\text{chlorite}}{(Fe_5Al)(Si_3Al)O_{10}(OH)_8} + 5\ CO_2 + 2\ H_2O$$

The ore solutions are assumed to have been brines of low pH that mixed with a hydrocarbon reductant to reduce iron and deposit copper. Conditions favoring copper precipitation were widespread in the Altiplano, but large deposits formed only near evaporite diapirs. Elevated temperatures near these diapirs accelerated convective flow of brines that leached copper from large volumes of sedimentary rock. Flow was focused along the flanks of the diapirs. Mixing of brines with reducing fluids in the sedimentary wall rocks caused copper deposition.

Geologic Map of the Sierrita-Mogollon Corridor (Arizona-New Mexico) and Implications for Mineral Resources

By Leslie J. Cox, Brenda B. Houser, Eric R. Force, Mark E. Gettings, Alison Burchell, *and* Frederick S. Fisher

The U.S. Geological Survey is conducting a multidisciplinary study of a geologic transect across the southern Basin and Range province (fig. 1). The Sierrita-Mogollon transect corridor contains abundant known mineral resources that include copper, precious metals, diatomite, and zeolites. Undiscovered mineral deposits may be concealed beneath a thin cover of basin fill, Tertiary lava flows, or the upper plates of detachment faults. Highlights of recent and (or) unpublished data used to compile the geologic map of the transect corridor are summarized below.

Sierrita and Tucson Mountains.—Recognition of a Cretaceous caldera in the Sierrita Mountains that was tilted to the southwest during middle Tertiary extensional tectonism led to reinterpretation of the positions of ore deposits relative to what may be a subcaldera batholith. The deposits formed in and around the roof of the batholith rather than down along its side (Lipman and Fridrich, 1990). Reinterpretation of movement along faults between precaldera and intracaldera volcanic units indicates that some present-day reverse faults were steep normal faults prior to southwest rotation.

Santa Catalina Mountains.—Previous interpretations of the Catalina detachment fault in the Santa Catalina Mountains assigned the entire mountain mass to the lower plate. New work suggests that the forerange is in the lower plate but that the main range occupies a structurally intermediate position above an older, deformed mylonite and below a younger mylonite, most of which has been eroded away. Within this intermediate plate are several newly mapped granitic intrusions that apparently postdate the emplacement of Eocene two-mica granites. A sequence of Precambrian to Upper Cretaceous supracrustal stratified rocks in the intermediate plate is host to several small mineral deposits and, potentially, could host large deposits.

San Manuel-Mammoth area.—Three generations of extensional faulting have affected the Mammoth vein set and other middle Tertiary mineralized and altered zones of the San Manuel-Mammoth area. From youngest to oldest, these are (1) middle Miocene or younger, steep Basin-Range faulting on the Mammoth fault zone, (2) early Miocene low-angle normal faulting and rotation on the San Manuel fault system, and (3) late Oligocene detachment on the Cloudburst fault and its side ramp, the Turtle fault. For the early Miocene and younger faults that offset the Mammoth vein set, precise vectors have been calculated that permit vein reconstruction. The late Oligocene detachment faulting apparently is genetically related to the vein mineralization.

Galiuro Mountains.—Reconnaissance and detailed geologic mapping in the Galiuro Mountains shows that the central part of the range consists of intermediate-composition lava flows overlain by local pyroclastic flow and air-fall deposits and by a previously unrecognized, areally extensive complex of dacitic to rhyolitic flows and domes. Possibly compatible hypotheses as to the source of the Galiuro volcanic field include (1) a volcano-tectonic depression inferred from a pattern of gravity lows that straddles the flow and dome complex and part of the San Pedro basin and (2) a large eruptive center that may have formed along an east-northeast-trending zone of crustal weakness that developed within an extensional accommodation zone.

The Galiuro Mountains are flanked by northwest-trending normal faults and are between the Catalina and Pinaleno metamorphic core complexes. Tectonic interpretations inferred for the structure of the Galiuro Mountains suggest the possibility of detachment faults at shallow depths. If correct, this interpretation has implications for the

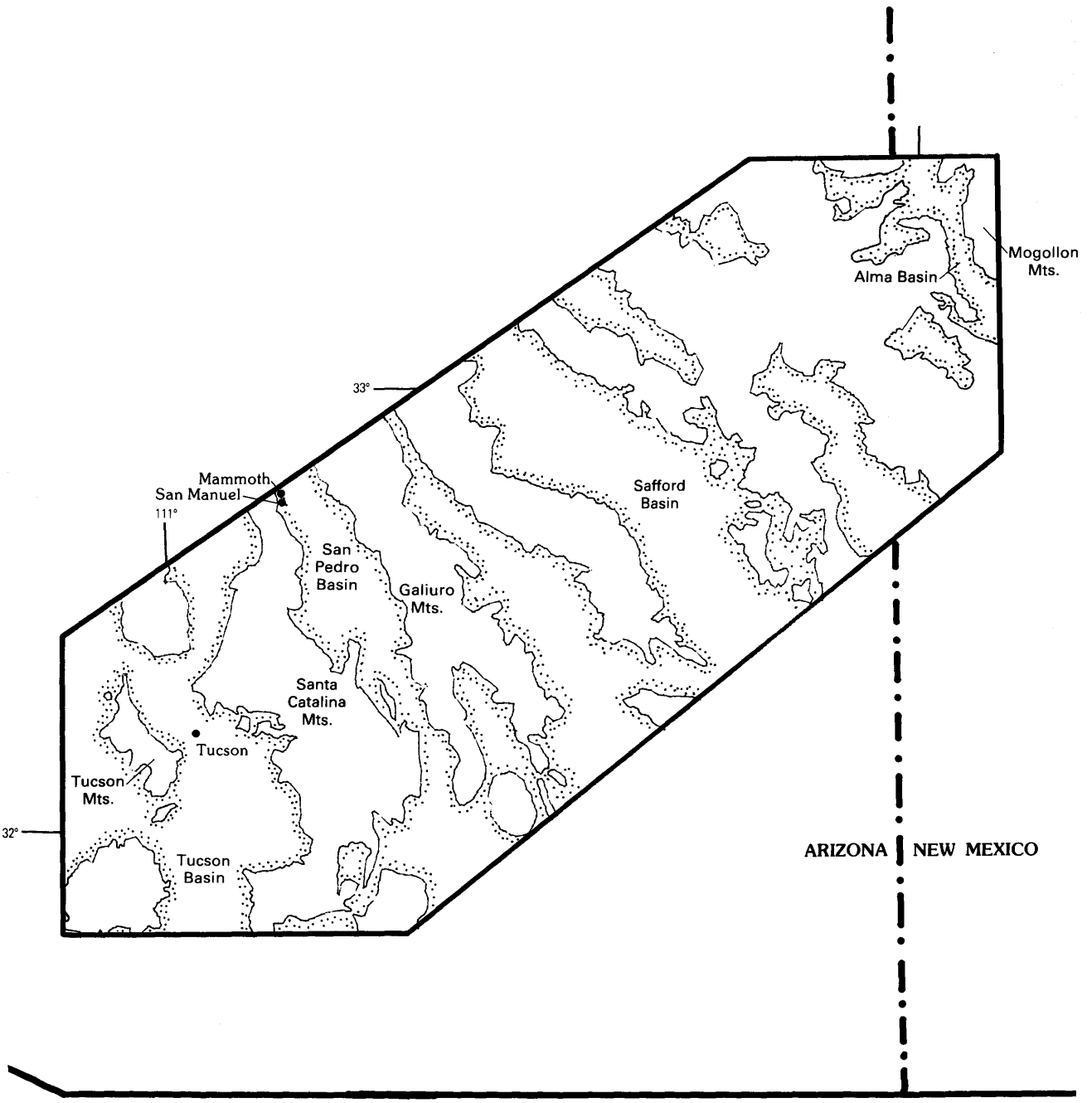

Figure 1 (Leslie Cox and others). Mountains and basins (stippled) in the Sierrita-Mogollon corridor, Arizona and New Mexico.

potential for detachment-fault-related precious metals in the range.

Alma basin, New Mexico.—Oblique-slip normal faults around the margins of the Alma basin in basin-fill units as young as early Pliocene suggest that the basin may have been rotated slightly counterclockwise during Basin and Range extension. The Alma basin is near the edge of the Colorado Plateau, between the Morenci-Reserve fault zone on the northwest and the Mogollon Mountains on the east. This tectonic setting suggests that the inferred rotation of the basin block may have been in response to interactions between the northeast-trending Morenci-Reserve fault zone, the relatively stationary Colorado Plateau, and east-west-directed Basin and Range extension. Stratigraphic evidence from Miocene conglomerates indicates that an early stage of the inferred rotation may have been coeval with mineralization in the Mogollon mining district.

REFERENCE CITED

Lipman, P.W., and Fridrich, C.J., 1990, Cretaceous caldera systems: Tucson and Sierrita Mountains, *in* Gehrels, G.E., and Spencer, J.E., eds., Geologic excursions through the Sonoran Desert region, Arizona and Sonora: Arizona Geological Survey Special Paper 7, p. 51–65.

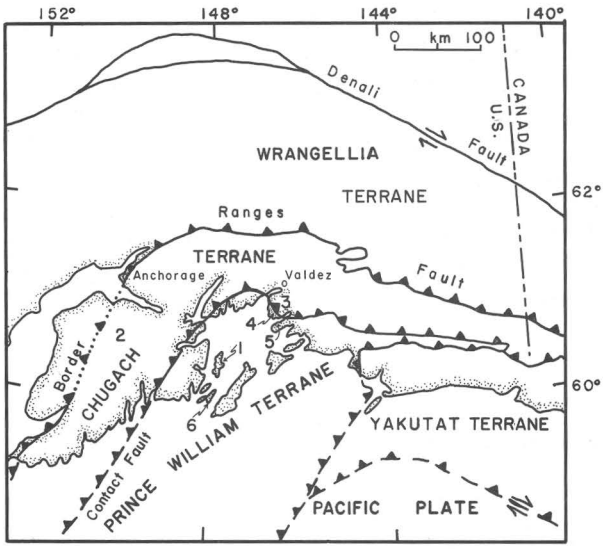

Figure 1 (Crowe and others). Tectonostratigraphic terranes and locations of mines in selected historically significant massive sulfide deposits in south-central Alaska. 1, Rua Cove mine; 2, Lynx Creek mine; 3, Standard Copper mine; 4, Ellamar mine; 5, Port Fidalgo mine; 6, Beatson mine.

Laser-Microprobe Studies of Sulfur Isotopes in Stockwork and Massive Sulfide Ores, Rua Cove Mine, South-Central Alaska

By Douglas E. Crowe, Wayne C. Shanks III, *and* John W. Valley

Many of the massive sulfide deposits in the Prince William Sound district of south-central Alaska (fig. 1), which historically were interpreted as epigenetic vein and replacement deposits, recently have been reinterpreted as volcanogenic massive sulfide (VMS) deposits formed syngenetically on or near the sea floor (Wiltse, 1973; Koski and others, 1985; Crowe and others, 1988). Understanding the origin of the deposits is critical for defining this region as a potential exploration target for VMS deposits. The morphologies and geologic settings of the deposits are consistent with Cyprus- and Besshi-type VMS models. The host rocks are predominantly flysch and dismembered ophiolite of the Chugach (Late Cretaceous) and Prince William (early Tertiary) terranes, which constitute the bulk of the rocks exposed in southern Alaska. Conventional analyses of stable sulfur isotopes show $\delta^{34}S$ ranging from +3.5 to +4.5 per mil; these values are consistent with a VMS model for the deposits but are not definitive. The major limitation to obtaining meaningful isotope data is the fine-grained, intergrown nature of the sulfide ores that typify the deposits.

A new laser-microprobe technique for performing micro-scale stable-isotope analyses (Crowe and others, 1990) allows us to measure sulfur-isotope ratios of individual minerals in fine-grained slabbed samples. Sulfur-isotope data were collected at the University of Wisconsin, Madison, by using a Nd-YAG (yttrium-aluminum-garnet) laser connected to an isotope-ratio mass spectrometer. A similar system (which uses a CO_2 laser) at the U.S. Geological Survey in Reston, Va., is shown in figure 2. Laser-microprobe sulfur-isotope data for samples from the Rua Cove mine, Prince William Sound, provide new evidence that many of these deposits are syngenetic.

Conventional combustion-extraction measurements of $\delta^{34}S$ from hand-picked coexisting chalcopyrite-pyrrhotite (cp-po) pairs (fig. 3) from both the massive sulfide blanket and the underlying stockwork feeder zone indicate isotopic disequilibrium; pyrrhotite is slightly depleted in ^{34}S, in contrast to the expected equilibrium enrichment with respect to chalcopyrite. The conventional data are inconsistent with ore formation by epigenetic replacement and vein mineralization or by syngenetic precipitation in the stockwork zone of a VMS deposit. Physical separation of the cp-po pairs is difficult because the samples are fine grained; thus, the results obtained conventionally are suspect.

Laser-microprobe analyses of the same samples (fig. 3) reveal that the stockwork sulfide pairs *are* in isotopic equilibrium if $\Delta_{cp-po} = 1.4$ per mil at the 300 °C temperature indicated by fluid-inclusion homogenization data. However, the massive sulfide sample analyzed by laser microprobe shows an average $\Delta_{cp-po} = 2.1$ per mil; this value suggests either lower temperature precipitation or rapid quenching. These data are inconsistent with epige-

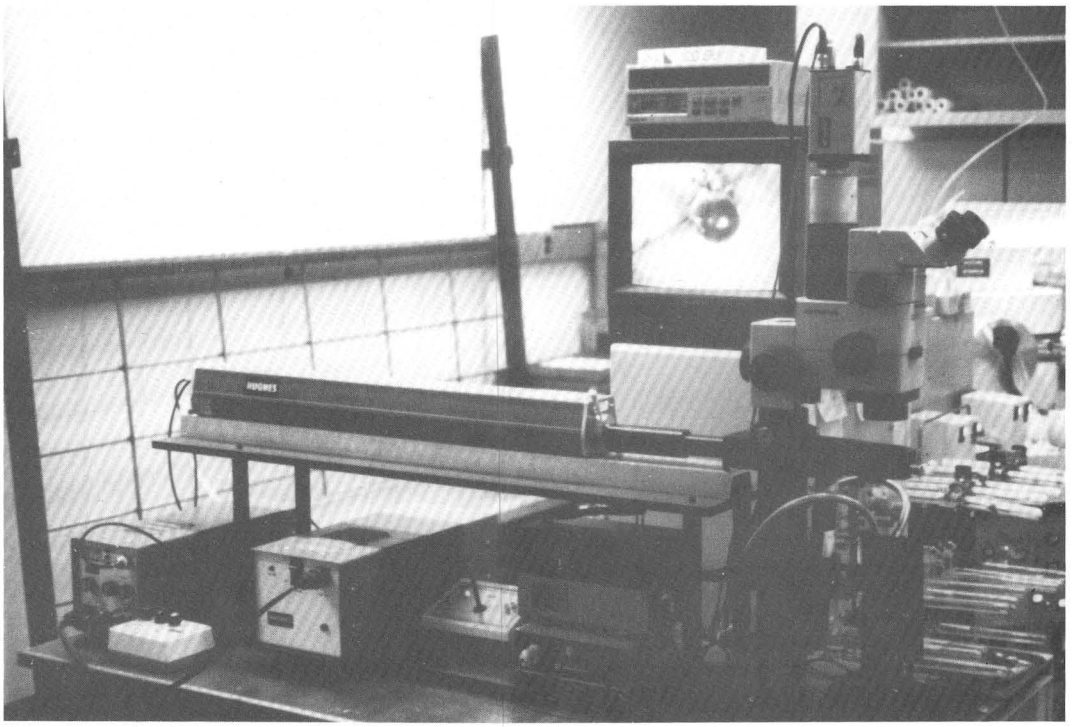

Figure 2 (Crowe and others). CO_2 laser microprobe connected to an isotope-ratio mass spectrometer at the U.S. Geological Survey in Reston, Va. The equipment is used to determine sulfur-isotope ratios for individual minerals in fine-grained slabbed rocks. Photograph by W.C. Shanks III in 1990.

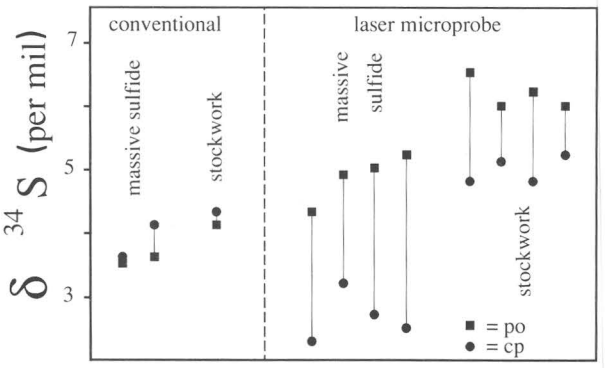

Figure 3 (Crowe and others). Conventional and laser-microprobe data for sulfur isotopes from the Rua Cove mine. The fine-grained, intergrown nature of the chalcopyrite-pyrrhotite (cp-po) pairs made conventional mineral separation difficult; this difficulty is reflected in the nearly identical $\delta^{34}S$ values for these sulfides. The laser-microprobe data indicate equilibrium $\delta^{34}S$ values for the stockwork pairs and lower temperature or disequilibrium $\delta^{34}S$ values for the massive sulfide pairs.

netic vein or replacement formation under equilibrium conditions at similar temperatures, where spatial variations in temperature required to produce Δ_{co-po} variations of this magnitude are uncommon. The laser-microprobe data are consistent with the predicted isotopic values for sulfide mineral pairs from the physicochemically distinct stockwork and massive sulfide environments.

REFERENCES CITED

Crowe, D.E., Nelson, S.W., Brown, P.E., and Shanks, W.C., III, 1988, Stable isotope and fluid inclusion investigation of massive sulfide deposits, Orca and Valdez Groups, Alaska—Evidence for syngenetic sulfide deposition [abs.]: Geological Society of America Abstracts with Programs, v. 20, no. 7, p. 153.

Crowe, D.E., Valley, J.W., and Baker, K.B., 1990, Micro-analysis of sulfur-isotope ratios and zonation by laser microprobe: Geochimica et Cosmochimica Acta, v. 54, p. 2075–2092.

Koski, R., Silberman, M.L., Nelson, S.W., and Dumoulin, J.A., 1985, Rua Cove—Anatomy of volcanogenic Fe-Cu sulfide deposit in ophiolite on Knight Island, Alaska [abs.]: American Association of Petroleum Geologists Bulletin, v. 69, p. 667.

Wiltse, M.A., 1973, Fe-Cu massive sulfide deposits in ancient outer-arc ridge-trench slope environments [abs.]: Geological Society of America Abstracts with Programs, v. 5, no. 1, p. 122–123.

Exploration Guides for Precious-Metal Deposits in Volcanic Domes

By Charles G. Cunningham *and* George E. Ericksen

Volcanic domes are common in intermediate to silicic volcanic fields and are exploration targets for epithermal precious-metal deposits. Domes occur throughout volcanic fields, but they are most common along structural margins and radial faults associated with calderas, within and on the flanks of stratovolcanoes (fig. 1), and along regional faults, especially where an inflection occurs along the fault. Domes generally form late in the magmatic evolution of an eruptive center and typically are cupolas above larger magma bodies at depth that were sources of much of the metals and fluids in addition to the magma.

The Neogene to Quaternary volcanic complex in the Andean Highlands of Peru, Bolivia, and Chile contains many excellent examples of mineralized volcanic domes. These domes have well-preserved features, commonly exposed during mining, that record the evolution of the domes and provide insight into the controls on the distribution of associated hydrothermal ore deposits. Some of these controls are described below and are illustrated in figure 2.

Forceful emplacement of silicic magma may cause development of outward-flaring cone fractures above a magma chamber that serve as natural conduits for hydrothermal fluids. As magma rises toward the surface, interaction with ground water may result in phreatomagmatic explosions that open a conical vent and deposit a surrounding apron of crudely bedded breccia fragments. This explosion breccia generally consists of fragments of the country rock and the carapace of the intrusive body in a tuffaceous matrix. This heterogeneous mixture can be highly porous and, consequently, is a favorable site for mineralization. The breccia commonly is overlain by bedded air-fall tuff resulting from subsequent explosive activity in the vent. Where it is well preserved, the tuff ring is draped over the mound of breccia and dips outward at the periphery as well as inward into the vent.

Viscous, flow-banded magma may then be extruded and expand over, and shoulder aside, the breccia and tuff; these magma movements cause the formation of both radial and concentric faults and fractures. Obsidian rings may

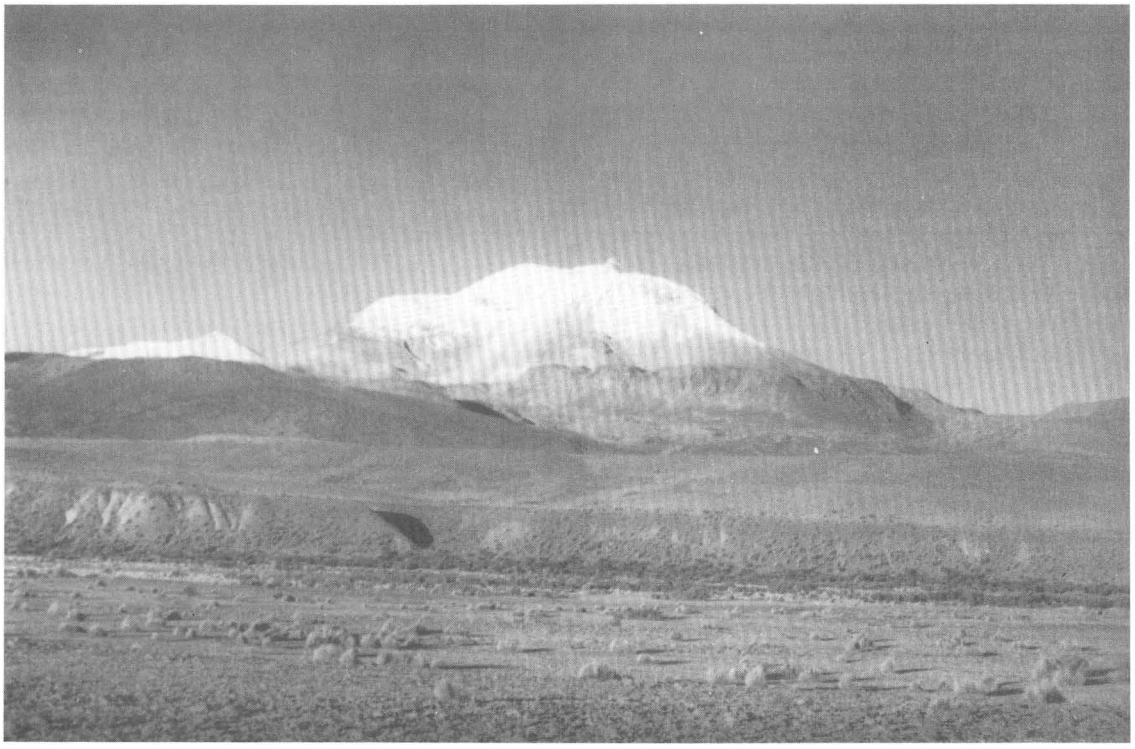

Figure 1 (Cunningham and Ericksen). Volcan Guallatiri, an ice-covered andesitic stratovolcano in northernmost Chile, near the Bolivian border, showing fumarolic activity (tiny white plume at highest point) and active deposition of native sulfur. The distribution of ore deposits in this region indicates that a newly formed or presently forming gold-silver deposit may exist deep within or beneath this volcano. Hydrothermal alteration zones in deeply eroded volcanoes of this type are prime exploration targets for new gold-silver deposits in this part of the Andes. Photograph by George E. Ericksen in 1979.

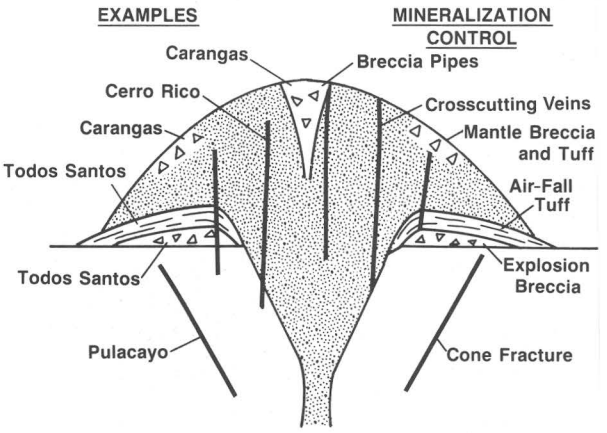

Figure 2 (Cunningham and Ericksen). Exploration guides for precious-metal deposits in volcanic domes, showing examples from Bolivia. Faults, fractures, and breccias are permeable features that are favorable sites for ore deposition.

form at the base of the dome where the magma is quenched as it overrides the cooler tuff ring. Continued extrusion of magma causes the dome to expand and break its solidified carapace to form mantle breccias. Hydrothermal and intrusive breccia pipes may form; they range from those less than a meter in diameter to those that encompass most of the dome. Eroded fragmental material accumulates as porous volcaniclastic sediments and talus along the flanks and base of the dome. Reactivation of faults that initially guided magma emplacement can cause development of fracture systems within the dome in which crosscutting epithermal veins may form.

Origin of Iron, Rare-Earth Elements, Copper, and Gold in Middle Proterozoic Deposits of the Midcontinent Region, U.S.A.

By W.C. Day, G.B. Sidder, A.E. McCafferty, L.E. Cordell, E.B. Kisvarsanyi, R.O. Rye, *and* L.M. Nuelle

Middle Proterozoic anorogenic rocks of the midcontinent region of the United States host several magnetite-hematite deposits rich in rare-earth elements (REE) and locally rich in copper and gold. The anorogenic rocks exposed in Missouri represent the root zone of an eroded volcano-plutonic terrane that developed on rocks of the Early Proterozoic Central Plains orogen. Subvolcanic biotite granite massifs are overlain by comagmatic high-silica rhyolite, which erupted from caldera complexes that locally underwent resurgence. The resurgent cauldrons are cored by plutons of high-silica, two-mica granite that have characteristic magnetic lows; amphibole granite and a magnetite-trachyte suite form ring intrusions along the margins of the calderas. The magnetite-hematite ore deposits are cut by aplite and postvolcanic mafic dikes indicating ore emplacement during the waning stages of igneous activity.

A 20-mgal, northwest-trending steep gravity gradient, as well as several smaller (5–10 mgal) en echelon gradients, transects the anorogenic terrane. Most of the magnetite-hematite ore deposits are spatially associated with the gravity gradients. Although the depth and precise geologic cause of the gravity gradients are unknown, the gradients require fairly abrupt density discontinuities over a vertical zone of more than 4 km and may represent a deep-seated fracture system that provided structural conduits for the magmatic and mineralizing systems.

The Pea Ridge magnetite deposit in Missouri is the best studied ore deposit of this class in the midcontinent region. The volcanic-rock-hosted ore body is steeply dipping, lenticular, and zoned outward from a magnetite-rich core through a footwall hematite zone to a quartz-potassium feldspar zone. The hanging wall is an amphibole-quartz-magnetite skarn. REE-rich breccia pipes composed of barite, potassium feldspar, monazite, xenotime, and local gold cut the footwall margins of the magnetite ore body. Total REE oxide and gold contents of the breccia pipes reach 20 percent and several parts per million, respectively; however, gold distribution is erratic.

New major- and trace-element chemical data indicate that the iron-REE±copper±gold deposits are genetically related to the host anorogenic terrane. The rhyolitic and granitic rocks represent lower crustal melts generated in response to mantle upwelling during the Middle Proterozoic. The magnetite-trachyte suite represents either a high degree of partial melting of the lower crust or crust-contaminated mantle melts. The rhyolitic and granitic magmas ascended into the upper crust and formed volcano-plutonic complexes. One scenario allows that the magnetite-trachyte suite underwent fractionation and liquid immiscibility and generated an Fe-P-REE-rich phase and a Si-Al-K-rich phase. The Fe-P-REE-rich phase was the progenitor of the ore deposits, whereas the Si-Al-K-rich phase was the precursor of the quartz-potassium feldspar alteration zone at Pea Ridge. These fluids may have been channeled along the deep-crustal discontinuities and emplaced into the volcano-plutonic complexes.

Anomalous Concentrations of Fine-Grained Native Gold in Stream Sediments of East-Central Lemhi County, Idaho

By George A. Desborough, William H. Raymond, *and* Karl V. Evans

Preliminary reconnaissance studies of heavy minerals in stream sediments show that anomalous amounts of fine-grained (microscopic) native gold in concentrations >0.05 ppm are present in a large area around Salmon, Idaho (fig. 1). Native gold in anomalous amounts was

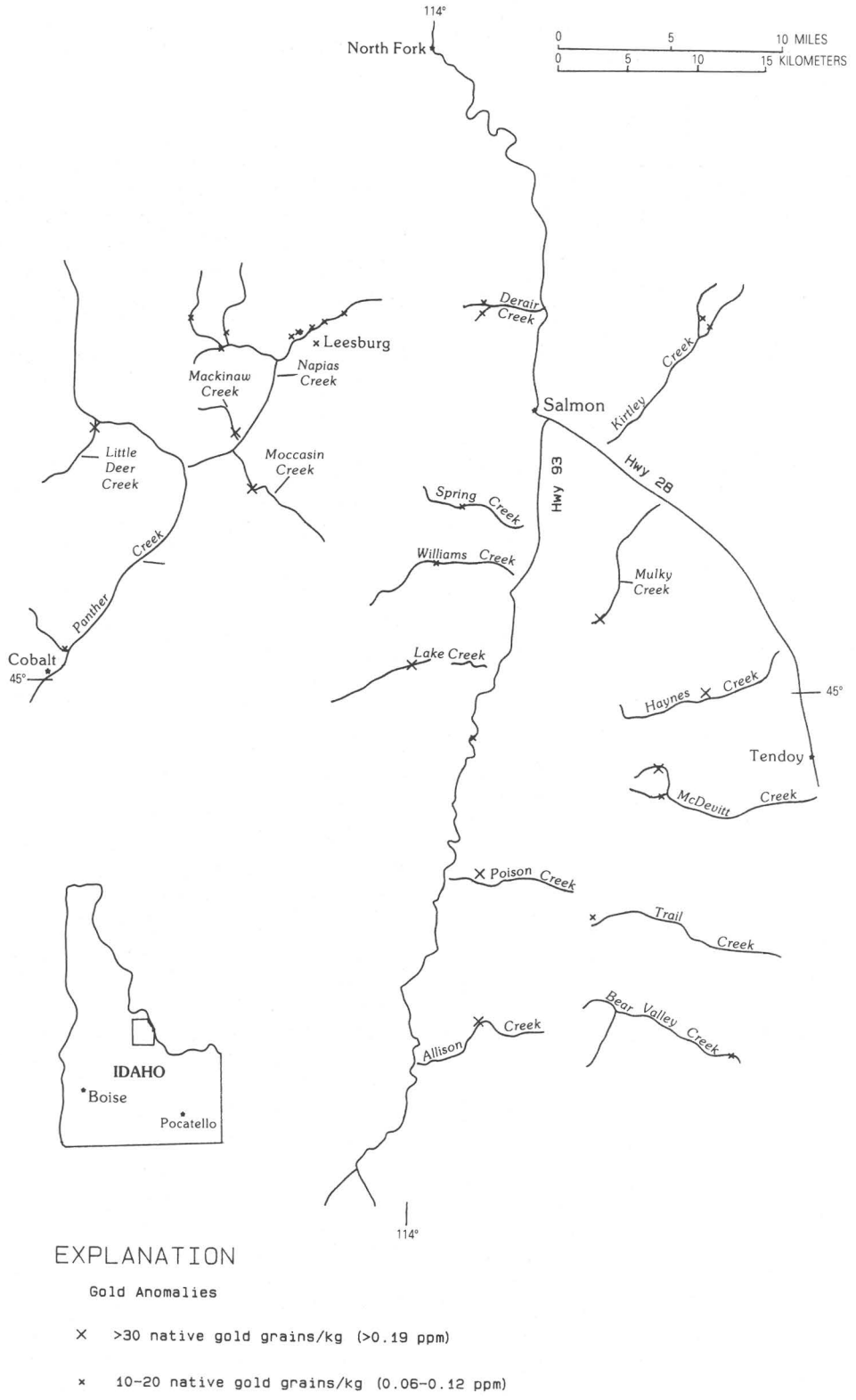

Figure 1 (Desborough and others). Locations of stream-sediment gold anomalies in east-central Lemhi County, Idaho.

recovered from samples of bulk stream sediment by using laboratory panning methods that effectively recover gold grains in the size range of 50–200 μm, as counted and measured by using a microscope. Many of the gold anomalies are in areas that have not been recognized for potential gold resources. Nine localities have what we consider highly anomalous concentrations of native gold (>30 grains/kg or 0.2–0.3 ppm). Ten other localities are considered to have anomalous gold concentrations (10–20 grains/kg or 0.06–0.12 ppm).

More than 100 sites were sampled. Nine samples from streams that drain the Leesburg area of lode-gold mineralization average 13 grains/kg (range of 8–22 grains/kg). Twenty percent of the other sample sites have anomalous amounts of gold (that is, >0.06 ppm); in contrast, 25 percent of the sample sites lack detectable gold.

Results of these studies suggest that fine-grained native gold is widely dispersed by streams because of small grain size, but that other heavy minerals or metals that locally are associated with native gold in lode deposits elsewhere are absent from the Salmon area.

Figure 1 (Detra and others). The Rabbit Creek open-pit gold mine of Santa Fe Pacific Mining, Inc., in Kelly Creek valley, Humboldt County, Nev. The pit exposes 120 m of Tertiary basin-fill sediments; each bench is 12 m high. View to the southwest; Osgood Mountains in background. Photograph by Steven M. Smith, August 25, 1990.

Element Dispersion in Alluvium Covering Gold Deposits in the Kelly Creek Valley, Getchell Gold Trend, Humboldt County, Nevada

By D.E. Detra, S.M. Smith, P.K. Theobald, *and* P.M. Theodorakos

The Chimney Creek and Rabbit Creek sedimentary-rock-hosted gold deposits are covered by 15–185 m of basin-fill alluvium in the Kelly Creek valley in Humboldt County, north-central Nevada (fig. 1). These are two of the deposits that define the Getchell gold trend. The exploration and development of these two deposits provide a unique opportunity to define three-dimensional element-dispersion patterns in the alluvium away from the ore bodies and to study the geochemical and physical processes that produced these patterns.

In this multidisciplinary study, reverse-circulation rotary drill cuttings of alluvium were obtained from 25 vertical exploration and development holes drilled by Gold Fields Mining Corporation and Santa Fe Pacific Mining, Inc. Cuttings generally were sampled at 6-m intervals within the alluvial sequence, were sieved to obtain the fraction from −20 to +100 mesh, and then were ground to −100 mesh for analysis. Total and oxalic-acid partial-leach analyses for 35 elements were performed by direct-current-arc atomic-emission spectrography. Results of these analyses show a distinct vertical distribution of elements or element suites within the alluvium in a 21-km^2 study area around and over the Rabbit Creek and Chimney Creek deposits. Anomalous element concentrations were detected by both total and partial analyses; however, these anomalous values were significantly enhanced in results from the partial analyses. This enhancement suggests that the metals may be concentrated in clast coatings.

Vertical variations in the concentration of major and minor elements are related to lithologic changes within the alluvial sequence and (or) to later diagenetic changes and (or) water-rock reactions within the alluvium. For the most part, gold and base metals occur in low concentrations and lack a systematic distribution with depth. Of the trace elements determined, As, Ge, Sb, and W show the greatest contrast in concentration relative to position within the alluvial sequence. Anomalous concentrations of As, Ge, Sb, and W in the alluvium delineate a cohesive, laterally continuous blanket near the base of the alluvium. A three-dimensional model of the data for this suite shows that the blanket has a fairly flat upper surface and a lower surface that conforms to the irregular surface topography of the basement. The blanket is apparently offset by normal faults within the alluvium and lacks a spatial relationship to the present-day water table. These observations suggest that the As, Ge, Sb, and W suite may be a fossil geochemical anomaly that is largely unrelated to currently active element-dispersion processes in the basin. Three possible mechanisms could have created the blanket: (1) deposition early in the basin's history of mineralized or metal-enriched clastic detritus derived from the Osgood Mountains to the west; (2) percolation of fluids from a low-temperature hydrothermal system through the alluvium early in the basin's history; or (3) migration downgradient along the bedrock-alluvium interface of a plume of ground water slightly enriched in trace elements.

Anomalous trace-element concentration patterns in the deeper parts of the alluvial sequence do not appear to be reflected in surface soil and plant geochemical anomalies and do not coincide vertically with any ore body at depth. In addition, there is no evidence that surface geochemical anomalies in the Kelly Creek valley are a direct reflection of individual ore bodies beneath the alluvium.

Advances in Plumbic Prospecting

By Bruce R. Doe

Since publication of the original paper on plumbic prospecting and the application of lead isotopes to evaluating mineral prospects in Cretaceous and Tertiary magmatothermal ore deposits in the Western United States (Doe, 1979), effort has concentrated on these types of deposits in the Northwestern United States. Emphasis is herein placed on the Butte and Dillon 1° × 2° quadrangles in western Montana (Doe and others, 1986) and the current study of the Challis and Hailey 1° × 2° quadrangles in central Idaho (Doe and Delevaux, 1985). These studies include an initial evaluation of the benefits of adding sulfur-isotope data in prospect evaluation. The original lead-isotope paper (Doe, 1979) was based largely on data for ore deposits where the oldest basement is 1,800–1,200 Ma. Previously, the only known Cretaceous and Tertiary supergiant deposit (that is, one having production worth more than $1.5 billion) in the Northwestern United States was the Butte, Mont., copper deposit, which may be partly underlain by Archean basement. Since 1979, the Thompson Creek porphyry-molybdenum deposit has opened in central Idaho; it also may be underlain by basement like that of the Basin and Range province.

The largest magmatothermal ore bodies (such as the Butte and Thompson Creek deposits) generally have lead-isotope ratios like those of igneous rocks and nonradiogenic $^{206}Pb/^{204}Pb$ ratios that are less than 18.1; this isotopic range undoubtedly characterizes many small prospects as well. Giant deposits (such as those at Tintic and Park City, Utah) that have produced ore worth $150 million to $ 1.5 billion may be somewhat more radiogenic ($^{206}Pb/^{204}Pb$ ratios are less than 18.6). Moderate-sized deposits (for example, Ag-Au deposits at Creede, Colo.) may show values of $^{206}Pb/^{204}Pb$ ratios up to 19.1. The largest deposits having $^{206}Pb/^{204}Pb$ ratios greater than 19.1 are in the Wood River district, Idaho, and at the Nancy Hanks mine, Montana; these deposits have total production worth more than $15 million but much less than $150 million. Although such radiogenic lead-isotope values are not encouraging for discovery of major magmatothermal ores, consideration might be given to Mississippi Valley-type deposits (such as those at the Pacific Mountain mine, Idaho).

At Liver Peak, Idaho, lead isotopes were used by Kleinkopf and others (1972) to define the cupola of a buried Tertiary stock. More examples are now known where lead-isotope signatures of igneous rocks are found in galena-bearing deposits within sedimentary rocks and suggest a cupola at depth (for example, the Iron Mask mine, Bannock area, Montana). The galenas also may contain $\delta^{34}S$ values typical of igneous rocks (−3 to +3 per mil). In some deposits (for example, the Cannivan Gulch porphyry-molybdenum prospect, Montana), a halo of more radiogenic lead-isotope ratios is suggested away from the cupola, and sulfides may show enrichment in $\delta^{34}S$.

Use of sulfur-isotope analyses can improve a plumbic prospecting evaluation by providing another indication of the magmatothermal origin for a deposit. Care must be taken, however, for $\delta^{34}S$ values can be negative in deposits formed under oxidizing conditions (for example, gold ores of the Alder district, Montana). A radiogenic lead-isotope composition with a very negative $\delta^{34}S$ value, however, would not be encouraging evidence for an economic deposit. Normally nonradiogenic lead with a heavy $\delta^{34}S$ value would not be encouraging, but, in central Idaho, $\delta^{34}S$ values can be unusually heavy (for example, Thompson Creek samples have $\delta^{34}S = +8$ to $+12$); thus, the largest deposits there may result from more assimilation of country rock than is typical of igneous terranes. Studies during the last decade reinforce the value of plumbic prospecting in the Western United States, but it should be extended to new areas with care.

REFERENCES CITED

Doe, B.R., 1979, The application of lead isotopes to mineral prospect evaluation of Cretaceous-Tertiary magmatothermal ore deposits in the Western United States, *in* Watterson, J.R., and Theobald, P.K., eds., Geochemical exploration 1978, Proceedings of the Seventh International Geochemical Exploration Symposium, Golden, Colorado: Association of Exploration Geochemists, p. 227–232.

Doe, B.R., Berger, B.R., and Elliott, J.E., 1986, Lead-isotope evaluation of selected ores and mineral prospects in the Butte and Dillon 1° × 2° quadrangles, Montana: U.S. Geological Survey Open-File Report 86–111, 40 p.

Doe, B.R., and Delevaux, M.H., 1985, Lead isotope characteristics of ore systems in central Idaho [abs.], Chapter O *of* McIntyre, D.H., ed., Symposium on the Geology and Mineral Deposits of the Challis 1° × 2° Quadrangle, Idaho: U.S. Geological Survey Bulletin 1658, p. 181.

Kleinkopf, M.D., Harrison, J.E., and Zartman, R.E., 1972, Aeromagnetic and geologic map of part of northwestern Montana and northern Idaho: U.S. Geological Survey Geophysical Investigations Map GP–830, scale 1:250,000.

Farah Garan, Saudi Arabia—Bimodal-Volcanogenic Zn-Cu-Au Mineralization in a Late Proterozoic Rift Basin, Southeastern Arabian Shield

By Jeff L. Doebrich, Arthur A. Bookstrom, *and* Richard B. Carten

The Farah Garan ancient mine site is in the Late Proterozoic Malahah rift basin in the southeastern Arabian Shield. Several small (<0.25 Mt) volcanogenic Zn-Cu-Au deposits at the site formed during the emplacement of a rhyolite dome into comagmatic sea-floor basalt. These deposits are among numerous volcanogenic Zn-Cu sulfide deposits (five containing more than 1 Mt of ore) that formed during the evolution of the Malahah rift basin. Metavolcanic rocks of the Malahah basin are mildly alkalic. Geochemistry of sulfide ores from the basin indicates high concentrations of components (for example, Te, Se, Mo, and CO_2) that are typically associated with alkalic magmatism. Field and geochemical evidence suggests that the Malahah basin evolved either as a rift marginal to a subduction-related volcanic arc or as a mid-ocean rift near plume-related oceanic islands.

At Farah Garan, a north-trending, west-facing sequence of intercalated metabasalt and metarhyolite is conformably overlain by graphitic, calcareous, and micaceous metasedimentary rocks. Mineralization is confined to three stratabound lenticular exhalative units (east, south, and west units) that are individually as much as 40 m thick and 300 m long. The east and south units were deposited immediately above a rhyolite dome and occur at the base of the metasedimentary section. The west unit was deposited farther above the dome after almost 200 m of sediment had accumulated. The exhalative units were deposited as dolomite mounds and are composed of intercalated layers of dolomite, talc, chlorite, chert, and massive and disseminated sulfides, sulfosalts, and tellurides. Though not present at the Farah Garan deposits, a dolomite-talc-breccia feeder zone is present below a dolomite mound at the Farah Garan East prospect (1 km to the east) and indicates that the mounds formed proximal to hydrothermal vents. Observations at Farah Garan and Farah Garan East indicate that a broad zone of footwall quartz-sericite-pyrite (QSP) alteration was overprinted by talc-chlorite alteration immediately below the stratabound exhalative units and along the margins of the feeder zones. Following exhalite deposition, accumulating sediments were altered to form a narrow QSP alteration zone in the hanging wall. These proximal alteration zones are enveloped by a carbonate-sericite alteration assemblage that extends 4 km north and south of the Farah Garan area.

Anomalous surface concentrations of Au, Ag, Zn, As, Sb, and Te in rock and electromagnetic geophysical anomalies aided in siting seven cored drill holes totaling 1,203 m. Significant mineralization was encountered only in the south exhalative unit. On the basis of two drill holes, the deposit is estimated to contain approximately 225,000 t averaging 2.5 percent Zn, 0.9 percent Cu, 2.8 ppm Au, and 33 ppm Ag.

Mineralization in the south unit exhibits distinct metal zonation. The Zn/Cu ratio increases gradually upsection. Au and Ag concentrations increase dramatically at the top of the mineralized section. Ore-mineral paragenesis occurred in three stages. Precipitation of base-metal sulfides was followed by the precipitation of As-Sb sulfosalts, which, in turn, was followed by the precipitation of tellurides. Metal zoning and mineral parageneses indicate that Cu sulfides (chalcopyrite and covellite) were precipitated proximal to hydrothermal vents during an early high-temperature phase of fumarolic activity; Zn and Pb sulfides (sphalerite and galena), followed by sulfosalts (tetrahedrite, tennantite, arsenopyrite, jamesonite, and boulangerite) and tellurides (altaite, hessite, and tellurobismuth), were deposited distally as hydrothermal fluids cooled.

Triassic-Jurassic Magmatic Arc of Western Nevada and Eastern California—Part III: Mineral Deposits

By J.L. Doebrich, L.J. Garside, D.R. Shawe, J.H. McCarthy, Jr., R.L. Turner, R.F. Hardyman, J.A. Erdman, H.F. Bonham, *and* J.V. Tingley

Mineral deposit studies in the Middle Triassic to Jurassic magmatic arc of western Nevada and eastern California were conducted (1) to characterize mineral systems hosted by the arc complex, (2) to evaluate the arc complex for volcanogenic massive sulfide (VMS) potential, and (3) to evaluate Neogene basins for concealed arc-hosted mineral systems.

Jurassic arc-related mineral deposits within the complex include porphyry-Cu, Cu-skarn, Fe-skarn, polymetallic replacement, epithermal Au-vein, polymetallic vein, and Al-silicate deposits. Most of these Jurassic deposits are related to the Yerington supersystem, which comprises at least three individual mineral systems (Yerington-Pumpkin Hollow(?), Ann Mason-Buckskin, and MacArthur-Bear-Lagomarsino-Airport), each of which produced porphyry-Cu deposits and related skarn, replacement, and vein deposits. Cretaceous and Tertiary deposits hosted by the arc complex include W skarns (Gardnerville district), W veins, a low-F porphyry-Mo deposit (Pine Nut deposit, Gardnerville district), Au-Cu quartz-tourmaline veins (Meadow Lake district), Au-Ag adularia-sericite and quartz-alunite veins (Ramsey and Peavine districts), Au-bearing polymetallic veins (Lucky Boy and Pamlico districts), barite veins, volcanogenic U deposits, and base-metal skarns.

The apparent absence of VMS deposits from the Triassic and Jurassic arc rocks is a consequence of the

subaerial to shallow-marine depositional environment that existed in the study area. Volcanic rocks deposited in subaerial and shallow subaqueous environments dominate the volcanic sections. Such shallow, near-shore, high-energy environments are not conducive to the formation and preservation of VMS deposits. Although thick sedimentary sections within the arc complex (Gardnerville Formation of Noble (1962) and Sailor Canyon Formation) provide evidence for local deep restricted basins, there is no evidence that they were sites of significant coeval magmatism, which would have been needed to generate sea-floor fumarolic activity.

Rock and stream-sediment geochemistry (from new data, data obtained by National Uranium Resource Evaluation studies, and data in the U.S. Geological Survey's Rock Analysis Storage System) was used to characterize deposit types and mineral systems as well as to identify new anomalous areas within exposed blocks. Reconnaissance of three Neogene basins (Smith Valley, Mason Valley, and Antelope Valley) for concealed mineral systems was conducted by using biogeochemical analysis of basin flora, soil geochemical sampling, a soil-gas geochemical survey, and a geobotanical survey of indicator plants. Anomalous areas in the basins were delineated for further assessment.

REFERENCE CITED

Noble, D.C., 1962, Mesozoic geology of the southern Pine Nut Range, Douglas County, Nevada: Stanford, Calif., Stanford University, Ph.D. thesis, 200 p.

Use of Landsat Thematic Mapper Images for Studying Volcanic-Rock-Hosted Precious-Metal Deposits in the Central Andean Region

By B.A. Eiswerth, T.L. Bowers, Lucia Cuitino, Felipe Diaz, Hugo Gumucio, Aldo Gutarra, Nestor Jimenez, J.L. Lizeca, Ramon Moscoso, Fernando Murillo, Luis Quispesivana, Jaime Rodriguez, L.C. Rowan, Rubén Tejada, *and* César Vilca

Landsat Thematic Mapper (TM) images are being analyzed to augment conventional methods of exploration for volcanic-rock-hosted epithermal precious-metal deposits in the Neogene-Quaternary volcanic complexes of the central Andean region. TM data were digitally processed for the regions of Berenguela, Bolivia; Maricunga, Chile; and Orcopampa, Peru; processing enabled us to distinguish lithologic units, especially hydrothermally altered rocks, and to delineate major volcanic and tectonic features.

Spectra of hydrothermally altered rocks typically exhibit more intense absorption features than do those of unaltered volcanic rocks (fig. 1). In the short-wavelength region, Fe^{3+} absorption may result from the oxidation of pyrite and ferromagnesian minerals. In the region from 2.0 to 2.5 μm, intense OH-absorption features are due to clays and other OH-bearing minerals produced by hydrothermal alteration of feldspars and ferromagnesian minerals. Spectra of carbonate minerals also may exhibit an absorption feature in this wavelength region.

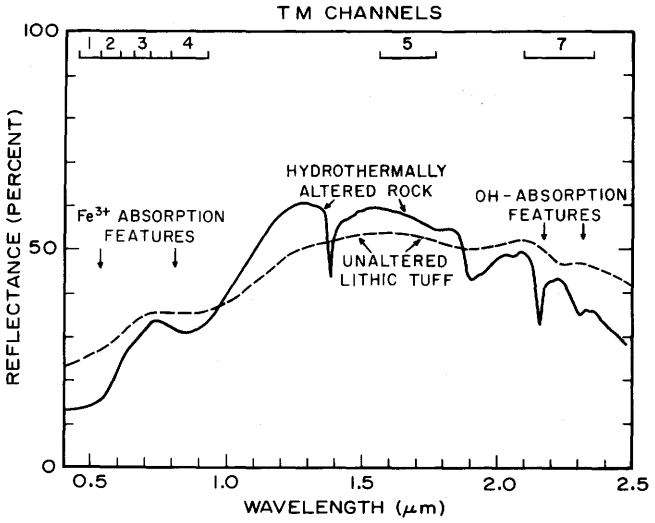

Figure 1 (Eiswerth and others). Reflectance spectra of hydrothermally altered rock and unaltered lithic tuff showing spectral contrast in Landsat Thematic Mapper (TM) channels (shown at the top).

The TM system records reflected solar radiation in six channels in the region from 0.4 to 2.4 μm and has a spatial resolution of 30 m. For each of the above-mentioned study areas, a single-channel black-and-white image and a color-composite image of three selected channels were used to distinguish volcanic and tectonic features. Color composites of selected ratio images were used to distinguish lithologies. The TM 5/7 ratio was included in the color-ratio composite images to display the spectral contrast between OH-bearing hydrothermally altered rocks and unaltered volcanic rocks in the region from 1.5 to 2.5 μm (fig. 1). The TM 3/1, TM 5/1, and (or) TM 5/4 ratios were used to display variations in Fe^{3+} absorption intensity. High values of these ratios are suggestive of alteration, but field evaluation is needed to resolve possible ambiguities, such as the presence of carbonate rocks. Where vegetation is an important component, TM 4/3 ratos were included to distinguish vegetation from hydrothermally altered rocks.

The false-color composite and black-and-white images outline numerous eruptive centers, which exhibit varying degrees of erosion. The color-ratio composite images delineate many zones of probable hydrothermal alteration in all three study areas. The most intense and widespread alteration is related to eroded stratovolcanoes and calderas. Variations in the color-ratio composite images suggest mineralogical differences that may reflect the type and intensity of alteration. Although a few of these altered areas have been explored by using modern techniques, most have not been studied in detail.

Can Trace and Rare-Earth Elements in Fluorite be Useful in Geochemical Exploration? Encouraging Evidence from the Sierra Cuchillo Area, New Mexico

By R.G. Eppinger, L.G. Closs, A.L. Meier, *and* J.M. Motooka

Fluorite was collected in the Sierra Cuchillo region of south-central New Mexico from four fluorite-bearing deposit types: Au-Ag veins, Ba-Pb veins, W-Be-Fe skarn, and barren quartz-calcite-fluorite veins apparently devoid of ore metals. The fluorite was analyzed for trace elements by inductively coupled plasma (ICP) atomic-emission spectrometry and for rare-earth elements (REE's) by ICP mass spectrometry.

Trace-element and REE patterns in fluorite samples are distinctive for the different deposit types. Fluorite from Au-Ag veins has positive Eu anomalies, a high Sr content, and low Be, Ba, Ti, U, and Y contents. Fluorite from Ba-Pb veins has negative Eu anomalies, high Ba and Pb contents, and low Sr and U contents. Fluorite from W-Be-Fe skarn has negative Eu anomalies, high Be, Ti, U, and Y contents, and low Sr and Ba contents. Fluorite from barren veins contains variable amounts of the above trace elements and exhibits variable Eu anomalies. The wide chemical variation in the fluorite studied may be due in part to changes in fluid chemistry resulting from reactions with feldspar in wall rock.

Fluorite from barren veins is more abundant than fluorite from other deposits and generally shows the most chemical variation. One group of fluorite samples from barren veins has chemical characteristics similar to those of fluorite from W-Be-Fe skarn. A second group of fluorite samples from barren veins exhibits chemical affinities with fluorite from Au-Ag veins. These similar geochemical signatures in the fluorite, coupled with favorable geologic settings, suggest the possibility of concealed skarn deposits underlying one barren vein group and the possibility of precious-metal deposits underlying the other barren vein group. Thus, the geochemistry of fluorite delineates potential concealed mineral deposits in the Sierra Cuchillo area and may be a useful tool for mineral exploration elsewhere.

Biogeochemical and Geochemical Expression of Poorly Exposed Epithermal Mineralization in the Southeastern Challis Volcanic Field, Idaho

By J.A. Erdman, Falma Moye, *and* P.K. Theobald

Biogeochemical and other geochemical exploration techniques were used in the Lava Creek mining district, north of Craters of the Moon National Monument, and in the Baker Creek area near Ketchum, Idaho, to assess the potential for new metallic mineral deposits. Stream sediments, soils, heavy-mineral concentrates, and several species of plants, principally big sagebrush (*Artemisia tridentata*), were collected in reconnaissance drainage-basin surveys (Adrian and others, in press; Erdman and others, 1990). Biogeochemical methods can be especially effective where surface expression of mineralization is poor.

The Lava Creek area was selected for study because of its historical importance as a producer of silver and byproduct gold. Most of this area is underlain by Eocene Challis Volcanics that have been so hydrothermally altered that good outcrop is extremely limited. At Lava Creek, initial results (Erdman and others, 1988) showed geochemical anomalies in sagebrush which suggested that a possible host for epithermal precious metals was the Lower Mississippian McGowan Creek Formation (chiefly turbidites), peripheral to the formerly active mines. Followup sampling of sagebrush, stream sediments, and soil defined the source of a Hg-Ag-Au-As-Sb anomaly in a fault breccia near a poorly exposed dacite porphyry intrusion.

Hydrothermal alteration east of Baker Creek chiefly affected dacitic lava; a central zone of intense argillic alteration is surrounded by a broader zone of propylitic alteration. The Baker Creek area lacked evidence of mineral prospecting when the survey was made, but it has geological characteristics indicating that an epithermal precious-metal system may be present.

In the Baker Creek area, heavy-mineral concentrates all contain abundant barite, even beyond the zone of propylitic alteration. Botryoidal pyrite was also found, but it is restricted to the alteration zones. Visible gold and pyromorphite, a lead phosphate, were found in heavy-mineral concentrates from a small drainage near a stockwork-veined outcrop in the central zone of argillic alteration. A grab sample of the outcrop contains 50 ppb Au, 1.5 ppm Ag, and 50 ppm Mo. The maximum concentration of Au in nearby stream sediments and upland soils is only 2 ppb, but aquatic mosses from within the argillically altered zone contain as much as 64 ppb Au in the ash. This intensely altered zone is characterized by anomalous levels of Ag, Mo, Pb, Cd, and Zn and, to a lesser extent, Au, Bi, Mn, As, Sb, and Tl in the various media sampled. The geochemical signature suggests a Ag- and Mo-rich, low-temperature, epithermal type of mineralization.

REFERENCES CITED

Adrian, B.M., Erdman, J.A., Bullock, J.H., and Hageman, P.L., in press, Analytical results and sample locality map of heavy-mineral-concentrate, stream-sediment, soil, and big sagebrush samples from the Lava Creek mining district, within the Idaho Falls 1° × 2° quadrangle, Butte County, Idaho: U.S. Geological Survey Open-File Report 90–545.

Erdman, J.A., Moye, Falma, Bailey, Betty, O'Leary, R.M., and Roemer, T.A., 1990, Analytical results and sample locality maps of soil, plant (Douglas-fir, sagebrush, sedge, aquatic moss), stream-

sediment, and heavy-mineral-concentrate samples from the Baker Creek study area, Blaine County, Idaho: U.S. Geological Survey Open-File Report 90–57, 16 p.

Erdman, J.A., Skipp, Betty, Theobald, P.K., and Moye, Falma, 1988, Drainage-basin geochemical survey of Lava Creek district in central Idaho using sagebrush and heavy-mineral concentrates—Preliminary evidence for sediment-hosted gold in McGowan Creek Formation [abs.]: Geological Society of America Abstracts with Programs, v. 20, no. 6, p. 414.

Volcanic-Hosted Epithermal Precious-Metal Deposits in the Central Andes—Geology, Resources, and Exploration Strategy

By George E. Ericksen, Charles G. Cunningham, *and* Barbara A. Eiswerth

The Neogene-Quaternary volcanic complex of the central Andes (fig. 1) contains hundreds of hydrothermally altered areas, many of which are associated with world-class silver-gold deposits; others are prime exploration targets. This complex, which constitutes a widespread volcanic cover in southern Peru, northern Chile, western Bolivia, and northwestern Argentina, is characterized by hundreds of andesitic to dacitic stratovolcanoes, at least 30 calderas related to widespread rhyolitic ash-flow tuffs, and many volcanic domes.

Three types of volcanic-hosted, epithermal precious-metal deposits are present: (1) silver-rich, locally gold-rich, polymetallic base-metal veins; (2) silver-rich, gold-poor, polymetallic tin veins and stockworks; and (3) low-grade gold-bearing stockwork or disseminated deposits, with or without silver and base metals. Many veins and districts show mineral zoning; in the central zones, base metals and, in some deposits, gold and tungsten are abundant, and, in the outer zones, silver, arsenic, and antimony are abundant. In the vertical zoning present at some places, base metals are most abundant at depth, and silver is abundant near the surface. Both adularia-sericite and acid-sulfate types of epithermal deposits are present; the former type is by far the more abundant and is characterized by intense sericitic and (or) argillic alteration, with or without adularia, and the latter is characterized by hypogene alunite and enargite.

Grade-tonnage data for both high-grade, multivein deposits and low-grade stockwork deposits show that most of the known epithermal deposits contain between 500 and 6,000 t of silver and less than 50 t of gold. Cerro Rico de Potosi, the world's largest silver deposit, has produced an estimated 30,000 to 60,000 t of silver from ores averaging about 0.5 kg/t Ag (fig. 2). A similar amount of silver is estimated to remain in Cerro Rico stockwork ores and waste dumps having grades ranging from 150 to 250 g/t Ag. A single vein at Pulacayo, Bolivia (about 135 km southwest of Cerro Rico de Potosi), which is 2.7 km long and was mined to a depth of 1,100 m below the surface, yielded about

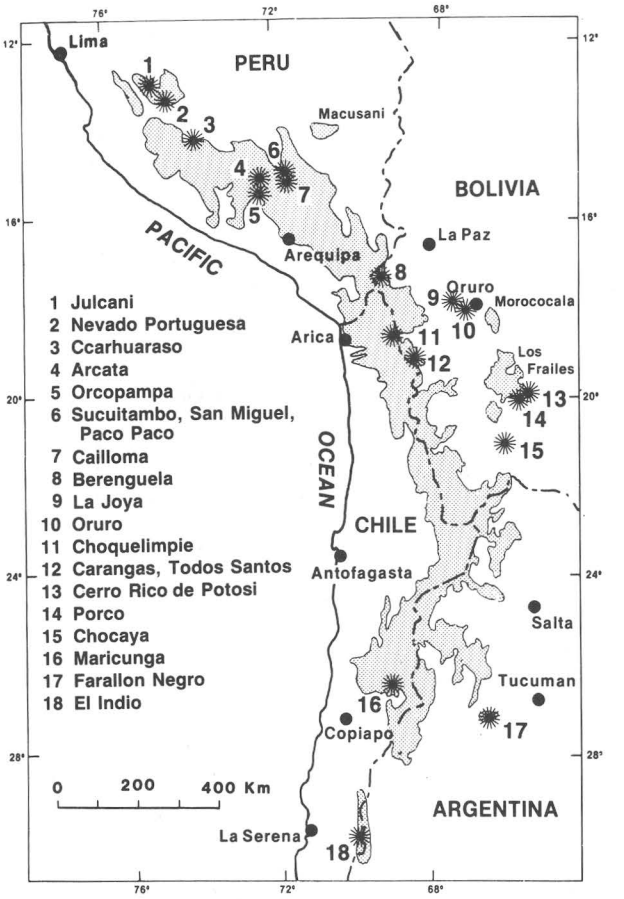

Figure 1 (Ericksen and others). Distribution of principal silver and gold deposits in the Neogene-Quaternary volcanic complex (stippled areas) of the central Andes. Most of the hundreds of andesitic to dacitic stratovolcanoes, at least 30 calderas, and many volcanic domes have associated hydrothermal alteration zones that are prime exploration targets for precious-metal deposits.

5,000 t of silver from ores averaging between 0.5 and 1 kg/t Ag. Gold grades in silver-rich veins generally are less than 1 g/t Au, but ore shoots in some veins may contain 100 or more g/t Au. Total gold production from silver-rich veins or districts is estimated to range from a few metric tons to about 30 t. The richest gold vein now being mined is the 3,500 vein in the El Indio district, Chile, which originally contained an estimated 37 t gold in ore that averaged about 0.25 kg/t Au. Low-grade ore (9 g/t Au) in this district is estimated to contain an additional 67 t of gold. Other low-grade stockwork deposits in Bolivia and Chile that are amenable to heap leaching have ores averaging between 1.2 and 2.1 g/t Au and containing up to 90 g/t Ag. Estimated resources of such deposits range from about 25 to 60 t gold and from little or no silver to a maximum of about 3,000 t Ag.

Digitally enhanced Landsat Thematic Mapper images of selected areas in Peru, Bolivia, and Chile show that most

Figure 2 (Ericksen and others). Cerro Rico de Potosi, Bolivia, a volcanic dome that hosts the famous Potosi tin-silver deposit. Since its discovery in the mid-l6th century, it has yielded an estimated 30,000–60,000 t of fine silver from ore averaging 0.5 kg/t Ag; thus, this hill is the world's largest silver deposit. Similar amounts of silver remain in low-grade ores in Cerro Rico and in waste dumps from earlier mining. Photograph by George E. Ericksen in 1984.

alteration zones considered to be favorable exploration targets are within or near deeply eroded stratovolcanoes and calderas. Analyses of geochemical samples of the alteration zones over ores may or may not detect gold and silver but generally do show anomalous values for arsenic. Copper, lead, and zinc, even though present in the ores, tend to show only background values in the surficial alteration zones. Some alteration zones are visible in aerial photographs (fig. 3). Additional study should provide new data about these zones and identify many as favorable exploration targets.

The Use of Lead-Isotope Geochemistry to Evaluate Economic Potential for Gold-Silver Mineralization—An Example from the North Amethyst Vein System and the Creede Mining District, Colorado

By Nora K. Foley *and* Robert A. Ayuso

Lead-isotope compositions of galenas were determined for ore deposits and volcanic wall rocks from the

Figure 3 (Ericksen and others). Aerial view of the Arcata mining district, one of the major silver producers in the Andean Highlands (4,000–5,000 m altitude) of southern Peru. The concentration plant and townsite are in the foreground, a 10- to 30-m-wide kaolinitic hydrothermal alteration zone (the linear light-colored band in the middle ground) marks the outcrop of one of the major veins in andesitic lavas of Pliocene age, and light-colored ash-flow tuffs and young basaltic (dark) lavas can be seen in the distance. Photograph by George E. Ericksen in 1987.

central San Juan Mountains, Colo., in an effort to evaluate the use of lead-isotope compositions for mineral prospecting (fig. 1). The study area includes the North Amethyst area and the central and southern parts of the Creede mining district. The North Amethyst vein contains two crosscutting mineral associations with contrasting mineral parageneses and metal associations (I, II in fig. 1) that are separated locally by breccias and sedimentary rock. The earlier, fine-grained association (I) has rocks from two stages that contain different mineral assemblages: Ia contains quartz, rhodonite, Mn-carbonates, and minor base-metal sulfides; Ib contains hematite, magnetite, electrum, Au-Ag-sulfides, Ag-sulfosalts, and base-metal sulfides. The second association (II) consists of coarser grained quartz, calcite, sericite, chlorite, hematite, adularia, fluorite, base-metal sulfides, and Ag-tetrahedrite. Veins of the central and southern parts of the Creede district (III, IV) consist primarily of coarse-grained quartz and base-metal sulfides, sericite, hematite, chlorite, adularia, fluorite, and barite and contain minor Ag-sulfides and Ag-sulfosalts.

Our detailed studies show that paragenetically early galenas from the Au-rich North Amethyst mineralization (Ib) have Pb-isotope compositions that are less radiogenic than those of galenas formed later in the North Amethyst area, during Ag and base-metal mineralization (II). Galenas from association Ia have lower $^{207}Pb/^{204}Pb$ ratios but are otherwise similar to galenas from association II. Their paragenesis is uncertain as they formed in a reaction zone involving associations I and II. New lead-isotope data for the central and southern parts of the Creede district agree with the lead-isotope data from a regional study by Doe and others (1979) that included five samples from the Creede district. Galenas and adularia of the central and southern Creede district (III) and galenas from the Bondholder district (V), north of Creede, are isotopically similar to North Amethyst II galenas. Galenas of the Alpha-Corsair vein (IV), which was mined for silver prior to 1910, are isotopically similar to North Amethyst Ib galenas. Unexplored segments of the Alpha-Corsair vein thus may be mineralogically similar to North Amethyst Ib assemblages; therefore, the Alpha-Corsair vein has the potential for high gold contents.

Lead-isotope data for the North Amethyst vein system and the rest of the Creede mining district generally define two distinct groups (fig. 1). Both groups are isotopically more radiogenic than the enclosing volcanic rocks of the central part of the San Juan volcanic field as defined by Lipman and others (1978) and Matty and others (1987). Our lead-isotope results indicate that Au mineralization in the North Amethyst area may represent the product of an older and relatively local hydrothermal system distinct from that of the younger base-metal and Ag mineralization found throughout the region. Fluids that deposited the Au may have derived their lead-isotope composition by a greater degree of interaction with shallow, relatively less radiogenic volcanic wall rocks. The Ag and base-metal-rich mineralization that overprints the Au mineralization in the North Amethyst area clearly has a more radiogenic isotopic signature, which implies that the later mineralization derived a greater component of its lead from Precambrian source rocks or sediments derived from them at depth.

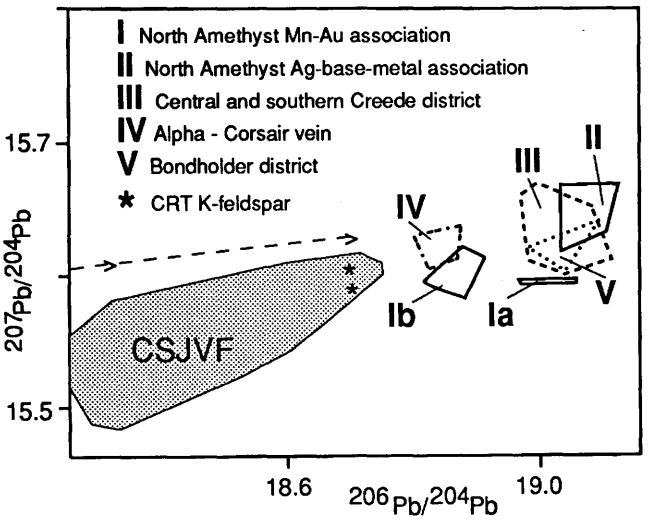

Figure 1 (Foley and Ayuso). Comparison of lead-isotope compositions of ore with those of volcanic rocks of the central part of the San Juan volcanic field (CSJVF); data are from Lipman and others (1978), Doe and others (1979), and Matty and others (1987). Asterisks identify additional analyses (this study) of the Carpenter Ridge Tuff (CRT) that hosts the ore. Dashed line is orogene reference curve of Doe and Zartman (1979).

Paragenetically early vein assemblages thus have the least radiogenic galenas and generally also have the highest gold contents. These characteristics may be related to temperature, as the early association formed from fluids hotter than those that deposited the later association. Identification of paragenetically early vein assemblages with relatively unradiogenic lead-isotope compositions similar to those of the North Amethyst area provides an additional exploration tool for gold in the central San Juan Mountains area.

REFERENCES CITED

Doe, B.R., Steven, T.A., Delevaux, M.H., Stacey, J.S., Lipman, P.W., and Fisher, F.S., 1979, Genesis of ore deposits in the San Juan volcanic field, southwestern Colorado—Lead isotope evidence: Economic Geology, v. 74, p. 1–26.

Doe, B.R., and Zartman, R.E., 1979, Plumbotectonics, the Phanerozoic, *in* Barnes, H.L., ed., Geochemistry of hydrothermal ore deposits (2d ed.): New York, Wiley, p. 22–70.

Lipman, P.W., Doe, B.R., Hedge, C.E., and Steven, T.A., 1978, Petrologic evolution of the San Juan volcanic field, southwestern Colorado—Pb and Sr isotope evidence: Geological Society of America Bulletin, v. 89, p. 59–82.

Matty, D.J., Lipman, P.W., and Stormer, J.C., Jr., 1987, Common-Pb isotopic characteristics of central San Juan ash flow tuffs [abs.]: Geological Society of America Abstracts with Programs, v. 19, no. 5, p. 319–320.

The Bisbee Group of the Tombstone Hills, Southeastern Arizona—Stratigraphy, Structure, Metamorphism, and Mineralization

By Eric R. Force

The Lower Cretaceous Bisbee Group (of Butler and others, 1938) is the host of most silver ores mined in the Tombstone district, southeastern Arizona. The group was locally subdivided by Butler and others (1938) only in the Tombstone basin, which forms the eastern of two main outcrop areas in the northern Tombstone Hills. In this study, I divided and mapped the Bisbee Group in both outcrop areas, which total about 7 km^2 and are about 1.5 km apart. Stratigraphic subdivision has allowed delineation of new structural features and has provided information on their histories. Contact-metamorphic isograds were also mapped; they reflect the shape and emplacement history of intrusions such as the Schieffelin Granodiorite.

The Bisbee Group can be divided into two informal units—an upper formation consisting mostly of argillite and having an upper part dominated by sandstone and a lower formation characterized by conglomerate and limestone. The lower formation includes the Glance Conglomerate and the "novaculite" and "blue limestone" of Butler and others (1938).

The two discrete outcrop areas of the Bisbee Group show reasonably similar stratigraphic sequences in the upper formation, which is more than 250 m thick. The argillite contains a thin cherty limestone bed, minor tuff, and petrified-wood horizons.

The lower formation shows a great transition in grain size, composition, and sequence from west to east. In the westernmost outcrop area, the lower formation is a sedimentary megabreccia of Paleozoic blocks, whereas in the easternmost Tombstone basin, 4.5 km away, it consists of a basal siliceous unit overlain by several limestone beds and intercalated argillite. A provenance difference between the two outcrop areas and a maximum thickness (300 m) along the western margin of the Tombstone basin may have been controlled by syndepositional movement on the intervening Ajax Hill fault, known to be pre-Schieffelin in age. The transition as a whole must have been controlled by a more important syndepositional fault farther west.

Folding of the Bisbee Group is of the dome-and-basin type. In the western outcrop area, folding is open and upright and is accentuated by steep faults. In the Tombstone basin, folding is of the same type, but some north-northwest-striking structures are tight and overturned to the west-southwest. The Lucky Cuss fault and related arcuate faults of the Tombstone basin appear to cut north-northwest-trending tight folds but are deformed by later west-trending open folds.

The Late Cretaceous augitic Schieffelin Granodiorite forms a flat-topped intrusion, probably a sill, underlying the Bisbee Group, which had been folded and extensively faulted by the time of intrusion. This intrusion fingers out toward the east, but a probable extrusive equivalent, the tuffaceous Uncle Sam unit, overlies the Bisbee Group toward the west. The Bisbee sequence shows three zones of contact metamorphism characterized by wollastonite, grossularite, and epidote; the zones have a total thickness of more than 200 m where the Schieffelin was sufficiently thick.

The east-trending Prompter fault has been thought to cut the Bisbee Group in the western outcrop area but previously could not be traced through it. Identification of separate stratigraphic units and metamorphic grades indicates its trace and suggests a two-stage movement history—the first and main movement was pre-Schieffelin and up on the south, and post-Schieffelin movement was down on the south.

Mineralization is mostly contained within the lower formation of the Bisbee Group, against its contact with the upper formation. It consists of veins within faults and replacements along certain beds and (or) anticlinal crests. The mineralization is apparently Laramide but probably is post-Schieffelin in age. Mined ore was at least partly supergene; it produced mainly silver and smaller amounts of gold, manganese, and base metals.

REFERENCE CITED

Butler, B.S., Wilson, E.D., and Rasor, C.A., 1938, Geology and ore deposits of the Tombstone district, Arizona: Arizona Bureau of Mines Bulletin 143, Geology Series 10, 114 p.

Concentration and Zonation of Copper and Palladium in the Mesozoic Belmont Diabase Sheet, Culpeper Basin, Northern Virginia—An Exploration Guide to Enrichment of Precious Metals in Mafic Magmatic Rocks

By A.J. Froelich, Laurel G. Woodruff, Harvey E. Belkin, *and* David Gottfried

Chemical zonation marked by intervals enriched in copper (Cu) and platinum-group elements (PGE) is present in a lensoid body of ferrogabbro, ferrodiorite, and granophyre about 150 m thick in the upper part of the Belmont diabase sheet in the Culpeper basin, Virginia. Five subhorizontal geochemical zones that thicken and thin reciprocally are best defined by variations in Cu abundance (table 1).

Zone 2 has the highest Cu content, but zone 3 shows the greatest enrichment in Pd and, to a lesser extent, Pt and Au. Other metals, such as Co and Ni, show little variation across the zones enriched in Cu (table 1). Various field, petrographic, geochemical, electron microprobe, SEM-EDXRF (scanning electron microscope-energy dispersive X-ray fluorescence spectroscopy), sulfur- and oxygen-isotope, and fluid-inclusion studies were conducted to understand the transport, alteration, and mineralization processes that occurred here.

The Belmont diabase sheet is an irregularly shaped Mesozoic intrusion as much as 600 m thick in Upper Triassic sedimentary rocks (fig. 1). The intrusive rock is composed of layered units resulting from differentiation of a high-TiO_2 (about 1.1 weight percent), quartz-normative ($SiO_2 \cong 51.5$ weight percent; MgO ≅ 7.5 weight percent), tholeiitic magma (HTQ, high-titanium quartz-normative, type). The lower few hundred meters of the sheet (MgO = 9–11 weight percent) is depleted in incompatible elements relative to the chilled margins and contains cumulus MgO-rich orthopyroxene (bronzite). The upper part of the sheet contains segregations of evolved rocks (granophyre and ferrodiorite, in which $SiO_2 \cong 53$ weight percent; MgO ≅ 3.5 weight percent; $TiO_2 \cong 2.5$ weight percent) that are enriched in Cu and have incompatible element abundances several times greater than those of the enclosing chilled margins; this element distribution indicates that these evolved rocks are complementary fractions to the cumulate rocks. As the orthopyroxene-rich cumulate rocks are about 10 km north of the evolved rocks in the upper part of the same sheet (fig. 1), considerable fractionation of the original magma by lateral and vertical migration and flow differentiation is indicated.

As shown in table 1, the ferrogabbro in zone 2 has the highest average Cu content (650 ppm); it overlies ferrogabbro in zone 3 having the greatest Pd enrichment (average 100 ppb, locally 500 ppb) and having an average Cu abundance of 220 ppm. Zone 3 also is locally enriched in FeO_{Total} (to 21.5 weight percent), TiO_2 (to 4.8 weight percent), Cl (to 2,900 ppm), Ba (to 1,550 ppm), S (to 760 ppm), V (to 350 ppm), As (to 19.4 ppm), Se (to 6.4 ppm), Mo (to 5.2 ppm), U (to 2.15 ppm), Ag (to 0.3 ppm), Au (to 137 ppb), Pt (to 41 ppb), and Rh (to 11 ppb). This enrichment suggests late- or post-magmatic concentration of some precious metals.

The degree and mode of alteration vary systematically with the zones defined by Cu and Pd abundances and ratios (table 1). During alteration, primary clinopyroxene was replaced by iron- and halogen-rich amphiboles and chlorite, and plagioclase was converted to fine-grained sheet silicates, such as sericite. Chalcopyrite is the most abundant sulfide in the altered rock, and its texture suggests that it is a very late phase. Chalcopyrite occurs with bornite, galena, sphalerite, chlorine-rich amphibole, quartz, apatite, and ilmenite. Also occurring with this late-stage alteration assemblage are micrometer-sized grains of electrum (Au > Ag) and phases containing Pd+Bi+Sb and Co+Fe+As (fig. 2). Sulfides in zones 2 and 3 show a restricted range in $\delta^{34}S$ of −0.47 to +1.26 per mil. Oxygen-isotope ratios from whole-rock core samples collected from the same zones indicate a narrow range of $\delta^{18}O$ from +7.1 to +7.7 per mil, whereas $\delta^{18}O$ in the pyroxene mineral separates ranges from +6.12 to +6.66 per mil. Both the oxygen- and sulfur-isotope data suggest a magmatic source. Multiphase fluid inclusions (containing NaCl+other chlorides+liquid +vapor) occur in quartz throughout the entire range of studied samples (fig. 3). The common occurrence of coeval vapor-rich and high-salinity multiphase fluid inclusions suggests pervasive boiling conditions, at least during some stages of alteration.

The zones of Cu and PGE enrichment at Belmont are believed to have formed from late magmatic, chlorine- and sulfur-rich aqueous solutions that hydrothermally altered the original ferrogabbro, granophyre, and diorite. Petro-

Table 1 (Froelich and others). Variations in average abundance and ratios of selected metals in the upper part of the Belmont diabase sheet, northern Virginia

[n = number of core samples analyzed from five coreholes 60–150 m deep. Analyses by U.S. Geological Survey analytical laboratories in Reston, Va., and Lakewood, Colo. Pd and Pt determined by graphite-furnace atomic-absorption spectrometry (GFAAS); Co, Ni, and Cu determined by flame atomic-absorption spectrometry and GFAAS]

Lithology	Zone	Approximate distance below upper contact (meters)	Cu (ppm)	Pd (ppb)	Pt (ppb)	Pd/Pt	Cu/Pd	Ni (ppm)	Co (ppm)	Cu/Ni
Ferrodiorite	1 (n=5)	450	420	1.6	1.0	1.6	400,000	8	38	75
Ferrogabbro and minor granophyre	2 (n=35)	500	650	15	5	3	45,000	15	50	43
Ferrogabbro and minor granophyre	3 (n=66)	510–550	220	100	12	8	2,000	15	50	15
Ferrodiorite and granophyre	4 (n=29)	530–570	150	17	4	4	8,000	20	40	7.5
Diorite and diabase	5 (n=3)	560–600	120	6	7	1.0	20,000	65	50	2.0

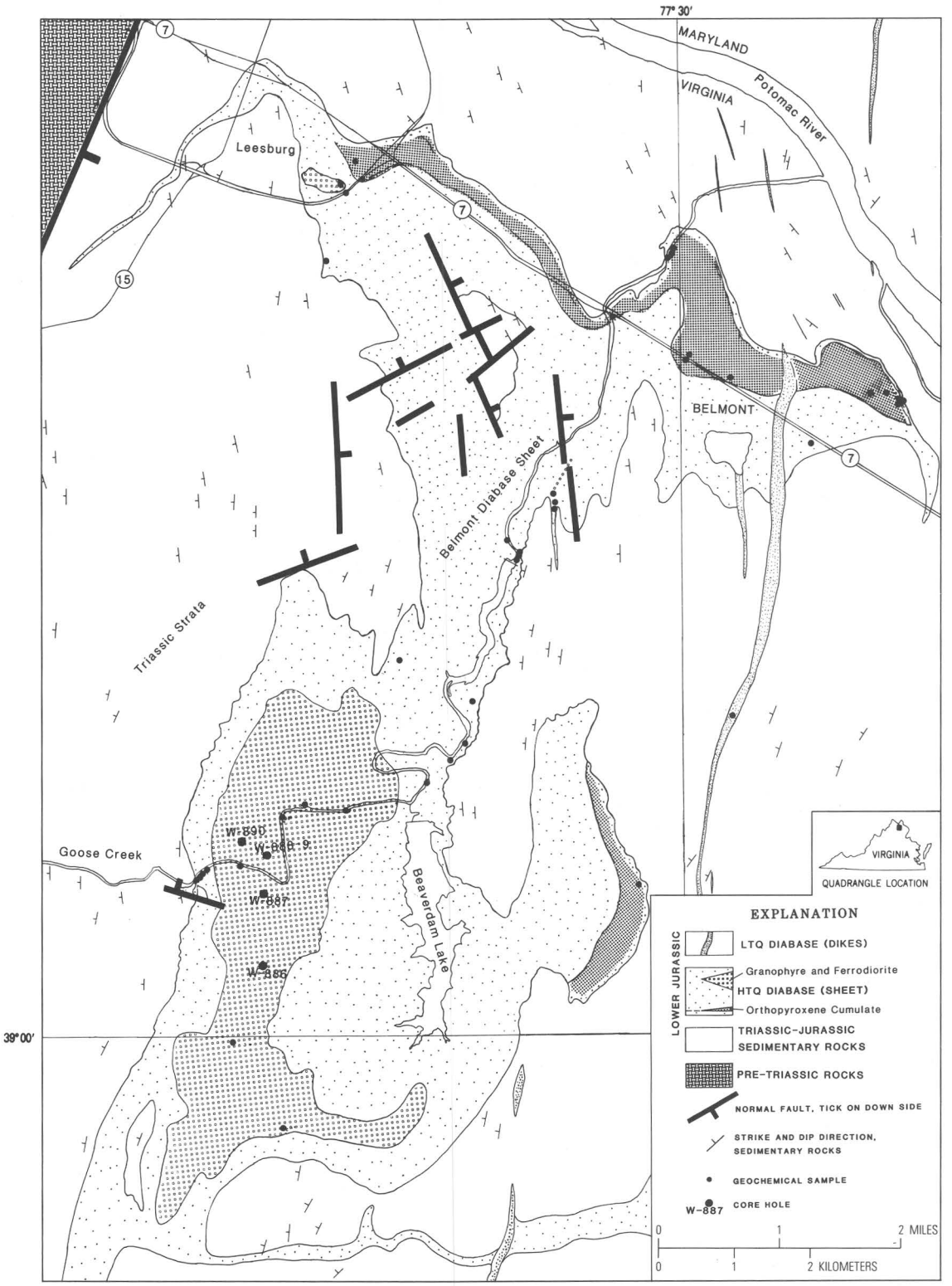

Figure 1 (Froelich and others). Simplified geology of the Belmont diabase sheet in the early Mesozoic Culpeper basin, northern Virginia. LTQ, low-titanium quartz-normative diabase; HTQ, high-titanium quartz-normative diabase.

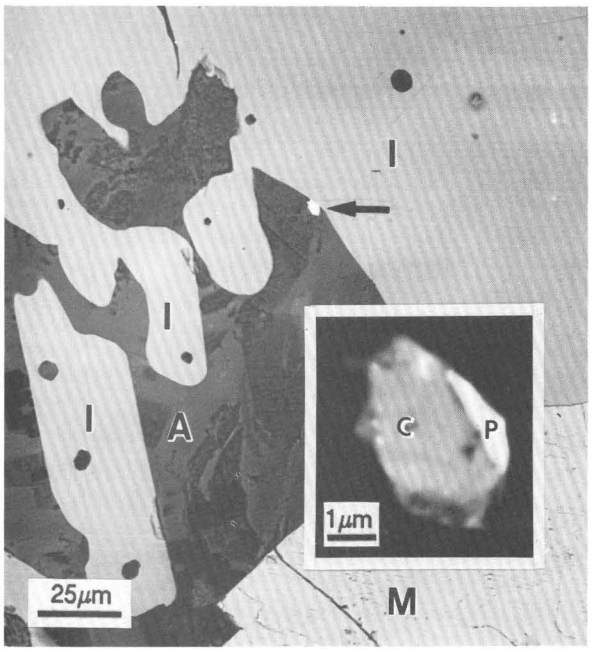

Figure 2 (Froelich and others). Palladium mineral (P) along a silicate-oxide grain boundary in a backscattered electron image taken with a scanning electron microscope (I = ilmenite, A = chlorine-rich amphiboles, M = titanomagnetite). Arrow indicates grain shown in the enlargement inset; P = Pd + Bi + Sb, and C = Co + Fe + As according to SEM-EDXRF analysis. Belmont corehole W-886, sample depth 55.5 m below land surface, zone 3.

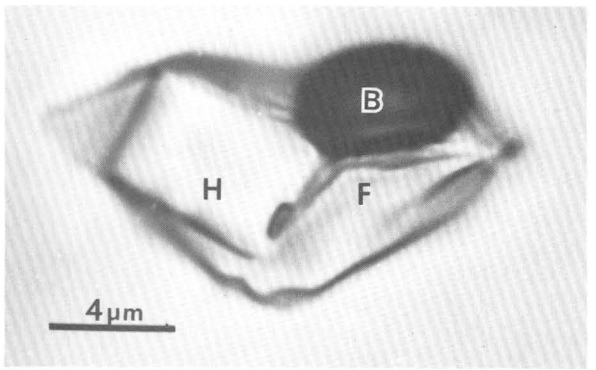

Figure 3 (Froelich and others). Primary multiphase fluid inclusion in quartz, plane-polarized transmitted light photomicrograph (H = halite, B = vapor bubble, F = birefringent daughter crystal(s)). Belmont corehole W-890, sample depth 38.7 m below land surface, zone 1.

graphic and fluid-inclusion evidence also suggest that the alteration was a multistep, nonisothermal process during which metals were deposited by a chemically evolving, cooling, magmatic hydrothermal fluid. More than two dozen thick Mesozoic diabase sheets of the HTQ magma type are known in the Eastern United States from Connecticut to Virginia, and most of these contain large bodies of ferrodiorite and ferrogabbro. To date, four (Palisades sheet, New York and New Jersey; Reesers Summit and Orrtanna sheets, Pennsylvania; and Belmont sheet, Virginia) have shown 10- to 50-fold enrichment in Pd. The evidence presented here indicates that exploration for precious metals in the HTQ-type diabase sheets should focus on the late-stage ferrogabbro and ferrodiorite differentiates enriched in Cu.

Lithologic and Tectonic Controls on Mercury Mineralization in the Bethel 1° × 3° Quadrangle, Southwestern Alaska

By Thomas P. Frost *and* Stephen E. Box

As part of the Alaska Mineral Resources Assessment Project (AMRAP), 1,486 stream-sediment and 1,104 heavy-mineral-concentrate samples were collected from first- and second-order streams from 1987 to 1989 in the Bethel 1° × 3° quadrangle and in the southern part of the Russian Mission quadrangle in southwestern Alaska. In addition, 1,375 bedrock samples were analyzed. Mercury and, to a lesser extent, arsenic contents are closely linked to locally subtle variations in bedrock lithology and to major structural elements in the area.

The region is underlain by at least five pre-mid-Cretaceous tectonostratigraphic terranes (fig. 1). Proterozoic orthogneisses and granitic rocks make up the Kilbuck terrane; Paleozoic and Mesozoic arc- and oceanic-affinity metabasalts, metacherts, clastic rocks, and minor marble are present in the Goodnews, Togiak, and Tikchik terranes; and Mesozoic arc volcanic rocks make up the Nyac terrane. Unconformably overlying all but the Nyac terrane is the Lower and Upper Cretaceous Kuskokwim Group, which consists predominantly of marine turbidites. Shallow-marine to deep-marine conglomerates and sandstones are present above a basal unconformity in the central part of the Kuskokwim basin.

The Kuskokwim Group can be divided into three belts, each having a distinct provenance. The western belt consists of an eastward-prograding deltaic sequence derived from an enigmatic chert-rich source area not presently exposed in the Bethel region. The basement on which the westernmost chert-rich facies was deposited is also not exposed. The eastern belt rests unconformably on the Togiak terrane and consists of turbiditic base-of-slope deposits derived from an eroded volcanic source. The central belt was deposited in a northeastward-flowing submarine fan system, which received sediment from both flanks and from a southern high-grade metamorphic source. The Kuskokwim Group was complexly deformed prior to the Late Cretaceous to early Tertiary magmatic episode.

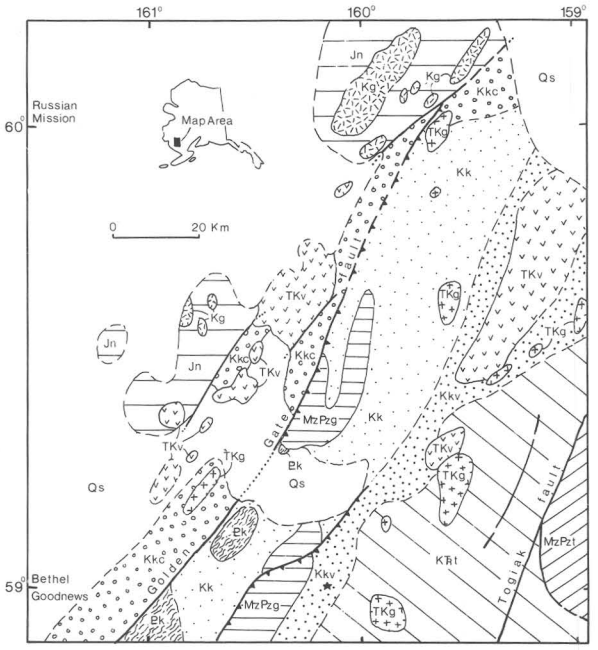

EXPLANATION

Contact - Dashed where inferred

Fault - Dashed where approximate, dotted where inferred

Thrust fault - Teeth on upper plate

Overlap sequences

Qs — Surficial deposits (Quaternary)

TKv — Volcanic rocks (early Tertiary and Late Cretaceous) -- Basalt to rhyolite flows and domes, includes some hypabyssal rocks.

TKg — Granitic to granodioritic plutons (early Tertiary and Late Cretaceous)

Kg — Granitic to granodioritic plutons (Early Cretaceous)

Kuskokwim Group (Late and Early Cretaceous) -- Consists of:

Kk — Undivided part

Kkc — Chert-clast facies

Kkv — Volcaniclastic facies

Pre-mid-Cretaceous terranes

KTt — Togiak terrane (Early Cretaceous to Late Triassic) -- Andesitic volcanic rocks, volcaniclastic rocks, and tuffaceous argillite

Jn — Nyac terrane (Late and Middle Jurassic) -- Andesitic volcanic rocks and minor volcaniclastic sedimentary rocks

MzPzg — Goodnews terrane (Mesozoic and Paleozoic) --- Tuffaceous argillite, chert, basalt, metabasite, metachert, and marble

MzPzt — Tikchik terrane (Mesozoic and Paleozoic) -- Metavolcanic rocks, metachert, graywacke, and limestone

Ek — Kilbuck terrane (Proterozoic) -- Amphibolite facies orthogneiss with minor amphibolite and quartz-mica schist

Figure 1 (Frost and Box). Regional geology of the Bethel quadrangle and parts of the Russian Mission and Goodnews quadrangles, southwestern Alaska. The Rainy Creek locality is indicated by a star.

Granitic to granodioritic rocks of Early Cretaceous age were emplaced only in the Nyac terrane. Similar plutons (73–55 Ma) were emplaced in the older terranes to the east and in the overlying Kuskokwim Group. Wall rocks generally are metamorphosed to biotite and cordierite hornfels within a kilometer of the intrusive contacts.

Latest Cretaceous and early Tertiary intermediate to silicic volcanic fields and hypabyssal intrusions were erupted through both the eastern volcaniclastic and western chert-rich facies of the Kuskokwim Group. Rhyolite domes and ash-flow tuffs, which may be part of the western volcanic field, also were erupted through the andesitic volcanic rocks of the Nyac terrane, the westernmost of the exposed basement terranes. Dikes of andesitic to dacitic composition are common throughout the Kuskokwim Group and older rocks, although their relationship to the volcanic fields is uncertain.

Anomalous mercury contents are present in sedimentary rocks of the Kuskokwim Group (0.5–1.1 ppm Hg), in overlying volcanic rocks (0.5–11 ppm Hg), and in stream sediments (1–>36 ppm Hg) wherever the eastern volcaniclastic facies of the Kuskokwim Group is exposed in the region. The epithermal Rainy Creek mercury prospect (Sainsbury and MacKevett, 1965) at the southern edge of the Bethel quadrangle is hosted by the eastern volcaniclastic facies of the Kuskokwim Group. Anomalous mercury concentrations (1–10 ppm) also are present in stream-sediment samples from just west of the eastern volcaniclastic facies of the Kuskokwim Group, where it is strongly deformed by east-dipping thrust faults in the southern part of the map area.

Despite similarities in age, lithology, and bulk chemistry, the western and eastern Late Cretaceous to early Tertiary volcanic fields have significant differences in their potential for mercury mineralization. The volcanic rocks emplaced through the eastern volcaniclastic facies of the Kuskokwim contain anomalous mercury, whereas those emplaced through the western chert-rich facies contain significantly less mercury. In addition to many stream-sediment samples that have anomalous mercury concentrations and to heavy-mineral concentrates that contain cinnabar, some rhyolite samples from the eastern field contain more than 36 ppm mercury. The western volcanic field has few mercury anomalies in any sample media that are clearly related to the volcanic rocks or to underlying Kuskokwim sedimentary rocks. Arsenic anomalies show some overlap with the mercury anomalies but are more heavily concentrated in the Togiak terrane beneath the eastern edge of the Kuskokwim Group. The difference in mercury content between the eastern and western volcanic fields appears to reflect variations in the composition of the underlying Kuskokwim Group and its basement.

Mercury anomalies also are present in sediments from streams that drain serpentinite having silica-carbonate alteration along the Golden Gate and related faults that form the

western boundary between the Kuskokwim Group and the Jurassic volcanic rocks of the Nyac terrane. Samples collected near the active Togiak fault in the southeastern corner of the area also contain anomalous mercury. Sediment samples from streams draining several of the Cretaceous granitic plutons also have anomalous mercury concentrations, which suggest that the plutons may have mobilized mercury from the Kuskokwim Group or the underlying basement.

Rocks having the greatest potential for undiscovered mercury deposits in the Bethel region are the eastern volcaniclastic facies of the Kuskokwim Group and volcanic rocks that were emplaced through the eastern volcaniclastic facies. Additional mercury deposits may be found in rocks associated with the major fault zones that form terrane boundaries.

REFERENCE CITED

Sainsbury, C.L., and MacKevett, E.M., Jr., 1965, Quicksilver deposits of southwestern Alaska: U.S. Geological Survey Bulletin 1187, 89 p.

Detailed Profiles of Southeastern Arizona Obtained by a Truck-Mounted Magnetometer—A Step Toward Better Utilization of the Information Content of Geophysical Data

By Mark E. Gettings, Mark W. Bultman, *and* Frederick S. Fisher

Computerized methods of data acquisition, processing, and analysis have made it possible to move geophysical surveying into a realm of very high data density, where the data are nearly continuous. Although significant problems remain for truly high density map coverage, profile data at very closely spaced intervals can now be accommodated. The U.S. Geological Survey has embarked on a program to develop better methods of extending bedrock mapping beneath cover, mainly in basins. Part of this program is the collection of detailed geophysical data from a truck-mounted platform. A proton precession magnetometer and a computer-controlled data-acquisition system have been installed on a four-wheel-drive vehicle. An electromagnetic system utilizing 60-Hz powerlines as a source is being constructed for installation into the truck, and a gamma-ray spectrometer will be incorporated so that the profiles will be essentially the horizontal equivalent of borehole logging. The system is capable of sampling at intervals from 25 cm to 25 m; work to date has used an interval of about 5 m. Because closely spaced data are used, problems such as aliasing of spectra and loss of signal from small local sources are eliminated. Profiles collected over several porphyry copper deposits and several replacement deposits strongly suggest that alteration zonation is detectable in the magnetic signatures of some deposits. The major objectives of the research program are to devise new methods of inferring the history of geochemical transport of metals in and around ore deposits and to find new ways to visualize and interpret data to define geologic structure.

A magnetometer profile consisting of about 20,000 observations over a distance of 111 km was used for an initial data set. This profile begins in the Tucson basin, crosses the Santa Catalina metamorphic core complex, passes through the copper deposits at the base of the sedimentary section, continues onto the gravels of the San Pedro Valley, and ends in the volcanic andesites and rhyolites of the Galiuro Mountains. A comparison of the observed magnetic data with the surface lithologies shows distinct correlations of the textures or "noisiness" of the magnetic field with various rock units. Two approaches were attempted to create a quantitative measure of this relation. The first used traditional Fourier analysis, which resulted in a spectrum over each rock unit. The spectra were successful in demonstrating some relations. For example, the spectrum of the central part of the San Pedro basin is quite different from that of the gravel sheets on the edges of the basin, presumably because allochthonous material has been transported by the river and lake system in the central basin. Finally, the gravels northeast of the basin center have a spectrum similar in shape to that of the Galiuro volcanic rocks and different from that of the gravels on the southwest side of the basin. However, the spectra are ambiguous and must be used with other data if lithologies are to be predicted reliably.

The second approach used some of the ideas of fractal geometry to describe the various "magnetic textures." The fractal dimension is commonly used to describe roughness. In a magnetometer profile, the coordinates are in different units, and, providing the profile can be described by a fractal, common methods of determining the dimension are dependent on the relative scaling between the distance and magnetic field coordinates; these methods require computations at several scaling factors to determine the fractal dimension. Two other measures have been used to reduce computation. They are computationally efficient and are fractal measures in the sense that they describe the tendency of the profile to fill the two-dimensional space. The two measures are applied within a window moving along the profile and consist of calculating the total "length," S, of the data (in mixed units of kilometers and nanoteslas) and counting the number of peaks and troughs, N. Both numbers measure the relative roughness of the data, and the parameter $S/(2N)$ describes the average anomaly amplitude relative to the regional variation within the window and thus characterizes the short-wavelength sources. The mean, minimum, maximum, and standard deviation are also computed. For the profile studied, N appears to be a useful

discriminant for shallow sources and may be especially useful for helping to distinguish between alluvial gravel units; *S* appears to be most useful in discrimination of lithologies.

Multidimensional plots where each measure is plotted along an axis have proved useful in studying the information contained in the various measures in a combined way. In this method, clustering among the measures is sought by viewing different projections of the plot ("cloud plot"), and lithologies are characterized on the basis of their cluster response to several measures. Efforts to find and apply other methods of plotting the data have been undertaken. New techniques have been developed to combine multiple data layers into one composite map in order to reduce the dimensionality of the data. In one technique to integrate the magnetometer profile data with geophysical and geologic map data, the magnetometer profile data are displayed as gray-scale or color stripes or as projected profiles that are superimposed on a traditional or composite map. In this context, the use of the profile data often simplifies or highlights the images of the geophysical or geologic data sets and can clarify relations in regional data.

Multidimensional plots of magnetometer and other data are also used to study structural relations in basins. The three-dimensional models of the basins can be viewed from any angle, can be cut in any location, and can have individual lithologies, such as basin fill, removed. These techniques enable one to explore the consequences of the model and often lead to the discovery of new relations.

Synorogenic Auriferous Fluids of the Juneau Gold Belt, Southeast Alaska—Stable-Isotope Evidence for a Deep Crustal Origin

By R.J. Goldfarb *and* W.J. Pickthorn

Mesothermal gold deposits of the Juneau gold belt extend for 200 km along both sides of the Coast Range megalineament, a major steeply dipping shear zone about 125 km inland of the continental margin. Gold-bearing fissure veins, stockworks, and stringers were deposited in a variety of igneous and metasedimentary host rocks at 55 Ma; deposition took place at depths of at least 5–8 km during the late stages of activity in the mid-Cretaceous to Eocene southeast Alaska-British Columbia orogen. Fluid migration and vein emplacement were coeval with rapid uplift of host rocks along the western edge of the orogen. The source of the fluids responsible for mesothermal gold veins throughout the accreted terranes of the northern part of the cordillera is controversial. New stable-isotope data for minerals from auriferous veins and country rocks along the Juneau gold belt provide new information on the source of these ore fluids.

The $\delta^{18}O$ values of gold-bearing quartz from mines of the gold belt range from +15.2 to +20.8 per mil and thus indicate ore fluid values of $+10.0 \pm 2.8$ per mil at about 300 °C, as determined from fluid-inclusion studies. Similar $\delta^{18}O$ values for quartz veins hosted by igneous and metasedimentary rocks indicate little local wall-rock control on oxygen-isotope compositions. The $\delta^{18}O$ values are best interpreted as representative of a fluid in isotopic equilibrium with pelitic metasedimentary rocks. The narrow range in oxygen-isotope compositions precludes the use of any fluid-mixing model for gold deposition along the gold belt. Calculated $\Delta^{18}O_{qtz\text{-}kspar}$ values of −0.2 to + 1.1 per mil for igneous rocks in the vicinity of the gold belt are suggestive of postcrystallization exchange between an isotopically heavy metamorphic fluid and the igneous rocks.

Hydrothermal micas from many of the gold deposits are characterized by δD values of −75 to −53 per mil. Ore fluids calculated to be in equilibrium with the micas have values of −35 to −15 per mil. These data, as well as the gas geochemistry of the fluids determined by fluid-inclusion investigations, are most consistent with a metamorphically derived ore fluid (fig. 1). Extracted fluid-inclusion waters from gold-bearing quartz have a broader range of δD, from −48 per mil in relatively undeformed veins to about −110 per mil for more deformed veins. This range of greater than 60 per mil reflects various mixtures of fluids from inclusions containing isotopically heavy primary ore solutions

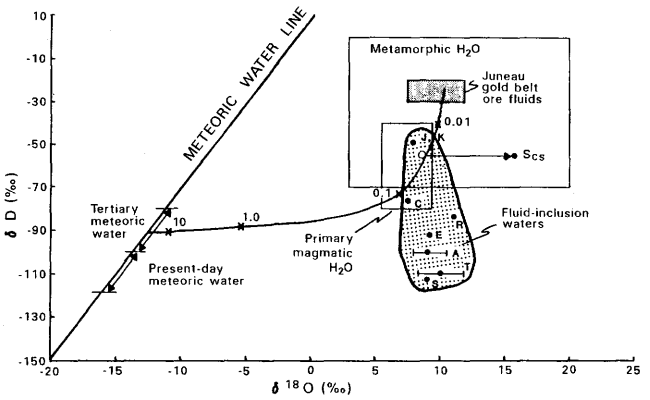

Figure 1 (Goldfarb and Pickthorn). Plot of $\delta^{18}O$ versus δD showing the composition for the ore fluids calculated on the basis of isotopic measurements of quartz and micas. The field for δD values determined from fluid-inclusion waters in quartz is significantly lighter. Specific deposits: J, Jualin; K, Kensington; S_{CS}, glassy quartz in calc-silicates at Sumdum Chief—figure shows a shift to an anomalously heavy oxygen value because of low water:rock ratios in calc-silicates; C, Crystal; R, Reagan; E, EPU; A, Alaska-Juneau; T, Treadwell; S, Sumdum Chief. A meteoric water evolution path, calculated for Tertiary waters at 300 °C, indicates water:rock ratios required to reach various isotopic compositions. In the calculations for the path, metasedimentary rocks are assumed to have an average $\delta^{18}O$ value of +16 per mil and δD of −60 per mil.

and those containing isotopically light meteoric waters trapped during uplift of the veins to shallow crustal levels.

The large isotopic shifts from the meteoric water line required to attain the $\delta^{18}O$ and δD values of the ore fluids preclude significant contributions from meteoric sources in the ore-forming process. Required oxygen shifts of about 20 per mil would necessitate water:rock ratios of less than 0.1; required hydrogen shifts demand ratios of even less than 0.01 (fig. 1). Such rock-dominated conditions are unlikely for any type of channelized, downward flow of meteoric waters into the deep crust. Rather, isotopically heavy fluids produced through prograde metamorphic reactions are more likely to have migrated upward during periods of failure along the Coast Range megalineament.

Black Shales as Hosts for Unconventional Platinum-Group-Element Resources? Examples from Southern China and the Yukon, Canada, and Implications for U.S. Resources

By Richard I. Grauch, Raymond M. Coveney, Jr., James B. Murowchick, *and* Chen Nansheng

Black shales in China and Canada host Mo- and Ni-sulfide deposits and occurrences that contain significant and potentially byproduct amounts of platinum-group elements (PGE's) and precious metals. The ores contain similar suites of metals (although the metal ratios differ), have very similar and unusual textures, and are hosted by black shales that were probably deposited in similar tectonic and metallogenic environments. The presence of analogous black shale sequences in Alaska and in the conterminous United States suggests a strong possibility of discovering comparable mineral resources in the United States.

Lower Cambrian black shales in nine provinces of southern China host Mo- and Ni-rich sulfide deposits and occurrences that contain up to several hundred parts per billion each of PGE's and Au. The mineralization at any specific locality is a single stratiform, metal-rich sulfide layer. The layer (≅2–15 cm thick, reported up to 35 cm thick) occurs within 10 m of the Proterozoic-Cambrian unconformity and crops out discontinuously along an approximately linear belt for 2,000 km. The Mo cutoff grade in the Zunyi area (the only active mining area), in Guizhou Province, is 4.1 percent. Annual production (from hand-driven adits) within the area during the last several years has been between 500 and 1,000 t having grades between 4.1 and 7.1 percent Mo. The ores also contain as much as 7 percent Ni, 2 percent Zn, and 2.5 percent As.

The sulfide layer commonly overlies thin (up to a meter thick) phosphorite rich in rare-earth elements. In some locations, the sulfide layer is separated from the phosphorite by thin layers of black shale that contain calcareous concretions. The sulfide layer is apparently lithified clastic sediment (up to 90 percent sulfide clasts) comprising interlayered conglomeratic, granule to very fine sand-sized, well to poorly sorted black sandstones and black, finely laminated siltstones and claystones. Clast types include, in order of abundance, (1) sulfide clasts and nodules, some of which are finely laminated, (2) phosphatic organic-carbon-rich nodules, some of which are sulfide rich; and (3) organic-carbon-rich clasts, either layered or massive. One sample, from near Dayong, Hunan Province, contains what appear to be fossilized worm tubes. The sediments are cemented by sulfides, calcium phosphate, quartz, and (or) carbonate. Ore mineralogy is complex; the major phases include pyrite, millerite, bravoite, and gersdorffite. Sphalerite and chalcopyrite are minor ore phases. Molybdenum occurs as a Mo sulfide (probably jordisite) and in organic matter.

Middle Devonian black shales in the central Yukon Territory, Canada, host a stratiform Ni-rich sulfide layer that is very similar to the metal-rich layer in China. The sulfide layer in the Yukon contains an average of 5.7 percent Ni, 1.2 percent Zn, and 0.24 percent Mo and contains up to 700 ppb Pt, 900 ppb Pd, 46 ppm Re, and 6 ppm Ag (L. Hulbert, Geological Survey of Canada, oral commun., 1990; Hulbert and others, 1990). The layer is up to 10 cm thick, crops out discontinuously for approximately 14 km along the strike of a doubly plunging synclinal structure, and has been intersected by several drill holes within the syncline (R. Carne, Archer-Cathro and Associates, oral commun., 1990). The clastic texture of the sulfide layer is remarkably similar to that of the Chinese layer. Significantly, it also contains fossils, which are sulfide replacements of plant material. However, the mineralogy of the layer (pyrite, vaesite, wurtzite, and organic matter, according to R. Carne, oral commun., 1990) is apparently less complex than that of the Chinese layer. The shales and metals were deposited in an anoxic basin related to an Atlantic-type passive margin (Goodfellow, 1990). Within the same environment and generally in the same time frame, barite and sedimentary-exhalative (SEDEX) base-metal deposits formed elsewhere in the Selwyn basin. The basin can be traced into Alaska, and the possibility exists, therefore, that similar occurrences are present in the United States.

REFERENCES CITED

Goodfellow, W.D., 1990, Processes of metal accumulation in Paleozoic basinal shales, North American passive margin, Canadian Cordillera (Yukon) [abs.]: International Association for the Genesis of Ore Deposits (IAGOD) Symposium, 8th, Ottawa, Canada, Program with Abstracts, p. A109–A110.

Hulbert, L., Carne, R., Gregoire, C., and Paktunc, D., 1990, Sediment-hosted Ni-Zn-PGE mineralization in the Selwyn basin, Yukon—A new environment for nickel and platinum-group element mineralization [abs.]: IAGOD Symposium, 8th, Ottawa, Canada, Program with Abstracts, p. A111.

Subsurface Structure and Lithology near the Getchell Gold Trend, Osgood Mountains, Nevada—Geophysical Insights

By V.J.S. Grauch, Donald B. Hoover, *and* Wayne S. Wojniak

A complicated picture of subsurface structure and lithology is emerging from the interpretation of aeromagnetic, airborne electromagnetic (AEM), and gravity data on the eastern side of the Osgood Mountains, Nevada, where six sedimentary-rock-hosted disseminated-gold deposits define the Getchell gold trend. This integrated interpretation has provided new information on the three-dimensional geologic setting of the Getchell trend, although the details of the picture are still unclear.

The three geophysical data sets were collected as part of a U.S. Geological Survey program to evaluate applications in mineral-deposit studies of geophysical data collected by various airborne geophysical instruments. Each data set represents the response to different physical properties at different depths within the subsurface and provides unique information for geophysical interpretation. The AEM data, collected at three different frequencies (900, 7,200, and 56,000 Hz), best define lithologic and structural features in the shallow subsurface and can be used to distinguish some areas of hydrothermal alteration. The aeromagnetic data best delineate the subsurface configuration of igneous rocks and associated faults and altered areas. The gravity data, acquired along three profiles, best distinguish major normal faults that juxtapose bedrock against basin fill.

Interpretation of the geophysical data involved application of mathematical filters to gridded data, digital comparison of data grids, and modeling of profiles and isolated anomalies. Many poorly defined or previously unknown geologic features were better defined or discovered during the interpretation; several are of particular interest. The Osgood Mountains pluton, which is adjacent to several of the gold deposits, extends laterally east and west to some depth; previous geologic interpretations suggested that the buried part of the pluton did not extend west of the exposed west side. Shallow dikelike apophyses may be common on the west side. Knowledge of the subsurface extension of the pluton is important if gold mineralization is genetically related to the pluton (the origin of the gold deposits is still controversial). The overall fault pattern delineated by the geophysical data is presumably related to Basin and Range structure and consists of four sets of approximately parallel faults that follow different trends in different parts of the study area. The fault sets trend north-northeast to the northeast of the Osgood Mountains pluton, north-south next to the pluton, northeast just south and southeast of the pluton, and north-south further south, east of the Preble gold deposit. The AEM data suggest that

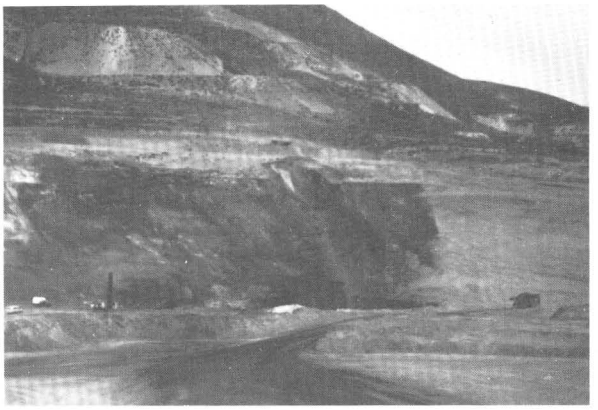

Figure 1 (V.J.S. Grauch and others). Looking north across the Mag pit, which is along the Getchell gold trend, at a normal fault that cuts bedrock, basin fill, and gold ore. Photograph by James A. Pitkin in 1989.

hydrothermal alteration occurred along many of the faults, especially those related to gold mineralization. Modeling results suggest that episodic faulting, basin filling, and volcanism have resulted in step-down faults or grabens where bedrock is covered by a variable amount of alluvium intermixed with volcanic flows. A fault cutting both bedrock and alluvium is shown in figure 1.

Drill-hole information has revealed a few unexpected sources for certain local geophysical anomalies. North of the Chimney Creek gold deposit, an anomalous aeromagnetic high is probably produced by pyrrhotite interspersed in pillow lavas, rather than by an intrusion as previously thought. North of the Mag open pit, an aeromagnetic high over an area of low resistivity may be produced by secondary magnetite in carbonaceous argillite. These unusual results suggest that the details of the subsurface picture are far from being established and indicate the direction for future work.

Geochemical Exploration Criteria for Epithermal Cinnabar and Stibnite Deposits, Southwestern Alaska

By J.E. Gray, D.E. Detra, R.J. Goldfarb, *and* K.E. Slaughter

Epithermal cinnabar- and stibnite-bearing vein systems are scattered over several thousand square kilometers in southwestern Alaska. More than 40,000 flasks of mercury have been produced in the region, mostly from the Red Devil mine. Mineralized quartz-carbonate veins and stockworks are found within Cretaceous basin-fill sedimentary rocks of the Kuskokwim Group and adjacent accretionary terranes. Many of the deposits are in or adjacent to brittle rocks, largely mafic dikes, rhyolite dikes and sills, and

intermediate to felsic stocks, that intrude sedimentary rock. Mineralized veins are commonly localized where bedding-plane faults in surrounding sedimentary rocks intersect these more competent units. Cinnabar is the dominant ore mineral; it typically is accompanied by stibnite. Realgar, orpiment, pyrite, limonite, hematite, and native mercury are less common. Dickite is a typical alteration mineral at many of these occurrences.

In 1989, a geochemical orientation survey was conducted around several cinnabar and stibnite vein deposits. Stream-sediment, heavy-mineral-concentrate, stream-water and vegetation samples were collected in drainages surrounding the Red Devil, Cinnabar Creek, White Mountain, Rhyolite, and Mountain Top deposits. Three size fractions of the stream-sediment samples were selected for analysis. The heavy-mineral-concentrate samples were split into nonmagnetic, paramagnetic, and magnetic fractions. These samples and the stream-water and vegetation samples were analyzed for multielement suites by different chemical procedures. Nonmagnetic heavy-mineral concentrates were also examined microscopically to identify their mineralogy.

Results confirm that Hg, Sb, and As in minus-80-mesh stream sediments are effective pathfinder elements in exploration for epithermal cinnabar and stibnite occurrences. Concentrations greater than 3 ppm Hg, 1 ppm Sb, and 15 ppm As in the minus-80-mesh stream sediments, regardless of the host lithology, are indicative of upstream cinnabar and stibnite occurrences in the Kuskokwim River region. Stream sediments coarser grained than minus-80-mesh are less useful in the exploration for these mineral occurrences. Base metals in stream sediments and heavy-mineral concentrates are ineffective pathfinders for this epithermal type of occurrence.

Heavy-mineral concentrates provide little additional advantage in the exploration for these mineral systems. Sb and As dispersion patterns downstream from mineralized areas are generally more restricted in heavy-mineral concentrates than they are in the stream sediments. Distribution patterns of placer cinnabar observed in heavy-mineral concentrates are similar to those of anomalous Hg and Sb in corresponding stream sediments. Stream waters are a less effective geochemical sample medium than stream sediments or heavy-mineral concentrates, and vegetation samples are ineffective geochemical sample media in exploration for this type of mineral occurrence.

Several of the epithermal cinnabar and stibnite vein deposits in the Kuskokwim River region contain anomalous gold concentrations. Gold contents in vein samples containing cinnabar and stibnite range from 0.05 to 6.9 ppm. These concentrations indicate that gold may be a byproduct of some of these epithermal systems, which were previously recognized only for their Hg and Sb contents. The gold anomalies suggest the potential for significant gold concentrations deeper in some of these cinnabar- and stibnite-bearing deposits.

Geochemical Investigation of Ground Water Associated with Disseminated Gold Deposits along the Getchell Trend, Northern Nevada

By D.J. Grimes, W.H. Ficklin, J.B. McHugh, *and* A.L. Meier

Ground-water samples were collected from wells and a drill hole near the Chimney Creek and Rabbit Creek disseminated gold deposits along the Getchell trend in northern Nevada to study the chemistry, distribution, and mobility of ore-associated elements such as Au, As, Sb, and W. A custom-built double-check valve bailer was used to obtain ground-water samples from various depths in the drill hole at and below the water table. The deepest sample was from 700 ft below the ground surface.

The samples were analyzed for a number of constituents, including Au, at the 1-part-per-trillion (ppt) level by anion-exchange graphite-furnace atomic-absorption spectrometry (GFAAS). As, Sb, and W contents were determined by inductively coupled plasma-mass spectrometry (ICP-MS), and concentrations of As species (arsenite or As(III) and arsenate or As(V)) were determined by ion-exchange GFAAS.

Water samples from nine observation wells around the perimeter of the Rabbit Creek deposit contain variable concentrations of As, Sb, and W. In these waters, As concentrations range from 19 to 540 μg/L (ppb); Sb, from 0.4 to 140 μg/L; and W, from 2 to 120 μg/L. High concentrations appear to be very local. In general, the higher concentrations of these constituents occur where measured Eh values indicate reducing conditions. Thus, it appears that the increased concentrations of these elements in water are derived from contact with the sulfidic parts of the gold deposit. Ordinarily, Sb and W contents are not determined in water samples because their abundances are so low that spectrophotometric methods are not effective; however, given the ease of determination provided by ICP-MS, we were able to establish background concentrations and confirm that anomalous concentrations of Sb and W occur in ground water near sedimentary-rock-hosted gold deposits.

As, Sb, W, and Au concentrations were determined from ground-water samples taken at various depths in a drill hole between the Rabbit Creek and Chimney Creek deposits (fig. 1). Concentrations of As range from 600 to 710 μg/L at five different depths in the water column; Sb concentrations range from 110 to 140 μg/L; W concentrations range from 130 to 150 μg/L; and Au concentrations range from 1 to 11 ng/L (parts per trillion). The values suggest that these elements are derived from mineralized rock.

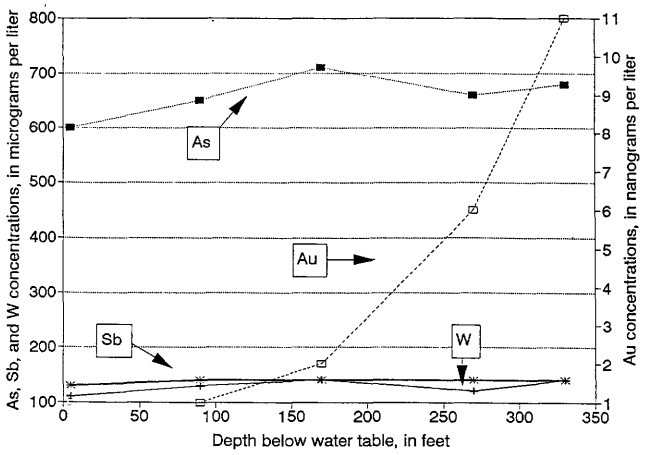

Figure 1 (Grimes and others). Depth below water table versus concentrations of As, Sb, W, and Au in ground-water samples from a drill hole between the Rabbit Creek and Chimney Creek gold deposits in northern Nevada.

Results for the determination of arsenic species, ferrous iron, and oxidation-reduction potential are presented in figure 2. The data suggest that vertical ground-water "redox zones," which may affect the mobility of some of the ore-associated elements, can occur in the water column of a drill hole. The highest redox readings occur near the water table, where all the As is As(V) and ferrous iron concentrations are low. In contrast, the reduced zone of the water column is characterized by the predominance of As(III), the reduced form, and by greater concentrations of ferrous iron.

Our data indicate that many chemical and physical parameters affect the mobility of ore-associated elements in ground water. A better understanding of these parameters will enable us to use water geochemistry more effectively as an exploration tool.

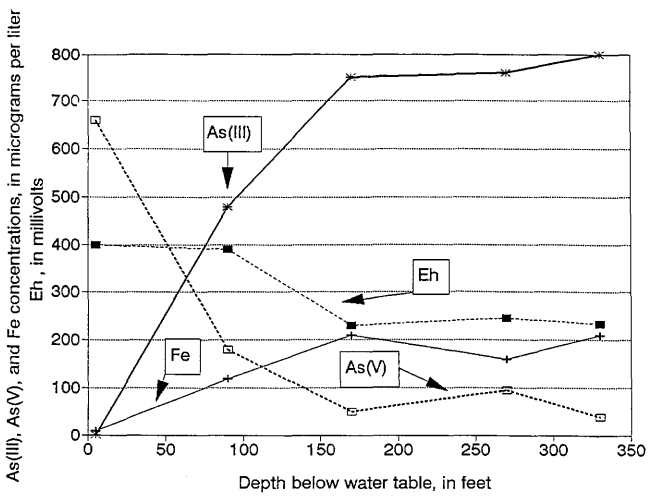

Figure 2 (Grimes and others). Depth below water table versus concentrations of arsenic species and ferrous iron and redox potential for ground-water samples from the same drill hole for which data are plotted in figure 1.

Comparative Metallogeny of the Soviet Far East and Alaska

By Donald J. Grybeck, Warren J. Nokleberg, *and* Thomas K. Bundtzen

For the last year and a half, we have been engaged in a systematic study with Soviet geologists from the Academy of Science and the Ministry of Geology of the metallogeny of the Soviet Far East and Alaska. In 1989, we spent more than a month visiting mineral deposits throughout the Soviet Far East and participated in extended discussions with Soviet geologists at numerous mines and research institutes. In return, last summer, two groups of Soviet geologists visited Alaska to examine important mineral deposits and to participate in workshops with American geologists.

The work to date has been productive. Numerous maps, publications, and data have already been exchanged and are in the process of being integrated into a consistent description of the geology and metallogeny of the Soviet Far East and Alaska. Differences remain, partly because of our different approaches to geology, but more often because both sides of the exchange have been introduced to new facets of the geology of the northern Pacific and to new types of mineral deposits. For instance, we visited the "Bor" deposit at Dalnegorsk in Primorye, which is a unique skarn deposit that is the major source of boron in the Soviet Union. It was certainly unknown to us and apparently was unmentioned in the Western literature. As the work has progressed, we feel that there has been marked convergence in our thinking. We are confident that the result will be a joint publication (in English and Russian versions) describing the mineral deposits of Alaska and the Soviet Far East in mutually agreeable terms and relating them to the geologic history of the two areas. Plans are underway to extend the work to the Canadian Cordillera.

This study is useful to both Soviet and American geologists because new knowledge and ideas are being exchanged across the northern Pacific. In addition, it is particularly germane at this time because of the opportunities that seem to be opening up for foreign investment in Soviet mineral deposits.

Seasonal Variation in the Silver Concentration in Mesquite (*Prosopis juliflora*) Collected near Globe, Arizona

By Thelma F. Harms

Biogeochemical prospecting, which depends on chemical analyses of vegetation, can be an effective tool in the search for buried mineral deposits. The extensive root systems of plants accumulate aqueous fluids from ground

water or pore water and transport these fluids along with the metal ions in solution to the upper parts of plants. In this way, plants concentrate metals from a large volume of ground. In areas containing relatively shallow layers of transported overburden, vegetation may give a better reflection of buried mineral deposits than the soils derived from the overburden.

Mesquite (*Prosopis juliflora*), a common tree species in the Southwest, ranges from Texas to California and southern Utah but grows best at elevations below 1,500 m. It is a phreatophyte; that is, a species whose roots tap a zone of water saturation or its capillary fringe. Well-established mesquite trees have taproots that penetrate vertically 12–15 m; mesquites also have an extensive lateral root system that may extend 15 m beyond the base of the tree. Mesquite has been widely used in biogeochemical surveys in the arid Southwest, especially in studies of porphyry copper deposits.

To determine the feasibility of using mesquite for biogeochemical studies of silver and to determine the optimum sampling time, a study of the seasonal variation in the silver content of mesquite was undertaken in an area northwest of Globe, Ariz., where the ground water may contain as much as 1–3 μg/L (ppb) of silver (J.H. Eychaner, U.S. Geological Survey, oral commun.). Samples of velvet mesquite were collected at monthly intervals from individual marked trees at three sites. Mesquite leaves were collected from late April 1990 until late autumn, when the leaves fell from the trees; mesquite twigs were collected for a full year. Mesquite inflorescences (flowers) and beans, though of less use for biogeochemical studies because of their ephemeral nature, were collected when available. The samples were washed to remove surface dust and were ground and ashed. The silver content of the ash was determined by atomic-absorption spectroscopy. The data collected through mid-August show silver accumulations of up to 3.5 ppm in the ash. With the results of this study, sampling plans can be designed to maximize the contrast between background and anomalous values where silver is an element of interest.

Marine Ferromanganese Deposits near the Marshall Islands

By James R. Hein, Jung-Keuk Kang, Marjorie S. Schulz, Suk-Hoon Yoon, *and* Virginia K. Smith

In September and October 1989, the U.S. Geological Survey and the Korea Ocean Research and Development Institute (KORDI) cooperated in two joint oceanographic cruises to study marine mineral deposits. The first cruise was dedicated to the study of Co-rich and Pt-bearing Fe-Mn crusts within the Exclusive Economic Zone (EEZ) of the Republic of the Marshall Islands. The second cruise was dedicated to the study of Fe-Mn nodules at the western margin of the Clarion-Clipperton Fe-Mn nodule belt. In September and October 1990, two additional joint cruises were undertaken. The first cruise was dedicated to the study of Fe-Mn nodules in an area adjacent to that studied in 1989, and the second cruise was dedicated to the study of Fe-Mn crusts, island-arc hydrothermal deposits, and phosphorites in the EEZ of the Federated States of Micronesia. Following is a summary of the results obtained from the 1989 cruise to the Marshall Islands.

The two main objectives of the cruise were to determine the geological, oceanographic, and geochemical controls on the origin and evolution of Co-rich Fe-Mn crusts that occur on seamounts in the Marshall Islands EEZ and to determine the origin and evolution of the seamounts and atolls in the region. Shipboard operations included collecting CTD (conductivity-temperature-density)-oxygen profiles of the water column, dredge hauling, and conducting video-camera surveys of the ocean bottom and bathymetric, seismic-reflection, gravity, and magnetic surveys. With completion of this work, the Marshall Islands became the most extensively studied area for Co-rich Fe-Mn crusts.

All dated seamounts in the Marshall Islands are of Cretaceous age; most are Late Cretaceous. Volcanic rocks are chiefly alkalic basalt, and some are strongly alkalic. Seamounts lack simple or consistent morphologies and structures; even adjacent seamounts differ significantly. The summit platforms have complex, rugged surfaces that may be tilted. Summits may have a sediment cap; where one is present, the sediment shows evidence of erosion and slumping. The flanks of some seamounts have multiple terraces that vary in water depth and width. Seamount flanks are sites of extensive slumping and mass failures.

Oxygen and temperature profiles in the water column vary with latitude and longitude and show greater depletion in oxygen to the east and south. Oxygen content of the seawater influences the metal contents of the Fe-Mn crusts. A direct correlation exists between low oxygen contents in seawater and high concentrations of Co, Cd, Mn, K, and Ti (manganophile elements) in the crusts and between low oxygen contents in seawater and low concentrations of Y, Cu, As, and Fe (siderophile elements) in the crusts. Oxygen content controls the Fe/Mn ratio and, thereby, the minor elements associated with each of the major phases.

The thickest Co-rich crusts known in the world were collected on the 1989 cruise; they were as thick as 180 mm. Inferred growth rates range from 1.5 to 16 mm/m.y. and average 4.7 mm/m.y. The thickest crusts began to form between about 30 and 16 Ma, long after the formation of the Cretaceous seamounts. The crusts average 16.6 percent Fe, 25.6 percent Mn, 2.06 percent P, 0.70 percent Co, 0.11 percent Cu, 0.57 percent Ni, and 0.67 ppm Pt. Crusts from the Marshall Islands have higher mean Pt contents than do crusts from other central Pacific areas. Co content (grade) varies inversely with crust thickness (tonnage). The platinum-group elements (PGE's = Pt, Rh, Pd, Ru, and Ir)

in bulk crusts show significant enrichments over their lithospheric averages and seawater abundances. PGE ratios indicate that Pt, Ir, and Rh are derived from seawater and that Pd and Ru are derived from seawater and clastic debris.

Contents of all rare-earth elements (REE's) range from 0.09 to 0.28 percent for bulk crusts and up to 0.37 percent for individual crust layers. Many chondrite-normalized REE patterns show either a small positive Ce anomaly or no anomaly; several have a negative anomaly. These patterns differ from those of other central Pacific crusts. The REE compositions and chondrite-normalized patterns change with depth in the crusts, but the changes are not consistent from one crust to another nor are the REE's consistently associated with the same crust phases. The geographic distribution of the REE's, particularly Ce and Eu, in the crusts may reflect the regional oxidation potential of seawater.

U.S. Geological Survey Research on Agricultural Industrial Minerals in the United States—Implications for Exploration

By James R. Herring, David Z. Piper, Sherilyn Williams-Stroud, Charles S. Spirakis, *and* Richard A. Sheppard

The indisputable need for the agricultural minerals, used principally as fertilizers, will parallel the increasing need for food to support population growth. U.S. Geological Survey (USGS) research on the agricultural mineral commodities includes studies of phosphate, sulfur, potash, and zeolites. The agromineral industries provide 41 percent of U.S. industrial mineral revenue and 7 percent of all U.S. nonfuel mineral revenue. USGS research on deposits of these commodities principally focuses on their geology, geochemistry, and mineralogy; production figures are provided by the U.S. Bureau of Mines. Overall research goals of the USGS are to understand the nature of existing deposits and to be able to use this information to benefit future exploration. A change in the classic exploration attitude, which considered mainly ore grade and tonnage, has been forced by modern societal values. Consequently, current USGS research also focuses on additional aspects important to the mining and use of the agromineral commodities. These aspects include, for example, determination of potentially useful byproducts or of material that adversely affects mining, processing, and eventual use of the commodity.

Phosphate rock is the most valuable nonenergy industrial mineral in the United States; it accounts for slightly over a quarter of the annual revenue from all industrial minerals, which are collectively valued at about $4 billion. The United States is the world's largest producer of phosphate, supplying its own needs and about one-quarter of world exports. Of domestic phosphate production, 90 percent is used for fertilizer and other agrochemicals. Phosphate is produced from two principal phosphorite deposits: (1) the western field, which includes the Permian Phosphoria Formation in Idaho, Montana, Wyoming, and Utah, and (2) Neogene deposits of the Atlantic Coastal Plain, principally in Florida and North Carolina. Tennessee has minor production, which is included with production in the western field for U.S. production statistics. The Neogene deposits account for 88 percent of the U.S. annual production of 49 Mt of phosphate rock. Three countries, the United States, the U.S.S.R., and Morocco, account for about two-thirds of world production, which totaled 163 Mt in 1989. The United States has sufficient phosphate resources to last well into the next century, but availability of this phosphate will be determined by international pricing and mining costs. Many of these deposits can be mined only at much greater cost than the presently developed deposits and may require new, as yet unproved, technologies for ore processing. Specific USGS studies focus on the use of new analytical techniques to provide geochemical traverses of deposits showing, in addition to phosphate, the distributions of major and trace elements that are of concern to mining or the environment. The goal is to understand the controls affecting these distributions and to predict how these elements vary in the deposits that may become future exploration targets.

U.S. sulfur production in 1989 was 12 Mt (worth $1 billion) while consumption was 13 Mt. About 70 percent of sulfur is used for agricultural chemicals, mostly for phosphate processing, but also as a soil amendment. Total world production in 1989 was 59 Mt. About 57 percent of the sulfur produced in the United States was recovered from oil and gas processing, 33 percent was from Frasch mining of sulfur deposits in west Texas and the Gulf of Mexico Coast, and 10 percent was SO_2 recovery from smelters. To satisfy domestic sulfur requirements, about 8 percent was imported, principally from Canada and Mexico. As environmental regulations further limit atmospheric sulfur emissions from industrial processes, increasing amounts of sulfur will be recovered. Nevertheless, native sulfur deposits in salt domes of the Gulf of Mexico Coast and in sedimentary basins of west Texas will continue to be attractive exploration targets. USGS studies of sulfur deposits in caves of the Guadalupe Mountains of New Mexico may provide clues to the genesis of nearby, similar deposits of west Texas and may help to identify additional commercial deposits.

The U.S. potash production in 1989 of 1.5 Mt (valued at $280 million) supplied only 27 percent of domestic consumption. Major imports were from Canada, Israel, the U.S.S.R., and the German Democratic Republic. Most U.S. potash comes from salt deposits in New Mexico, where it is produced by conventional underground mining techniques at depths of 100 to 200 m. The limiting depth for

underground mining, around 1,100 m, is constrained by the low strength of the salt. The United States has estimated potash reserves of 90 Mt, while total estimated resources are about 6,000 Mt. Most of the potash resources are in the Williston Basin in Montana and North Dakota and in the Paradox Basin in Utah, but the deposits occur between 2 and 3 km depth. These two basins present important research possibilities for deposit characterization and new production methods, such as solution mining. Because there are no substitutes for potash as an essential plant nutrient, a continued supply is necessary for the United States to meet present agricultural needs and to become less dependent on imports. Current USGS research focuses on creating a new model for the deposition of sylvite (KCl, the principal ore mineral of potassium compounds), which may shift approaches in exploration.

Zeolites are important agricultural minerals for the future. Presently, they are used in agriculture as slow-release fertilizers, carriers for herbicides and pesticides, and traps for heavy metals in soils. Commercial use of natural zeolites in the United States is in its infancy; production and use in Japan, eastern Europe, the U.S.S.R., and Cuba exceed those in the United States. Most U.S. zeolites occur in Cenozoic tuffaceous rocks west of the Mississippi River. Major objectives of USGS investigations are to locate new high-grade deposits and characterize their grade, tonnage, and thickness of overburden as well as their mineralogy and chemical composition. A long-term goal is to develop and refine models of zeolite deposits as an aid in future exploration. As new markets open, the United States should become a major exporter of zeolites.

Low-Level Gold Determinations by Use of Flow Injection Analysis-Atomic Absorption Spectrophotometry—An Application to Precious-Metal-Resource Assessment in the Iditarod 1° × 3° Quadrangle, Southwestern Alaska

By D.M. Hopkins, J.E. Gray, *and* K.E. Slaughter

Low-level gold determinations were performed by the U.S. Geological Survey (USGS) to assess the precious-metal resources in the Iditarod 1° × 3° quadrangle, Alaska, as part of the ongoing Alaska Mineral Resources Assessment Project. Flow injection analysis-atomic absorption spectrophotometry (FIA-AAS) was used to determine gold concentrations in stream-sediment samples collected during a reconnaissance geochemical survey of the quadrangle.

The most common method for gold determination is separation from hydrochloric or hydrobromic acid solution with methyl isobutyl ketone (MIBK) and detection by means of flame atomic-absorption spectrophotometry (FAAS) or graphite-furnace atomic-absorption spectrophotometry (GFAAS). Although FAAS is less sensitive than GFAAS, some advantages of FAAS are (1) fewer problems with interference, (2) continuous monitoring of the analyte in a liquid stream, (3) suitability for online automated analysis, and (4) more rapid determinations. Furthermore, FAAS procedures can be transformed conveniently into a FIA-AAS technique that uses solvent extraction and a 10-fold analyte preconcentration to produce a lower limit of determination, one that approaches the crustal abundance of gold (3–5 ppb). Thus, the analysis of gold at concentrations that formerly required GFAAS is accomplished more effectively with the FIA-AAS technique.

The FIA-AAS technique uses a sample weight of 10 g for digestion with a hydrobromic acid-bromine solution. Gold is extracted from the acid mixture with 1 mL of MIBK; a 10-fold preconcentration and a detection limit of 5 ppb can be achieved. The flow injection device introduces 0.1 mL of MIBK extractant per determination into the spectrometer; more than 50 determinations per hour can be completed by this technique. Precision of the technique at the 100-ppb level is 14.3 percent relative standard deviation based on a 5-g aliquot of USGS reference GXR–2 in 1 mL MIBK. Results for reference standards by this FIA-AAS technique agree well with values reported in the literature.

Approximately 12 percent of the stream-sediment samples from the Iditarod quadrangle contain greater than 5 ppb gold. Most of these samples cluster into 13 distinct areas. Five of these areas are associated spatially with Cretaceous-Tertiary volcano-plutonic complexes that intrude sedimentary rocks of the Cretaceous Kuskokwim Group. Six other anomalous areas are near Cretaceous-Tertiary dikes or small stocks that intrude rocks of the Kuskokwim Group. One gold anomaly is found in an area underlain by Cretaceous-Tertiary volcanic rocks of the Yetna field; another occurs in an area underlain by rocks of the Kuskokwim Group.

Samples that contain anomalous gold cluster in areas of known placer districts such as Flat, Moore Creek, and Donlin Creek. Gold anomalies are observed also in areas in which little or no gold had been reported previously, such as the Beaver Mountains, Mount Joaquin, and Granite Mountain. These anomalies probably are related to (1) vein deposits containing quartz, carbonate, fluorite, stibnite, cinnabar, gold, scheelite, and arsenopyrite similar to those near Flat or (2) veins containing chalcopyrite, galena, sphalerite, cassiterite, tourmaline, and fluorite such as those in the Beaver Mountains. These gold anomalies correlate well with anomalous concentrations of Ag, Sb, As, Cu, Pb, Zn, Sn, or W in stream-sediment or heavy-mineral-concentrate samples. However, the low-level gold concentrations in the stream-sediment samples most effectively define areas of precious-metal favorability in the Iditarod quadrangle.

Geophysical and Geological Studies of the Roseau 1° × 2° Quadrangle, Minnesota and Ontario

By R.J. Horton, W.C. Day, T.L. Klein, *and* B.D. Smith

The U.S. Geological Survey (USGS), in cooperation with the Minnesota Geological Survey (MGS), the Minnesota Department of Natural Resources, and the Geological Survey of Canada (GSC), has compiled geologic, aeromagnetic, and gravity maps for the Roseau 1° × 2° quadrangle, Minnesota and Ontario. This compilation was done as part of the Conterminous United States Mineral Assessment Project (CUSMAP). More than 95 percent of the bedrock in the Roseau quadrangle is covered by westward-thickening Quaternary glacial deposits. Therefore, the geologic map is based on the interpretation of geophysical data supported by drill-core studies and studies of a limited number of outcrops.

The aeromagnetic map was produced by compiling existing data from the MGS and the GSC with new data collected by the USGS. The magnetic data were processed with a reduction-to-the-pole program to compensate for inclination and declination of the induced magnetic field that shifts the magnetic anomalies away from their source rocks. Shaded-relief (fig. 1) and first-vertical-derivative maps were also produced; they enhance such subtle bedrock features as dikes and faults. Other derivative maps were generated that define the boundaries of magnetic bodies from magnetic gradients and that outline terranes based on bedrock units having different magnetic susceptibilities.

The complete Bouguer anomaly map was produced by compiling existing data from the MGS, the GSC, and the U.S. Department of Defense. The USGS collected new gravity data to help fill the regional coverage and to better

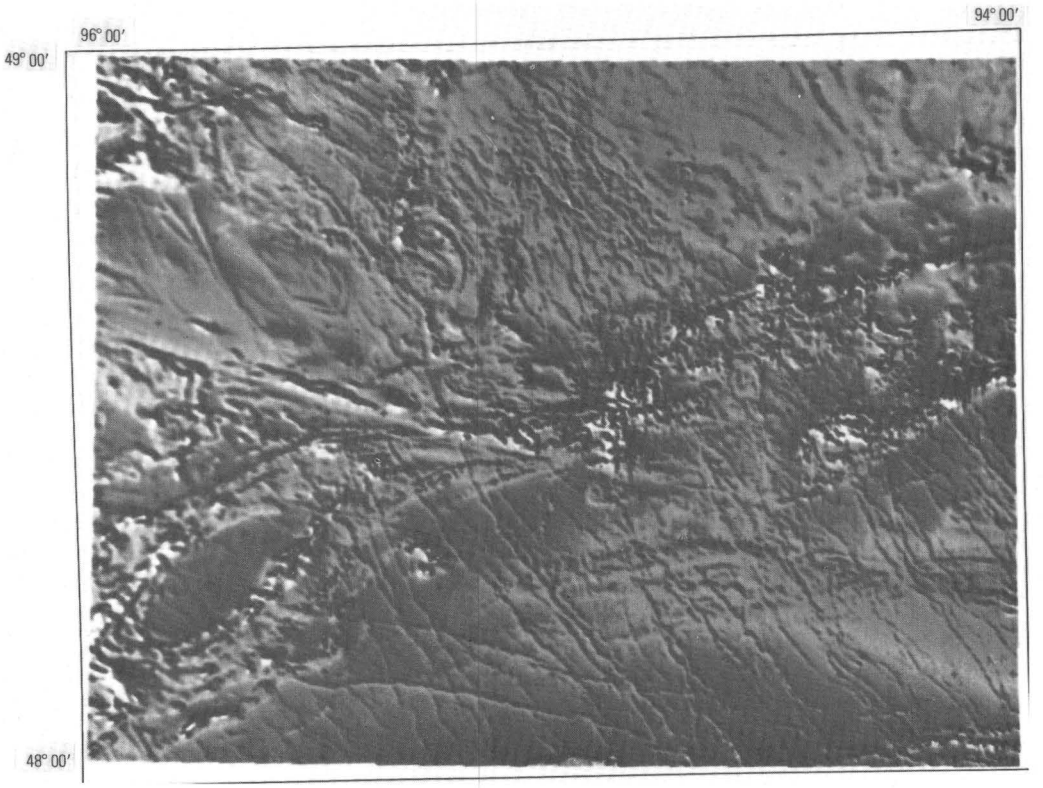

Figure 1 (Horton, Day, and others). Shaded-relief aeromagnetic map of the Roseau 1° × 2° quadrangle, Minnesota and Ontario. This map is a compilation of data from the U.S. Geological Survey, the Minnesota Geological Survey, and the Geological Survey of Canada. The lighter areas represent magnetic-field highs; the darker areas represent magnetic lows. The apparent relief is produced by computer-generated southwest illumination. The Vermilion fault can be seen striking west-northwest across the center of the map. A major northwest-trending dike swarm, readily seen in the southern part of the image, cuts metasedimentary and migmatite terrane of the Quetico subprovince. The oval feature in the southwest quarter of the map is a granitoid pluton surrounded by metavolcanic rocks of the Wabigoon subprovince. The area mapped is approximately 100 by 150 km.

define contacts. The combined data set was processed to produce a terrain-corrected Bouguer anomaly map. In addition, derivative maps were generated that enhance boundaries and define terranes based on bedrock units having different densities.

The above-mentioned geophysical data were combined with new geologic data to produce a comprehensive synthesis of the regional geology and mineral potential of the area. The Roseau quadrangle is underlain by Archean rocks of the following subprovinces: the Wabigoon in the north and west, the Quetico in the central part, and the Wawa-Shebandowan in the southeast. Rocks of the Wawa-Shebandowan subprovince are a continuation of the western Vermilion district greenstone belt, which crops out east and south of the quadrangle. The Wabigoon and Wawa-Shebandowan subprovinces are made up of rocks typical of greenstone-granite terranes, whereas the Quetico is dominantly composed of amphibolite-grade schists and migmatites.

Major high-angle transpressive fault zones delineate the boundary between the Wabigoon and the Quetico subprovinces. These faults, which are up to 2 km wide and more than 100 km long, are zones of intense ductile deformation that have pronounced aeromagnetic and gravity signatures. The latest ductile deformation, which had a dextral sense of shear, produced S-C mylonites, phyllonites, and mica schists that are variably altered to quartz, calcite, pyrite, and chlorite. Secondary ductile shear zones, which parallel the major bounding fault zones, locally have anomalous gold concentrations.

Although poorly exposed in the map area, the boundary between the Quetico and Wawa-Shebandowan subprovinces is interpreted to be gradational and without any abrupt change in lithology. The metamorphic grade gradually increases from low to medium grade northward into the metasedimentary rocks of the Quetico subprovince. No mineralization has been discovered to date in the subprovince within the Roseau quadrangle. However, Algoma-type iron deposits and shear-zone-hosted lode-gold prospects are present to the east in the Vermilion district.

Interpretation of New Geophysical Data Obtained by Airborne Instruments for the Effie-Coon Lake Area, Minnesota

By Robert J. Horton, Bruce D. Smith, Victor F. Labson, *and* Robert J. Bisdorf

New airborne geophysical instruments and data-processing methods developed by the U.S. Geological Survey (USGS) have been used to supplement standard aerial magnetic methods commonly used in regional subsurface mapping. The purpose of this study is to apply emerging technology in aerial geophysics and advanced data-processing methods to geologic mapping of an area covered by glacial overburden.

The study area is the Effie-Coon Lake area, Minnesota. It is underlain by a Late Archean granite-greenstone bedrock which is more than 95 percent concealed by Quaternary glacial deposits as much as 100 m thick. Within the study area, three large felsic plutons and a mafic sill complex (Deer Lake Complex) have intruded the steeply dipping metasedimentary and metavolcanic country rocks that also host several thin iron-formations. A northwest-trending Early Proterozoic mafic dike swarm cuts the Archean terrane. Records of the Minnesota Department of Natural Resources show that the Deer Lake Complex was previously explored for base-metal deposits. This exploration used detailed commercial aerial electrical and magnetic surveys, in which flightlines were spaced at 1/8-mi intervals. Recent mineral exploration just east of the study area has identified gold mineralization associated with iron-formations, such as those in the southeastern part of the study area.

New USGS aerial data presented here include standard total magnetic field data and data from USGS-developed electromagnetic (EM) very low frequency (VLF) and powerline-source instruments (fig. 1). The sources for VLF signals are distant radio transmitters operating at about 20 kHz. The powerline system measures the electromagnetic fields radiating from powerlines at 60 Hz and harmonic frequencies of 180 and 300 Hz, which penetrate much more deeply than do VLF signals.

The new aerial magnetic data were processed to produce color shaded-relief and first-vertical-derivative maps that enhance subtle bedrock geologic features. Other analysis techniques were used to generate "maxspot" and terrace maps, which can be used to interpret boundaries of subsurface magnetic sources on the basis of interpreted variations in magnetic susceptibility. This type of processing can enhance the variations of magnetic properties of iron-formations, which could indicate areas having structures or alteration zones favorable for gold mineralization.

USGS data from the VLF and powerline EM systems have been reduced to make apparent-resistivity maps of the survey area. In this glaciated terrain, the VLF data generally reflect near-surface (tens of meters) features, such as glacial deposits and shallow high-resistivity bedrock, and are useful in interpretation of more deeply penetrating powerline aerial EM data. In the south-central part of the survey area, eskers are associated with sinuous apparent-resistivity highs. Low apparent resistivities in the northwestern part of the survey area reflect thick glaciolacustrine clay deposits that can attenuate the aerial powerline EM anomalies.

In contrast to the VLF signals, the powerline EM system penetrates hundreds of meters as a result of its lower frequency and is less sensitive to the effects of glacial

Figure 1 (Horton, Smith, and others). The Fairchild Heli-Porter research aircraft operated by the U.S. Geological Survey. The turbo-prop, STOL (short takeoff and landing) aircraft is equipped with magnetic and electromagnetic instruments for airborne geophysical mapping. A very low frequency electromagnetic receiver is mounted in the boom or "stinger." A magnetometer and a powerline-source electromagnetic sensor are mounted in wing-tip instrument pods. Photograph by Herbert A. Pierce in 1989.

overburden. Individual anomalies from the powerline system compare favorably with those mapped by previous commercial aerial EM systems. However, the anomalies detected by the powerline system suggest that the low-resistivity zones in the Deer Lake Complex extend farther to the southwest than those mapped by the commercial EM systems.

Integrated interpretation of the geophysical, geological, and geographical data is facilitated by using geographic-information-system (GIS) software. GIS software can easily display overlays of various data sets to enhance their subtle features; for example, the magnetic and resistivity signatures of the intrusive complexes can be combined to enhance geologic features that may be associated with various types of mineral deposits.

An Overview of Industrial Minerals of the U.S. Atlantic and Gulf of Mexico Coastal Plains

By John W. Hosterman

Industrial minerals are an economically important, though often overlooked, part of the resource base of the United States. Recent advances in deposit models for industrial mineral commodities that include grade and tonnage data now allow attempts at quantitative assessments of industrial mineral resources. This report presents an overview of the industrial mineral resources of the U.S. Atlantic and Gulf of Mexico Coastal Plains States and represents the initial phase of a new effort to assess these resources of the Nation.

Industrial minerals are the principal mineral commodities produced in the following 16 States of the U.S. Atlantic and Gulf of Mexico Coastal Plains: New York, New Jersey, Delaware, Maryland, Virginia, North Carolina, South Carolina, Georgia, Florida, Alabama, Mississippi, Tennessee, Kentucky, Arkansas, Louisiana, and Texas. Approximately $5.4 billion worth of industrial minerals were produced by these States in 1987. Florida was the leading producer, with more than $1.3 billion worth of industrial minerals, and was followed by Georgia and Texas, each with about $800 million.

Sand and gravel are the leading bulk commodities produced in each Coastal Plain State. They have an average market value of about $3.50 per ton. Because of relatively high transportation costs, they are used near mining sites and processing facilities.

The second major commodity is clay, which is also produced in all the Coastal Plain States. The market value for clay ranges from about $4.50 per ton for common clay to $94.50 per ton for high-grade white kaolin. Consequently, some clay products are used locally, whereas high-grade clay products are transported to national or international consumers. Common clay in all the Coastal Plain States is used in the manufacture of face and structural bricks and lightweight aggregate. Georgia and South Carolina are the major producers of high-grade white kaolin, which is used for filling and coating paper and for white dinnerware. Georgia and Florida are the only producers of palygorskite (attapulgite), a type of fuller's earth, which is used chiefly to absorb grease, oil, and animal waste. Mississippi, Alabama, and Texas are the major producers of southern, or nonswelling, bentonite, which is used primarily for bonding foundry sand to make molds for metal castings. Kentucky and Tennessee are the major producers of ball clay, which is used in making pottery, sanitary ware, tile, and ceramics.

About 95 percent of the phosphate rock (89 percent of the P_2O_5) produced in the United States in 1987 was mined in Florida and North Carolina. Other commodities produced from the Atlantic and Gulf of Mexico Coastal Plains were

cement (limestone plus clay) from South Carolina, Florida, Mississippi, Louisiana, and Texas; peat from New Jersey, South Carolina, and Florida; salt from Alabama, Louisiana, and Texas; glauconite from Delaware and New Jersey; industrial sand from Tennessee and Texas; lime and aggregate from Florida and Texas; sulfur from Louisiana and Texas; staurolite, zircon, and rutile from placer deposits in Florida; and gypsum and bauxite from Arkansas.

The future demand for the unique palygorskite-type fuller's earth from Georgia and Florida and for the high-grade white kaolin from Georgia and South Carolina probably will increase at a rate approximately equal to the growth of the Gross National Product. In Florida, however, the phosphate mining industry may decline because of competing land uses (retirement housing, agriculture, tourism) and foreign competition.

Geology and Mineral-Resource Potential of Part of the Northern Safford Basin, Southeastern Arizona

By Brenda B. Houser, J.M. Kruger, *and* Roy A. Johnson

The 100-km-long part of the northern Safford basin between Fort Thomas and Interstate 10 in southeastern Arizona is within the Sierrita-Mogollon corridor being mapped by the U.S. Geological Survey (Leslie Cox and others, this volume). The stratigraphy and structure of the northern Safford basin are inferred to have been controlled in large part by late Cenozoic Basin and Range extension along preexisting low- to moderate-angle faults associated with the Pinaleno Mountains metamorphic core complex.

Basin geometry is revealed by test wells, residual Bouguer gravity maps, seismic-reflection data, and magnetic-anomaly data. These data show that between Fort Thomas on the north and the Graham-Cochise County line on the south, the northwest-trending Safford basin is a half graben, deepest on the southwest side. South of the county line, a west-northwest-trending bedrock high, covered by probably less than 0.5 km of basin-fill sedimentary rocks, crosses the Safford basin. This bedrock high may be associated with either the Stockton Pass fault or the Oak Draw detachment fault.

Seismic-reflection data indicate that the deep southwestern side of the Safford half-graben is bounded by a northwest-trending normal fault with a concave upward fault plane that dips northeast 25°–50° near the range front and has more than 7 km of structural relief. Well data show that, to the northeast across the basin near the Safford mining district, a low-relief surface on andesitic bedrock dips about 5° southwestward beneath basin-fill sedimentary rocks. Seismic-reflection and well data indicate that this surface has low to moderate relief farther to the southwest and dips about 10°–15° southwestward to the deep part of the basin, 10 km east of the Pinaleno range front. Bedrock is at a depth of 355 m in a well 4 km from the Gila Mountains on the northeast side of the basin. In contrast, a test well 4 km from the Pinalenos on the southwest side of the basin penetrated 2,590 m of semiconsolidated sand and gravel but did not reach bedrock.

Seismic-sequence analysis shows that the basin contains two major sedimentary sequences. The older sequence is inferred to have been deposited between 19 and 8 Ma on the basis of tentative correlation with other older sedimentary sequences exposed in the area, including sedimentary rocks of the Black Rock and Oak Draw detachments. The older sequence is 3–4 km thick in the deep part of the basin and wedges out against the bedrock slope on the northeastern side of the basin. Analysis of stacking velocities suggests that the older sedimentary sequence may contain evaporite deposits as thick as 0.5 km in the western half of the basin.

Seismic profiles show that bedding-plane reflectors in the older sequence bend abruptly downward within a few kilometers of the southwestern side of the basin and dip toward the inferred detachment fault. The dip of the bedding planes decreases with decreasing depth and age, overlying beds clearly onlap older, steeper beds, and the thickest part of each successively younger unit in the sequence lies westward of the thickest part of the underlying unit. These relationships suggest episodic eastward displacement of the older sequence during deposition. This displacement may have resulted from periodic reactivation of the Pinaleno detachment fault system during Basin and Range extension. These relationships are not seen in the younger sedimentary sequence.

The younger sedimentary sequence in the basin is probably late Miocene and Pliocene in age. It is as much as 1.5 km thick in a narrow, northwest-trending linear downwarp about 5 km northeast of the Pinaleno Mountains but is probably less than 0.6 km thick throughout most of the basin. The younger sequence overlies the older sequence unconformably in depositional onlap and appears to be relatively undeformed except for tectonic subsidence in the downwarp adjacent to the Pinalenos and minor but widespread normal faulting. Provenance studies of basin-fill sedimentary rocks indicate that the downwarped area was the depositional center of the Safford basin between Thatcher and the Graham-Cochise County line throughout the late Miocene and Pliocene. Fault scarps in Pleistocene and Holocene alluvium above the downwarped zone suggest that subsidence continues to the present.

The entire northeastern margin of the northern Safford basin has high potential for the occurrence of porphyry copper and copper vein deposits similar to those in the Safford mining district. This assessment of a high potential is based on the apparent continuation of the volcanic host rocks beneath a relatively thin cover of basin fill.

Seismic data indicate that the older sedimentary sequence in the northern Safford basin contains thick evaporite deposits that may be as shallow as about 0.6 km near the middle of the basin. However, test wells show that the shallower evaporite deposits generally are interbedded with significant amounts of mudstone. Sparse evidence suggests that there may be ground-water circulation between deep faults and some of the evaporite units. Wells drilled southwest of the Butte fault near the Safford mining district have encountered artesian water as warm as 65 °C that contains more than 2,000 ppm Cl. Base- and precious-metal deposits near detachment faults may have been deposited in the past by similar warm brines derived from evaporite sequences in overlying basin-fill sedimentary rocks. Thus, the Oak Draw and Black Rock detachment faults, which may be at fairly shallow depths along the southwest margin of the northern Safford basin, are proposed as target areas for geochemical study.

Geology and Genesis of the Baid Al Jimalah and Silsilah Tungsten-Tin Deposits, Kingdom of Saudi Arabia

By Robert J. Kamilli

The Baid al Jimalah and Silsilah tungsten-tin deposits are in the northeast Arabian Shield in Saudi Arabia. Baid al Jimalah (569 Ma) is a sheeted greisen-vein tungsten deposit containing minor tin; Silsilah (587 Ma) is a disseminated, tin-greisen deposit containing minor tungsten. Both deposits are spatially, temporally, and genetically associated with highly differentiated, peraluminous granites that intrude Late Proterozoic immature sandstones.

Most of the vein constituents at Baid al Jimalah came from hydrothermal fluids exsolved from a granitic magma during a single cycle of magma intrusion and hydrothermal activity. The hypogene mineralization can be divided into three main periods represented by three sets of veins: early quartz±molybdenite stockwork veins, wolframite- and scheelite-bearing greisen-bordered veins, and late quartz-carbonate-fluorite veins. Early stockwork mineralization occurred at near-magmatic temperatures (580–700 °C); a CO_2-rich, low-density fluid and an H_2O-rich, higher density fluid were present. The greisen mineralization formed from fluids in the liquid state at temperatures mostly between 390 and 430 °C. Late quartz-carbonate-fluorite veins formed from liquids at temperatures at least as low as 238 °C. These temperatures, corrected for pressure by assuming a depth of mineralization of 3.1 km, are 75–80 °C higher than fluid-inclusion filling temperatures. Important volatile constituents of the hydrothermal fluids were H_2O, CO_2, and CH_4.

At Silsilah, four distinct phases of peraluminous granite are recognized throughout a 16-km^2 area. However, only the most differentiated, cupola-shaped intrusions host significant volumes of greisen and related mineralization. Also, a strong correlation exists between the geometry of a given cupola and the intensity of alteration: the most intense apical greisenization is associated with small-diameter cupolas that have steeply dipping contacts.

The paragenetic sequence at Silsilah can be divided into five stages: pegmatite formation, pervasive albitization, pervasive greisenization with deposition of cassiterite, formation of quartz-wolframite veins, and formation of mostly barren quartz veins. Temperatures during albitization were higher than those during pervasive greisenization; mean filling temperatures of fluid inclusions are 412 and 359 °C, respectively. During the first three stages, two aqueous phases were present. Fluid inclusions in wolframite are characterized by two immiscible fluids, one rich in H_2O and the other nearly pure CO_2. The mean filling temperature of H_2O-rich fluid inclusions in the quartz-wolframite veins is 286 °C. Fluid-inclusion salinities at both deposits are generally less than 11 weight percent NaCl equivalent.

The Baid al Jimalah and Silsilah deposits share numerous characteristics with Climax-type molybdenum deposits. Silsilah has aplitic caps and the multiple intrusions typical of Climax-type deposits, but the intrusions are spread out and are not stacked vertically like those at the Climax and Henderson deposits, where overlapping mineralized zones form minable ore. Although Baid al Jimalah has only one cycle of mineralization and lacks the multiple intrusions of Climax-type deposits, the mineral assemblages and sequence of mineralization are almost identical. Only the relative intensities of the processes that caused the various periods of mineralization are reversed.

As of 1990, these deposits are economically marginal. Nevertheless, they do show that many of the processes needed to form an economically viable tin, tungsten, or molybdenum deposit occurred in the Late Proterozoic of the Arabian Shield and that there is significant potential for larger, higher grade deposits in the region.

The Mogollon Mining District, Southwestern New Mexico—Classic Epithermal Silver-Gold Vein Deposits Revisited

By Robert J. Kamilli

The Mogollon mining district in southwestern New Mexico comprises a number of Ag-Au-Cu epithermal veins of early to middle Miocene age. The district is in and near a north-northeast-trending segment of the structural wall of the late Oligocene Bursum caldera known as the Queen fault zone. This fault zone, which itself is mineralized, divides the district into two parts. Most of the past production has come from west-northwest-trending veins west of the Queen fault zone, in an area approximately 3×1.5 km.

Veins within the downthrown block east of the Queen fault zone lack recorded production. Wall rocks of the productive parts of veins are andesitic lava flows intruded by dikes and shallow, domal intrusions of rhyolite. Rhyolitic intrusion breccias are common in structures that later served as sites for vein mineralization.

The district is remarkable for the widespread distribution of hydrothermal breccias that are located in fault zones and throughout the country rock. The breccias range between two end-member types. One type consists of intrusive hydrothermal pebble dikes that contain clasts of wall rock, exotic rock types, and vein material; the matrix typically is quartz rich and contains much comminuted wall rock. The second type of breccia comprises zones in which angular wall-rock fragments have been hydraulically shattered, with little or no translation or rotation; the matrix is composed of quartz, calcite, and chlorite.

The hypogene paragenesis in the district is complex because of repeated episodes of hydrothermal brecciation, mineralization, and faulting; from oldest to youngest, the events were approximately as follows: (1) hydrothermal brecciation and injection of fluids along zones of weakness with concomitant deposition of minerals that form the breccia matrix; (2) deposition of finely banded, crustified, fine-grained quartz with chlorite, adularia, pyrite, electrum, and silver sulfides (principally argentite); (3) deposition of coarse quartz and white, lamellar calcite intergrowths; (4) partial to complete dissolution of calcite and concomitant replacement by quartz (commonly amethystine); (5) deposition of fluorite; (6) deposition of quartz, pyrite, chalcopyrite, and bornite; and (7) deposition of coarse, gray to black calcite. Events 1–5 occurred at least twice, and it is probable that this sequence of events (or parts of it) occurred many times in different parts of the hydrothermal system(s).

Certain district-wide, mineral zoning patterns are apparent, although the overall character of mineralization is similar throughout the district. Copper-bearing mineralization is more common in the north and west parts of the district, and the ratio of calcite to quartz increases with elevation at any given location.

The Mogollon district is currently being explored, and the probability is high for the discovery of additional silver-gold ore bodies with moderate grade and tonnage. Similar potential exists in the analogous Steeple Rock district to the southwest, where erosion was less extensive and a hot spring zone has been preserved above the veins. The presence of a complex, trellislike network of faults, abundant hydrothermal breccias, and copper mineralization at Mogollon suggests strongly that a porphyry-copper system is present at depth, although the age relations of mineralization and exposed igneous rocks need further study.

Mineral-Resource Potential of the Sitka 1° × 3° Quadrangle, Southeastern Alaska

By S.M. Karl, R.J. Goldfarb, K.D. Kelley, D.M. Sutphin, C.A. Finn, A.B. Ford, *and* D.A. Brew

The Sitka 1° × 3° quadrangle encompasses roughly 11,000 km^2 in southeastern Alaska and contains sedimentary, volcanic, and plutonic rocks derived from Paleozoic and Mesozoic arc settings. Paleozoic rocks are assigned to the Alexander and Wrangellia terranes; three different Mesozoic arc assemblages are assigned to the Wrangellia, Alexander, and Chugach terranes, respectively.

In the Sitka quadrangle, the Chichagof mining district, which has a history of activity that dates to the 1800's, was a leading producer of gold in Alaska until 1945. The opening of the Greens Creek mine, only a few kilometers north of the quadrangle, has renewed interest in the base- and precious-metal potential of the region.

Nine tracts have been identified as having potential for certain types of mineral deposits because of the presence of known deposits, specific lithologic types, and geochemical and geophysical anomalies:

(1) mafic-ultramafic synorogenic-synvolcanic Ni-Cu deposits in Tertiary norites on western Chichagof Island and eastern Yakobi Island;
(2) polymetallic veins and porphyry Mo-Cu deposits in Jurassic to Tertiary intermediate to felsic plutons on Chichagof and Baranof Islands;
(3) low-sulfide gold-quartz veins within major fault zones on western Chichagof Island and Baranof Island and along Lisianski Inlet-Hoonah Sound;
(4) U, Th, and rare-earth elements in Paleozoic alkalic plutons on eastern Chichagof Island;
(5) marine evaporite gypsum and hydrothermal gypsum in Mississippian limestone on eastern Chichagof Island;
(6) volcanogenic massive sulfide deposits in Permian and Triassic volcanic and sedimentary rocks on central and eastern Admiralty Island;
(7) epithermal vein and hot-spring Au and Ag deposits in Tertiary volcanic rocks on southern Admiralty Island;
(8) skarn, replacement, and polymetallic vein deposits in Paleozoic carbonate rocks intruded by late orogenic plutons on eastern Chichagof Island and Admiralty Island; and
(9) coal and sandstone U deposits in Tertiary nonmarine clastic rocks on southern Admiralty Island.

In addition, scattered low-temperature geothermal systems are active on Baranof and Chichagof Islands.

The greatest resource potential for the area lies in tracts 3 (gold-quartz veins) and 6 (volcanogenic massive sulfide deposits). The gold-quartz veins, identified in 59 deposits in the western Chichagof gold belt, have yielded 800,000 oz of gold, mostly from the Chichagof and Hirst-Chichagof deposits. These deposits consist of ribbon

quartz filling northwest-trending shears. Gold is accompanied by minor amounts of pyrite, arsenopyrite, galena, sphalerite, pyrrhotite, and chalcopyrite. Fluid-inclusion analyses indicate that ore-forming fluids were low-salinity, aqueous-dominant solutions having trapping temperatures between 190 and 238 °C and trapping pressures in excess of 500 bars; these characteristics suggest a metamorphic origin. The $\delta^{18}O$ values of quartz are 15.7–16.0 per mil, which are typical of mesothermal hydrothermal systems. The δD values of fluid inclusions are equivocal; they range from −55 to −110 per mil.

The main volcanogenic massive sulfide (VMS) deposits are Pyrola and several deposits near Pybus and Gambier Bays. They occur within the Retreat Group in a setting similar to that of the Greens Creek and other Triassic VMS deposits in a 350-km-long belt in southeastern Alaska. At Pyrola, massive basalt with chlorite-carbonate alteration overprinted by sericite-quartz-pyrite alteration is in contact with fine-grained clastic and chemical sedimentary rocks. At this contact, pods of massive pyrite, sphalerite, and Ag-rich barite contain minor associated galena, chalcopyrite, jamesonite, and boulangerite. The deposit is underlain by a siliceous stockwork containing auriferous pyrite, and remobilized mineralization is present in later quartz veins.

Mineral-Resource Assessment of the Goodnews 1° × 3° Quadrangle and Parts of the Hagemeister Island and Nushagak Bay Quadrangles, Southwestern Alaska

By J.E. Kilburn, S.E. Box, R.J. Goldfarb, J.E. Gray, *and* J.L. Jones

Mineral resources were assessed in the Goodnews 1° × 3° quadrangle and in parts of the Hagemeister Island and Nushagak Bay quadrangles, which are north of Bristol Bay in southwestern Alaska. The region is underlain largely by volcanic and sedimentary rocks of the northeast-trending Togiak and Goodnews tectonostratigraphic terranes. Jurassic ultramafic rocks and associated gabbros are most common in the west near Goodnews Bay and Island Mountain. Late Cretaceous to early Tertiary granitic stocks are widespread, though they are more prevalent in the central and eastern parts of the study area. The ultramafic rocks south of Goodnews Bay have yielded high-grade platinum placers in the Salmon River and its tributaries. A few minor gold placers, an isolated sphalerite-rich vein, and an epithermal cinnabar lode are the only other documented mineral occurrences in the study area.

During the mineral assessment of the region in 1975–77, stream-sediment and heavy-mineral-concentrate samples were collected and analyzed. Geochemical data from these media delineate areas characterized by large elemental anomalies. The samples are enriched in Ag, As, Au, Bi, Cr, Cu, Mo, Pb, Sn, W, or Zn (Cieutat and others, 1988).

During the summer of 1990, additional rock samples were collected from several of the areas having geochemical anomalies. In all the revisited drainage basins, strongly oxidized Cretaceous-Tertiary stocks of intermediate composition and associated hornfels zones were observed. During the followup study, geochemical anomalies were identified in the following areas:

(1) the Mt. Waskey-Rainbow basin region—samples of quartz-arsenopyrite-pyrite veins and stockworks in granite and silicified argillite collectively contain maximum concentrations of 1.5 ppm Ag, >10,000 ppm As, 1.4 ppm Au, 1,000 ppm Bi, 2,000 ppm Cu, 15 percent Fe, 50 ppm Mo, 200 ppm Sb, 20 ppm Sn, and 500 ppm Zn;
(2) a drainage basin south of Atshichlut Mountain—samples of silicified, bleached, and Fe-stained argillite with minor pyrite veinlets collectively contain maximum concentrations of 100 ppm Ag, 0.40 ppm Au, >5,000 ppm Ba, 200 ppm Cu, 10 percent Fe, 1.8 ppm Hg, 50 ppm Mo, 300 ppm Pb, and 1,000 ppm Zn;
(3) the Trail Creek-Mt. Oratia area—samples of silicified quartz vein breccia, Fe-stained hornfels containing quartz-tourmaline stockworks, and silicified graywacke with minor quartz veins contain maximum concentrations of 0.7 ppm Ag, 2,000 ppm As, 0.15 ppm Au, >2,000 ppm B, >5,000 ppm Mn, and 150 ppm Sb; and
(4) the west bank of the Togiak River—samples from an oxidized sphalerite-rich vein hosted in pillow basalt contain maximum concentrations of 5 ppm Ag, 0.35 ppm Au, 500 ppm Cd, 700 ppm Cu, 5 percent Fe, 10.4 ppm Hg, >5,000 ppm Mn, and >10,000 ppm Zn.

REFERENCE CITED

Cieutat, B.A., Goldfarb, R.J., and Speckman, W.S., 1988, Analytical results and sample locality map of stream-sediment, heavy-mineral-concentrate, and organic material samples from the Goodnews, Hagemeister Island, and Nushagak Bay quadrangles, southwest Alaska: U.S. Geological Survey Open-File Report 88–591, 188 p., 1 oversize sheet, scale 1:250,000.

Large Sulfide-Sulfate Mounds, Hydrothermal Fluids, and Altered Sediment in Escanaba Trough, Southern Gorda Ridge—Elements of a Mature Hydrothermal System at a Sediment-Covered Spreading Axis

By Randolph A. Koski, Janet L. Morton, Robert A. Zierenberg, Wayne C. Shanks III, Andrew C. Campbell, *and* Keith A. Kvenvolden

Large sulfide-sulfate mounds (lengths measured in hundreds of meters and widths and heights in tens of

meters) and hydrothermal vents are the surface manifestations of past and present hydrothermal activity in the sediment-covered axial valley of Escanaba Trough, southern Gorda Ridge. The slow-spreading (2.4 cm/yr) Escanaba Trough has a morphology like that of the Mid-Atlantic Ridge; a deep (3,300 m) and wide (5 to 15 km) axial valley is flanked by ridges that rise 1,000–1,500 m above the valley floor. The southern two-thirds of the Escanaba Trough is covered by 300–700 m of Quaternary sediment, including turbidites and hemipelagic muds derived from the continental margin of Washington, Oregon, and California. Seismic profiles reveal highly reflective horizons 2–10 m apart that probably represent coarse-grained intervals in the mud-rich uppermost sediment section. Within the axial valley, a series of volcanic edifices spaced 10–15 km apart penetrate the sediment cover; sill-like bodies of basaltic magmas have intruded and dilated the sediment and have resulted in uplift of 1-km-wide sediment hills (fig. 1). Where the edifices breach the sediment pile, pillow lavas and sheet flows are locally extruded onto the sea floor.

Hydrothermal deposits are concentrated along the perimeters of several sediment-covered hills where bounding faults provide cross-stratal permeability (fig. 1). Sand layers between relatively impermeable silt and mud layers in the sediment pile also provide a favorable milieu for lateral fluid flow and subsurface mineralization. The rapid alteration of terrigenous organic matter in the sediment has resulted in the formation of asphaltic petroleum, that is, an admixture of products formed over a wide range of thermal regimes. The insulating effect of the sediment blanket has produced relatively long lived (hundreds to thousands of years) geothermal systems along the ridge axis and relatively large and mature hydrothermal deposits.

The mineral deposits in the Escanaba Trough have been sampled by dredge, gravity core, and submersible; they include large pyrrhotite-rich mounds, polymetallic (Zn-Pb-Cu-As-Sb-Ag) sulfide structures, and barite chimneys. Sulfate (barite+anhydrite) sinters are forming around active vents (maximum measured fluid temperature = 220 °C). Compared to massive sulfide deposits formed at sediment-starved ocean ridges, sulfide samples from the Escanaba Trough sites are enriched in As (to 2.8 percent), Pb (to 14 percent), Ag (to 680 ppm), Bi (to 820 ppm), Sb (to 8,700 ppm), and Sn (to 1,500 ppm). Au occurs in amounts up to 10.1 ppm in Cu-rich samples. Pyrrhotite is the predominant mineral phase, but isocubanite, sphalerite, marcasite, and galena are abundant in some samples. Minor phases include arsenopyrite, löllingite, stannite, boulangerite, native bismuth, and alabandite. Sulfur-isotope values for sulfides range from −0.7 to +11.6 per mil; the lighter values indicate the presence of bacteriogenic sulfide whereas heavier values may reflect sulfide derived from reduction of seawater sulfate in the sediment pile. Compositional characteristics of the hydrothermal fluids (near-neutral pH; high alkalinity; high concentrations of NH_4^+, Li, Rb, Cs, B, I, and Tl; high $^{87}Sr/^{86}Sr$ ratios; low concentrations of H_2S, Fe, Mn, Cu, Zn, Cd, and Ag; low values for $\delta^{11}B$) are consistent with extensive interaction between hydrothermal fluid and terrigenous sediment that contains a small amount of organic matter.

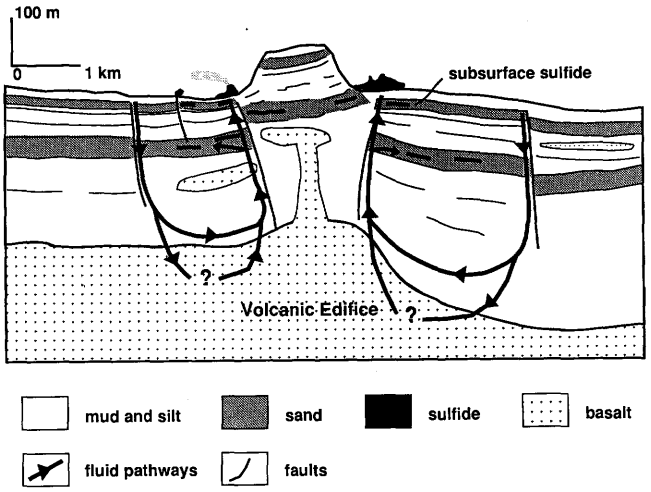

Figure 1 (Koski and others). Schematic cross section showing the relations among a sediment-covered volcanic edifice, an uplifted sediment hill, hydrothermal circulation, and location of sulfide deposits in Escanaba Trough. Faults bounding the sediment hill provide cross-stratal permeability for upwelling hydrothermal fluids and focused flow for deposition of sea-floor sulfide-sulfate mounds. Sand layers in the sediment pile provide favorable permeability and porosity for lateral fluid flow and subsurface sulfide deposition.

Sediment samples recovered in gravity cores are characterized by Mg metasomatism and the formation of smectite and chlorite. The alteration of fine-grained sediment to nearly monomineralic aggregates of clinochlore (Fe/(Fe+Mg) = 0.21) was accompanied by an increase in Mg from 4 to 25 weight percent and the nearly complete removal of Na, K, Rb, Ca, and Sr. Oxygen-isotope fractionation temperatures calculated for smectite (181–235 °C) and chlorite (203–223 °C) are consistent with measured temperatures of vent fluids. The alteration of surficial sediment at temperatures near 200 °C took place during the mixing of upwelling hydrothermal fluid with shallowly circulating seawater.

Natural Aggregates—Mining Challenge of the 1990's

By William H. Langer

Crushed stone and sand and gravel are the two main sources of natural aggregates. These essential construction materials frequently are used interchangeably with one another throughout the United States. U.S. aggregate pro-

duction in 1989 had a value of approximately $8.5 billion (U.S. Bureau of Mines, 1990); thus, aggregates are among the leading nonfuel mineral commodities in the United States. Their value by far exceeds those of iron ore ($1.7 billion), copper ($4.4 billion), or the precious metals, including gold, silver, and the platinum-group metals (combined production in 1989 worth $4.3 billion).

In the United States, natural aggregates are not universally available for use. In addition to the highly visible land-use and zoning conflicts, the aggregate industry is faced with a variety of source and utilization problems. Some areas are devoid of sand and gravel, and potential sources of crushed stone may be covered with sufficient unconsolidated material to make surface mining impractical. In other areas, aggregates do not meet the physical-property requirements for certain uses, or they contain mineral constituents that react adversely when used in concrete. Proper long-range planning based on an understanding of aggregate availability and physical properties can help assure adequate supplies. In order to obtain an overview of the availability of natural aggregates, two 1:5,000,000-scale maps (Langer, 1988) were prepared for the conterminous United States: (1) a map showing the major potential sources of sand and gravel and (2) a map showing the distribution of selected types of bedrock normally considered for use as crushed stone.

Natural aggregates are distributed throughout the United States in a variety of geologic environments. The map showing potential sources of sand and gravel is divided into geographic regions based, in general, on geologic history and physiography. The mode of distribution of sand and gravel is similar within a region and is fairly distinct from that of other regions. Within each of these regions, major areas of sand and gravel resources are shown.

Crushed-stone aggregates are derived from a wide variety of parent bedrock materials. Limestone and other carbonate rocks account for approximately three-quarters of the rocks used for crushed stone; granite and other igneous rocks make up most of the remainder. Limestone deposits are widespread throughout the Central and Eastern United States and are scattered in the West. Granites are widely distributed in the Eastern and Western United States and in the Lake Superior region; they are exposed in only a few other places in the midcontinent. Igneous rocks (excluding granites) are largely concentrated in the Western United States and in a few isolated localities in the East.

Aggregates are in short supply or of poor quality in approximately one-third of the conterminous United States. In the High Plains, aggregate is largely restricted to river channels and terraces and commonly lacks coarse fractions. Large areas of glaciolacustrine deposits in Michigan and North and South Dakota lack significant deposits of sand and gravel. The seaward sections of the Coastal Plain are primarily composed of sand that commonly lacks coarse fractions. Much of the Mississippi River alluvial plain and loessial upland lack significant deposits of sand and gravel. In some areas, aggregates contain mineral constituents that limit their use. When some aggregates are used in concrete, alkali-silica reactions or alkali-carbonate reactions cause the concrete to break up. When other aggregates are used in bituminous mixes, reactions between minerals and water may cause the bituminous film to be stripped.

Identification of areas having adequate sources of aggregate represents only the first step in commercial exploitation. In areas having limited aggregate sources, geophysical or other remote-sensing techniques can be used to help locate deposits. Geochemical analyses and geologic mapping can identify areas where deleterious constituents are absent from the aggregate source. Research can be conducted on processing techniques to improve aggregate quality and on methods to improve concrete and bituminous products. Zoning, regulations, and competing land uses further restrict or preclude mining. The problems associated with aggregate availability, aggregate quality, and socio-economic restrictions present a challenging environment for the development of new techniques and methodologies.

REFERENCES CITED

Langer, W.H., 1988, Natural aggregates of the conterminous United States: U.S. Geological Survey Bulletin 1594, 33 p., 2 pls.

U.S. Bureau of Mines, 1990, Mineral commodity summaries, 1990: 199 p.

Heavy-Mineral Placers at the Fall Zone

By Curtis E. Larsen

Placers are concentrations of heavy minerals sorted by density and shape through fluvial, littoral, and eolian processes. The specific gravity and hydraulic equivalence of a mineral relative to quartz determine the type of sedimentary deposit in which it is found; for example, a grain of gold or a titanium mineral, such as ilmenite or rutile, in the very fine sand range (0.06–0.12 mm) tends to concentrate in deposits having dissimilar grain sizes. Gold of this size occurs with very coarse quartz sand (1.0–2.0 mm) or gravel. Very fine grained titanium minerals, as well as zircon and monazite, typically are deposited with fine quartz sand (0.13–0.25 mm).

In a river system, the size of the sediment it carries and subsequently deposits depends on its discharge, slope, depth, and velocity. Sediments with limiting grain sizes that host placers are deposited in predictable reaches of the system where slope and velocity decrease. In the Southeastern United States, rivers draining the eastern Appalachian Mountains commonly decrease in gradient and velocity until they reach the outer edge of the Piedmont Lowlands.

Here, gradients typically steepen abruptly at structural boundaries and then flatten at the Fall Zone before the rivers enter the Coastal Plain. The abrupt change in river dynamics preferentially deposits coarse-grained sediments near the Fall Zone and medium and fine sand at the edge of the Coastal Plain. Depending on the mineralogy of upstream source terranes, the Fall Zone may have potential for placer gold, and the inner edge of the Coastal Plain may have potential for monazite, zircon, rutile, and ilmenite.

The effect of stream gradient changes at the Fall Zone has geologic longevity; as an example, placer gold is found in the basal Triassic gravels of the North Carolina Mesozoic basins in settings downstream from the Carolina slate belt. Similarly, small amounts of placer gold are reported from the basal units of Cretaceous and Cenozoic fluvial deposits near the Fall Zone and at the innermost edge of the Coastal Plain. Upper Cretaceous fluvial sediments near the Fall Zone in Georgia and South Carolina contain small concentrations of monazite, zircon, rutile, and ilmenite. Finer grained Cretaceous upper delta and delta facies deposited on the basement tend to concentrate less dense, but hydraulically equivalent, heavy-mineral suites characterized by staurolite, kyanite, amphiboles, pyroxenes, epidote, and rutile. Similar gradation of heavy minerals is present within the Cenozoic fluvial facies of the Coastal Plain.

Although a qualitative relation between certain heavy-mineral suites and fluvial deposits of the inner Coastal Plain has been known for some time, the role of stream gradient has not been critically examined. Detailed geomorphologic and stratigraphic research in the Fall Zone region will allow more effective predictive models of placer mineral occurrence to be developed. Drainage-basin analysis utilizing stream discharge, gradient, channel width, and depth can be linked with geologic studies of source terranes to target river reaches that have sediment sizes conducive to concentration of specific heavy-mineral suites. Such studies will allow the extensive data base of streamflow characteristics in the Southeastern States to be combined with economic geologic knowledge so that heavy-mineral prospecting techniques in the Fall Zone region can be refined.

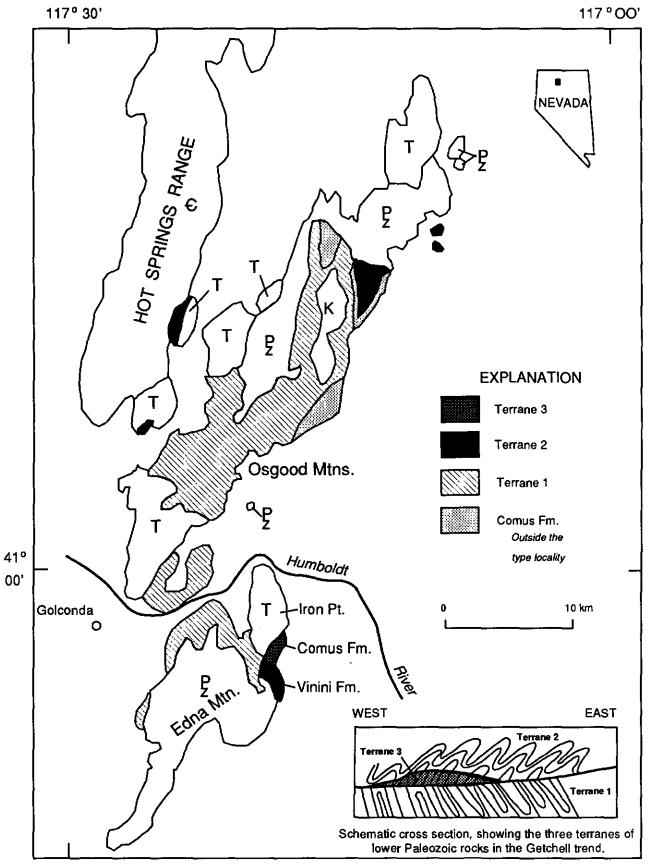

Figure 1 (Madden-McGuire and Marsh). Simplified geologic map of the Osgood Mountains, Edna Mountain, and surrounding areas, showing outcrops of rocks that definitely fit into terrane 1 (Preble Formation and Osgood Mountain Quartzite), terrane 2 (Vinini and Valmy Formations), and terrane 3 (Comus Formation in its type locality) and rocks currently mapped as the Comus Formation in the Osgood Mountains, outside the type locality. Abbreviations: €, Upper Cambrian sedimentary rocks; P_z, upper Paleozoic rocks; K, Late Cretaceous granodiorite; T, Tertiary volcanic rocks.

Recognition of Distinct Terranes in Lower Paleozoic Host Rocks in the Getchell Gold Trend, Humboldt County, Nevada

By Dawn J. Madden-McGuire *and* Sherman P. Marsh

The lower Paleozoic rocks that host gold deposits along the Getchell gold trend in Humboldt County, Nev., represent several allochthonous blocks (fig. 1) rather than a simple sequence of continuous deposition. We are calling the allochthons "terranes," a term used in a descriptive sense. Evidence for allochthonous terranes in this area includes fault boundaries and differences in age, rock type, and structural style among several rock packages.

The two most widespread and distinct terranes in the area are (1) intensely deformed and uniformly regionally metamorphosed marine rocks (Lower Cambrian Osgood Mountain Quartzite, Lower Cambrian to Lower Ordovician Preble Formation, and some of what is currently mapped as the Comus Formation) and (2) generally less deformed chert, clastic sedimentary rocks, and volcanic rocks (Ordovician Valmy and Vinini Formations). Bedding and foliation in terrane 1 dip predominantly eastward and folds verge westward, whereas folds in terrane 2 verge southeastward.

Lower Paleozoic rocks in this area and their contact relations are regionally significant. Exposures of terranes 1 and 2 might preserve evidence for Paleozoic metamorphism and deformation. Terrane 1 is intensely folded and region-

ally metamorphosed at map and outcrop scales. The same rock type, structural style, and predominance of west-verging folds (and east-dipping foliation) are consistently displayed along the strike of terrane 1 for 60 km from Anderson Canyon (on the northwestern flank of the Osgood Mountains) southward past Hot Springs Ranch (on the east side of the Sonoma Range). Regional deformation and metamorphism of terrane 1 might have been post-Early Ordovician and pre-Middle Pennsylvanian, because Lower Ordovician strata occur in terrane 1, and the conglomerate subunit of the Middle Pennsylvanian Highway Limestone at Edna Mountain contains clasts of phyllite and reddish limestone of the Preble Formation. The Upper Permian Edna Mountain Formation contains lithic fragments thought to be Preble phyllite (terrane 1) and overlies the Preble Formation along a contact mapped as depositional at Edna Mountain; these features further suggest that deformation and metamorphism of terrane 1 occurred in Paleozoic time. In the northern Osgood Mountains, outcrops of terrane 2 are overlain depositionally by the Middle Pennsylvanian to Upper Pennsylvanian or Lower Permian Etchart Limestone. This contact suggests that terrane 2 was emplaced before Middle Pennsylvanian time. The age of the low-angle structure separating terranes is uncertain; the limited geologic evidence available suggests that it is Paleozoic, but no Mesozoic sedimentary rocks are preserved to overlie the structure and confirm a Paleozoic age.

The Comus Formation, which is Middle Ordovician in age in its type locality at Edna Mountain (south of Iron Point), might represent a third terrane (fig. 1) situated structurally between terranes 1 and 2. Use of the name "Comus Formation" outside the type locality (particularly in the Osgood Mountains) has created confusion and needs reevaluation. Some of the rocks currently mapped as Comus Formation belong to the other terranes.

Areas of Mineral-Resource Favorability (with Emphasis on Gold and Chromite) in the Anchorage 1° x 3° Quadrangle, Southern Alaska

By D.J. Madden-McGuire *and* G.R. Winkler

The U.S. Geological Survey conducted geologic, geochemical, and geophysical investigations to determine areas of mineral-resource favorability in the Anchorage 1°×3° quadrangle. The quadrangle contains three major fault-bounded terranes that were accreted between mid-Cretaceous and early Tertiary time. The Peninsular terrane, bounded on the south by the Border Ranges fault system, comprises intrusive and extrusive phases of an early Mesozoic intraoceanic magmatic arc and late Mesozoic marine sedimentary rocks deposited in forearc basins. The Peninsular terrane is intruded by voluminous composite plutons of Late Cretaceous and Paleocene age. Paleocene and younger nonmarine volcanic and coal-bearing sedimentary rocks overlap both the Peninsular terrane and the Chugach terrane to the south. The Chugach terrane consists of Mesozoic polygenetic melange and accreted wedges of Upper Cretaceous flysch and minor metatuff. South of the Contact fault, the Prince William terrane consists of an accreted Paleogene deep-sea fan complex interbedded with minor tholeiitic basalt.

Gold, which is currently the commodity of greatest economic interest, has been produced from gold-quartz veins and related placer deposits in the Peninsular and Chugach terranes, primarily in the Willow Creek and Girdwood mining districts (fig. 1). The two areas that include the historic mining districts are assigned the highest and most certain levels of potential for gold-quartz veins and gold-placer deposits in the quadrangle.

In the Willow Creek district, high-sulfide gold-quartz-carbonate veins cut a pluton dated at 79–72 Ma (recording multiple stages of alteration) and adjacent pelitic schist. A fault contact between these host rocks might have served as a conduit for mineralizing fluids (mineralization occurred at 66 Ma and at 57–55 Ma). The extent of the high-potential area is defined by mineral deposits, geologic contacts, and panned concentrates that contain gold and are enriched in As, Ag, Sb, and Pb; stream sediments have anomalous As contents.

In the Girdwood district, Au and Ag are concentrated in quartz-carbonate veins within joints and shears in greenschist-facies metasedimentary rocks of Cretaceous age and Eocene quartz diorite (53 Ma). Mineralization is younger than 53 Ma. Elsewhere in the Valdez Group (in adjacent quadrangles), gold-quartz veins are younger than 34 Ma. Panned concentrates from Crow Creek and surrounding drainages contain gold and locally are enriched in Ag, As, and Sb.

In Prince William Sound, areas around Harriman Fiord and the Coghill River have been assigned a moderate resource potential because gold-quartz veins are exposed in a mine, in prospects, and in outcrop. Additional areas of moderate potential for gold-quartz veins in the Chugach terrane have been identified on the basis of the presence of gold in panned concentrates and, locally, in mineralized outcrops. A particularly large area of moderate potential for gold-quartz veins is between Mount Marcus Baker and the Border Ranges fault.

Podiform chromite occurs in the Peninsular terrane within two fault-bounded ultramafic complexes near Eklutna and in the upper part of Wolverine Creek on the north side of the Border Ranges fault (fig. 1). Cumulate chromitite, having a moderate potential for Cr_2O_3, occurs within deformed cumulate dunite and wehrlite. Adjacent outcrops of ultramafic rocks have a moderate potential for Cr_2O_3 but a lower level of certainty. Chromitite has not been observed in the serpentinized ultramafic rocks that

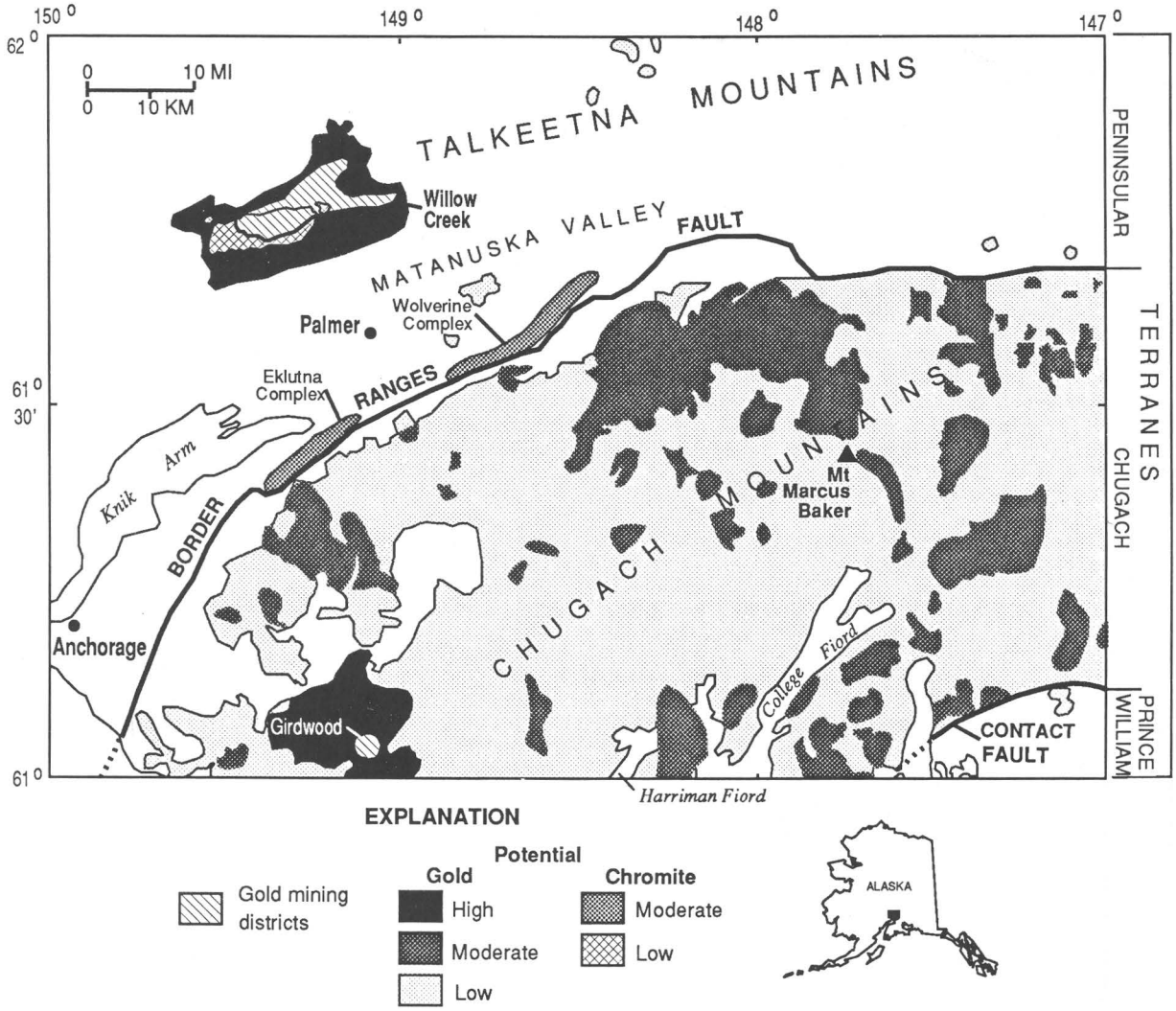

Figure 1 (Madden-McGuire and Winkler). Areas of favorability for gold-quartz veins and podiform chromite in the Anchorage 1° x 3° quadrangle, southern Alaska. Wolverine and Eklutna Complexes of Burns (1985).

occur within pelitic schist in the Willow Creek district, and nearby stream sediments are not enriched in chromium; the area of exposed serpentinite is therefore assigned a low potential for Cr_2O_3.

The Peninsular terrane includes areas that have low potential for porphyry-copper deposits, copper-silver skarns, volcanic-rock-hosted stratiform and stratabound mineralization, and uranium mineralization associated with granitic rocks. Coal has been mined from the Chickaloon and Tyonek Formations north of the Border Ranges fault. The Chugach and Prince William terranes include areas of moderate and low potential for base-metal veins, massive sulfide deposits, and uranium mineralization. A moderate potential for base metals has been assigned to a prospected area in the southeastern corner of the quadrangle between Kadin and Miners Lakes, where veins and massive sulfide occurrences in the Prince William terrane are locally enriched in Zn, Cu, Pb, and Ag, and panned concentrates contain chalcopyrite and sphalerite.

REFERENCE CITED

Burns, L.E., 1985, The Border Ranges mafic and ultramafic complex, south-central Alaska—Cumulate fractionates of island-arc volcanics: Canadian Journal of Earth Sciences, v. 22, no. 7, p. 1020–1038.

Mineral-Resource Assessment of the Altiplano and Cordillera Occidental, Bolivia—A Progress Report

By Sherman P. Marsh, Dan H. Knepper, Jr., Keith R. Long, *and* John W. Cady

In early 1990, the U.S. Geological Survey (USGS) and the Geological Survey of Bolivia (GEOBOL) initiated a Trade Development Program (TDP), which is funding a collaborative mineral-resource assessment of the 150,000-km^2 Altiplano and Cordillera Occidental, Bolivia. This area of Bolivia ranges between 3,500 and 6,000 m in elevation and consists primarily of Tertiary volcaniclastic sedimentary rocks and volcanic rocks.

The goal of the joint project is to produce a mineral-resource assessment of the Altiplano and Cordillera Occidental by using innovative digital techniques. Geologic maps are vital to the assessment. Geologic data were obtained from paper maps compiled by GEOBOL geologists at 1:250,000 scale; they were digitized and converted into ARC/INFO files. The ARC/INFO geographic information system (a product of Environmental Systems Research Institute (ESRI), Inc., Redlands, Calif.) was used to produce colored digital geologic maps at 1:250,000 scale and a regional colored geologic map at 1:500,000 scale.

Data on mineral deposits, mines, alteration zones, salars, and other features related to mineralization were compiled from hundreds of unpublished Bolivian reports, from observations made during field investigations, and from the published literature. The area has a long history of mostly small-scale mining activity. Deposit locations were digitized from large-scale topographic maps by using the USGS GSDIG software. USGS GSMAP software was used to generate a map showing the locations of mineral deposits.

Thirteen Landsat Thematic Mapper (TM) scenes have been digitally processed to assist in site identification for field examination and in preparing a map of the entire Altiplano showing areas of possible hydrothermal alteration. Images prepared at a scale of 1:250,000 include (1) a simulated natural color (SNC) composite image that shows the terrain much as it would appear on color air photographs and (2) a color infrared (CIR) composite image that depicts the sparse vegetation cover in shades of red and enhances the expression of geologic structure and geomorphic features. The SNC and CIR images are digital contrast stretched for color display and are enhanced by a nondirectional edge technique to sharpen the display of the high-frequency components of the image data. These images are useful as index maps of the region and for general geologic and structural mapping.

Ratio images have been prepared by dividing the data numbers (DN) of each picture element (pixel) in one band of data by the DN of the corresponding pixels of another band of data. TM ratio images provide information about the mineralogic composition of exposed surface materials. A color-ratio composite (CRC) image shows the distribution of two classes of minerals: (1) iron oxides and hydroxides and (2) minerals that contain hydroxyls and carbonates. Both groups include minerals formed during hydrothermal alteration or derived from the weathering of hydrothermally altered rocks. Because vegetation produces a spectral response similar to those of the clays, hydrated sulfates, and carbonates, a version of the CRC image has been prepared with vegetation, water, shadows, clouds, and snow masked from the CRC image. This masked color-ratio composite image is the fundamental image used for targeting areas of possible hydrothermally altered rocks in the Altiplano.

Aeromagnetic data, which were compiled from existing surveys and from a GEOBOL commercial survey, have been processed and analyzed. The resulting low-level, 2-km-line-span data are available for over 60 percent of the Altiplano and Cordillera Occidental.

Mercury-Sulfur-Gypsum Mineralization at Crater, California—A Suggestion of Gold Mineralization at Depth

By Sherman P. Marsh, Chester T. Wrucke, *and* Kevin P. Corbett

A large deposit of native sulfur and gypsum at Crater, Calif., in the Last Chance Range of the northern Death Valley region is the surface expression of a hot spring system that has potential for concentrations of gold at depth. Hydrothermal alteration characterized by the elemental suite of As, Sb, Hg, and Au and nearby concentrations of mercury at the El Capitan mine are indicators of possible gold mineralization at Crater.

The sulfur deposit at Crater is mainly in limestone of the Carrara Formation of Cambrian age in a structurally complex setting in the upper plate of the Last Chance thrust. At Crater, upper plate strata are Cambrian carbonate and siliciclastic rocks that were emplaced above Mississippian phyllitic and coarse clastic rocks, probably in the Late Permian or Triassic. Probable renewed offset along northeast-trending faults in the Tertiary helped prepare the ground for a postulated igneous intrusion in the Pliocene. Sulfur-gypsum alteration is exposed intermittently for a distance of nearly 2 km along the northeast-trending faults. Exposures of jasperoid and quartz breccia show evidence of multiple stages of brecciation. Available evidence, including K-Ar ages from a nearby basalt-rhyolite suite, indicates that hot spring discharge to the surface may have begun in the Pliocene and continued into the Quaternary.

Native sulfur and gypsum deposits at Crater resulted from intense alteration in a vapor-dominated acid sulfate hot spring system. This system developed as the postulated igneous intrusion rose to shallow crustal levels in a drainage basin having a small capacity for ground-water recharge. Intensely altered rock high in the system was depleted in most metals but retained traces of the gold geochemical suite, as evidenced by gold values as high as 1.7 ppm in a small quartz vein near the El Capitan mine. Much of the limestone host rock has been altered to silica minerals, sulfur, and gypsum. Samples of siliceous sinter give X-ray patterns for quartz and cristobalite. Most of the mercury was deposited in peripheral areas because of its high volatility; the mercury deposit at the El Capitan mine is 3.5 km north of Crater. Significant concentrations of gold, if present, would be at depth in a zone where boiling took place in late Tertiary hydrothermal systems.

Regional Aeromagnetic and Gravity Data Bases for Studies Centered on the Idaho Batholith and Challis Volcanic Field

By Anne E. McCafferty *and* Viki Bankey

Recently compiled aeromagnetic and gravity data for most of Idaho and adjoining parts of Montana, Wyoming, Oregon, and Washington (an area bounded by lats 42° and 47° N. and longs 110° and 118° W.) were used to produce a series of maps in support of investigations of the mineral-resource potential of National Forest Wilderness Study Areas in Idaho. An immediate objective of the project was to assemble all available magnetic and gravity data into digital composite data sets. The aeromagnetic compilation includes a synthesis of digital data acquired from more than 60 separate surveys flown at different times with varied flight elevations, flight spacings, and data-reduction procedures. The complete Bouguer gravity anomaly data were compiled using data obtained from 32,152 stations extracted from State and Federal Government gravity data bases and from data collected as part of university theses and dissertations. The initial products include an aeromagnetic anomaly grid at a datum level of 305 m above terrain, a complete Bouguer gravity anomaly grid, and an isostatic gravity anomaly grid. All are being prepared in color at a scale of 1:1,000,000.

A second objective of the project was to apply analytical methods and digital filtering to enhance selected attributes of the anomaly fields and provide new interpretive information. One recently developed technique, called the "terrace method," has been applied to the aeromagnetic and isostatic gravity data in an effort to map geologic terranes and structures delineated by physical-property boundaries as calculated from the anomalous fields. The resulting products are a terrace-magnetization map and a terrace-density map.

The terrace-magnetization map is roughly equivalent to a geologic map of magnetic rocks; in places, the edges of the magnetization units can be equated with mapped faults and other lithologic discontinuities. The magnetization domains themselves generally correspond to geologic bodies, such as buried or exposed intrusions or volcanic strata that contain enough magnetic minerals to produce discrete anomalies.

The terrace-density map mimics a geologic map by theoretically outlining domains having sufficient density contrast to produce gravity anomalies. These domains may or may not correspond to real geologic formations. The terrace method is particularly helpful in delineating low-amplitude features not clearly visible on the original magnetic and gravity maps.

The third and culminating objective of the project is to integrate the aeromagnetic and gravity data with geologic, geochemical, and other geophysical data in order to refine interpretations of the structural and lithologic setting of the Idaho batholith and Challis volcanic field and to assess resource potential. This phase of the project is currently in progress.

Application of Grade and Tonnage Models to the Development of Strategies for Mineral Deposit Exploration

By Gregory E. McKelvey *and* James D. Bliss

Mineral deposit models developed by the U.S. Geological Survey (Cox and Singer, 1986) give the characteristics and the range in size and tenor of 71 types of mineral deposits. In order to construct these models and to compare tonnage and metal contents of the models, the following criteria must be met: (1) mineral deposits must be assigned specific deposit types by using geologic knowledge, (2) adequate data must be available to define grade and tonnage models, and (3) for each deposit type, a median grade and a median tonnage must be identified. An example of an application of these methods is presented by Bliss and others (1990). They identified exploration opportunities suitable for small-scale mining by using median deposit sizes for the 71 deposit types.

The relative importance of each deposit type can be demonstrated by using the amount of contained metal of the median deposit. Contained metal is computed from the median tonnage and median grade, and grade and tonnage are assumed to be independent variables. For each deposit type, the amount of contained metal of the median deposit

is compared to the estimated world annual production in 1989 (U.S. Bureau of Mines, 1990) to gauge its relative importance. In our study, only base and precious metals are considered. For a particular metal to be considered, at least half the deposits of the specific deposit type must report a grade for that metal. This information can be used to adjust exploration efforts to search for the deposit type best suited to the investor.

Twenty of the 71 deposit types under consideration have a gold grade reported for their median deposits. In two of the deposit types, the contained gold of the median deposits exceeds 1 percent of the world's annual gold production; they are the hot-spring Au-Ag deposit type (1.1 percent of world production) and the porphyry Cu-Au deposit type (2 percent). Sixteen deposit types have silver grades in at least half their deposits. Four deposit types have median deposits with amounts of contained silver greater than 1 percent of the world's annual silver production (table 1). Of these four, the median porphyry Cu-Mo deposit type contains the most silver—4.3 percent of the world's annual production.

Fifteen deposit types have median deposits that contain copper, seven have median deposits that contain lead, and nine have median deposits that contain zinc. Median deposits of four of the deposit types with contained copper have copper contents greater than 5 percent of the annual world production (table 1); the greatest amount of contained copper is in the median deposit of the porphyry Cu-Mo deposit type (24 percent of world production). The median deposits of six of the seven deposit types with contained lead have amounts of lead exceeding 1 percent of the world's annual lead production (table 1); the largest amount of contained lead is in the median deposit of the sedimentary exhalative Zn-Pb deposit type, which contains 12 percent of the world's annual production of lead. Three of the nine deposit types with contained zinc, Southeast Missouri Pb-Zn & Appalachian Zn (20 percent), sedimentary exhalative Zn-Pb (12 percent), and Pb-Zn skarns (1.2 percent), have amounts of zinc exceeding 1 percent of the world's annual zinc production.

In general, the median deposits of the porphyry Cu, porphyry Cu-Au, and porphyry Cu-Mo deposit types have two orders of magnitude more copper, gold, and silver than the median deposits of other deposit types. Porphyry Cu deposits may also be sources of cobalt, platinum, molybdenum, and rhenium. Sedimentary-exhalative and carbonate-hosted deposits may also contain recoverable zinc, lead, and cadmium.

Although the amount of contained metal of a median deposit can be used to rank the relative importance of its deposit type, exceptions exist. For example, there are several large deposits of the Kuroko massive sulfide deposit type that produce zinc. These individual deposits account for a significant amount of the world's annual zinc production. However, the median deposit of the Kuroko massive sulfide deposit type does not contain zinc because fewer than half of the deposits have a reported zinc grade. Some deposit types of major importance (for example, the Witwatersrand gold type) do not yet have grade and tonnage models constructed for them; therefore, they cannot be evaluated.

Table 1 (McKelvey and Bliss). Estimated contained metals in the median deposits for selected deposit types defined by Cox and Singer (1986)

[Values are percentages of world annual production (1989) for each commodity as reported by the U.S. Bureau of Mines (1990). Only deposit types whose median deposits have amounts of contained metal greater than 1 percent of world annual production are given]

Deposit type	Contained metal in median deposits as a percentage of 1989 world production				
	Au	Ag	Cu	Pb	Zn
Hot spring Au-Ag	1.1	—	—	—	—
Porphyry Cu-Au	2.0	—	5.7	—	—
Porphyry Cu-Mo	—	4.3	24	—	—
Distal disseminated Ag-Au	—	2.2	—	—	—
Polymetallic replacement	—	1.9	—	2.7	—
Creede epithermal veins	—	1.3	—	1.0	—
Porphyry Cu	—	—	8.6	—	—
Sedimentary-hosted Cu	—	—	5.2	—	—
Sedimentary exhalative Zn-Pb	—	—	—	12	12
Southeast Missouri Pb-Zn & Appalachian Zn	—	—	—	8.8	20
Sandstone Pb-Zn	—	—	—	3.4	—
Pb-Zn skarns	—	—	—	1.1	1.2

REFERENCES CITED

Bliss, J.D., McKelvey, G.E., and Allen, M.S., 1990, Applications of grade and tonnage deposit models; the search for ore deposits possibly amenable to small-scale mining: U.S. Geological Survey Open-File Report 90–412, 24 p.

Cox, D.P., and Singer, D.A., eds., 1986, Mineral deposit models: U.S. Geological Survey Bulletin 1693, 379 p.

U.S. Bureau of Mines, 1990, Mineral commodity summaries, 1990: 199 p.

A Reconnaissance Study of Gold Mineralization Associated with Garnet Skarn at Nambija, Zamora Province, Ecuador

By Gregory E. McKelvey *and* Jane M. Hammarstrom

A group of gold deposits in southeastern Ecuador, near the town of Nambija, has recently become the focus of intensive mining activity because of extremely high gold grades (unconfirmed reports of 50 g/t or more). The deposits at Nambija and at other prospects in the district are hosted by a sequence of sedimentary and volcanic rocks that form a xenolith within alkalic phases of the Jurassic Zamora batholith. Mineralization appears to be localized within a structural breccia zone that crosscuts a complex calcic skarn assemblage within the xenolith. The xenolith is composed of various lithologies (limestones, shales, sandstones, tuffs, and flows), all of which have been affected to some degree by skarn alteration. Although the nature of the host rocks has exerted some control on mineralization, high-grade ore is concentrated along north-northeast-trending breccias, faults, and dikes that crosscut the stratigraphy and skarn alteration. In addition, the strong linear trend of workings in the district suggests a major structural control on mineralization.

Chemical analyses for a suite of 15 representative samples of skarn, porphyry endoskarn, breccia, tuff, and intrusive rocks show the following: (1) highest gold values are observed for garnet-rich skarn samples (Au in skarn, <0.002–47.0 ppm; Au in breccia, trace to 0.034 ppm; and Au in altered igneous rock, ≤0.002 ppm); (2) gold/silver ratios are high; silver was detected (3 ppm Ag) in gold-rich massive garnetite skarn; all other samples contain <2 ppm Ag; (3) copper contents are quite variable but are generally low (2–745 ppm Cu); samples that contain 1 ppm Au or more have extremely low Cu/Au ratios (0.04–208); and (4) none of the samples is enriched in elements commonly associated with gold skarns, such as Bi, As, or Te.

Coarse-grained veinlets and pods of electrum ($Au_{77}Ag_{23}$) are associated with quartz veinlets in massive garnet skarn (fig. 1) that has undergone little retrograde alteration. In high-grade samples, garnet is much more abundant than pyroxene, and sulfides are rare. Chalcopyrite, pyrite, sphalerite, galena, arsenopyrite, hematite, and magnetite are recognized in the Nambija deposits; electrum does not appear to be intimately associated with sulfides in the samples studied so far. Gangue minerals include zoned anisotropic garnets ($Ad_{34}Sp_4Gr_{62}$ to $Ad_{62}Sp_3Gr_{35}$), pods of yellow, isotropic pure andradite, pyroxene ($Hd_{22-28}Di_{66-72}Jo_6$), epidote, actinolite, potassium feldspar, apatite, chlorite, calcite, quartz, goethite, and clay. Feldspar phenocrysts in porphyry endoskarn are altered to nearly pure albite and orthoclase.

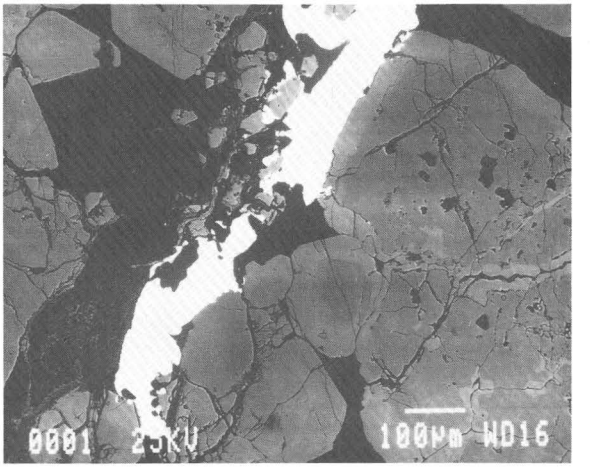

Figure 1 (McKelvey and Hammarstrom). Backscattered electron image taken with a scanning electron microscope of high-grade gold ore in garnet skarn from Nambija, Ecuador, showing electrum veinlets (white), quartz (black), and zoned garnets. Iron content of garnet increases from core (dark gray) to rim (light gray).

The Nambija deposits share some characteristics of relatively oxidized gold skarns (for example, volcaniclastic host rock, mineralogy). More extensive studies are needed to determine the nature of these important deposits and to design exploration strategies for the region.

Hydrogeochemical Exploration in Areas of Thin Glacial Overburden, Northeastern Minnesota

By W.R. Miller, W.H. Ficklin, *and* J.B. McHugh

Water can be used as a medium for geochemical exploration in areas of thin glacial overburden. In addition, modeling of the water chemistry contributes to an understanding of the chemical processes that are taking place in the surficial weathering environment.

Hydrogeochemical exploration was used to detect a known but undisturbed Cu-Ni sulfide body along the basal zone of the Duluth Complex in an area in northeastern Minnesota covered by less than 3 m of glacial ground moraine. The most important pathfinders for detection of the sulfide body are Ni, Cu, and SO_4^{2-} and, to a lesser extent, Mg and SiO_2. A map plot that uses the normalized sum of the concentrations of the pathfinders,

$$\frac{Ni/\bar{x}_{Ni} + SiO_2/\bar{x}_{SiO_2} + Cu/\bar{x}_{Cu} + Mg/\bar{x}_{Mg} + SO_4^{2-}/\bar{x}_{SO_4^{2-}}}{5},$$

($\bar{x}$=geometric mean concentration) defines the mineralized zone more consistently than a single-element plot, mainly because the absence of any one variable will not significantly influence the value of the normalized sum.

The study area is characterized by numerous hills and ridges interspersed with bogs and wetlands. Surficial material is mainly ground moraine. Shallow and immature soils are developed on ridges, and gray-brown podzolic soils are developed on the lower slopes. Modeling the chemistry of waters collected from swamps, streams, springs, and a well indicates that the waters are oxidizing. The dominant trace-metal species in these waters are Cu^{2+}, Ni^{2+}, and SO_4^{2-}, which are derived from the oxidation and dissolution of sulfide minerals. During glaciation, rocks become fragmented and mechanically abraded, thus significantly reducing the grain size and making them particularly susceptible to chemical weathering. Most of the sulfide minerals in the glacial drift probably were destroyed by oxidation and dissolution during glacial melting. Therefore, most of the Ni^{2+}, Cu^{2+}, and SO_4^{2-} in the waters of the study area are coming from the dissolution of sulfide minerals in nearby mineralized outcrops or shallowly buried bedrock. Areas containing sulfide-bearing rocks would have been particularly susceptible to intense chemical weathering and subsequent differential glacial ablation. As a result, these areas typically would be low lying and, in this environment, would tend to form wetlands. The possibility exists that sulfide-bearing zones may underlie some of the wetlands in this environment. Trace-metal concentrations in the water can be used to detect the underlying mineralization if the waters in contact with the mineralized bedrock are oxidizing.

Plots of Cu and Ni contents in soils from the data reported by Alminas (1975) show that the most useful indicator elements for delineating the sulfide body are Cu and Ni. The ability of soil and water geochemical data to delineate the sulfide body supports the use of both media for geochemical exploration in this environment. In the wetlands, water is abundant, and soils are scarce or absent; conversely, where soils are abundant, waters are usually scarce or absent. The use of both media is recommended for geochemical exploration in areas covered by thin glacial overburden.

REFERENCE CITED

Alminas, H.V., 1975, Soil anomalies associated with a Cu-Ni mineralization in the South Kawishiwi area, northern Lake County, Minnesota: U.S. Geological Survey Open-File Report 75–158, 20 p., 6 pls.

Reconnaissance Geologic Mapping Using Digital Aeromagnetic Data and Space-Shuttle Radar Data for a Heavily Forested Area of the Guayana Shield, Northwestern Brazil

By Fernando P. Miranda, Anne E. McCafferty, *and* James V. Taranik

The part of the Guayana Shield in northwestern Brazil is one of the least geologically known regions of the country. The area is completely covered by rainforest, and lithologic boundaries and geologic structures lack obvious geomorphic expression. It is characterized by a complex association of gneissic and granitoid rocks of Middle Proterozoic age (Guianense Complex), which are not individually shown as distinct units on the geologic map published by the RADAMBRASIL Project at the scale of 1:1,000,000 (Pinheiro and others, 1976). The project was sponsored by the Brazilian government to acquire X-band radar images and other data for the whole country.

In 1984, the Shuttle Imaging Radar-B (SIR-B) acquired digital data over the Guayana Shield. This L-band (23.4-cm wavelength) synthetic-aperture radar system operated at a fixed incidence angle of 35.7° over flat terrain. On the SIR-B image, brighter tones outline the flood plains of some streams. These tones are due to the presence of standing water beneath canopy layers, which strongly increases SIR-B backscatter. Linear geomorphic features were identified on the SIR-B image on the basis of (1) the spatial distribution of flooded vegetation indicative of subtle topographic relief of up to 8 m and (2) tonal linear features associated with drainage divides.

The digital aeromagnetic data used in this research were obtained in 1987. Measurements were made by using a proton-precession magnetometer having a sensitivity of 1.0 nT. Flightlines were north-south at a 2.0-km spacing. The survey was performed in a draped mode 150 m above relatively flat terrain. The following products were derived by digital data manipulation: (1) a gray-scale image of the reduced-to-pole magnetic anomalies, constructed in order to highlight zones of distinct magnetic signature; (2) a terrace-magnetization map that delineates induced-magnetization boundaries and theoretically outlines geologic structures and terranes having different magnetic characteristics; and (3) a map showing the location of maximum values of the horizontal component of the pseudogravity gradient (boundary lines) that represent abrupt lateral changes in magnetization interpreted as steep structural or lithologic contacts.

Comparison of the magnetic and radar results with the geologic field data acquired by the RADAMBRASIL Project allows two broad terrane categories to be delineated for the first time. Areas characterized by intermediate brightness levels on the gray-scale magnetic image and by low to intermediate magnetization values on the terrace map correspond to sphene- and amphibole-bearing biotite granitoids having a Rb-Sr age of 1,640±26 Ma and a mantle derivation ($^{87}Sr/^{86}Sr$ initial ratio = 0.703). Areas characterized by very bright signatures on the gray-scale image and by high terrace-magnetization values correspond to a granitic and quartz-monzonitic intrusive body of unknown age that crosscuts the mantle-derived granitoids. The limits of this intrusive body are inferred by magnetization boundary lines, which are coincident with linear geomorphic features identified on the SIR-B image.

REFERENCE CITED

Pinheiro, S.S., and others, 1976, Geologia, Chapter 1 *of* Projeto RADAMBRASIL, folha NA.19, Pico da Neblina: Rio de Janeiro, Brazil Departamento Nacional da Produção Mineral, p. 17–137, 5 pls., scale 1:1,000,000.

Tourmalinite and Iron-Formation in the Yellowjacket Formation, Idaho Cobalt Belt, Lemhi County, Idaho

By Peter J. Modreski *and* Jon J. Connor

Stratabound concentrations of cobalt, copper, and iron exist at two stratigraphic levels within the Yellowjacket Formation (Middle Proterozoic) in the Idaho cobalt belt, Lemhi County, Idaho. The principal cobalt-copper deposits are near the Blackbird mine; they occur in northwest-trending, biotite-rich strata within the middle unit (argillite-siltite-quartzite) of the >13,000-m-thick Yellowjacket Formation (Modreski, 1985; Nash and Hahn, 1989; Connor, 1990). Sulfide minerals within this 1,000-m-thick Blackbird zone include cobaltite, chalcopyrite, arsenopyrite, pyrrhotite, and pyrite. A second interval of mineralization, the Jackass zone, is stratigraphically lower, is a few hundred meters thick, and contains abundant magnetite plus cobalt-bearing pyrite (Nash, 1989).

Tourmaline occurs in veins and breccias that cut greenschist-facies metasedimentary rocks of the Yellowjacket Formation and in quartz-tourmaline pods and lenses within more strongly deformed rocks of higher metamorphic grade. In the vicinity of Iron Creek, in and near the Jackass zone, black, flinty veins and breccia matrices are composed of a fine-grained intergrowth of tourmaline and quartz, locally with orthoclase, albite, muscovite, biotite, apatite, magnetite, and rutile. Clasts in the breccias are angular and commonly consist of bleached, pale greenish-white sericitic quartzite. In contrast to the silicified, tourmalinized breccias of the Blackbird district, which contain cobaltite at the Patty B prospect and the Haynes-Stellite mine, the tourmalinite veins and breccias near Iron and Jackass Creeks are essentially barren of cobalt (<4 to 28 ppm). Tourmaline throughout the district appears black in hand specimen but ranges from blue to olive-green and brown in thin section; some is color zoned. It is of intermediate schorl-dravite composition and is generally richer in iron than magnesium; atomic Fe/(Fe+Mg) ratios range from about 0.4 to 0.7, and weight FeO/(FeO+MgO) ratios range from 0.50 to 0.80. Some tourmalinites in the Jackass zone are associated with bedded magnetite-rich iron-formation.

The mineralized zones in the Yellowjacket Formation are interpreted to have been loci of sea-floor hot-spring activity. The magnetite-rich iron-formation consists of exhalative deposits that formed from hydrothermal fluids that were more oxidized than those that precipitated the sulfide-arsenide deposits in the Blackbird zone; the more oxidizing nature of the fluid probably resulted from greater mixing with seawater. The tourmalinites appear to have formed by venting of hydrothermal fluids through the mostly lithified sediment column beneath and in the vicinity of the exhalative deposits.

REFERENCES CITED

Connor, J.J., 1990, Geochemical stratigraphy of the Yellowjacket Formation (Middle Proterozoic) in the area of the Idaho cobalt belt, Lemhi County, Idaho: U.S. Geological Survey Open-File Report 90–234 (Part A, discussion, 38 p.; Part B, diskette).

Modreski, P.J., 1985, Stratabound cobalt-copper deposits in the Middle Proterozoic Yellowjacket Formation in and near the Challis quadrangle, *in* McIntyre, D.H., ed., Symposium on the Geology and Mineral Deposits of the Challis 1° × 2° Quadrangle, Idaho: U.S. Geological Survey Bulletin 1658–R, p. 203–221.

Nash, J.T., 1989, Geology and geochemistry of synsedimentary cobaltiferous-pyrite deposits, Iron Creek, Lemhi County, Idaho: U.S. Geological Survey Bulletin 1882, 33 p.

Nash, J.T., and Hahn, G.A., 1989, Stratabound Co-Cu deposits and mafic volcaniclastic rocks in the Blackbird mining district, Lemhi County, Idaho, *in* Boyle, R.W., Brown, A.C., Jefferson, C.W., Jowett, E.C., and Kirkham, R.V., eds., Sediment-hosted stratiform copper deposits: Geological Association of Canada Special Paper 36, p. 339–356.

Geophysical Logs in an Oxide Copper Deposit near Casa Grande, Arizona

By Philip H. Nelson, David J. Johnston, Henry G. Kreis, *and* Jon L. Mikesell

A joint industry-government project, cosponsored by the Santa Cruz Joint Venture (a joint venture between wholly owned subsidiaries of Asarco, Inc., and Freeport McMoRan, Inc.) and the U.S. Bureau of Mines, is investigating the use of in-place leaching to recover copper from an oxide ore deposit near Casa Grande, Ariz. Chemical solutions will be circulated through boreholes penetrating the deposit so that copper may be dissolved from chrysocolla and atacamite and brought to the surface in solution. At this stage, test holes have been drilled and logged, and some preliminary hydrologic tests have been completed. Objectives of the logging effort are to provide the following information: structure and fracturing, alteration mineralogy, and properties related to fluid flow.

By using logging technology developed for the petroleum industry, Schlumberger has acquired a complete suite of logs in five 9.9-in. rotary boreholes, including caliper, density, neutron, electrical-resistivity, dipmeter, gamma-spectrometry, sonic-waveform, and neutron-activation-spectrometry logs. The U.S. Geological Survey acquired logs in a nearby 3.6-in. borehole, including caliper,

neutron, resistivity, gamma-ray, sonic-velocity, induced-polarization, and magnetic-susceptibility logs. Asarco has contributed geologic descriptions, copper analyses, data on fracture density, and mineralogic estimates.

The data set is unique in that neutron activation spectrometry logs have been collected for the first time in a mineral deposit. These logs provide direct estimates of the concentrations of the elements Al, C, Ca, S, Si, Fe, and Ti. Natural gamma-ray spectrometry adds data on K, U, and Th abundances. Compensation for the effects of borehole fluid, cement, and fiberglass casing is required before the elemental concentrations of the rocks can be estimated. Mineral abundances are estimated by applying an element-to-mineral transformation. Use of such transformations requires that the suite of permissible minerals be carefully restricted and that the results be checked against geologic and petrologic data. Results obtained thus far produce reasonable estimates of the proportions of quartz, K-feldspar, and clay minerals within the granite host rock. Although copper has not been detected directly as an element, the estimated amounts of atacamite and chrysocolla are encouraging at this stage of the investigation.

Porosity is best calculated as part of the procedure used to determine the mineralogy; alternatively and more conventionally, it may be estimated from the density and neutron logs. Because the host rock is granitic, fluid flow probably is controlled by fractures. A correlation between sonic velocity and rock quality (that is, fracture counts) indicates that the rock is so pervasively fractured that porosity is controlled by the fracture density. If so, permeability can be estimated directly from porosity. The hydrologic tests will be used to check and refine the permeability estimates.

Regional Structural Setting of Gold Deposits in the Carolina Slate Belt of North Carolina

By Terry W. Offield *and* Terry L. Klein

Reconnaissance geologic mapping at the scale of 1:250,000 and new interpretations of the lithotectonic framework and structural history of the Carolina slate belt in North Carolina offer insights useful in gold exploration. The slate belt is anomalous relative to other terranes of the Piedmont, not only for its low intensity of deformation and metamorphism, but also for its wrong-way vergence. Much of the belt is characterized by west-dipping cleavage axial planar to folds overturned eastward and by east-directed thrust faults; the principal deformation and accompanying greenschist-facies metamorphism have been dated as Late Ordovician (Taconian).

Taconian thrusting produced shear zones in which tectonite fabric shows west-over-east dip slip as the dominant movement. These shear zones display phyllite and quartz veins where they occur in arc volcanic rocks that make up the northeastern structural slice of the slate belt. Large areas of these rocks are volcanogenically altered, and some have anomalous gold values. The ductility contrast of the altered rocks served to focus and intensify shearing during thrust faulting; phyllites are almost continuous across a zone 24 km wide in one area of widespread alteration. West of the volcanic arc rocks, in a structural slice of felsic volcanic rocks and an arc-basin sequence, thrust-related shears (some at gold deposits) served as conduits for fluid flow during metamorphism.

Late Paleozoic Alleghanian strike-slip faulting produced vertical shear zones that mark the east and west boundaries of the slate belt. The west (Gold Hill) shear zone has gold, silver, and base-metal deposits, some of which are exhalative deposits modified during subsequent structural events, whereas other deposits formed during phyllitization related to the Alleghanian wrench faulting. The east boundary, structurally analogous, also may be prospective but is largely covered by Triassic or Coastal Plain rocks. Other zones of anomalous, steeply dipping cleavage or phyllite found in many places within the slate belt typically trend north or east-northeast athwart the grain of the belt. All these zones, the boundary shears, and the rhombic shape of the slate belt are believed to be related to the wrench-faulting event. In several areas (for example, Gold Hill shear zone, Sawyer/New Sawyer and Russell Au deposits, pyrophyllite deposits), wrench shearing overprinted earlier thrust shears. In such areas, tectonite fabrics record both dip-slip and strike-slip movement, and these fabrics commonly are most intense where the rocks earlier were prepared by volcanogenic alteration.

Recent gold occurrence models for the Carolina slate belt have focused on either an epithermal hot-spring model related to felsic volcanic centers or a mesothermal shear-zone model requiring neither specific source nor specific host rocks. Our studies indicate that two episodes of shearing localized gold mineralization and that many intensely sheared areas were volcanogenically altered before deformation. Exploration efforts during the past decade have concentrated on areas of known gold occurrence or former production; however, a great deal of sheared ground (some previously altered) exists outside such areas, and so exploration targets may be abundant. The three producing gold deposits in South Carolina appear to be examples of (1) a volcanogenic deposit little modified structurally (Brewer), (2) a volcanogenic deposit modified by both thrust and wrench shearing (Haile), and (3) a deposit formed in a thrust shear zone (Ridgeway). If this interpretation is correct, it is reasonable to expect similar deposits in analogous settings in the North Carolina part of the slate belt. Structural targets are good starting places for exploration, but whether volcanogenic solutions deposited gold and whether shear-related processes enhanced or destroyed preexisting gold concentrations or formed

entirely new deposits cannot be known without geochemical sampling or drilling; these questions remain to challenge future explorers.

Latin American Mineral-Resource Data Available through the U.S. Geological Survey

By Frances Wahl Pierce *and* Karen Sue Bolm

The Minerals Information Offices (MIO's) were established by the U.S. Geological Survey (USGS) to facilitate use of USGS mineral-resource data and to encourage cooperation with other Federal and State agencies and with private organizations. The MIO's have access to several digital data bases and to the scientific expertise within the USGS. The four MIO's are in Washington, D.C.; Spokane, Wash.; Reno, Nev.; and Tucson, Ariz.

The Center for Inter-American Mineral Resource Investigations (CIMRI) in Tucson, Ariz., was established by the USGS to assess the mineral resources and to understand the metallogeny of Latin American countries. The center collects geological, geochemical, geophysical, and remote-sensing information relevant to mineral resources in South and Central America and the Caribbean.

Recently, the Tucson MIO has collaborated with CIMRI to update, collect, and enter data on mineral deposits and occurrences in northern Mexico, the Guayana Shield of Venezuela, northern Chile, Honduras, and the Altiplano of Bolivia. CIMRI and the Tucson MIO have produced files of news clippings and mineral-resource bibliographies for Bolivia and the Guayana Shield of Venezuela, partial bibliographies of geophysical data from the Caribbean and Latin America, and archives of maps, books, and papers on Latin American geology. The Tucson MIO helps CIMRI compile and distribute these collections.

Figure 1 shows the Latin American and Caribbean locations for which the Mineral Resources Data System (MRDS) contains information. The MRDS is a digital data base maintained by the USGS. It includes data from the "Preliminary Deposit-Type Map of Northwestern Mexico" (Leonard, 1989) and the "Mineral Resource Assessment of the Republic of Costa Rica" (USGS and others, 1987). The data can be manipulated, combined, and displayed to help formulate exploration strategies for specific deposit types, including those potentially amenable to small-scale mining (Bliss and others, 1990).

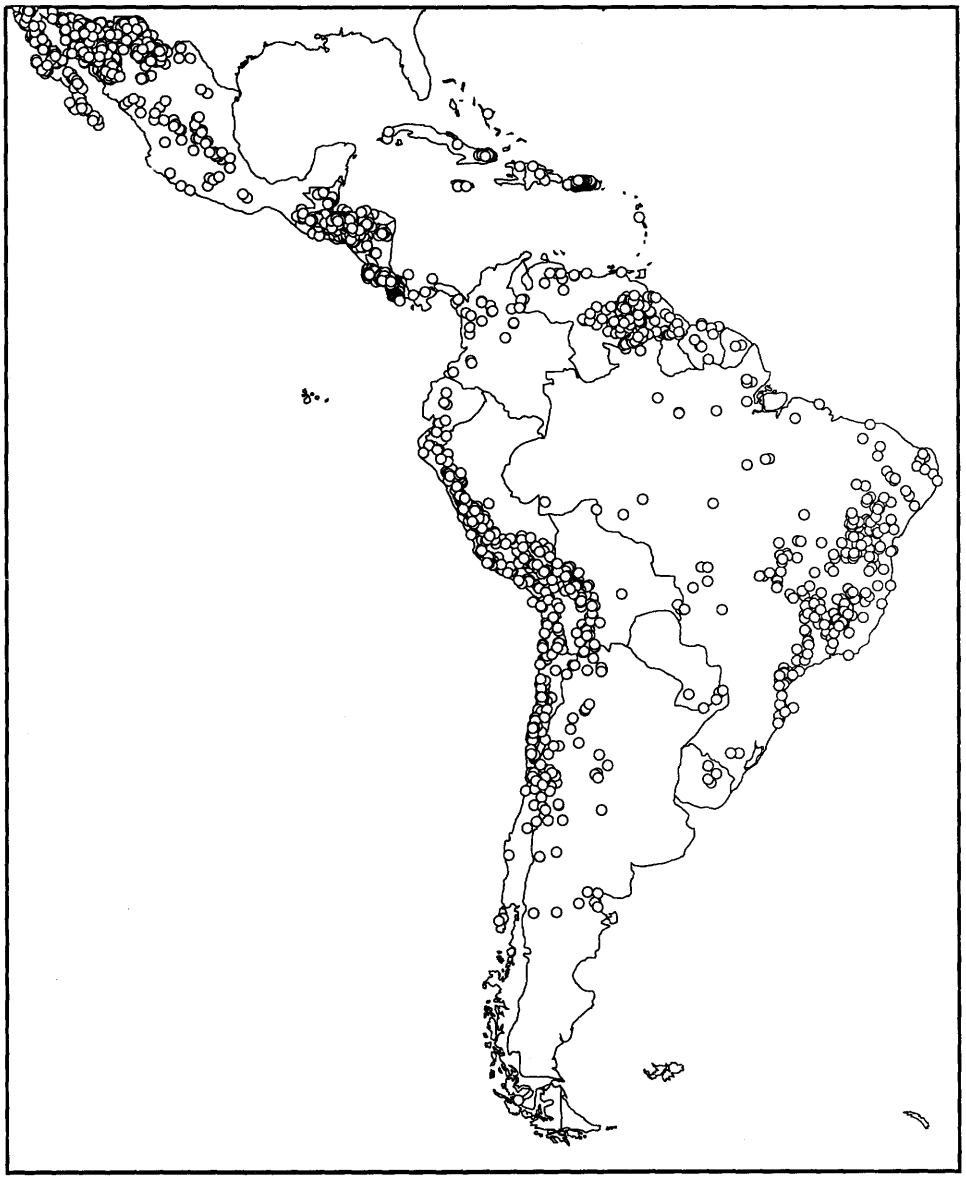

Figure 1 (Pierce and Bolm). Mineral sites in Latin America and the Caribbean for which the U.S. Geological Survey's Mineral Resources Data System contains information.

Companies interested in investing in foreign mineral projects may find that unpublished data on the mineral resources of a country are scattered among several agencies and are difficult to locate. Once these data are collected by CIMRI, the MIO's make them readily available in an easily transportable, digital format.

We welcome contributions of mineral-resource data from all sources. Data can be entered into the MRDS on paper forms sent to an MIO, or they can be entered directly into a data base on computers compatible with Macintosh or IBM personal computers. Once these data have been checked for quality and completeness, they are ready to be accessed, manipulated, and interpreted by the general public.

REFERENCES CITED

Bliss, J.D., McKelvey, G.E., and Allen, M.S., 1990, Application of grade and tonnage deposit models; the search for ore deposits possibly amenable to small-scale mining: U.S. Geological Survey Open-File Report 90–412, 24 p.

Leonard, K.R., 1989, Preliminary deposit-type map of northwestern Mexico: U.S. Geological Survey Open-File Report 89–158, 366 p., 1 map.

U.S. Geological Survey, Dirección General de Geología, Minas e Hidrocarburos, and Universidad de Costa Rica, 1987, Mineral resource assessment of the Republic of Costa Rica: U.S. Geological Survey Miscellaneous Investigations Series Map I–1865, 76 p., scale 1:500,000.

Preliminary Results of Geochemical Investigations of Aerial Gamma-Ray Anomalies in the Getchell Gold Trend, Humboldt County, Nevada

By James A. Pitkin

Selected anomalies in aerial gamma-ray data for the Getchell gold trend in Humboldt County, Nev., are being investigated for their significance in gold exploration. The aerial gamma-ray data were obtained by a contract helicopter survey (TerraSense, Inc., 1989) as part of the U.S. Geological Survey's Getchell trend airborne geophysics demonstration project (Hoover and others, in press). The demonstration area is on the east side of the Osgoood Mountains and includes six Carlin-type gold deposits.

The aerial data portrayed as radioelement (U, K, Th) contour and color-composite maps include relatively anomalous areas in phyllitic shale and phyllite of the Preble Formation of Paleozoic age and in pediment detritus east of the mountain front. During October and November of 1989, anomalous sites along flight lines were located by using a calibrated, hand-portable gamma-ray spectrometer that measures radioelement concentrations; rock and soil samples were obtained.

Geochemical analyses focused on Au, As, Hg, Sb, W, Ag, and F as major elements of interest for the gold deposits and on U, Th, and K for comparison of ground and aerial radioelement data. Analyses included Au by graphite-furnace atomic-absorption spectroscopy; Hg by cold-vapor atomic-absorption spectroscopy; F by specific ion electrode; W by visible spectrophotometry; As, Ag, Sb, and K by inductively coupled plasma-atomic emission spectroscopy, and U and Th by delayed neutron activation analysis. All the methods were described in Baedecker (1987).

Comparison of analytical results for U, K, and Th with concentrations determined by ground and aerial measurements shows good agreement. The data indicate that anomaly sites were successfully located and sampled, despite the disparity between the 3-ft sample diameter of the portable detector and the 800-ft-wide swath of the aerial detector (defined as twice survey altitude of 400 ft above ground level).

Analyses of 14 rock samples show that eight contain detectable Au; seven have <0.002 to 0.004 ppm, and one sample has 0.05 ppm. The highest Au value of 0.05 ppm is from a quartz vein in phyllite that has the highest As value of 210 ppm, 0.02 ppm Hg, probable background values of W, F, and Sb, and no detectable Ag. A sample of phyllite has a Au content of <0.002 ppm, the second highest As value of 140 ppm, background values of W, F, and Sb, and no Hg or Ag. The other 12 samples, all of phyllite or phyllitic shale, include two with detectable Hg, five with Sb, and three with Ag (none thought significant) and have probable background values of As, W, and F. Three of the 14 rock samples were collected in Felix Canyon just south of the granodiorite of the Osgood Mountains; they may have a geochemical character different from that of the other 11 and may reflect the alteration halo surrounding the pluton.

Eleven soil samples were obtained in the pediment south of the Pinson mine. Analyses show that eight samples contain Au in the range of <0.002 to 0.006 ppm and that one sample has 0.014 ppm. The sample with the highest Au value (0.014 ppm) is on the upthrown side of a fault that parallels the mountain front; except for Au, the geochemical character of this sample is similar to that of the other 10 samples. The 11 soil samples all contain detectable As, W, F, Sb, and Ag, and Hg occurs in four of them. The concentrations determined are believed to represent background values for an area probably affected by hydrothermal alteration associated with formation of the gold deposits of the Pinson mine and the nearby Mag mine.

Many of the 25 samples discussed here contain detectable Au, some have Hg, Sb, and Ag, and all have detectable As, W, and F, although not in any pattern thought significant in this preliminary study. These and the other samples, as well as additional geochemical data, are being evaluated to test the use of gamma-ray measurements in gold exploration.

REFERENCES CITED

Baedecker, P.A., ed., 1987, Methods for geochemical analysis: U.S. Geological Survey Bulletin 1770, 132 p.

Hoover, D.B., Grauch, V.J.S., Pitkin, J.A., Krohn, M.D., and Pierce, H.A., in press, An integrated airborne geophysical study along the Getchell trend of gold deposits, north-central Nevada, *in* Raines, G.L., Lisle, R.E., Schafer, R.W., and Wilkinson, W.W., eds., Geology and ore deposits of the Great Basin—Symposium Proceedings: Reno, Geological Society of Nevada.

TerraSense, Inc., 1989, Uranium, potassium, and thorium contour maps derived from a helicopter gamma-ray spectrometer survey of the Getchell trend, Humboldt County, Nevada: U.S. Geological Survey Open-File Report 89–287, 8 p., 12 sheets, scale 1:24,000.

Phosphorite Deposits of the Northern Blake Plateau as Observed From the *NR-1* Submarine and *Delta* Minisubmersible

By Peter Popenoe *and* Frank T. Manheim

The Charleston Bump is a bathymetric ramp on the northern part of Blake Plateau offshore of the Carolinas that deflects the Gulf Stream (fig. 1). It is capped by a nearly continuous layer of cemented phosphorite gravel (pavement) winnowed from Miocene sediments by the intensification of Gulf Stream currents caused by constriction over

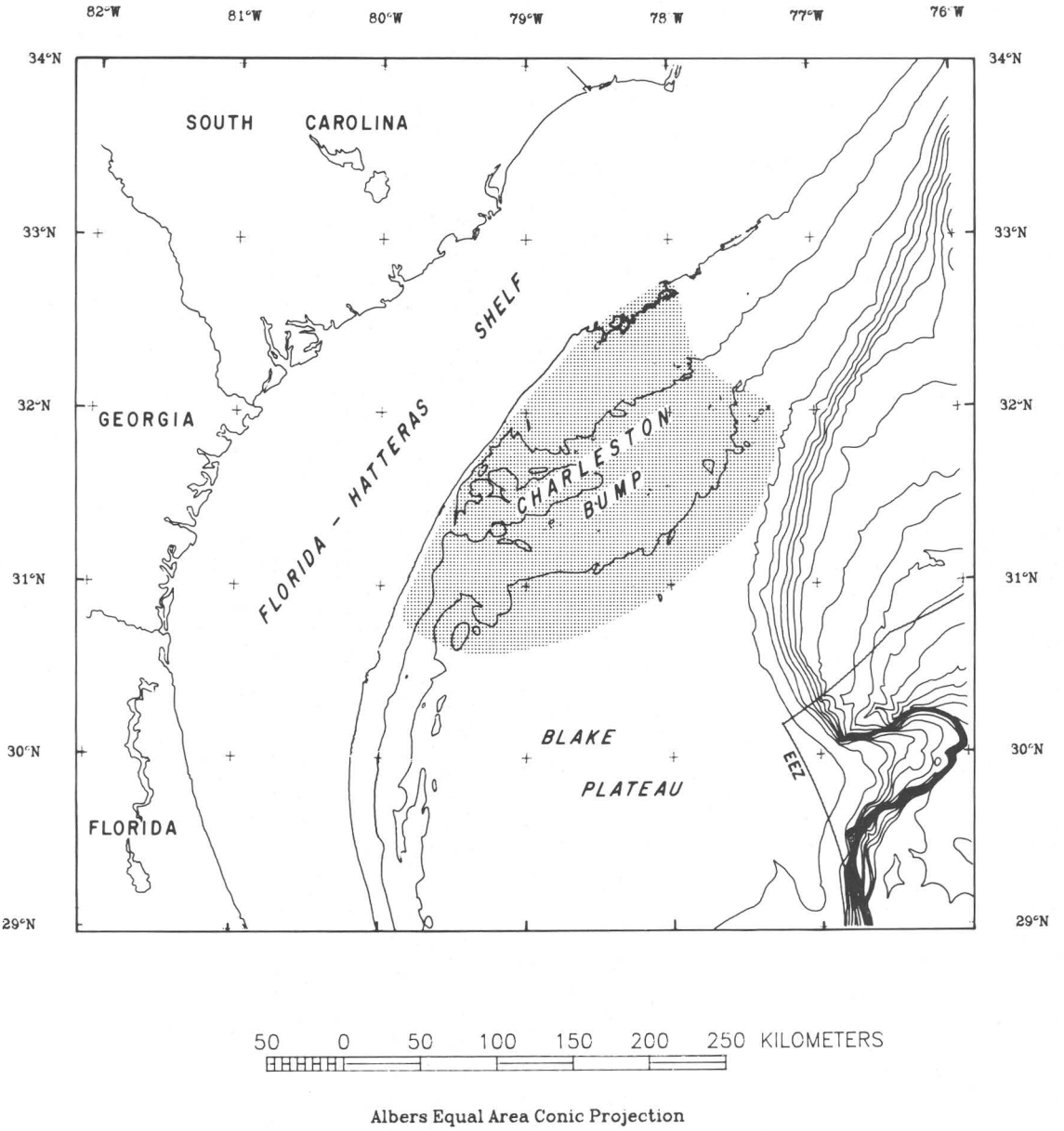

Figure 1 (Popenoe and Manheim). Area capped by phosphorite pavement (pattern) on the northern Blake Plateau. EEZ, Exclusive Economic Zone.

Figure 2 (Popenoe and Manheim). Phosphorite cobbles capping the sea floor of the northern Blake Plateau. The sponge near the right-center of the picture is about 18 cm across. Photograph by Peter Popenoe.

the shoal bathymetry. This pavement is overlain by a thin surficial layer of modern glauconitic carbonate sand and by residual phosphorite slabs, boulders, and gravel (fig. 2). The pavement is broken in many areas by large depressions associated with Gulf Stream scour.

Two series of dives totaling about 12 days bottom time were made in 1989 and 1990 by U.S. Geological Survey and cooperating scientists to assess the thickness and extent of the phosphorite pavements and the presence and thickness of manganese rinds and to sample both the pavements and underlying sediments. The first dives to greater than 600 m depth were made in strong currents on the central plateau by the U.S. Navy nuclear submarine *NR-1*. These dives investigated two large scour depressions, which are more than 100 m deep and have near-vertical walls; the depressions expose well-indurated, layered siliceous limestone and chert of Paleocene and Eocene age. The upper edges of these scour depressions are rimmed by a 1-m-thick phosphorite pavement that overhangs in places by about 9 m; the top of this pavement is littered with broken phosphorite slabs and boulders. Farther down the Charleston Bump, the pavement is breached, and erosion has cut down to a second hard layer, presumably another phosphorite pavement.

A second dive series was made as part of the U.S. National Oceanic and Atmospheric Administration's National Undersea Research Program. Scientists in the minisubmersible *Delta* investigated the shallower part of the Charleston Bump at depths of 300–400 m in an area of rugged, broken bottom. Here, a series of ridges about 10–15 m high, whose sides and tops are capped by phosphorite boulders and slabs, alternate with depressions whose bottoms are composed mainly of carbonate sand. In some areas, phosphorite boulders and slabs exceeding 1.5 m in thickness are piled one upon another at varying angles. In other areas, a level bottom littered with phosphorite boulders, cobbles, and gravels is underlain by continuous, unbroken phosphorite pavement.

The dive series documents an enormous resource of phosphorite on the northern Blake Plateau. Over 14,000 km^2 of ocean bottom in this area is covered by a phosphorite cap that exceeds 1 m in thickness. These dimensions indicate the presence of about 19 billion metric tons of equivalent phosphate rock concentrate. Because the phos-

phorite is at depths of 300 to 800 m, it cannot be considered a reserve base at the present time. However, the enormous mass and easy accessibility on the sea floor suggest that these phosphorite deposits should not be excluded from consideration as a possible resource for the future.

Silt-Fraction Mineralogy of Unconsolidated Sediment Samples from the Continental Shelf, Slope, and Rise off the Northeastern United States

By L.J. Poppe *and* J.A. Commeau

Heavy-mineral analyses are useful as sedimentologic and stratigraphic tools and may provide information on the resource potential of sediments. However, studies involving heavy minerals have usually been conducted on the sand fraction because of difficulties in using organic heavy liquids on silts and the inability to study this finer size fraction under the petrographic microscope. A new technique allows the efficient examination of heavy minerals in the silt fraction (4–62 μm) and, thus, broadens the scope of mineral studies of unconsolidated sediments. We separated the heavy minerals by centrifugation in sodium polytungstate and then identified them with a scanning electron microscope equipped with an automated image analyzer and an energy-dispersive X-ray spectrometer. Polymorphs and minerals having similar compositions were grouped or differentiated on the basis of X-ray diffractograms.

Whereas heavy minerals from the continental shelf off southeastern New England average only 1.5 percent of the sand fraction, heavy minerals in the silt fraction (fig. 1) range from 11.8 percent in sandy, higher energy environments near Georges Bank to 3.4 percent in clayey silt south of Martha's Vineyard. Corundum and minerals of the TiO_2, epidote, and phosphate groups are enriched in the silt fraction; spinel, the amphiboles, garnet+staurolite, and kyanite-group minerals are relatively concentrated in the sand fraction. Opaque minerals in the silt heavy fraction average 27.8 percent ilmenite, 4.8 percent magnetite+hematite+goethite+siderite, 1.6 percent ferromanganese-coated grains, and 0.9 percent pyrite. Lateral mineralogic variability within the silt-sized heavy-mineral assemblage is considerable. Zircon and ilmenite occur most commonly as coarse silt and progressively decrease in concentration to the west. Conversely, concentrations within the characteristically finer grained suites of amphibole- and epidote-group minerals increase westward.

Quartz dominates the silt-sized light mineral+phyllosilicate group on the shelf off southeastern New England; on average, it makes up 70.3 percent of that fraction. The potassium feldspar/plagioclase ratio and the 10Å/14Å ratio of phyllosilicate-group minerals average 0.38 and 2.61, respectively. The potassium feldspar/plagioclase ratio is higher in the sand fraction than in the silt fraction. Phyllosilicates are more concentrated in the finer grained sediments.

Preliminary studies of surficial sediment samples collected from the U.S. mid-Atlantic continental slope and rise show that heavy minerals in the silt fraction average 6.89 percent on the slope and 5.71 percent on the rise. However, unlike the silt fraction on the continental shelf off southeastern New England, sediments from these deeper water environments contain a more extensive authigenic mineral suite.

This study has revealed several important relationships with regard to the composition, abundance, and areal distribution of silt- and sand-sized heavy minerals on the continental shelf off southeastern New England: (1) regardless of sediment texture, heavy minerals constitute a substantially greater weight percentage of the silt fraction than of the sand fraction; (2) the silt-sized heavy-mineral assemblage is diverse and predominantly detrital; (3) pronounced mineralogical differences exist between the silt and sand fractions; (4) TiO_2 is enriched to an average of 0.67 weight percent in the silty sands southwest of Nantucket Shoals; and (5) the distribution trends observed in the sediments are largely due to sorting by westward-flowing bottom currents and are related to the specific gravity and characteristic shapes and sizes of the mineral grains.

Basin Evolution and Petroleum Studies in the U.S. Eastern Great Basin—Relevance to Mineral Investigations

By Christopher J. Potter, John A. Grow, Charles H. Thorman, Harry E. Cook, *and* James A. Peterson

The U.S. Geological Survey is undertaking two complementary, multidisciplinary regional projects in the eastern Great Basin (eastern Nevada and western Utah), with the goal of providing a better definition of the geologic framework of hydrocarbon and mineral deposits. The two projects are part of the Evolution of Sedimentary Basins (ESB) and Onshore Oil and Gas (OOG) programs and have a duration of 5 yr (1990–95). In the eastern Great Basin, the ESB project involves systematic studies of Paleozoic through modern sedimentary basins and their tectonic settings, and the OOG project is concerned more specifically with the geologic controls on hydrocarbon occurrences. Both projects include several detailed investigations (site studies) that emphasize the geologic evolution of specific resource-bearing (or potentially resource-bearing) horizons or areas. The ESB project will also produce regional transects consisting of cross sections and palinspastic restorations. In the OOG project, organic geochemical studies associated with regional stratigraphic investigations of major petroleum source rocks will produce hundreds of new

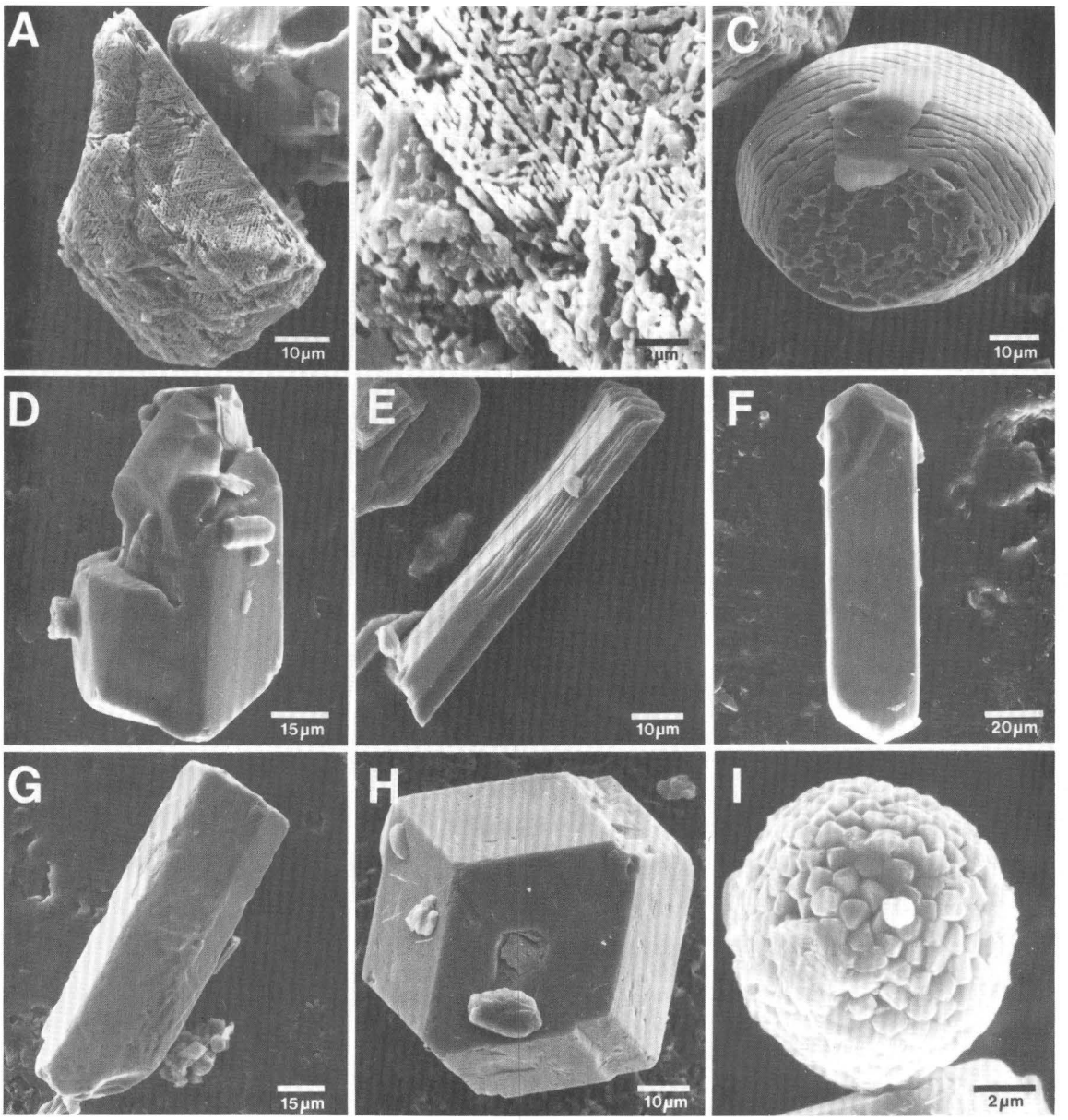

Figure 1 (Poppe and Commeau). Scanning electron microscope photomicrographs of silt-sized heavy-mineral grains representative of those found on the southeastern New England outer continental shelf. *A*, Corroded grain of altered ilmenite (originally ilmenomagnetite?). *B*, Higher magnification photomicrograph of grain pictured in fig. 1*A* showing lattice of diagenetic rutile prisms (trellis structure). *C*, Subrounded detrital ilmenite grain; voids probably represent hematite exsolution lamellae removed during transport or diagenesis. *D*, Prismatic crystal of epidote. *E*, Slender, elongate grain of the kyanite group. *F*, Tetragonal, dipyramidal grain of zircon. *G*, Hexagonal calcium phosphate grain (apatite). *H*, Dodecahedral garnet (almandite?). *I*, Framboidal pyrite showing the spheroidal agglomeration of euhedral pyrite crystals.

analytical measurements. Together, the two projects provide an integrated approach to eastern Great Basin geology and related resources. Elements of the integrated study are summarized below.

Detailed site studies are underway in the Adobe Range and Snake Mountains, the Pine Valley area, the Grant Range and Railroad Valley area, the Hot Creek Range, and the Mesquite Valley and Virgin Mountains area;

they include stratigraphic, sedimentologic, structural, geophysical, geochemical, and thermal history investigations. East-west regional transects (from approximately long 111°30′ W. to 117° W.) will be constructed at lats 38°30′ N., 40° N., and 41°30′ N. Several north-south transects will provide complementary data. The transects will incorporate regional geologic and geophysical information, including new geologic mapping and newly available seismic data, as well as data from the detailed site studies. As an example, work is currently underway with regional seismic lines from Railroad Valley to Lake Valley, along the transect at lat 38°30′ N. To establish fault geometries, we are using new geologic mapping in the Grant Range, well data, and gravity and magnetic data in conjunction with the reflection survey. New mapping is planned in the Egan and Schell Creek Ranges along this 91-km-long seismic line in order to provide new data on Basin and Range and older structures. Another broad-scale investigation is underway in the Toano-Goshute Range, Feber Flats, and the Deep Creek Range to evaluate multiple large-scale younger-over-older faulting events and their relation to mineralization and possible petroleum accumulation.

Synthesis of the structural and geophysical framework with studies of the Paleozoic through Tertiary sedimentary rocks and with the thermal histories of the basins will allow construction of cross sections and palinspastic restorations that will provide useful contributions for mineral and hydrocarbon exploration in the eastern Great Basin. A better understanding of the depositional environments and structural evolution of the region is critical to determining the timing and paths of fluid migration, for both hydrocarbon and mineralizing fluids. This determination will lead to an understanding of how and when potential traps formed and of how and when mineral or hydrocarbon deposits became localized in the traps.

Resource Assessment of the Mount Katmai 1° × 2° Quadrangle and Adjacent Parts of the Naknek and Afognak Quadrangles, Alaska Peninsula

By J.R. Riehle, S.E. Church, *and* L.B. Magoon

Geologic and geochemical field studies have been completed in 15,000 km^2 of the Mount Katmai 1° × 2° quadrangle and adjoining parts of the Naknek and Afognak quadrangles on the Alaska Peninsula as part of the Alaska Mineral Resources Assessment Project (AMRAP). Nearly the entire study area is within either the Katmai National Park and Preserve or the Becharof National Wildlife Refuge. The area is, in some ways, a geologic frontier: gravity data comprise only a few profiles or isolated measurements, aeromagnetic data are restricted to the Naknek quadrangle, and there are neither drill-hole data nor published reports on the several unpatented lode and placer claims.

The study area is within the Peninsular terrane. The Bruin Bay reverse fault (fig. 1) separates Middle Jurassic plutonic rocks and roof pendants in the northwest part of the area from Upper Jurassic sandstones and siltstones of the Naknek Formation to the southeast. Upper Cretaceous flysch occurs near Cape Douglas. Early to middle Tertiary volcanic rocks of the Aleutian arc are exposed northwest of the Bruin Bay fault, and middle Tertiary plutonic rocks are intruded along and adjacent to the fault in the north-central part of the study area. Late Tertiary volcanic and hypabyssal rocks occur in the central and eastern parts of the area. Quaternary volcanoes (fig. 2) of the active part of the Aleutian arc are constructed on some of the late Tertiary hypabyssal and volcanic rocks along the crest of the Aleutian Range.

Contributions of the Katmai AMRAP study to a fuller understanding of the geology and mineral potential of the Alaska Peninsula are (1) a better definition of the age and distribution of volcanic and plutonic rocks in the western, north-central, and northeastern parts of the area, (2) subdivision of the Naknek Formation, (3) discovery of a 50-km-long belt of hypabyssal rocks adjacent to the Valley of Ten Thousand Smokes (fig. 1), (4) systematic reconnaissance geochemical coverage throughout the area, and (5) a mineral-resource assessment.

Bedrock and stream-sediment geochemical data outline areas of anomalous concentrations of base and precious metals. The most important are (1) around Tertiary plutons in the north-central part of the study area; (2) within late Tertiary plutonic rocks and Tertiary sedimentary wall rocks near Cape Douglas; (3) in late Tertiary volcanic and hypabyssal intrusive rocks in the eastern part of the study

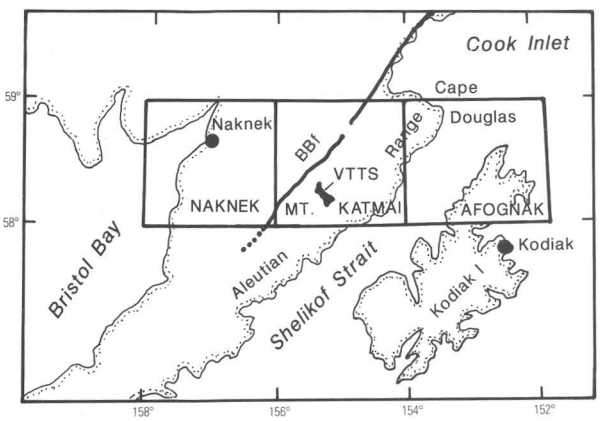

Figure 1 (Riehle and others). The Katmai AMRAP (Alaska Mineral Resources Assessment Project) study area on the Alaska Peninsula. The study area consists of the Mount Katmai 1° × 2° quadrangle and adjacent parts of the Naknek 1° × 2° and Afognak 1° × 2.5° quadrangles. The trace of the Bruin Bay fault (BBf), the major structural feature of the Alaska Peninsula, is interrupted by middle Tertiary plutons. VTTS, the Valley of Ten Thousand Smokes.

Figure 2 (Riehle and others). View to the north of Griggs Volcano, a Quaternary stratovolcano of the Aleutian arc. Griggs Volcano is built on Upper Jurassic sandstones and siltstones of the Naknek Formation that have been intruded by Tertiary sills, dikes, and shallow porphyritic plutons. The head of the Valley of Ten Thousand Smokes, site of the 1912 eruption of Novarupta dome (the "Katmai eruption"), is in the middle foreground. Two glaciers are visible in the lower right, and thick fallout deposits of the 1912 eruption can be seen mantling the lower slopes of Griggs Volcano. Griggs Volcano is about 8 km across at its base. Photograph by J.R. Riehle in July 1983.

area; (4) in Mesozoic sedimentary wall rocks and Tertiary hypabyssal rocks in the central part of the study area; and (5) in volcanic rocks of the Aleutian arc and underlying Naknek Formation near the southern margin of the area. On the basis of element suites, followup studies of selected areas, and permissive geologic attributes, we infer, at the 10 percent level of confidence, the existence of one or more porphyry Cu systems. Geochemical and geologic data suggest that polymetallic vein and epithermal gold systems are also present; however, the lack of subsurface data and the low density of our surface data preclude our making a quantitative estimate of the number of such deposits present where these deposits occur within an area of <1 km^2. These inferred deposit types are similar to porphyry deposits or occurrences and to vein occurrences south of the Katmai area and to vein occurrences associated with Tertiary plutonic rocks in the Iliamna quadrangle to the north. Other deposit types known elsewhere in southern Alaska (for example, tin-bearing granites, skarn deposits, syngenetic sea-floor gold in Jurassic volcanic rocks) are unlikely to be present in the Katmai area, where the geology is unfavorable for their occurrence.

The potential for producible hydrocarbons in the study area is small, primarily because the most favorable reservoir rocks have been uplifted and dissected by erosion. Thermal springs near Quaternary volcanoes in the eastern part of the area indicate some low-temperature geothermal potential. Surficial sand and gravel deposits are abundant in the western half of the study area.

Triassic-Jurassic Magmatic Arc of Western Nevada and Eastern California—Part IV: A Model for the Evaluation of Cenozoic Basins for Concealed Mineral Systems

By D.L. Sawatzky, G.L. Raines, J.L. Doebrich, R.L. Turner, L.J. Garside, *and* J.H. McCarthy, Jr.

A computerized geologic information system based on several geographic-information-system (GIS) computer programs provides data management, digitizing and plotting, and powerful GIS functions. These functions provide the analytical tools for spatial analyses of map data bases for evaluation of mineral resources in basins. We used these tools to study Cenozoic basins in the Middle Triassic to Jurassic magmatic arc of western Nevada and eastern California.

Data bases were compiled from new data and several existing sources of digital data. These data sets include (1) digital data on Nevada geology, (2) geologic maps at scales larger than 1:500,000, (3) mine and prospect data from the Mineral Resource Data System of the U.S. Geological Survey (USGS), (4) stream-sediment and soil geochemical data collected during National Uranium Resource Evaluation (NURE) studies and data from the Rock Analysis Storage System (RASS) of the USGS, (5) NURE aeroradioactivity data, (6) USGS aeromagnetic and gravity data, and (7) USGS digital-elevation-model (DEM) topographic data, audio-magnetotelluric profile data, biogeochemical data, and soil-gas data.

The basin evaluation model is based on maps of pre-Cenozoic rocks, depth-to-basement maps, and maps of proximity to mines and prospects, geochemical anomalies, hydrothermal alteration, limonite anomalies, and radiometric anomalies. A digital subcrop map of pre-Cenozoic rocks was prepared by extrapolating basement geology beneath Cenozoic basins, utilizing known geologic relations in the ranges and structural data relating to folding and faulting, and interpreting magnetic, gravity, and electrical geophysical data. Depth to basement is estimated from complex physical relations among geologic, topographic, gravity, and magnetic data. It is used to estimate the thickness of Cenozoic fill on basement rocks. The proximity maps show prospective areas around mines and prospects and around geochemical and geophysical anomalies; they also show hydrothermal alteration zones.

The geologic, depth-to-basement, and proximity maps are combined by using a linear weighting procedure to produce the evaluation model. The weights reflect the importance of each data type as a predictor of mineralization. Weights are determined intuitively or from statistical analysis of the distribution of the data. The result is a map of the areas favorable for mineralization at depths of less than 1 km under Cenozoic cover rocks in the basins.

Triassic-Jurassic Magmatic Arc of Western Nevada and Eastern California—Part I: Geology

By R.A. Schweickert, J.H. Stewart, J.H. Dilles, L.J. Garside, R.C. Greene, R.F. Hardyman, D.S. Harwood, *and* N.J. Silberling

Metavolcanic and metasedimentary rocks and plutons that represent a Middle Triassic to Jurassic magmatic arc crop out at scattered localities throughout a large region of western Nevada and eastern California. These rocks have recently been studied in an area extending northwestward from the Gillis Range near Walker Lake through Lake Tahoe to the northern Sierra Nevada near Bowman Lake and near Reno. Geologic relations of the arc have been complicated by the intrusion of younger Jurassic and Cretaceous plutons of the Sierra Nevada batholith, concealment beneath Cenozoic volcanic rocks, fragmentation by large-magnitude Cenozoic extension and strike-slip faulting, and burial beneath Neogene basin fill.

The Mesozoic strata can be separated into at least four stratigraphic packages. The oldest package includes Middle to Late Triassic (Carnian) lava flows, breccias, and ash-flow tuffs that range in composition from andesite to rhyolite. These rocks were deposited in both subaerial and marine environments and locally are intercalated with shallow-marine carbonate rocks. This package extends westward from the Gillis Range to the Carson City area but does not occur in the northern Sierra Nevada.

Conformably overlying the oldest package are Upper Triassic (Carnian to Norian) platform to basinal marine limestones and local intercalated marine tuffs and pyritic argillites. This carbonate-rich package is overlain, apparently conformably, by a third package of uppermost Triassic to lower Middle Jurassic (Bajocian) basinal siltstone, argillite, and dark limestone. Shallow-marine to nonmarine quartz sandstone and evaporites occur near the top of the sequence. This general stratigraphy exists throughout much of the study area. The basinal units include the well-known Sailor Canyon Formation and the Gardnerville Formation of Noble (1962).

The fourth, and youngest, stratigraphic package, which may include several unrelated sequences, consists of a diverse assortment of Middle and Middle(?) Jurassic volcanic units that include felsic ash-flow tuff, dacite and andesite porphyry, fluvial conglomerate, and hypabyssal intrusions. In some areas, rocks of the youngest package apparently rest unconformably upon the older units. Major- and trace-element analyses of volcanic rocks from all four packages suggest that they represent a calc-alkalic suite related to a magmatic arc developed along an active continental margin.

Uncertainties about age(s) of stratigraphic units in some areas and of deformational events create problems of

interpretation. Geologic maps, geochronologic data for plutons, and structural data indicate that, in the central part of the study area, the oldest three packages were deformed, folded, and faulted prior to the intrusion of the Yerington batholith (169 Ma). However, the possibility that regional deformation occurred at different times in different parts of the region cannot be excluded. The intensity of deformation varied markedly. Rocks in some parts of the region are highly deformed tectonites, whereas those in other parts are folded but lack foliation. The extent, geometry, timing, and significance of the regional deformation are still being studied.

The relation of the youngest stratigraphic package to the regional deformation varies across the study area. For example, Middle and Middle(?) Jurassic volcanic rocks in the Yerington area appear to postdate the regional deformation. In contrast, in the northern Sierra Nevada, the youngest Middle(?) Jurassic units were involved in regional deformation together with older units.

The oldest Mesozoic rocks in the study area are interpreted to have formed in a low-relief, shallow-marine to subaerial volcanic terrane during the Middle to Late Triassic. As volcanism waned in the Late Triassic, subsidence occurred and one or more intra-arc or fringing basins developed. Continued subsidence and (or) sea-level rise deepened and enlarged the basin(s) during most of the Early Jurassic, as basinal marine siltstone, mudstone, and limestone were deposited. Late in the Early Jurassic, the region shoaled and nonmarine sedimentary deposits accumulated. Subsequently, Middle Triassic to Middle(?) Jurassic units were regionally deformed. At least locally, the deformed rocks were intruded by younger Middle Jurassic batholiths and were overlain by younger Middle(?) Jurassic volcanic sequences. An unresolved tectonic problem is whether major Mesozoic strike-slip or thrust faults proposed by various authors divide the Mesozoic units into different tectonostratigraphic terranes.

REFERENCE CITED

Noble, D.C., 1962, Mesozoic geology of the southern Pine Nut Range, Douglas County, Nevada: Stanford, Calif., Stanford University, Ph.D. thesis, 200 p.

Triassic-Jurassic Magmatic Arc of Western Nevada and Eastern California—Part II: Audio-Magnetotelluric Survey near Reno and Carson City, Nevada

By R.M. Senterfit *and* D.P. Klein

Audio-magnetotelluric (AMT) data in the frequency range of 4.5-27,000 Hz were used to investigate the resistivity structure of a Middle Triassic to Jurassic magmatic arc near Reno and Carson City, Nev. Sixty-one AMT stations were occupied. The data for each station consist of scalar electromagnetic measurements at 16 discrete frequencies for two orthogonal magnetic and electric field pairs. The fields are measured by electrodes and a magnetic coil at the ground surface (fig. 1). The goal was to provide information on lithologic or structurally controlled resistivity contrasts that may provide insight into the distribution of buried parts of rock units associated with the magmatic arc. Data were compiled as contoured maps showing the lateral variations in apparent resistivity and also as 10 resistivity cross sections based on composited one-dimensional modeling.

The areas studied include (1) the Churchill Butte-Ramsey mine area, which is about 55 km east of Carson City, and the Carson River plain, (2) Carson Valley, including the western flank of the Pine Nut Mountains, and (3) the western side of Smith Valley, including the eastern edge of the Pine Nut Mountains; this last area is about 55 km southeast of Carson City. Three exploratory stations were occupied on Peavine Peak near Reno.

The cross sections show the approximate thickness of alluvial material and indicate locations of low-resistivity (3–30 ohm-m) units believed to represent volcanic and sedimentary rocks. The locations of several alluvium-covered, north-trending faults are also suggested by the data, especially in the valley between Churchill Butte and the Ramsey mine area in the Virginia Range. The data suggest that the thickness of the alluvial fill in parts of Smith Valley may exceed 3 km. In conjunction with geologic mapping, the data appear to identify the basement structure, notably variable basement relief on the east edge of Carson Valley and various lateral resistivity contrasts within the bedrock that suggest lithologic and structural contacts.

Figure 1 (Senterfit and Klein). Preparing to record an audio-magnetotelluric sounding. Photograph by Carl L. Long.

Early to Middle Proterozoic Supracrustal Rocks and Mineralization of the Southern Guayana Shield, Venezuela

By Gary B. Sidder, William E. Brooks, Yasmin Estanga, Fernando Nuñez, *and* Andres Garcia

Recent mapping in southern Venezuela has provided new insights into the geology of the southern Guayana Shield. Felsic to mafic volcanic rocks of the Early Proterozoic (about 1,900 to 1,700 Ma) Caicara Formation and associated hypabyssal granitic intrusions are conformably and disconformably overlain by quartz sandstone and conglomerate of the Early to Middle Proterozoic Roraima Group. Intermediate to mafic dikes, sills, and small bodies of gabbro intrude the volcanic and sedimentary rocks. Field, petrographic, and chemical characteristics of the volcanic rocks indicate that they are correlative with the Early Proterozoic Surumu Formation in northern Brazil.

The volcanic rocks are dominantly rhyolite and trachyte, with lesser amounts of andesite, basaltic andesite, and basalt. They are characteristically crystal-lithic ash-flow tuff with minor flows and breccia. Whole-rock geochemical analyses demonstrate that the volcanic rocks are calc-alkalic. These rocks are not penetratively deformed. They lack index minerals indicative of regional metamorphism, although, adjacent to granitic and gabbroic intrusions, they contain contact metamorphic mineral assemblages.

Mineralized volcanic rock is present in scattered areas of hydrothermal alteration and is characterized by propylitization, silicification, and as much as 10 modal percent pyrite and traces of associated chalcopyrite. Some quartz veins and altered rhyolite contain anomalous values of gold, silver, bismuth, and molybdenum and may constitute exploration targets. A deposit model for epithermal precious-metal veins best represents these mineral occurrences in the Caicara Formation. In addition, cassiterite locally forms disseminated grains in rhyolite and occurs in panned concentrates of stream sediment.

The gabbro bodies and intermediate to mafic dikes and sills that cut the volcanic rocks are typically deuterically altered, medium to coarse grained, and equigranular to porphyritic. Andesitic to basaltic (diabasic) dikes and sills, some as much as 8 m thick, are moderately altered and contain sulfides. Some dikes have a distinctive chicken-track porphyritic texture. The mafic intrusive rocks, which represent different suites and ages of intrusion, are tholeiitic, alkalic, and calc-alkalic in affinity. The calc-alkalic basaltic andesite to basalt dikes and sills may be comagmatic with the volcanic rocks. However, the tholeiitic and alkalic basaltic dikes and sills and the gabbro bodies may be part of the Middle Proterozoic Avanavero Suite, or they may belong to the Mesozoic diabase dike swarms.

Evolution of an Early Proterozoic Rift Basin in the La Esmeralda Area, Guayana Shield, Venezuela

By G.B. Sidder, W.C. Day, R.M. Tosdal, S.D. Olmore, Luis Guzman, *and* Freddy Prieto

New geologic mapping and geochemical and isotopic data help unravel the geologic history of an Early Proterozoic greenstone belt near La Esmeralda, 100 km southwest of Ciudad Bolívar, Venezuela. Supracrustal rocks within the area include basal feldspathic quartzite approximately 100 m thick, which is overlain by tholeiitic metabasalt, microgabbro, and thin beds of metashale, chert, and quartzite. These supracrustal rocks form an east-trending synclinal structural basin 16 km wide and 40 km long, which is underlain both on the north and south by gneissic basement of the Guayana Shield. The basal supracrustal quartzite lies conformably on basement granitic gneiss, whereas thrust faults occur locally near the upper contact of the quartzite with the overlying metabasalt. The granitic gneiss was previously assigned to the Early to Middle Archean Imataca Group. However, new U-Pb zircon data indicate that this gneiss is 2,240±44 Ma and, therefore, that the basement in this area is in part Early Proterozoic.

Two types of gold mineralization are known in the La Esmeralda area. An epigenetic type is represented by the Hueco Rico prospect, in which gold is localized within a shear-zone-hosted quartz-chlorite vein that cuts ductilely deformed mafic metavolcanic rocks; S-C mylonitic fabrics are preserved within the shear zone. A syngenetic type of mineralization is observed at the Cerro La Pinto mine, where gold occurs within a finely laminated, rhythmically bedded sequence of deeply weathered graphitic metashale, mafic metavolcanic rocks, and metachert.

The supracrustal rocks formed in an Early Proterozoic intracratonic basin or along a continental margin during the early rifting phase of the Trans-Amazonian orogeny. Deposition of the basal quartzite within the incipient rift was followed by tholeiitic basaltic volcanism. Although tectonism has obscured the original texture of the mafic rocks, the presence of metashale and metachert interbedded with the basal part of the mafic metavolcanic rocks at Cerro La Pinto suggests that the volcanism was subaqueous.

Closure of the basin was accompanied by regional compressive tectonism during the later phases of the Trans-Amazonian orogeny. The tectonism produced regional amphibolite-grade metamorphic rocks that show a penetrative structural fabric. Metabasalt has a moderately strong schistosity as well as a mineral lineation. The compressive regime deformed the basin into a synclinal structure and variably thrust the metabasaltic rocks over the basal quartzite; mylonites formed locally within the basal thrust zone.

The U-Pb zircon data place a maximum age of about 2,240 Ma for rifting during the early stages of the Trans-Amazonian orogeny. The penetrative fabric preserved in the rocks of the La Esmeralda area is associated with subsequent compressional stages of the Trans-Amazonian orogeny, which took place from 2,150 to 1,960 Ma.

Gold-Bearing Quartz Veins Along the Mojave-Sonora Megashear Zone, Northern Sonora, Mexico

By Miles L. Silberman, Anita Moore-Nall, *and* Brian M. Smith

Gold-bearing quartz veins, quartz-vein stockworks, and silicified breccias occur in most of the gold deposits and prospects along the trend of the Mojave-Sonora megashear zone, northern Sonora, Mexico (fig. 1). Gold has been mined intermittently since the early 1700's, largely by primitive methods. An abandoned crusher at the Quitovac prospect is shown in figure 2. The deposits and prospects are hosted by sedimentary, metamorphic, and igneous rocks of Precambrian through Mesozoic age along or near low-angle structures such as thrust faults, shear zones, or detachment faults (Silberman and others, 1988). Relatively continuous, steeply dipping quartz veins several meters thick, such as those at Tajitos, are less common than stockworks and breccias.

Reconnaissance petrographic data, fluid-inclusion data, and oxygen-isotope measurements were collected on gold-bearing quartz veins from seven deposits and prospective areas along the megashear trend from Sonoita through Santa Ana; they are Quitovac, Banco de Oro, Tajitos, Basura, Altar, Lluvia de Oro, and Llano. The rocks and quartz veins show evidence of both ductile and brittle deformation. Ductile deformation is indicated by ribbon texture in the quartz veins, foliation in the host rocks, rounding of porphyroblasts, augen of feldspar encased in mica, pressure shadows, and suturing of quartz-grain contacts. Brittle deformation is represented by fractures that cut all veins and host rocks and contain sericite and limonite (after pyrite). Sericitic alteration appears to have affected almost all the host rocks. Sericite replaces feldspars and occurs in highly fractured zones in many places with calcite and limonite. Adularia has crystallized in the groundmass of some sericitically altered rocks, but no quartz-adularia veins were seen.

Three types of quartz were identified on the basis of petrographic and fluid-inclusion study of approximately 30 quartz-vein samples:

(1) Cloudy bull quartz—Milky quartz containing many healed microfractures arranged in sheetlike wispy textures. Crushing the quartz in oil indicates that the tiny inclusions defining the microfractures contain gases under pressure.
(2) Clear bull quartz—White quartz similar to the cloudy bull quartz but having fewer and larger inclusions, which are mostly irregular in shape and contain two or three phases, including $(H_2O)_L + (CO_2)_V + (CO_2)_L$.
(3) Clear euhedral quartz—Clear quartz with euhedral terminations in vugs. Fluid inclusions in this quartz are irregular in shape and have inconsistent liquid/vapor ratios. Filling temperatures are less than 200 °C, and salinities are less than 1.5 equivalent weight percent NaCl.

Quartz types 1 and 2 are dominant; typically one or the other makes up more than 90 percent of a sample. Where they occur together, type 2 quartz always replaces or, less commonly, cuts type 1. More detailed studies of other deposits indicate that these textural types of quartz are characteristic of relatively deep, magmatic or metamorphic environments. Type 3 quartz is always paragenetically late and cuts other types present. Low temperatures and salinities are suggestive of shallow, epithermal environments of deposition. Type 3 rarely makes up more than 10 percent of the quartz in any sample, but, where present, it appears to contain sulfide or oxide minerals.

Oxygen-isotope compositions of 21 quartz samples from all seven deposits and prospective areas with one exception are in the range from +10 to +15.5 per mil relative to SMOW (standard mean ocean water). One prospect, Basura, has a lower $\delta^{18}O$ value of +8 per mil and has a larger proportion (20 percent) of the late, type 3 quartz. Only one sample from a vein at Banco de Oro consists of a single type of quartz, type 2; fluid-inclusion homogenization temperatures average 265 °C. Water in equilibrium with this quartz would have had a minimum $\delta^{18}O$ value of approximately +4 per mil. A fluid of this composition could result from a mixture of magmatic or metamorphic water with meteoric water (at this latitude). If the actual temperature of formation were higher, on the order of 400 °C (due to depth of burial during vein formation), then the oxygen-isotope composition of the fluid would be in the magmatic or metamorphic range.

The oxygen-isotope ratios for Sonoran quartz are approximately the same as those measured for gold-bearing type 1 quartz veins formed along low-angle shear zones at Cargo Muchacho, San Bernadino County, Calif. The geologic setting there is similar to that for many of the Sonoran gold occurrences. The ore fluid at Cargo Muchacho was largely magmatic in origin (Branham, 1987).

Our reconnaissance results suggest (1) that most of the Sonoran gold-quartz deposits and prospects occur in host rocks that underwent complex deformation and (2) that gold-bearing quartz veins within them are complex and multistage. The veins formed or were recrystallized during both ductile and brittle deformation. The last stage of hydrothermal activity was evidently epithermal and may

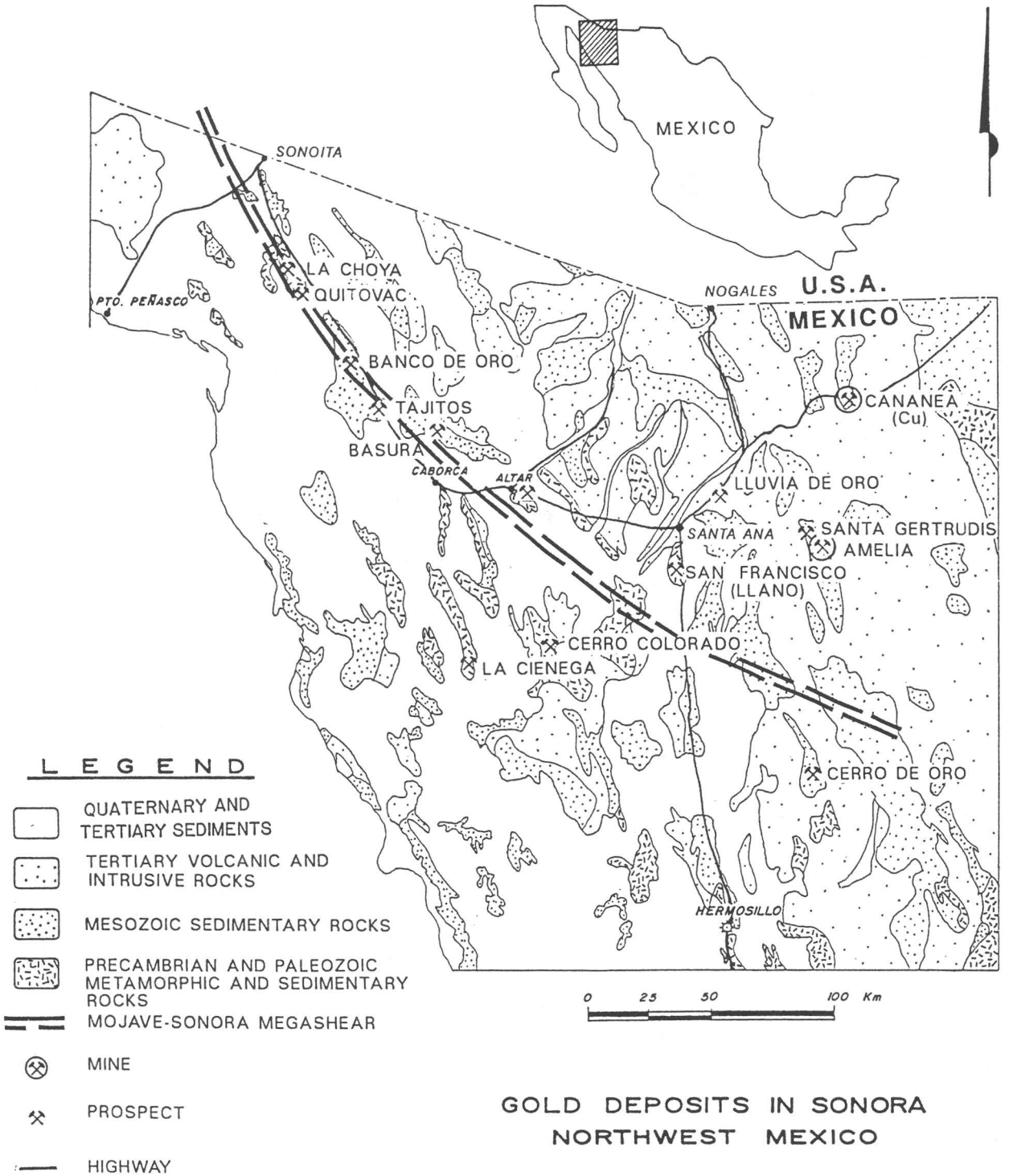

Figure 1 (Silberman and others). Gold mines and prospects and generalized geology of northern Sonora, Mexico. Modified from Silberman and others (1988).

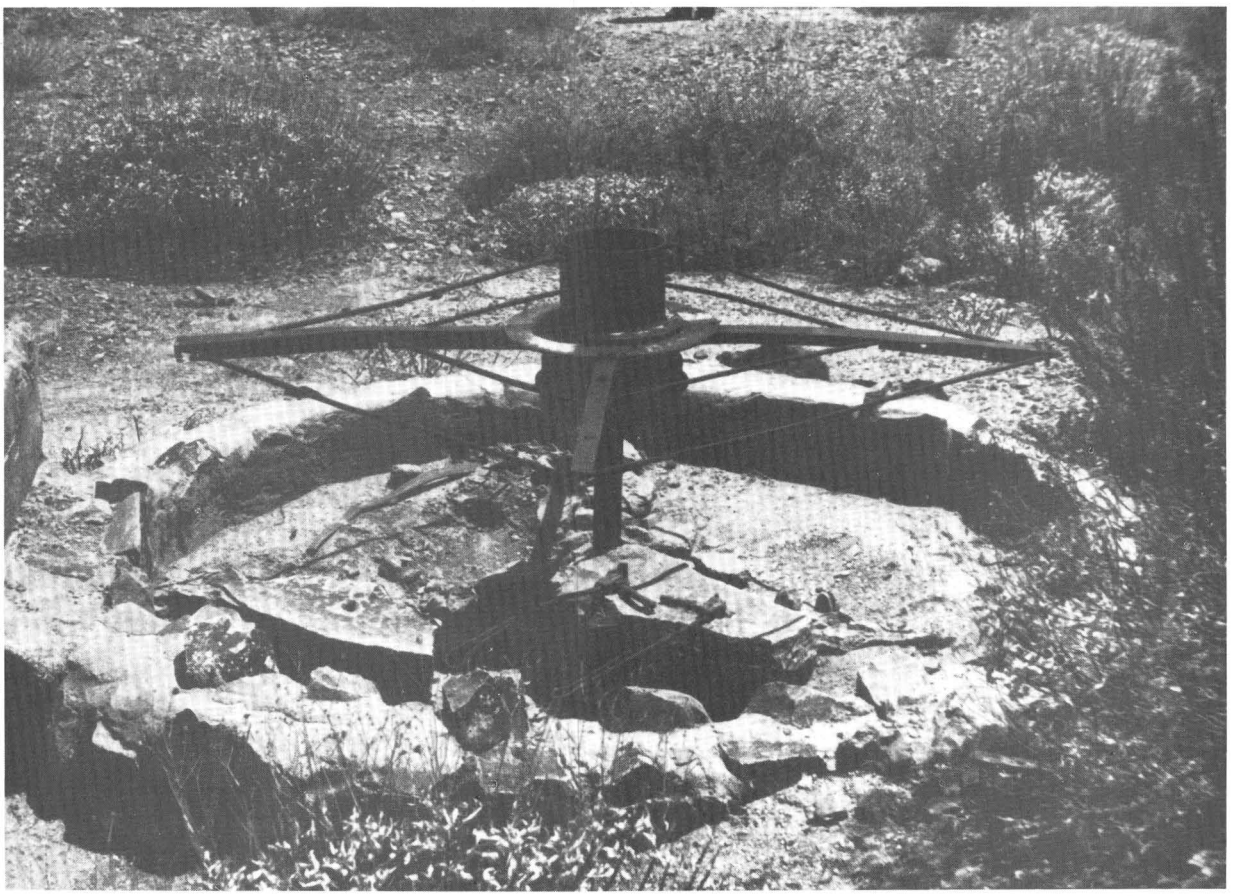

Figure 2 (Silberman and others). Abandoned arastra (crusher) at Quitovac, near old open pit. Diameter of circle is about 2 m. Photograph by M.L. Silberman in 1984.

have remobilized gold deposited by earlier magmatic or metamorphic fluids into brittle fractures.

REFERENCES CITED

Branham, A.D., 1987, Geology of the American Girl and Padre y Madre gold deposits, Imperial County, California: Pullman, Wash., University of Washington, unpub. M.S. thesis, 144 p.

Silberman, M.L., Giles, D.A., and Graubard, Cinda, 1988, Characteristics of gold deposits in northern Sonora, Mexico—A preliminary report: Economic Geology, v. 83, p. 1966–1974.

Geology and Mineral Potential of Precambrian Basement Rocks of the Trans-Hudson Orogen, U.S.A.

By P.K. Sims, Zell E. Peterman, *and* T.G. Hildenbrand

Geological, geophysical, and well-log data were analyzed to map the subsurface geology and basement topography of the Early Proterozoic Trans-Hudson orogen and adjacent tectonostratigraphic terranes (fig. 1). The map (Sims and others, in press) was compiled as part of a cooperative project between the U.S. Geological Survey and the geological surveys of Minnesota, Montana, Nebraska, North Dakota, South Dakota, and Wyoming.

The Trans-Hudson orogen is a north-trending orogenic belt of Early Proterozoic (1,910–1,800 Ma) age that extends from outcrop areas in Manitoba and Saskatchewan southward beneath Phanerozoic cover into the subsurface of the northern Great Plains. It mainly comprises Early Proterozoic arc-related rocks but locally includes Archean basement rocks. The western boundary of the Trans-Hudson orogen is marked by two major Archean faults that displace the basement rocks—the Cedar Creek fault and the Hartville-Rawhide fault. The Hartville-Rawhide fault possibly merges with the much younger (about 1,700 Ma) Cheyenne belt. The eastern boundary of the orogen is marked by the Superior-Churchill boundary zone, a 55-km-wide zone of low magnetization, which abruptly truncates the east-northeast-trending structural fabric of the Superior craton.

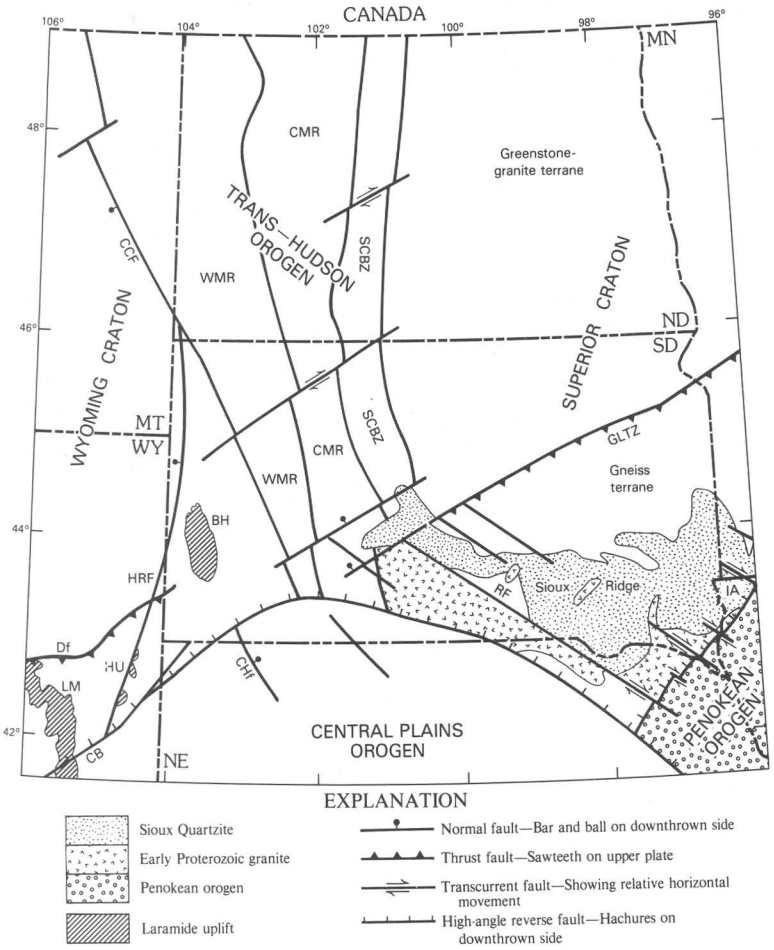

Figure 1 (Sims and others). Tectonic map of Precambrian basement, northern Great Plains, U.S.A. The Archean Superior and Wyoming cratons are separated by the Early Proterozoic Trans-Hudson orogen. The Superior craton is flanked on the southeast by the Early Proterozoic Penokean orogen. The Early Proterozoic Central Plains orogen truncates both cratons and older Proterozoic orogens on the south. BH, Black Hills; CB, Cheyenne belt; CCF, Cedar Creek fault; CMR, central magnetic region; CHf, Chadron fault; Df, Douglas fault; GLTZ, Great Lakes tectonic zone; HRF, Hartville-Rawhide fault; HU, Hartville uplift; LM, Laramie Mountains; RF, Reservation fault; SCBZ, Superior-Churchill boundary zone; WMR, western magnetic region.

Aside from the Black Hills uplift, mineral resources of the Trans-Hudson orogen must be sought in the subsurface. Stratabound gold deposits of the Homestake type could be present beneath a shallow cover of Phanerozoic rocks around the northern margin of the Black Hills uplift. Nickel and copper deposits similar to those in the Thompson nickel belt in Manitoba may exist in the ultramafic-mafic rocks of the Superior-Churchill boundary zone.

REFERENCE CITED

Sims, P.K., Peterman, Z.E., Hildenbrand, T.G., and Mahan, Shannon, compilers, in press, Precambrian basement map of the Trans-Hudson orogen and adjacent terranes, northern Great Plains, U.S.A.: U.S. Geological Survey Miscellaneous Investigations Series Map I–2214, scale 1:1,000,000.

Development and Testing of the CHIM Electrogeochemical Exploration Method

By David B. Smith, Donald B. Hoover, *and* Richard F. Sanzolone

The CHIM electrogeochemical exploration technique was developed in the Soviet Union approximately 20 yr ago and has become a routine mineral exploration tool in that country. CHIM is an acronym for the Russian phrase "*ch*astichnoe *i*zvlechenniye *m*ettalov," which means "partial extraction of metals." The method is claimed to be particularly effective in the exploration for concealed mineral deposits that are not detectable by other geochemical or geophysical techniques. Soviet explorationists cite case histories in which concealed mineral deposits have been found through several hundred meters of barren cover in a variety of geologic settings. The People's Republic of China has been using a variation of this method for almost a decade, and the Geological Survey of India has recently begun to test the method.

The basics of the CHIM method are relatively simple. A stable, high-voltage, direct-current electrical source provides current to an anode and to an array of special collector cathodes. Electric current to the individual collector cathodes is in the range of 0.1 to 0.5 A, and collection times range from 6 to 48 h. The anode may be an iron, steel, or carbon rod. The collector cathodes consist of a graphite or titanium rod inside a cylinder containing a solution of nitric acid. Electrical contact with the earth is made through a semipermeable membrane at the base of the cylinder (fig. 1). Mobile cations from soil near the cylinder are collected in the nitric acid or on the inner rod during passage of the current. Upon cessation of the electric current, the cathodes are retrieved, and both the nitric acid solution and the graphite or titanium rod are analyzed for metallic elements that accumulated under the influence of the electric field.

The U.S. Geological Survey is in the process of developing CHIM capabilities and testing the technique on various types of mineral deposits. Early work consisted of developing and testing electronics, testing electrode designs, and testing different types of semipermeable membranes in the laboratory. This work was successfully completed, and the first field tests were begun at the Kokomo mine near Central City, Colo., in May 1990.

The current field system obtains power from a trailer-mounted 15-kW, 400-Hz diesel generator and a Zonge Engineering induced-polarization transmitter using 50–1,000 V and 0.2–4.3 A; the transmitter is mounted in a pickup truck. Direct-current output goes to a multichannel ampere-hour meter having 32 anode and 32 cathode positions to monitor the total charge transfer during a run. Electric current from the meter is adjusted for individual collector electrodes in an optional rheostat bank and is distributed through multiconductor cables to the electrodes.

Figure 1 (Smith and others). Large (4-in. diameter) CHIM electrode emplaced in soil. Photograph by Misac Nabighian (Newmont Exploration) in September 1990.

Cathodes for the field test consist of a titanium or graphite rod suspended in 4 *N* nitric acid housed in a polyvinyl chloride body. A parchment membrane, through which current passes, is held in place on the base of the unit with an O-ring.

The field tests at the Kokomo mine were conducted over a 2-m-wide vein containing Cu, Pb, and Zn sulfides and precious metals. The vein is covered by approximately 3 m of colluvial material. Standard geochemical soil sampling failed to delineate the vein except that a weak Ag anomaly was detected (5 ppm compared to a background of 1–2 ppm). The CHIM method successfully defined the vein on the basis of Cu, Ag, and Zn distribution. Figure 2 shows CHIM results for Zn obtained during a test in which samples of the nitric acid solution were collected 6 times from 12 sample sites positioned at 10-m intervals during a 25-h run.

$^{40}Ar/^{39}Ar$ Thermochronology of Fracture-Controlled Mineral Deposits of the Idaho Batholith—Age, Thermal History, and Origin

By L.W. Snee, Karen Lund, K.V. Evans, C.H. Gammons, *and* M.J. Kunk

$^{40}Ar/^{39}Ar$ age-spectrum dating is a highly precise (<0.25 percent absolute analytical uncertainty) and accurate isotopic technique that is a powerful tool for solving some long-standing problems in economic geology, including the age, duration, number of stages and (or) episodes, and temperature of mineralization. This method offers the temporal resolution necessary for dating different stages of mineralization and alteration in hydrothermal systems. An age-spectrum or isochron analysis of the data from a sample

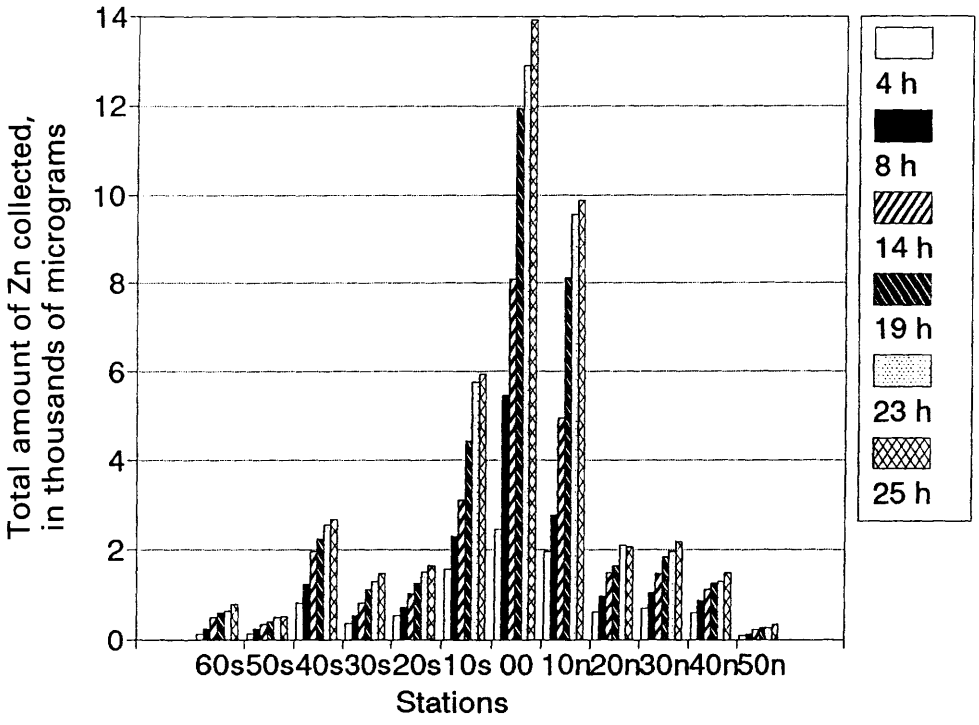

Figure 2 (Smith and others). Total micrograms of zinc collected at CHIM collector electrodes spaced at 10-m intervals over a mineralized vein at the Kokomo mine, Colorado. Six samples were taken at each electrode during the 25-h run. The vein is approximately under station 00.

provides information about the distribution of argon in the analyzed mineral or whole rock and can indicate whether the dated material formed before, during, or after alteration. Duration of mineralization and number of episodes can be evaluated by comparing mineral data from veins that formed during multiple stages with data from associated wall rocks. $^{40}Ar/^{39}Ar$ age-spectrum dates are unique because the time when various minerals close to diffusion of argon can be related to temperature; thus, the dates provide a thermochronology. These time-temperature data are useful for understanding details of ore-forming processes and for planning mineral exploration. $^{40}Ar/^{39}Ar$ thermochronologic data have been used to provide valuable constraints on the age, thermal history, and origin of fracture-controlled mineral deposits of the Idaho batholith.

The age and origin of gold-bearing quartz veins hosted in Cretaceous rocks of the Idaho batholith or older rocks in central Idaho were the subject of debate prior to detailed isotopic dating. Eocene plutonic and dike rocks crop out in many of the mining districts, and, locally, disseminated gold deposits are present in Eocene volcanic rocks such as in the Thunder Mountain district. It has been long argued that the numerous gold-bearing quartz veins distributed throughout the Idaho batholith were genetically related to the Eocene plutonic and volcanic event.

Many quartz veins in the southern part of the Idaho batholith (within the Elk City, Challis, Hailey, and Twin Falls 1° × 2° quadrangles) are near the roof zones of Late Cretaceous (78–70 Ma), marginally peraluminous, granite-granodiorite (primarily biotite granodiorite and muscovite-biotite granite) plutons; other quartz veins are in older metaluminous granodiorite-tonalite plutons (93–87 Ma) and metamorphic rocks that were intruded by the younger plutons. The deposits are both in discrete quartz-filled fissure veins and in disseminated deposits along silicified shear zones. All the deposits are characterized by quartz flooding, episodic brecciation, and open-space filling. Wall-rock alteration is minor. The fissure-vein and shear-zone deposits contain sulfides and have produced gold, silver, copper, lead, zinc, molybdenum, tungsten, antimony, and mercury. Sulfide minerals of the veins vary from district to district, perhaps because of the depth of formation of the vein systems and possibly because of different sources of the metals. Although parallel Eocene dikes are common in several districts, the dikes cut mineralized rock and are neither silicified nor mineralized; thus, the Eocene dikes formed after the mineralization.

High-precision $^{40}Ar/^{39}Ar$ age-spectrum dates of muscovite and potassium feldspar from quartz veins and altered host rock from 15 districts range from 78 to 57 Ma. Ages of the deposits within any district tend to form clusters; locally, multiple mineralization events occurred in some districts (for example, Edwardsburg, Profile Gap, Yellow Pine, Atlanta). Ages of the deposits are slightly younger

than cooling ages of the peraluminous granites in most districts. Therefore, the vein deposits are Cretaceous or, less commonly, Paleocene and were not formed by hydrothermal activity associated with Eocene plutons. Furthermore, the $^{40}Ar/^{39}Ar$ age spectra for minerals from the deposits and the cooling history of the region after emplacement of Cretaceous granites quantify the thermal and spatial effects of younger events. In particular, age spectra of quartz-vein muscovites commonly show ^{40}Ar loss that occurred during younger Cretaceous and Paleocene mineralization; only those samples collected within a few meters of Eocene dikes, plutons, and volcanic centers display partial ^{40}Ar loss incurred during Eocene events. In addition, microcline from nearby Cretaceous plutons yields Late Cretaceous to Paleocene $^{40}Ar/^{39}Ar$ dates which indicate that the ambient temperature of host rocks and mineral deposits was already below about 150 °C (the argon closure temperature of microcline) before Eocene magmatic events. Thus, only Cretaceous or Paleocene mineral deposits that were cut by Eocene plutons or dike swarms show the effects of temperatures exceeding 150 °C. Mixed-layer illite/muscovite, which has an estimated argon closure temperature of less than 150 °C, was collected from two alteration zones adjacent to Eocene dikes and yielded $^{40}Ar/^{39}Ar$ ages of 52 Ma. Therefore, metals were remobilized locally during Eocene magmatic activity, but the importance of such an event has not been evaluated.

In summary, most of the studied mineral deposits were episodically formed in fractures at or near the roof of marginally peraluminous, Cretaceous granite plutons, either in extensional fissures that opened during postemplacement cooling and uplift of the plutons or in preexisting and long-lived shear zones near the roof of the plutons. The Paleocene metallogenic activity may have been related to local slow cooling after the Cretaceous magmatic event or to undocumented Paleocene magmatism. Subsequently, most of these same fracture systems served as avenues for the emplacement of Eocene dikes and local remobilization of metals.

The Re-Os Isotope System as a Tracer in the Study of Platinum-Group-Element and Gold Deposits

By R.J. Walker, J.W. Morgan, D.D. Lambert, A.J. Naldrett, J.K. Bohlke, *and* V. Rajamani

^{187}Re decays to ^{187}Os and has a half-life of approximately 43 b.y. The long half-life of ^{187}Re and the large fractionations of Re from Os that take place during many magmatic and aqueous processes make the Re-Os system valuable for dating ores. The initial Os isotopic composition is a useful geochemical indicator for assessing the origin of the noble metals, of which Os is one. We have utilized the Re-Os system to study four ore occurrences.

Re-Os isotopic analysis of rocks from the Late Archean Stillwater Complex, Montana, that have high Re/Os ratios yielded an isochron age of 2,710±20 Ma. This age indicates that the Re-Os system, unlike the Rb-Sr system, remained closed following crystallization. Analyses of sulfides and chromitites from the J-M reef revealed that the complex crystallized from melts having very different initial Os isotopic compositions ($^{187}Os/^{186}Os$ = 0.90–1.3). We infer from the isotopic evidence that magma mixing may have occurred throughout the crystallization of parts of the Stillwater Complex. The J-M reef contains platinum-group elements (PGE's) and has a much higher initial Os isotopic composition than that thought to prevail in the bulk mantle; ores in the reef were likely derived from melt containing a significant proportion (approximately 10 percent) of crustal material.

A Re-Os study of sublayer ores from the Sudbury Complex, Ontario, also revealed a significant contribution to the ores from a crustal source. Like those for Stillwater rocks, Re-Os isochrons for individual Sudbury ores (Levack West, Falconbridge, Strathcona) indicate closed-system behavior since the 1,850-Ma crystallization age of the complex. Very large initial Os isotopic variations exist for the different ores; $^{187}Os/^{186}Os$ ratios range from 4.7 to 8.7. These compositions indicate the presence of at least two isotopically distinct sources for the PGE's (and probably the Cu and Ni). It is likely that the chief source of the PGE's in at least some of the ores was predominantly the Late Archean Superior Province crust. Mixing calculations suggest that one ore (Strathcona) may contain >95 percent crustal Os.

The Re-Os systematics of Au ores and related mafic and ultramafic rocks of the 2.7-Ga Kolar schist belt, Karnataka, India, suggest a complex secondary history for many of the rocks. Several rocks and a sulfide lode ore have highly radiogenic initial $^{187}Os/^{186}Os$ ratios of 33–39. Probably these rocks were equilibrated with fluids containing very radiogenic Os derived from ancient crust; some Au also may be derived from ancient crustal sources. In contrast, two quartz-carbonate vein ores have Re-Os systematics consistent with the derivation of Os from 2.7-Ga mantle-derived rocks. Sources for this Os (and related Au) may have been the komatiites and basalts within the schist belt.

To test the use of Os isotopes as tracers for fluid-deposited Au, we have begun an examination of the isotopic systematics of Au ores and related rocks from the Allegheny district of northern California. Initial results show that relatively unaltered samples of granite, basalt, and harzburgite have initial Os isotopic compositions that are similar to those of related rocks that have been altered by Au-bearing fluids to quartz-carbonate schist and to sulfidic albitites. Presumably the Re-Os systematics of the altered

rocks were affected only slightly by the alteration. Several ore samples, however, have Os isotopic compositions consistent with the incorporation of highly radiogenic Os from much older crustal sources.

The Getchell Gold Trend, Northwestern Nevada—Geologic Structure Delineated by Further Processing of Electromagnetic Data Collected During a Helicopter Survey

By W.S. Wojniak *and* D.B. Hoover

The U.S. Geological Survey used a helicopter to conduct a low-altitude electromagnetic survey of the Getchell gold trend in the Osgood Mountains of northwestern Nevada as part of its Development of Assessment Techniques Program. The Getchell gold trend includes six Carlin-type gold deposits (fig. 1), tungsten and barite deposits, and potential for additional mineral deposits. The electromagnetic data were collected at three frequencies (56,000, 7,200, and 900 Hz) and were processed into apparent electrical resistivities by Dighem, Inc. The flight-line data tapes are publicly available from the National Geophysical Data Center in Boulder, Colo.

Faults and fractures associated with the gold deposits produce linear, low-resistivity anomalies of 1–10 ohm-m on the maps of Dighem's computed apparent resistivities. In an attempt to enhance anomalies that may indicate such structures, the data were further processed as digital images. First, the logarithmic electrical resistivities were processed into color shaded-relief images, and horizontal-gradient maps were calculated for the three logarithmic electromagnetic resistivity maps and the map of the total magnetic field reduced to the pole. Maps of the ratios between the resistivities at the three frequencies were prepared. Various multiplications of the linear and logarithmic horizontal gradients of the 900-Hz resistivity and total magnetic field were mapped, and the multiplications of horizontal gradient maps were multiplied by their correlation coefficients. A map of the two-layer Bostick inversion of the three apparent resistivities was also prepared.

Of all the maps prepared, those showing (1) the horizontal gradient of the 900-Hz logarithmic resistivity and (2) the horizontal gradient of the 900-Hz logarithmic resistivity multiplied by the logarithm of the horizontal gradient of the total magnetic field were the most successful in enhancing and extending the representations of known faults, such as the Getchell fault zone. The horizontal gradient enhances areas where the physical properties of the rocks change sharply, such as boundaries between lithologies having different resistivities. When the horizontal gradients of the apparent resistivity and the magnetic field are multiplied together, the zones, such as faults, where both electrical and magnetic properties are changing are enhanced.

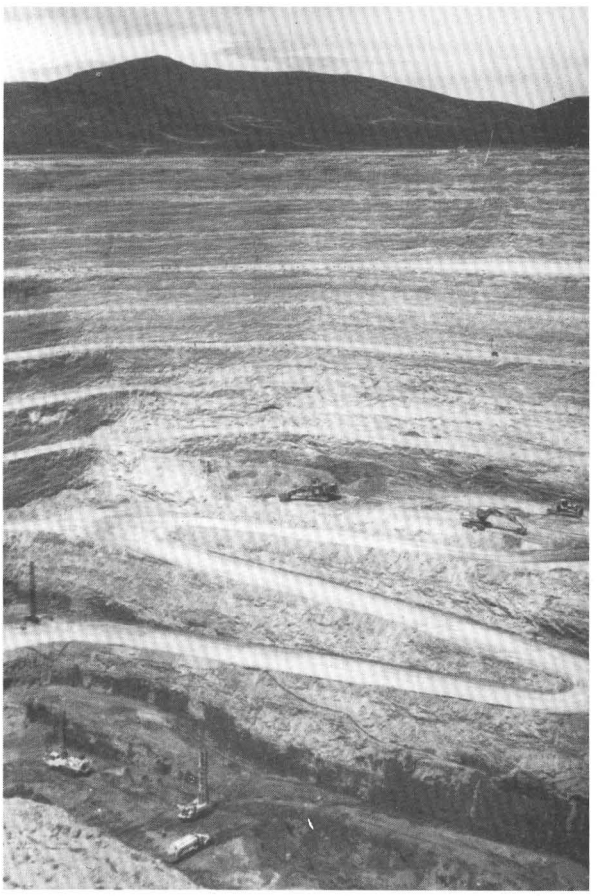

Figure 1 (Wojniak and Hoover). The Rabbit Creek open-pit gold mine of Santa Fe Pacific Mining, Inc., along the Getchell trend, Nevada. The pit exposes 120 m of Tertiary basin-fill sediments; each bench is 12 m high. View looking northwest toward the Dry Hills. Photograph by Steven M. Smith, August 25, 1990.

The airborne resistivity data best detect the low-resistivity anomalies along the known faults over bedrock outcrops and over the upper pediment of the valley east of the Osgood Mountains where alluvial cover is the thinnest. The effective penetration of the electromagnetic fields into the electrically conductive alluvial cover is only tens of meters; nevertheless, linear structural trends were detected in the thick alluvium of the valley east of the Osgood Mountains. We therefore conclude that differences in the resistivity of the alluvial cover are present and that these differences reflect deep underlying structure.

SOPAC—A Decade of Research on Mineral and Hydrocarbon Resources in the South Pacific

By F.L. Wong, B.A. Richmond, H.G. Greene, J.R. Dingler, J.R. Hein, K.A. Kvenvolden, M.S. Marlow, J.L. Morton, D.M. Rubin, D.W. Scholl, *and* J.G. Vedder

The U.S. Geological Survey (USGS) has been investigating mineral and hydrocarbon resources in the South Pacific for the past 10 yr through unilateral and cooperative programs with island nations and international agencies. The main program, referred to as SOPAC, was a cooperative effort among the USGS and agencies in Australia and New Zealand; it was coordinated by the multinational Committee for Coordination of Joint Prospecting for Mineral Resources in South Pacific Offshore Areas (CCOP/SOPAC). The SOPAC program (which included major USGS cruises in 1982 and 1984) focused on the mineral resources and hydrocarbon potential of the island nations of Tonga, Vanuatu, Solomon Islands, Fiji, and Papua New Guinea (fig. 1). Additionally, as part of an ongoing cooperative program with CCOP/SOPAC, USGS personnel have completed and continue to produce economic mineral assessments in connection with studies of nearshore sedimentological processes for these and other South Pacific nations.

Nearshore mineral resources of value to the island nations include sand and gravel, gold and other placers, phosphorite, and precious coral. Rapid economic growth in many South Pacific island countries has led to an increased demand for aggregate material used in the construction industry. In response to the gradual depletion of the most readily available source of aggregate, the surrounding beaches, and to the attendant coastal erosion, the USGS and CCOP/SOPAC have explored and identified alternate sources of sand and gravel in diverse island and reef environments in Tonga, the Cook Islands, Tuvalu, and Western Samoa. The USGS has done similar work in American Samoa.

In 1986, a USGS-CCOP/SOPAC-Cook Islands mineral exploration program drilled for phosphorite in Aitutaki lagoon in the Cook Islands. No extensive deposits were found, but the mud deposits recovered were leached from mafic and ultramafic rocks that contained anomalous con-

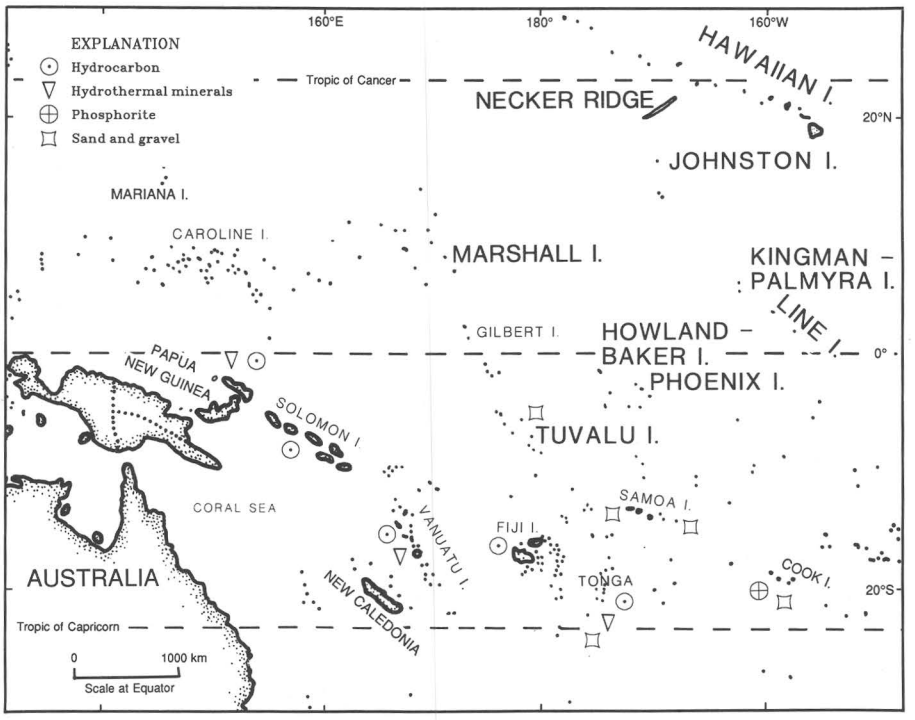

Figure 1 (Wong and others). Sites of mineral and hydrocarbon exploration in the South Pacific.

centrations of strategically and economically important metals including Al, Fe, Ti, Cr, Ni, Mn, U, and As. The metal concentrations are not of immediate economic interest but warrant further studies because similar processes have produced minable Ni-rich laterites in New Caledonia.

Geophysical surveys of the Valu Fa Ridge region west of the Tonga arc conducted by the USGS in 1982 and 1984 provided the basis for subsequent international exploration programs that led to the discovery of sea-floor sulfide deposits and active hydrothermal vents. USGS investigators used multichannel seismic-reflection data to locate the magma chamber under the Valu Fa Ridge. The presence of fresh andesite and dacite, warm bottom water and cored sediment, and abundant oxide deposits indicated extensive hydrothermal activity. Sites with high resource potential were outlined for future exploration. Later geophysical and photographic surveys and submersible exploration by French and German agencies have located polymetallic sulfide deposits along the ridge crest above the Valu Fa magma chamber.

Hydrothermal mineralization has also been investigated in shallow-water and onshore environments. In conjunction with earlier work by the Australian Bureau of Mineral Resources (BMR), the USGS sampled volcanic deposits associated with active cones perched on Epi caldera offshore of Epi Island, Vanuatu. Anomalous Fe and Mo contents in two of the five samples collected by the USGS were similar to the metal enrichment determined by the BMR in this area. Volcanic rocks of quartz trachyte and trachyte composition were dredged from offshore of the Tabar-Lihir-Tanga-Feni island chain north of New Ireland, Papua New Guinea, during the 1984 USGS survey. Analysis of the dredge samples for precious metals has not yet detected any gold, but subsequent release of proprietary data by Papua New Guinea revealed that similar rocks do host epithermal gold deposits (18.4×10^6 oz at 3.4 g/t) on Lihir Island.

The USGS hydrocarbon resource assessment program in the South Pacific refined knowledge of the factors for hydrocarbon generation and accumulation in the southern Tonga platform in Tonga; the Central Basin of Vanuatu; the complex of basins in the Central Solomons Trough, Solomon Islands; and the New Ireland basin in Papua New Guinea. Adequate sediment thickness (>3 km), geothermal gradients (>30 °C/km), structural traps (anticlines, fault traps), and reservoir rocks of varying quality are present in each area. Hydrocarbon gases commonly found in near-surface sediment from various offshore sites in the South Pacific appear to be mainly biogenic. Oil seeps, such as those reported from onshore Tonga, Fiji, and Vanuatu, indicate hydrocarbon generation in the arc regions, but onshore source-rock analyses suggest only a remote potential for significant quantities of oil and gas. However, the USGS is reevaluating old proprietary and public single- and multi-channel seismic-reflection data and those more recently acquired by the USGS to focus study on the most promising targets for future exploration.

The Origin of Evaporite Deposits—A Model Based on a Hydrologically Open System

By Warren W. Wood *and* Ward E. Sanford

The origin of large thicknesses of commercially valuable evaporite minerals has, for many deposits, been difficult to explain on the basis of known or likely solute input to topographically closed basins. Our proposed leakage model suggests that a hydrologically open basin, having either seepage loss to surrounding ground-water systems or interchange with an adjacent ocean, is the dominant control on the thickness and suite of evaporite minerals forming within the basin. For a specific solute composition, the chemical divide determines the potential suite of minerals that can form in a chemically closed basin undergoing evaporation. However, the flux ratio (the ratio of water outflow to inflow) determines the minerals in the suite that actually precipitate, as well as their respective thicknesses. Attainment of hydrologic steady-state conditions permits large thicknesses of one or two evaporite minerals to form rather than the equilibrium sequence of several minerals that typically forms in a closed basin.

The code PHRQPITZ (Plummer and others 1988) is a chemical-equilibrium model incorporating Pitzer's equations for calculating ion activity in a high-ionic-strength solution. By using the code with a lumped-parameter hydrologic model, we calculated the variation in thickness of gypsum, dolomite, glauberite, mirabilite, bloedite, polyhalite, halite, and hexahydrite deposits as a function of subtle changes in ground-water seepage rates (Wood and Sanford, 1990). These calculations utilized a typical mixed cation-anion ground water from the southern High Plains of Texas and New Mexico. We also calculated the mineral suite and thickness of variable leakage of seawater and a sodium carbonate ground water from southern Idaho typical of that found in many volcanic terrains. In addition to mineral thickness, the model provides the concentration of the individual solutes as a function of leakage and amount of evaporation and, thus, documents the evolution of the brine during evaporation. The model is general and is applicable for any solute composition and can be used to simulate (1) evaporite deposition in a topographically closed continental basin, (2) the interchange between a restricted evaporating basin and the ocean, and (3) reflux conditions, where certain solutes return to the ocean through seepage. Knowledge of the mechanism controlling evaporite thickness and mineral suites can aid in the exploration for evaporite resources by eliminating unneces-

sary exploratory drilling, explaining the absence of certain brines, and predicting the mineral suite of active systems from the results of inexpensive solute analyses of ground water surrounding the basin.

REFERENCES CITED

Plummer, L.N., Parkhurst, D.L., Fleming, G.W., and Dunkle, S.A., 1988, A computer program incorporating Pitzer's equations for calculation of geochemical reactions in brines: U.S. Geological Survey Water-Resources Investigations Report WRI 88–4153, 310 p.

Wood, W.W., and Sanford, W.E., 1990, Ground-water control of evaporite deposition: Economic Geology, v. 85, p. 1226–1235.

U.S. Geological Survey Mineral-Resource and Tectonic Studies in Venezuela

By J.C. Wynn, S.D. Olmore, Floyd Gray, W.C. Day, G.B. Sidder, *and* N.J Page

A cooperative project was established in 1987 between the U.S. Geological Survey (USGS) and C.V.G.-Técnica Minera, C.A. (TECMIN), a mining company owned by the Venezuelan Government. The project is centered in Puerto Ordaz and Ciudad Bolívar, Venezuela, and is staffed by 3 resident USGS scientists and up to 10 visiting scientists per year. The 5-yr cooperative agreement encompasses training in geophysics, geochemistry, and economic geology, evaluating mineral sites, and upgrading laboratory and data-processing capabilities. A primary goal of the project is to complete a mineral-resource inventory of the Precambrian Venezuelan Guayana Shield (fig. 1) by the end of 1991. Intermediate steps in this effort include evaluation of known mineral deposits, exploration for new deposits, and a geologic inventory program. A major new Tectonic and Geologic Map Series will form an important milestone in this effort; maps in this series will incorporate available geophysical data and will be published at a scale of 1:500,000.

The Puerto Ayacucho sheet (fig. 2) is representative of the new Tectonic and Geologic Map series. The map is being compiled from aeromagnetic data, radiometric data, gravity data, side-looking radar images, air photos, and reconnaissance field work. The mapped area is about the size of West Virginia. It contains a large granite pluton, which has potential for gold and rare-earth-element mineralization; the area also may contain possible kimberlites along Mesozoic fractures. Three previously unknown ring-like structures, one with a uranium association that may be a large carbonatite intrusion, have been identified during data interpretation and assembly of the map. Numerous small to medium-sized buried magnetic bodies are also being incorporated into the map representation, making it effectively a map of the top 10–15 km of the crust. This series of maps thus will become the foundation for a detailed mineral-resource appraisal of the Venezuelan Guayana Shield.

The mineral-deposit map being compiled for the Guayana Shield shows several interesting associations. Shear-zone-hosted quartz veins within an Early Proterozoic greenstone belt are the primary source of gold in Venezuela. Districts such as El Callao, Lo Increible, and Kilometer 88 currently produce gold from low-sulfide gold-quartz veins. Placer deposits are associated with rocks of the greenstone belt and with conglomerate lenses and beds of the Uairén Formation of the Early to Middle Proterozoic Roraima Group. Diamond-bearing kimberlite has been identified only in the Quebrada Grande district in the northeastern part of the Guayana Shield, but diamonds are mined in numerous areas in the central, eastern, and southern parts. World-class deposits of banded iron-formation in the Archean Imataca Complex are mined at Cerro Bolívar, San Isidro, El Pao, and several other places. Deposits of bauxite and aluminum-rich laterite are products of intense weathering of granitic (Los Pijiguaos) and mafic intrusive rocks (Upata, Nuria, and Gran Sabana). Placer, eluvial, and lode occurrences of tin are associated with the Middle Proterozoic Parguaza Granite along the western margin of the shield.

The Lo Increible gold district is important because of its close spatial association with the El Callao mining district, which by 1906 was the largest gold producer in the world at over 7,000,000 oz. The Lo Increible district lies along a major ductile shear zone within the Early Proterozoic Pastora Group. Although the tropical weathering is intense, S-C mylonitic fabric is well preserved. The mineralization is typical of shear-zone-hosted lode-gold deposits in that native gold occurs in quartz-tourmaline veins that contain a quartz-calcite-chlorite-sericite alteration assemblage.

Sierra Verdun is a long, linear structure associated with mafic and ultramafic bodies that stands out sharply in SLAR (side-looking airborne radar) imagery from an otherwise flat Proterozoic granitic terrane. Geologic mapping reveals a structurally disjointed terrane that includes a folded and multiply deformed greenstone belt dominated by volcanic flows and tuffs of intermediate composition that are intruded by gabbroic and ultramafic rocks, perhaps representing multiple intrusive phases. These gabbroic and ultramafic rocks include komatiitic lavas, a sequence of pyroxene-rich cumulus rocks, and diabase dikes. Substantial gold production is associated with a distinctive magnetic anomaly caused by a large pluton overlain by many shallow, east-trending apophyses. Other similar anomalies in the region, as well as the occurrence of sulfides in the mafic-ultramafic sequence, suggest additional potential target zones for hydrothermal gold and for magmatic deposits of platinum-group elements.

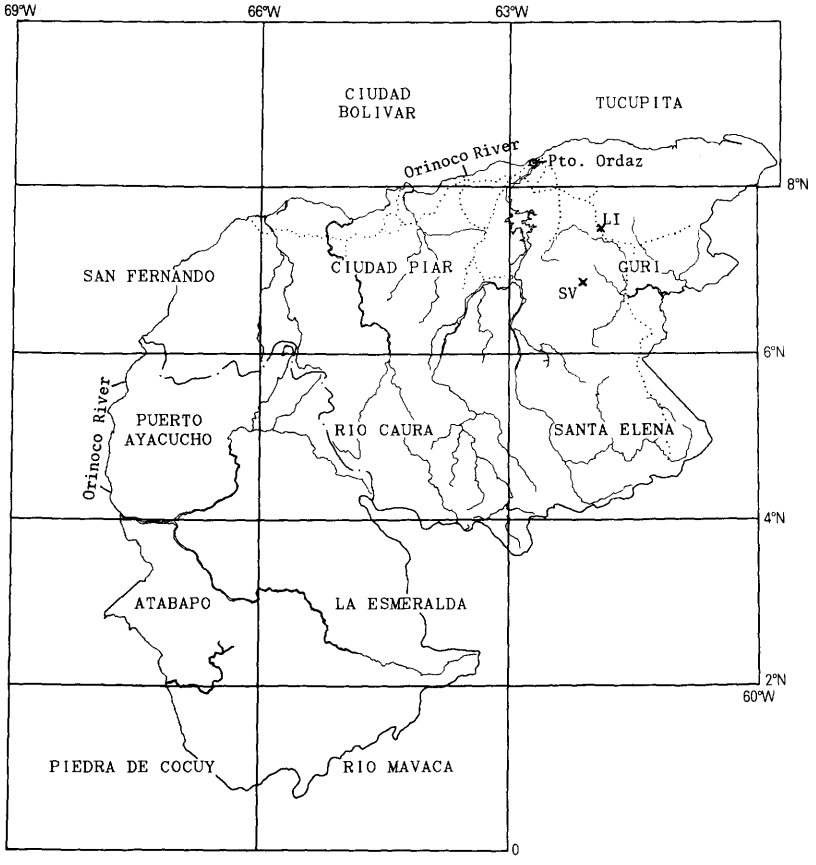

Figure 1 (Wynn and others). The Venezuelan Guayana Shield, showing locations of the Puerto Ayacucho area and the Sierra Verdun (SV) and Lo Increible (LI) study areas.

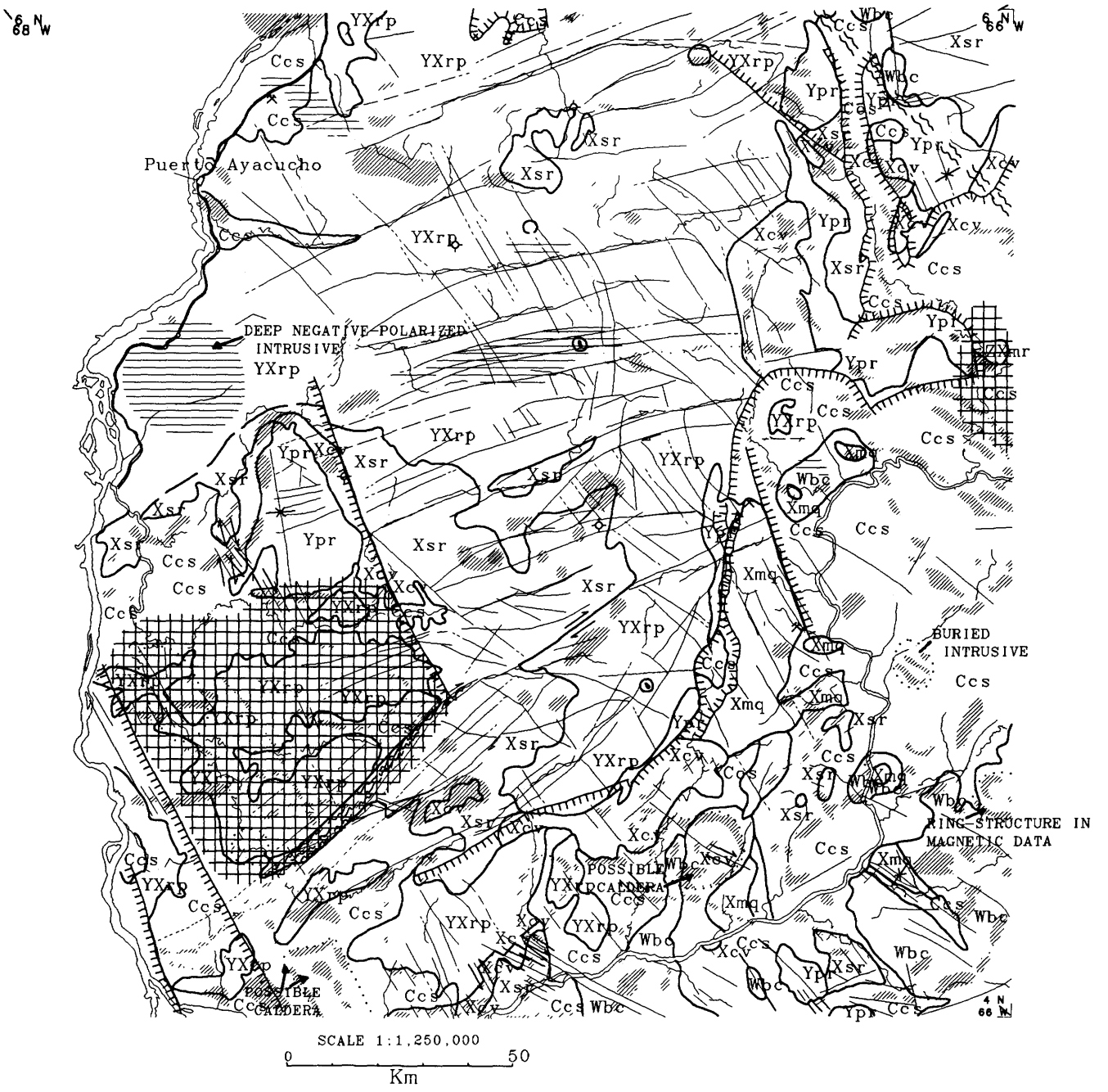

Figure 2 (Wynn and others). Geology and tectonic features in the Puerto Ayacucho area, Venezuela.

Platinum-Group Mineral Investigations, East and South Kalimantan, Indonesia

By Michael L. Zientek *and* Bambang Pardiarto

Information was gathered by the U.S. Geological Survey (USGS) and the Directorate of Mineral Resources of the Republic of Indonesia on occurrences of platinum-group-elements (PGE's) in Indonesia. The goal was to define the source of platinum-group minerals (PGM's) found in placers in East and South Kalimantan. USGS activities in PGM exploration in Indonesia were done in conjunction with the Geological and Mineral Survey Project, Asian Development Bank Loan No. 641 INO.

For East Kalimantan, two new placer PGM localities (Tabang area and Sungai Marah area) were documented, as well as an additional area, the Pasir area, that has anomalous Pt contents (8 and 12 ppm) in panned concentrate samples. A detailed mineral-resource assessment of southeastern Kalimantan identified four permissive areas for the occurrence of primary PGE deposits and a large region where diamond, gold, and PGM placers are derived from

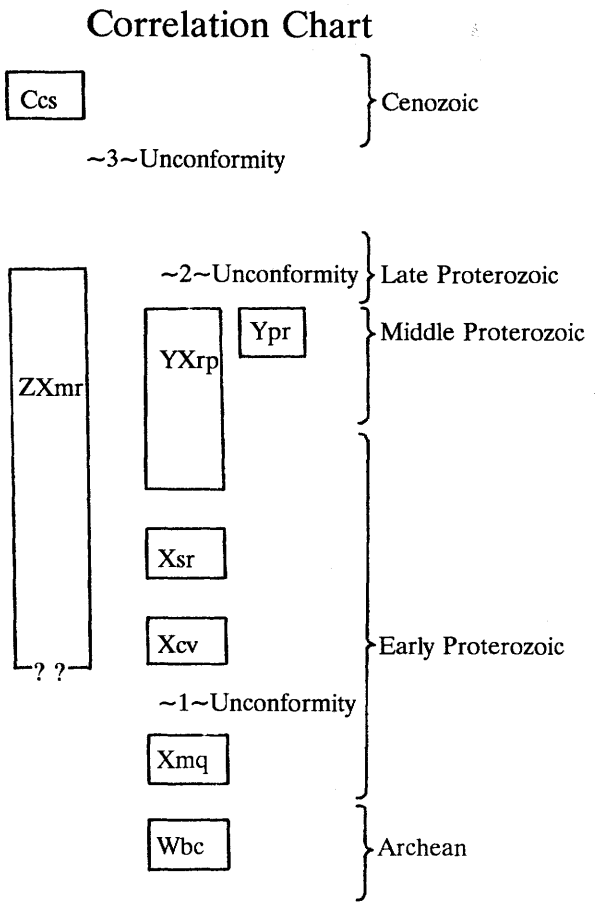

EXPLANATION

Ccs Cenozoic deposits and surfaces, including both depositional and erosional surfaces, alluvium, colluvium, and lag gravels.

~3~ Period of regional uplift and erosion.

~2~ Continental rifting in eastern Venezuela.

Ypr Middle Proterozoic platform sedimentary rocks (Roraima Group).

YXrp Middle Proterozoic Rapakivi-textured sodic granite to quartz monzonite (Parguaza Granite).

ZXmr Alkalic mafic rocks (where hatched, visible in the magnetic data only).

Xsr Middle Proterozoic calc-alkalic to alkalic granite (Santa Rosalia Granite).

Xcv Early Proterozoic calc-alkalic volcanic rocks; extrusive manifestation of the Santa Rosalia Granite?

~1~ Early Proterozoic Trans-Amazonian orogeny; northwest-striking shear zones and fold axes.

Xmq Early Proterozoic supracrustal quartzites, conglomerates, and volcanic rocks (highly magnetic unit: locally called the Moriche Formation).

Wbc Archean soda-granodiorite basement complex (highly magnetic unit: equivalent to the Imataca Group?).

Figure 2 (Wynn and others).—Continued.

Cretaceous conglomerates. The mineralogy and textures of the PGM's from the placers and detailed investigations of one of the permissive areas indicate that the primary source of the PGM's is most likely chromitite schlieren associated with Alaskan-type ultramafic intrusions.

In southeastern Kalimantan, pre-Tertiary rocks and folded and faulted Eocene to Miocene sedimentary rocks are flanked by two late Cenozoic sedimentary basins. The pre-Tertiary rocks consist of an Early to Middle Cretaceous accretionary complex hosting deposits of podiform chromitite; iron±Au skarns; Fe-Cr oxide segregations in cumulate dunite, clinopyroxenite, and gabbro; epithermal Mn deposits; low-sulfide Au-quartz veins; and Au in sheared serpentinite. These rocks are unconformably overlain by the Late Cretaceous (Senonian) Manunggul Formation, a sequence of sedimentary and mafic volcanic rocks that are a source of placer diamond, gold, and PGM's found in younger deposits. Eocene to Miocene sedimentary rocks of mixed shallow-marine, deltaic, and continental facies were deposited in stable shelf and epicontinental conditions over much of this area. After uplift of the Meratus Mountains, Pliocene and Pleistocene coarse clastic sediments were deposited on the western and southeastern flank of the mountains; the sediments contain Au-PGM and diamond-Au-PGM placer deposits.

Detailed investigations of one of the areas permissive for a bedrock source for PGM's in South Kalimantan (Riam Pinang area) indicate at least two sources for the PGM's in the alluvial deposits in this area: (1) alluvial deposits on terraces 20–30 m above the present drainages and (2) dunitic bodies intrusive into clinopyroxene cumulates that are probably parts of Alaskan-type ultramafic complexes in the pre-Tertiary accretionary complex. A chromitite schlieren found during the trenching of one of these dunitic bodies contained an anomalous Pt concentration; analysis by NiS fire assay-inductively coupled plasma-mass spectroscopy yielded the following results: Pt = 580 ppb; Pd = 3.4 ppb; Rh = 10 ppb; Ru = 9 ppb; and Ir = 21 ppb. The

chondrite-normalized PGE pattern for this rock is characterized by elevated Pt and Ir contents and is similar to patterns for chromitites in Alaskan-type ultramafic intrusions. Chromitite schlieren made up approximately 11 percent of the analyzed rock sample; therefore, concentrations of Pt in the chromitite alone may exceed 5 ppm.

The two most valuable exploration methods for defining prospective targets in the Riam Pinang area are recording the PGM's seen in panned concentrate samples in the field and analyzing the panned concentrate samples for Pt, Pd, and Au. Up to 29 grains of PGM's were observed in panned concentrate samples in the field. Pt contents of the concentrates range from <5 ppb to 85.9 ppm. Fifty percent of the samples have more than 107 ppb Pt; 25 percent have greater than 1,250 ppb Pt. Au contents range from 1.2 ppb to 291.3 ppm. Fifty percent of the samples have greater than 1.43 ppm Au; 25 percent have greater than 13.4 ppm Au. High Pt and Au contents do not have a one-to-one correspondence (as would be expected because Au and PGM's are derived from different sources). Pd contents are all low, less than 33 ppb. In contrast, only three of the stream-sediment samples have slightly anomalous PGE contents (their Pt contents are 394, 138, and 100 ppb). The rest of the samples have less than 44 ppb Pt and 23 ppb Pd. Au values are typically higher, averaging 90 ppb, with a high value of 130 ppb.

U.S. Geological Survey chemist William d'Angelo running samples on the inductively coupled plasma-atomic emission spectrometer (ICP-AES) in Reston, Va. By using a dedicated computer to record emission intensities, the ICP-AES can determine the concentrations of 51 elements in solution simultaneously. Photograph by Philip J. Aruscavage.

ADDRESSES AND TELEPHONE NUMBERS OF CONTRIBUTING AUTHORS

H.V. Alminas
U.S. Geological Survey
Mail Stop 973
Box 25046, Denver Federal Center
Denver, CO 80225
(303) 236–9674

Orlando André
Servicio Geólogico de Bolivia
Casilla 2729
La Paz, Bolivia
011–591–237–4544

Joseph G. Arth
U.S. Geological Survey
Mail Stop 937
345 Middlefield Road
Menlo Park, CA 94025
(415) 329–4670

Roger P. Ashley
U.S. Geological Survey
Mail Stop 901
345 Middlefield Road
Menlo Park, CA 94025
(415) 329–5416

Robert A. Ayuso
U.S. Geological Survey
954 National Center
Reston, VA 22092
(703) 648–6347

Viki Bankey
U.S. Geological Survey
Mail Stop 964
Box 25046, Denver Federal Center
Denver, CO 80225
(303) 236–1348

David F. Barnes
U.S. Geological Survey
Mail Stop 989
345 Middlefield Road
Menlo Park, CA 94025
(415) 329–5315

Walter J. Bawiec
U.S. Geological Survey
920 National Center
Reston, VA 22092
(703) 648–6148

Harvey E. Belkin
U.S. Geological Survey
959 National Center
Reston, VA 22092
(703) 648–6162

Robert J. Bisdorf
U.S. Geological Survey
Mail Stop 964
Box 25046, Denver Federal Center
Denver, CO 80225
(303) 236–1377

H. Richard Blank
U.S. Geological Survey
Mail Stop 964
Box 25046, Denver Federal Center
Denver, CO 80225
(303) 236–1341

James D. Bliss
U.S. Geological Survey
210 E. 7th Street
Tucson, AZ 85705
(602) 629–5502

J.K. Bohlke
U.S. Geological Survey
954 National Center
Reston, VA 22092
(703) 648–6325

Karen Sue Bolm
U.S. Geological Survey
210 E. 7th Street
Tucson, AZ 85705
(602) 670–5508

H.F. Bonham
Nevada Bureau of Mines and Geology
University of Nevada–Reno
Reno, NV 89557–0088
(702) 784–6691

Arthur A. Bookstrom
U.S. Geological Survey
Saudi Arabian Mission
APO New York 09697–7002
011–966–2–667–4188

T.L. Bowers
U.S. Geological Survey
927 National Center
Reston, VA 22092
(703) 648–6354

Stephen E. Box
U.S. Geological Survey
Room 656 U.S. Courthouse
W. 920 Riverside Ave.
Spokane, WA 99201
(509) 353–2467

David A. Brew
U.S. Geological Survey
Mail Stop 904
345 Middlefield Road
Menlo Park, CA 94025
(415) 329–5726

William E. Brooks
U.S. Geological Survey
Mail Stop 905
Box 25046, Denver Federal Center
Denver, CO 80225
(303) 236–5627

Mark W. Bultman
U.S. Geological Survey
University of Arizona
Gould-Simpson Building #77
Tucson, AZ 85721
(602) 670–5503

Thomas K. Bundtzen
Alaska Division of Geological
and Geophysical Surveys
3700 Airport Way
Fairbanks, AK 99709
(907) 451–2771

Alison Burchell
U.S. Geological Survey
University of Arizona
Gould-Simpson Building #77
Tucson, AZ 85721
(602) 670–5572

John W. Cady
U.S. Geological Survey
Mail Stop 964
Box 25046, Denver Federal Center
Denver, CO 80225
(303) 236–1330

Andrew C. Campbell
Department of Earth, Atmospheric,
and Planetary Sciences
Massachusetts Institute of Technology
Cambridge, MA 02139
(617) 253–5790

William F. Cannon
U.S. Geological Survey
954 National Center
Reston, VA 22092
(703) 648–6345

ADDRESSES AND TELEPHONE NUMBERS OF CONTRIBUTING AUTHORS

Raul Carrasco
Servicio Geólogico de Bolivia
Casilla 2729
La Paz, Bolivia
011–591–237–4544

Richard B. Carten
U.S. Geological Survey
Saudi Arabian Mission
APO New York 09697–7002
011–966–2–667–4188

Chen Nansheng
Institute of Geochemistry
Academia Sinica
Guiyang, Guizhou Province
People's Republic of China

S.E. Church
U.S. Geological Survey
Mail Stop 973
Box 25046, Denver Federal Center
Denver, CO 80225
(303) 236–1900

Roger N. Clark
U.S. Geological Survey
Mail Stop 964
Box 25046, Denver Federal Center
Denver, CO 80225
(303) 236–1332

Sandra H.B. Clark
U.S. Geological Survey
954 National Center
Reston, VA 22092
(703) 648–6331

L.G. Closs
Department of Geology and
Geological Engineering
Colorado School of Mines
Golden, CO 80401
(303) 273–3856

J.A. Commeau
U.S. Geological Survey
Woods Hole, MA 02543
(508) 548–8700

Jon J. Connor
U.S. Geological Survey
Mail Stop 905
Box 25046, Denver Federal Center
Denver, CO 80225
(303) 236–5614

Clay M. Conway
U.S. Geological Survey
2255 N. Gemini Drive
Flagstaff, AZ 86001
(602) 527–7199

Harry E. Cook
U.S. Geological Survey
Mail Stop 999
345 Middlefield Road
Menlo Park, CA 94025
(415) 329–3007

Theresa M. Cookro
U.S. Geological Survey
Mail Stop 937
Box 25046, Denver Federal Center
Denver, CO 80225
(303) 236–5706

Kevin P. Corbett
Department of Geology
School of Natural Sciences
Weber State University
Ogden, UT 84408–2507
(801) 626–7954

L.E. Cordell
U.S. Geological Survey
Mail Stop 964
Box 25046, Denver Federal Center
Denver, CO 80225
(303) 236–1204

Raymond M. Coveney, Jr.
Department of Geosciences
University of Missouri
Kansas City, MO 64110–2499
(816) 276–2980

Dennis Cox
U.S. Geological Survey
Mail Stop 984
345 Middlefield Road
Menlo Park, CA 94025
(415) 329–5364

Leslie J. Cox
U.S. Geological Survey
University of Arizona
Gould-Simpson Building #77
Tucson, AZ 85721
(602) 670–5505

Douglas E. Crowe
U.S. Geological Survey
954 National Center
Reston, VA 22092
(703) 648–6338

Lucia Cuitino
Servicio Nacional de
Geologia y Mineria
Casilla 10465
Santiago, Chile
011–56–237–5050

Charles G. Cunningham
U.S. Geological Survey
959 National Center
Reston, VA 22092
(703) 648–6121

W.C. Day
U.S. Geological Survey
Mail Stop 905
Box 25046, Denver Federal Center
Denver, CO 80225
(303) 236–6483

George A. Desborough
U.S. Geological Survey
Mail Stop 905
Box 25046, Denver Federal Center
Denver, CO 80225
(303) 236–5611

D.E. Detra
U.S. Geological Survey
Mail Stop 973
Box 25046, Denver Federal Center
Denver, CO 80225
(303) 236–2449

Felipe Diaz
Servicio Nacional de
Geologia y Mineria
Casilla 10465
Santiago, Chile
011–56–237–5050

J.H. Dilles
Department of Geology
Oregon State University
Corvallis, OR 97331–5506
(503) 737–1245

John R. Dingler
U.S. Geological Survey
Mail Stop 999
345 Middlefield Road
Menlo Park, CA 94025
(415) 329–3109

Bruce R. Doe
U.S. Geological Survey
923 National Center
Reston, VA 22092
(703) 648–6205

ADDRESSES AND TELEPHONE NUMBERS OF CONTRIBUTING AUTHORS

Jeff L. Doebrich
U.S. Geological Survey
Mackay School of Mines
University of Nevada-Reno
Reno, NV 89557–0047
(702) 784–5596

Lawrence J. Drew
U.S. Geological Survey
920 National Center
Reston, VA 22092
(703) 648–6483

Barbara A. Eiswerth
U.S. Geological Survey
927 National Center
Reston, VA 22092
(703) 648–6379

R.G. Eppinger
U.S. Geological Survey
Mail Stop 973
Box 25046, Denver Federal Center
Denver, CO 80225
(303) 236–2468

J.A. Erdman
U.S. Geological Survey
Mail Stop 973
Box 25046, Denver Federal Center
Denver, CO 80225
(303) 236–5512

George E. Ericksen
U.S. Geological Survey
954 National Center
Reston, VA 22092
(703) 648–6323

Yasmin Estanga
Corporación Venezolana de
Guayana-Compañía Técnica
Minera, C.A.
Edificio Sede CVG
Ciudad Bolívar, Venezuela
011–58–85–25334

Karl V. Evans
U.S. Geological Survey
Mail Stop 905
Box 25046, Denver Federal Center
Denver, CO 80225
(303) 236–5625

Russell C. Evarts
U.S. Geological Survey
Mail Stop 901
345 Middlefield Road
Menlo Park, CA 94025
(415) 329–5415

W.H. Ficklin
U.S. Geological Survey
Mail Stop 973
Box 25046, Denver Federal Center
Denver, CO 80225
(303) 236–1904

C.A. Finn
U.S. Geological Survey
Mail Stop 964
Box 25046, Denver Federal Center
Denver, CO 80225
(303) 236–1345

Frederick S. Fisher
U.S. Geological Survey
University of Arizona
Gould-Simpson Building #77
Tucson, AZ 85721
(602) 670–5501

Nora K. Foley
U.S. Geological Survey
959 National Center
Reston, VA 22092
(703) 648–6179

Eric R. Force
U.S. Geological Survey
University of Arizona
Gould-Simpson Building #77
Tucson, AZ 85721
(602) 670–5506

A.B. Ford
U.S. Geological Survey
Mail Stop 904
345 Middlefield Road
Menlo Park, CA 94025
(415) 329–5723

A.J. Froelich
U.S. Geological Survey
926 National Center
Reston, VA 22092
(703) 648–6950

Thomas P. Frost
U.S. Geological Survey
Room 656 U.S. Courthouse
W. 920 Riverside Ave.
Spokane, WA 99201
(509) 353–2165

Andrea J. Gallagher
U.S. Geological Survey
Mail Stop 964
Box 25046, Denver Federal Center
Denver, CO 80225
(303) 236–1388

C.H. Gammons
Department of Earth Sciences
Monash University
Clayton, Victoria 3168
Australia
011–61–3–565–5772

Andres Garcia
Corporación Venezolana de
Guayana-Compañía Técnica
Minera, C.A.
Edificio Sede CVG
Ciudad Bolívar, Venezuela
011–58–85–25334

L.J. Garside
Nevada Bureau of Mines and Geology
University of Nevada-Reno
Reno, NV 89557–0088
(702) 784–6691

Mark E. Gettings
U.S. Geological Survey
University of Arizona
Gould-Simpson Building #77
Tucson, AZ 85721
(602) 670–5507

R.J. Goldfarb
U.S. Geological Survey
Mail Stop 973
Box 25046, Denver Federal Center
Denver, CO 80225
(303) 236–2441

David Gottfried
U.S. Geological Survey
954 National Center
Reston, VA 22092
(703) 648–6310

ADDRESSES AND TELEPHONE NUMBERS OF CONTRIBUTING AUTHORS

Richard I. Grauch
U.S. Geological Survey
Mail Stop 973
Box 25046, Denver Federal Center
Denver, CO 80225
(303) 236–5551

V.J.S. Grauch
U.S. Geological Survey
Mail Stop 964
Box 25046, Denver Federal Center
Denver, CO 80225
(303) 236–1393

Floyd Gray
U.S. Geological Survey
c/o U.S. Embassy
Caracas, Venezuela
APO Miami 34037
011–58–86–223–655

J.E. Gray
U.S. Geological Survey
Mail Stop 973
Box 25046, Denver Federal Center
Denver, CO 80225
(303) 236–2446

H.G. Greene
U.S. Geological Survey
Mail Stop 999
345 Middlefield Road
Menlo Park, CA 94025
(415) 329–3078

R.C. Greene
U.S. Geological Survey
Mail Stop 901
345 Middlefield Road
Menlo Park, CA 94025
(415) 329–5420

D.J. Grimes
U.S. Geological Survey
Mail Stop 973
Box 25046, Denver Federal Center
Denver, CO 80225
(303) 236–5510

Andrew Griscom
U.S. Geological Survey
Mail Stop 984
345 Middlefield Road
Menlo Park, CA 94025
(415) 329–5302

John A. Grow
U.S. Geological Survey
Mail Stop 960
Box 25046, Denver Federal Center
Denver, CO 80225
(303) 236–5754

Donald J. Grybeck
U.S. Geological Survey
4200 University Drive
Anchorage, AK 99508–4667
(907) 786–7403

Hugo Gumucio
Servicio Geólogico de Bolivia
Casilla 2729
La Paz, Bolivia
011–591–237–7310

Aldo Gutarra
Oficina Nacional de Evaluación
de Recursos Naturales
Los Petirrojos 315 San Isidro
Lima, Peru
011–51–14–410425 A38

Luis Guzman
Corporación Venezolana de
Guayana-Compañía Técnica
Minera, C.A.
C.C. Chilemex
Puerto Ordaz, Venezuela
011–58–86–228377

Jane Hammarstrom
U.S. Geological Survey
959 National Center
Reston, VA 22092
(703) 648–6165

R.F. Hardyman
U.S. Geological Survey
Mackay School of Mines
University of Nevada-Reno
Reno, NV 89557–0047
(702) 784–5379

Thelma F. Harms
U.S. Geological Survey
210 E. 7th Street
Tucson, AZ 85705
(602) 670–5514

D.S. Harwood
U.S. Geological Survey
Mail Stop 975
345 Middlefield Road
Menlo Park, CA 94025
(415) 329–4932

James R. Hein
U.S. Geological Survey
Mail Stop 999
345 Middlefield Road
Menlo Park, CA 94025
(415) 329–3150

James R. Herring
U.S. Geological Survey
Mail Stop 939
Box 25046, Denver Federal Center
Denver, CO 80225
(303) 236–5559

T.G. Hildenbrand
U.S. Geological Survey
Mail Stop 989
345 Middlefield Road
Menlo Park, CA 94025
(415) 329–5303

Alberto Hinojosa
Servicio Geólogico de Bolivia
Casilla 2729
La Paz, Bolivia
011–591–237–4544

Donald B. Hoover
U.S. Geological Survey
Mail Stop 964
Box 25046, Denver Federal Center
Denver, CO 80225
(303) 236–1326

D.M. Hopkins
U.S. Geological Survey
Mail Stop 973
Box 25046, Denver Federal Center
Denver, CO 80225
(303) 236–1908

Robert J. Horton
U.S. Geological Survey
Mail Stop 964
Box 25046, Denver Federal Center
Denver, CO 80225
(303) 236–1338

John W. Hosterman
U.S. Geological Survey
954 National Center
Reston, VA 22092
(703) 648–6316

Brenda B. Houser
U.S. Geological Survey
University of Arizona
Gould-Simpson Building #77
Tucson, AZ 85721
(602) 670–5509

ADDRESSES AND TELEPHONE NUMBERS OF CONTRIBUTING AUTHORS

Donald F. Huber
U.S. Geological Survey
Mail Stop 984
345 Middlefield Road
Menlo Park, CA 94025
(415) 329–5358

Nestor Jimenez
Servicio Geólogico de Bolivia
Casilla 2729
La Paz, Bolivia
011–591–237–7310

Roy A. Johnson
Department of Geosciences
University of Arizona
Gould-Simpson Building #77
Tucson, AZ 85721
(602) 621–4890

David J. Johnston
Schlumberger Well Services
21250 E. 31st Circle
Aurora, CO 80011
(303) 375–8090

Janet L. Jones
U.S. Geological Survey
Mail Stop 973
Box 25046, Denver Federal Center
Denver, CO 80225
(303) 236–1865

Robert J. Kamilli
U.S. Geological Survey
University of Arizona
Gould-Simpson Building #77
Tucson, AZ 85721
(602) 670–5576

Jung-Keuk Kang
Korea Ocean Research and
Development Institute
An Sun, P.O. Box 29
Seoul 425–600 Korea
011–82–2–863–4770

S.M. Karl
U.S. Geological Survey
4200 University Drive
Anchorage, AK 99508–4667
(907) 786–7428

John S. Kelley
U.S. Geological Survey
4200 University Drive
Anchorage, AK 99508–4667
(907) 786–7414

K.D. Kelley
U.S. Geological Survey
Mail Stop 973
Box 25046, Denver Federal Center
Denver, CO 80225
(303) 236–2467

J.E. Kilburn
U.S. Geological Survey
Mail Stop 973
Box 25046, Denver Federal Center
Denver, CO 80225
(303) 236–1865

E.B. Kisvarsanyi
Missouri Department of
Natural Resources
Division of Geology and
Land Surveys
P.O. Box 250
Rolla, MO 65401
(314) 364–1752

D.P. Klein
U.S. Geological Survey
Mail Stop 964
Box 25046, Denver Federal Center
Denver, CO 80225
(303) 236–1313

Terry L. Klein
U.S. Geological Survey
954 National Center
Reston, VA 22092
(703) 648–6339

Dan H. Knepper, Jr.
U.S. Geological Survey
Mail Stop 964
Box 25046, Denver Federal Center
Denver, CO 80225
(303) 236–1385

Randolph A. Koski
U.S. Geological Survey
Mail Stop 999
345 Middlefield Road
Menlo Park, CA 94025
(415) 329–3208

Henry G. Kreis
Asarco, Inc.
P.O. Box 5747
1150 North 7th Avenue
Tucson, AZ 85703
(602) 792–3010

J.M. Kruger
Department of Geosciences
University of Arizona
Gould-Simpson Building #77
Tucson, AZ 85721
(602) 621–4890

Richard D. Krushensky
U.S. Geological Survey
917 National Center
Reston, VA 22092
(703) 648–6060

M.J. Kunk
U.S. Geological Survey
981 National Center
Reston, VA 22092
(703) 648–5332

Keith A. Kvenvolden
U.S. Geological Survey
Mail Stop 999
345 Middlefield Road
Menlo Park, CA 94025
(415) 329–3213

Victor F. Labson
U.S. Geological Survey
Mail Stop 964
Box 25046, Denver Federal Center
Denver, CO 80225
(303) 236–1312

D.D. Lambert
Department of Earth Sciences
Monash University
Clayton, Victoria 3168
Australia

William H. Langer
U.S. Geological Survey
Mail Stop 913
Box 25046, Denver Federal Center
Denver, CO 80225
(303) 236–1249

Curtis E. Larsen
U.S. Geological Survey
954 National Center
Reston, VA 22092
(703) 648–6342

Keenan Lee
U.S. Geological Survey
Mail Stop 964
Box 25046, Denver Federal Center
Denver, CO 80225
(303) 236–1375

ADDRESSES AND TELEPHONE NUMBERS OF CONTRIBUTING AUTHORS

J.L. Lizeca
Servicio Geólogico de Bolivia
Casilla 2729
La Paz, Bolivia
011–591–237–7310

Keith R. Long
U.S. Geological Survey
210 E. 7th Street
Tucson, AZ 85705
(602) 629–5512

Karen Lund
U.S. Geological Survey
Mail Stop 905
Box 25046, Denver Federal Center
Denver, CO 80225
(303) 236–5600

Dawn J. Madden-McGuire
U.S. Geological Survey
Mail Stop 973
Box 25046, Denver Federal Center
Denver, CO 80225
(303) 236–1856

L.B. Magoon
U.S. Geological Survey
Mail Stop 999
345 Middlefield Road
Menlo Park, CA 94025
(415) 354–3010

Frank T. Manheim
U.S. Geological Survey
Woods Hole, MA 02543
(508) 548–8700

M.S. Marlow
U.S. Geological Survey
Mail Stop 999
345 Middlefield Road
Menlo Park, CA 94025
(415) 329–3129

Sherman P. Marsh
U.S. Geological Survey
Mail Stop 973
Box 25046, Denver Federal Center
Denver, CO 80225
(303) 236–5521

Anne E. McCafferty
U.S. Geological Survey
Mail Stop 964
Box 25046, Denver Federal Center
Denver, CO 80225
(303) 236–1397

J. Howard McCarthy, Jr.
U.S. Geological Survey
Mackay School of Mines
University of Nevada-Reno
Reno, NV 89557–0047
(702) 784–5362

Teresa A. McGervey
U.S. Geological Survey
954 National Center
Reston, VA 22092
(703) 648–6345

J.B. McHugh
U.S. Geological Survey
Mail Stop 973
Box 25046, Denver Federal Center
Denver, CO 80225
(303) 236–1908

Gregory E. McKelvey
U.S. Geological Survey
210 E. 7th Street
Tucson, AZ 85705
(602) 629–5581

A.L. Meier
U.S. Geological Survey
Mail Stop 973
Box 25046, Denver Federal Center
Denver, CO 80225
(303) 236–1902

Jon L. Mikesell
U.S. Geological Survey
990 National Center
Reston, VA 22092
(703) 648–6996

William R. Miller
U.S. Geological Survey
Mail Stop 973
Box 25046, Denver Federal Center
Denver, CO 80225
(303) 236–5558

Fernando P. Miranda
Petrobras-CENPES
Cidade Universitaria-Ilha do Fundao
Rio de Janeiro RJ–21740
Brazil

Peter J. Modreski
U.S. Geological Survey
Mail Stop 905
Box 25046, Denver Federal Center
Denver, CO 80225
(303) 236–5639

Anita Moore-Nall
Box 453
Gardiner, MT 59030
(406) 848–7408

J.W. Morgan
U.S. Geological Survey
981 National Center
Reston, VA 22092
(703) 648–5334

Janet L. Morton
U.S. Geological Survey
Mail Stop 999
345 Middlefield Road
Menlo Park, CA 94025
(415) 329–3209

Ramon Moscoso
Servicio Nacional de
Geologia y Mineria
Casilla 10465
Santiago, Chile
011–56–237–5050

J.M. Motooka
U.S. Geological Survey
Mail Stop 973
Box 25046, Denver Federal Center
Denver, CO 80225
(303) 236–2460

Falma Moye
Idaho State University
Pocatello, ID 83209
(208) 236–3549

Fernando Murillo
Servicio Geólogico de Bolivia
Casilla 2729
La Paz, Bolivia
011–591–237–7310

James B. Murowchick
Department of Geosciences
University of Missouri
Kansas City, MO 64110–2499
(816) 276–2980

ADDRESSES AND TELEPHONE NUMBERS OF CONTRIBUTING AUTHORS

A.J. Naldrett
Department of Geology
University of Toronto
Toronto, Ontario M5S 1A1
Canada
(416) 978–3022

Philip H. Nelson
U.S. Geological Survey
Mail Stop 964
Box 25046, Denver Federal Center
Denver, CO 80225
(303) 236–1322

Warren J. Nokleberg
U.S. Geological Survey
Mail Stop 904
345 Middlefield Road
Menlo Park, CA 94025
(415) 329–5732

L.M. Nuelle
Missouri Department of
Natural Resources
Division of Geology and
Land Surveys
P.O. Box 250
Rolla, MO 65401
(314) 364–1752

Fernando Nuñez
Corporación Venezolana de
Guayana-Compañía Técnica
Minera, C.A.
Edificio Sede CVG
Ciudad Bolívar, Venezuela
011–58–85–25334

Terry W. Offield
U.S. Geological Survey
954 National Center
Reston, VA 22092
(703) 648–6135

S.D. Olmore
U.S. Geological Survey
c/o U.S. Embassy
Caracas, Venezuela
APO Miami 34037
011–58–85–25378

N.J Page
U.S. Geological Survey
210 E. 7th Street
Tucson, AZ 85705
(602) 670–5580

Bambang Pardiarto
Directorate of Mineral Resources
Jl. Diponegoro 57
Bandung 40133 Indonesia
011–62–22–73205

E.C. Perry, Jr.
Department of Geology
Northern Illinois University
De Kalb, IL 60115
(815) 753–1944

Zell E. Peterman
U.S. Geological Survey
Mail Stop 963
Box 25046, Denver Federal Center
Denver, CO 80225
(303) 236–7887

James A. Peterson
U.S. Geological Survey
301 Pattee Canyon Drive
Missoula, MT 59812
(406) 542–2087

W.J. Pickthorn
U.S. Geological Survey
Mail Stop 901
345 Middlefield Road
Menlo Park, CA 94025
(415) 329–5446

Frances Wahl Pierce
U.S. Geological Survey
210 E. 7th Street
Tucson, AZ 85705
(602) 670–5508

David Z. Piper
U.S. Geological Survey
Mail Stop 902
345 Middlefield Road
Menlo Park, CA 94025
(415) 329–5187

James A. Pitkin
U.S. Geological Survey
Mail Stop 964
Box 25046, Denver Federal Center
Denver, CO 80225
(303) 236–1387

Peter Popenoe
U.S. Geological Survey
Woods Hole, MA 02543
(508) 548–8700

L.J. Poppe
U.S. Geological Survey
Woods Hole, MA 02543
(508) 548–8700

Christopher J. Potter
U.S. Geological Survey
Mail Stop 939
Box 25046, Denver Federal Center
Denver, CO 80225
(303) 236–3282

Freddy Prieto
Corporación Venezolana de
Guayana-Compañía Técnica
Minera, C.A.
C.C. Chilemex
Puerto Ordaz, Venezuela
011–58–86–228377

Luis Quispesivana
Instituto Geologico Minero
y Metalurgico
Pablo Bermudez 211 Jesus-Maria
Lima, Peru
011–51–14–316233 A41

G.L. Raines
U.S. Geological Survey
Mackay School of Mines
University of Nevada-Reno
Reno, NV 89557–0047
(702) 784–5574

V. Rajamani
J. Nehru University
New Delhi 110067
India

William H. Raymond
U.S. Geological Survey
Mail Stop 905
Box 25046, Denver Federal Center
Denver, CO 80225
(303) 236–5622

B.A. Richmond
U.S. Geological Survey
Mail Stop 999
345 Middlefield Road
Menlo Park, CA 94025
(415) 329–3144

J.R. Riehle
U.S. Geological Survey
4200 University Drive
Anchorage, AK 99508–4667
(907) 786–7415

ADDRESSES AND TELEPHONE NUMBERS OF CONTRIBUTING AUTHORS

Jaime Rodriguez
Centro de Estudios Espaciales
Universidad de Chile
Arturo Prat 1171
Santiago, Chile
011–56–2–5553400

David H. Root
U.S. Geological Survey
920 National Center
Reston, VA 22092
(703) 648–6144

L.C. Rowan
U.S. Geological Survey
927 National Center
Reston, VA 22092
(703) 648–6381

D.M. Rubin
U.S. Geological Survey
Mail Stop 999
345 Middlefield Road
Menlo Park, CA 94025
(415) 329–3060

R.O. Rye
U.S. Geological Survey
Mail Stop 963
Box 25046, Denver Federal Center
Denver, CO 80225
(303) 236–7886

Ward E. Sanford
U.S. Geological Survey
431 National Center
Reston, VA 22092
(703) 648–5882

Richard F. Sanzolone
U.S. Geological Survey
Mail Stop 973
Box 25046, Denver Federal Center
Denver, CO 80225
(303) 236–2451

D.L. Sawatzky
U.S. Geological Survey
Mackay School of Mines
University of Nevada-Reno
Reno, NV 89557–0047
(702) 784–5379

Kathryn M. Scanlon
U.S. Geological Survey
Woods Hole, MA 02543
(508) 548–8700

Jeanine M. Schmidt
U.S. Geological Survey
4200 University Drive
Anchorage, AK 99508–4667
(907) 786–7494

D.W. Scholl
U.S. Geological Survey
Mail Stop 999
345 Middlefield Road
Menlo Park, CA 94025
(415) 329–3127

Marjorie S. Schulz
U.S. Geological Survey
Mail Stop 999
345 Middlefield Road
Menlo Park, CA 94025
(415) 329–3151

R.A. Schweickert
Geology Department
Mackay School of Mines
University of Nevada-Reno
Reno, NV 89557–0047
(702) 784–6901

R.M. Senterfit
U.S. Geological Survey
Mail Stop 964
Box 25046, Denver Federal Center
Denver, CO 80225
(303) 236–1355

Wayne C. Shanks III
U.S. Geological Survey
954 National Center
Reston, VA 22092
(703) 648–6336

D.R. Shawe
U.S. Geological Survey
Mail Stop 905
Box 25046, Denver Federal Center
Denver, CO 80225
(303) 236–5588

Richard A. Sheppard
U.S. Geological Survey
Mail Stop 939
Box 25046, Denver Federal Center
Denver, CO 80225
(303) 236–5563

Michael A. Shubat
Utah Geological and Mineral Survey
606 Blackhawk Way
Salt Lake City, UT 84108–1280
(801) 581–6831

Gary B. Sidder
U.S. Geological Survey
Mail Stop 905
Box 25046, Denver Federal Center
Denver, CO 80225
(303) 236–5607

N.J. Silberling
U.S. Geological Survey
Mail Stop 919
Box 25046, Denver Federal Center
Denver, CO 80225
(303) 236–5660

Miles L. Silberman
U.S. Geological Survey
Mail Stop 973
Box 25046, Denver Federal Center
Denver, CO 80225
(303) 236–5511

P.K. Sims
U.S. Geological Survey
Mail Stop 905
Box 25046, Denver Federal Center
Denver, CO 80225
(303) 236–5621

K.E. Slaughter
U.S. Geological Survey
Mail Stop 973
Box 25046, Denver Federal Center
Denver, CO 80225
(303) 236–2446

Brian M. Smith
Lawrence Berkeley Laboratory
Mail Stop 70A–3363
1 Cyclotron Road
Berkeley, CA 94720
(415) 486–6508

Bruce D. Smith
U.S. Geological Survey
Mail Stop 964
Box 25046, Denver Federal Center
Denver, CO 80225
(303) 236–1399

David B. Smith
U.S. Geological Survey
Mail Stop 973
Box 25046, Denver Federal Center
Denver, CO 80225
(303) 236–1800

ADDRESSES AND TELEPHONE NUMBERS OF CONTRIBUTING AUTHORS

Steven M. Smith
U.S. Geological Survey
Mail Stop 973
Box 25046, Denver Federal Center
Denver, CO 80225
(303) 236–1191

Virginia K. Smith
U.S. Geological Survey
Mail Stop 999
345 Middlefield Road
Menlo Park, CA 94025
(415) 329–3151

L.W. Snee
U.S. Geological Survey
Mail Stop 905
Box 25046, Denver Federal Center
Denver, CO 80225
(303) 236–5619

Charles S. Spirakis
U.S. Geological Survey
Mail Stop 939
Box 25046, Denver Federal Center
Denver, CO 80225
(303) 236–1558

W.D. Stanley
U.S. Geological Survey
Mail Stop 964
Box 25046, Denver Federal Center
Denver, CO 80225
(303) 236–1328

J.H. Stewart
U.S. Geological Survey
Mail Stop 901
345 Middlefield Road
Menlo Park, CA 94025
(415) 329–5412

D.M. Sutphin
U.S. Geological Survey
920 National Center
Reston, VA 22092
(703) 648–6134

Gregg A. Swayze
U.S. Geological Survey
Mail Stop 964
Box 25046, Denver Federal Center
Denver, CO 80225
(303) 236–1411

James V. Taranik
Desert Research Institute
University of Nevada System
P.O. Box 60220
Reno, NV 89506–0220
(702) 673–7312

Rubén Tejada
Instituto Geólogico Minero
y Metalurgico
Pablo Bermudez 211 Jesus-Maria
Lima, Peru
011–51–14–316233 A39

P.K. Theobald
U.S. Geological Survey
Mail Stop 973
Box 25046, Denver Federal Center
Denver, CO 80225
(303) 236–1853

P.M. Theodorakos
U.S. Geological Survey
Mail Stop 973
Box 25046, Denver Federal Center
Denver, CO 80225
(303) 236–2482

Charles H. Thorman
U.S. Geological Survey
Mail Stop 905
Box 25046, Denver Federal Center
Denver, CO 80225
(303) 236–5601

Joseph V. Tingley
Nevada Bureau of Mines and Geology
University of Nevada-Reno
Reno, NV 89557–0088
(702) 784–6691

R.M. Tosdal
U.S. Geological Survey
Mail Stop 901
345 Middlefield Road
Menlo Park, CA 94025
(415) 329–5423

Robert L. Turner
U.S. Geological Survey
Mackay School of Mines
University of Nevada-Reno
Reno, NV 89557–0047
(702) 784–5581

John W. Valley
Department of Geology and
Geophysics
University of Wisconsin
Madison, WI 53706
(608) 263–5659

J.G. Vedder
U.S. Geological Survey
Mail Stop 999
345 Middlefield Road
Menlo Park, CA 94025
(415) 329–3096

César Vilca
Instituto Geólogico Minero
y Metalurgico
Pablo Bermudez 211 Jesus-Maria
Lima, Peru
011–51–14–316233 A39

R.J. Walker
Department of Geology
University of Maryland
College Park, MD 20742
(301) 405–4089

Sherilyn Williams-Stroud
U.S. Geological Survey
Mail Stop 939
Box 25046, Denver Federal Center
Denver, CO 80225
(303) 236–8627

G.R. Winkler
U.S. Geological Survey
Mail Stop 905
Box 25046, Denver Federal Center
Denver, CO 80225
(303) 236–9232

Wayne S. Wojniak
U.S. Geological Survey
Mail Stop 964
Box 25046, Denver Federal Center
Denver, CO 80225
(303) 236–1351

Florence L. Wong
U.S. Geological Survey
Mail Stop 999
345 Middlefield Road
Menlo Park, CA 94025
(415) 329–3053

ADDRESSES AND TELEPHONE NUMBERS OF CONTRIBUTING AUTHORS

Warren W. Wood
U.S. Geological Survey
431 National Center
Reston, VA 22092
(703) 648–5875

Laurel G. Woodruff
U.S. Geological Survey
954 National Center
Reston, VA 22092
(703) 648–6327

Chester T. Wrucke
U.S. Geological Survey
Mail Stop 901
345 Middlefield Road
Menlo Park, CA 94025
(415) 329–5413

J.C. Wynn
U.S. Geological Survey
920 National Center
Reston, VA 22092
(703) 648–6463

Suk-Hoon Yoon
Korea Ocean Research and
Development Institute
An Sun, P.O. Box 29
Seoul 425–600 Korea
011–82–2–863–4770

Michael L. Zientek
U.S. Geological Survey
Room 656 U.S. Courthouse
W. 920 Riverside Ave.
Spokane, WA 99201
(509) 353–2166

Robert A. Zierenberg
U.S. Geological Survey
Mail Stop 901
345 Middlefield Road
Menlo Park, CA 94025
(415) 329–5437

U.S. Geological Survey geologists collecting samples below glaciers for a geochemical study, Chugach Mountains, south-central Alaska. Photograph by William R. Miller.

ORGANIZATION OF THE U.S. GEOLOGICAL SURVEY

Office	Name	Telephone	City
Office of the Director			
Director	Dallas L. Peck	703/648–7411	Reston
Associate Director	Doyle G. Frederick	703/648–7412	Reston
Assistant Director for Research	Stephen E. Ragone	703/648–4450	Reston
Assistant Director for Engineering Geology	James F. Devine	703/648–4423	Reston
Assistant Director for Administration	Jack J. Stassi	703/648–7200	Reston
Assistant Director for Programs	Peter F. Bermel	703/648–4430	Reston
Assistant Director for Intergovernmental Affairs	John J. Dragonetti	703/648–4427	Reston
Chief, Public Affairs Office	Donovan B. Kelly	703/648–4459	Reston
Assistant Director for Information Systems	James E. Biesecker	703/648–7108	Reston
National Mapping Division			
Chief	Lowell E. Starr	703/648–5748	Reston
Geologic Division			
Chief Geologist	Benjamin A. Morgan	703/648–6600	Reston
Water Resources Division			
Chief Hydrologist	Philip Cohen	703/648–5215	Reston
ORGANIZATION OF THE GEOLOGIC DIVISION			
Office of the Chief Geologist			
Chief Geologist	Benjamin A. Morgan	703/648–6600	Reston
Associate Chief Geologist	William R. Greenwood	703/648–6601	Reston
Assistant Chief Geologist for Program	David P. Russ	703/648–6640	Reston
Assistant Chief Geologist, Eastern Region	Jack H. Medlin	703/648–6660	Reston
Assistant Chief Geologist, Central Region	Harry A. Tourtelot	303/236–5438	Denver
Assistant Chief Geologist, Western Region	William R. Normark	415/329–5101	Menlo Park
Office of Mineral Resources			
Chief	Glenn H. Allcott	703/648–6100	Reston
Chief, Branch of Alaskan Geology	Willis H. White	907/786–7403	Anchorage
Chief, Branch of Eastern Mineral Resources	Klaus J. Schulz	703/648–6327	Reston
Chief, Branch of Central Mineral Resources	David A. Lindsey	303/236–5568	Denver
Chief, Branch of Western Mineral Resources	William C. Bagby	415/329–5477	Menlo Park
Chief, Branch of Geochemistry	David B. Smith	303/236–1800	Denver
Chief, Branch of Resource Analysis	W. David Menzie II	703/648–6125	Reston
Chief, Branch of Geophysics	David L. Campbell	303/236–1212	Denver
Office of Energy and Marine Geology			
Chief	Gary W. Hill	703/648–6472	Reston
Chief, Branch of Petroleum Geology	Donald L. Gautier	303/236–5711	Denver
Chief, Branch of Coal Geology	Harold J. Gluskoter	703/648–6401	Reston
Chief, Branch of Sedimentary Processes	Walter E. Dean, Jr.	303/236–1644	Denver
Chief, Branch of Pacific Marine Geology	David A. Cacchione	415/329–3184	Menlo Park
Chief, Branch of Atlantic Marine Geology	Bradford Butman	617/837–4211	Woods Hole

Office	Name	Telephone	City
Office of Regional Geology			
Chief	Mitchell W. Reynolds	703/648–6960	Reston
Chief, Branch of Eastern Regional Geology	Wayne L. Newell	703/648–6900	Reston
Chief, Branch of Central Regional Geology	David L. Schleicher	303/236–1258	Denver
Chief, Branch of Western Regional Geology	Rowland W. Tabor	415/329–4909	Menlo Park
Chief, Branch of Isotope Geology	Carl E. Hedge	303/236–7880	Denver
Chief, Branch of Astrogeology	Philip Davis	602/527–7015	Flagstaff
Chief, Branch of Paleontology and Stratigraphy	John Pojeta, Jr.	703/648–5288	Reston
Office of Earthquakes, Volcanoes, and Engineering			
Chief	Robert L. Wesson	703/648–6714	Reston
Chief, Branch of Engineering Seismology and Geology	Thomas L.Holzer	415/329–5613	Menlo Park
Chief, Branch of Global Seismology and Geomagnetism	Robert P. Masse	303/236–1510	Denver
Acting Chief, Branch of Seismology	John Van Schaack	415/329–4780	Menlo Park
Chief, Branch of Geologic Risk Assessment	Kaye M. Shedlock	303/236–1585	Denver
Chief, Branch of Tectonophysics	William H. Prescott	415/329–4860	Menlo Park
Chief, Branch of Igneous and Geothermal Processes	Robert L. Christiansen	415/329–5228	Menlo Park
Office of Scientific Publications			
Chief	John M. Aaron	703/648–6077	Reston
Chief, Branch of Eastern Technical Reports	Simon M. Cargill	703/648–6147	Reston
Chief, Branch of Central Technical Reports	Lawrence F. Rooney	303/236–5457	Denver
Chief, Branch of Western Technical Reports	James B. Pinkerton	415/329–5043	Menlo Park
Chief, Library and Information Services	Barbara A. Chappell	703/648–4305	Reston
Chief, Branch of Visual Services	John R. Keith	703/648–4357	Reston
Office of International Geology			
Chief	A. Thomas Ovenshine	703/648–6047	Reston

Addresses

U.S. Geological Survey
National Center
Reston, VA 22092

U.S. Geological Survey
Box 25046, Denver Federal Center
Denver, CO 80225

U.S. Geological Survey
345 Middlefield Road
Menlo Park, CA 94025

U.S. Geological Survey
4200 University Drive
Anchorage, AK 99508–4667

U.S. Geological Survey
2255 North Gemini Drive
Flagstaff, AZ 86002

U.S. Geological Survey
Quissett Campus, Building B
Woods Hole, MA 02543

Minerals Information Offices (MIO's)

MIO, U.S. Geological Survey
210 East 7th Street
Tucson, AZ 85705
(602) 670–5508

MIO, Department of the Interior
MS 2647-MIB, Room 2647
1849 C Street NW
Washington, DC 20240
(202) 208–5512

MIO, U.S. Geological Survey
Mackay School of Mines
Scrugham Engineering Mines Building
University of Nevada-Reno
Reno, NV 89557–0047
(702) 784–5552

MIO, U.S. Geological Survey
Room 656 U.S. Courthouse
W. 920 Riverside Ave.
Spokane, WA 99201
(509) 353–2649

INDEX OF AUTHORS

A

Alminas, H.V. 1
André, Orlando 11
Arth, Joseph G. 3
Ashley, Roger P. 2
Ayuso, Robert A. 3, 24

B

Bankey, Viki 6, 53
Barnes, David F. 3
Bawiec, Walter J. 4
Belkin, Harvey E. 26
Bisdorf, Robert J. 41
Blank, H. Richard 5
Bliss, James D. 53
Bohlke, J.K. 76
Bolm, Karen Sue 59
Bonham, H.F. 20
Bookstrom, Arthur A. 20
Bowers, T.L. 21
Box, Stephen E. 29, 46
Brew, David A. 6, 45
Brooks, William E. 69
Bultman, Mark W. 31
Bundtzen, Thomas K. 36
Burchell, Alison 11

C

Cady, John W. 6, 52
Campbell, Andrew C. 46
Cannon, William F. 7
Carrasco, Raul 11
Carten, Richard B. 20
Chen Nansheng 33
Church, S.E. 65
Clark, Roger N. 8
Clark, Sandra H.B. 8
Closs, L.G. 22
Commeau, J.A. 63
Connor, Jon J. 57
Conway, Clay M. 9
Cook, Harry E. 63
Cookro, Theresa M. 10
Corbett, Kevin P. 52
Cordell, L.E. 16
Coveney, Raymond M., Jr. 33
Cox, Dennis 11
Cox, Leslie J. 11
Crowe, Douglas E. 13
Cuitino, Lucia 21
Cunningham, Charles G. 15, 23

D

Day, W.C. 16, 40, 69, 80
Desborough, George A. 16
Detra, D.E. 18, 34
Diaz, Felipe 21
Dilles, J.H. 67
Dingler, J.R. 78
Doe, Bruce R. 19
Doebrich, Jeff L. 20, 67
Drew, Lawrence J. 6

E

Eiswerth, Barbara A. 21, 23
Eppinger, R.G. 22
Erdman, J.A. 20, 22
Ericksen, George E. 15, 23
Estanga, Yasmin 69
Evans, Karl V. 16, 74
Evarts, Russell C. 2

F

Ficklin, W.H. 35, 55
Finn, C.A. 45
Fisher, Frederick S. 11, 31
Foley, Nora K. 24
Force, Eric R. 11, 26
Ford, A.B. 45
Froelich, A.J. 26
Frost, Thomas P. 29

G

Gallagher, Andrea J. 8
Gammons, C.H. 74
Garcia, Andres 69
Garside, L.J. 20, 67
Gettings, Mark E. 11, 31
Goldfarb, R.J. 32, 34, 45, 46
Gottfried, David 26
Grauch, Richard I. 33
Grauch, V.J.S. 34
Gray, Floyd 80
Gray, J.E. 34, 39, 46
Greene, H.G. 78
Greene, R.C. 67
Grimes, D.J. 35
Griscom, Andrew 4
Grow, John A. 63
Grybeck, Donald J. 36
Gumucio, Hugo 21
Gutarra, Aldo 21
Guzman, Luis 69

H

Hammarstrom, Jane M. 55
Hardyman, R.F. 20, 67
Harms, Thelma F. 36
Harwood, D.S. 67
Hein, James R. 37, 78
Herring, James R. 38
Hildenbrand, T.G. 72
Hinojosa, Alberto 11
Hoover, Donald B. 34, 74, 77

Hopkins, D.M. 39
Horton, Robert J. 40, 41
Hosterman, John W. 42
Houser, Brenda B. 11, 43
Huber, Donald F. 6

J

Jimenez, Nestor 21
Johnson, Roy A. 43
Johnston, David J. 57
Jones, Janet L. 10, 46

K

Kamilli, Robert J. 44
Kang, Jung-Keuk 37
Karl, S.M. 45
Kelley, John S. 3
Kelley, K.D. 45
Kilburn, J.E. 46
Kisvarsanyi, E.B. 16
Klein, D.P. 68
Klein, Terry L. 40, 58
Knepper, Dan H., Jr. 52
Koski, Randolph A. 46
Kreis, Henry G. 57
Kruger, J.M. 43
Krushensky, Richard D. 4
Kunk, M.J. 74
Kvenvolden, Keith A. 46, 78

L

Labson, Victor F. 41
Lambert, D.D. 76
Langer, William H. 47
Larsen, Curtis E. 48
Lee, Keenan 6
Lizeca, J.L. 21
Long, Keith R. 11, 52
Lund, Karen 74

M

Madden-McGuire, Dawn J. 49, 50
Magoon, L.B. 65
Manheim, Frank T. 61
Marlow, M.S. 78
Marsh, Sherman P. 4, 49, 52
McCafferty, Anne E. 6, 16, 53, 56
McCarthy, J. Howard, Jr. 20, 67
McGervey, Teresa A. 7
McHugh, J.B. 1, 35, 55
McKelvey, Gregory E. 4, 53, 55
Meier, A.L. 22, 35
Mikesell, Jon L. 57
Miller, William R. 2, 55
Miranda, Fernando P. 56
Modreski, Peter J. 57
Moore-Nall, Anita 70
Morgan, J.W. 76
Morton, Janet L. 46, 78
Moscoso, Ramon 21
Motooka, J.M. 22
Moye, Falma 22
Murillo, Fernando 21
Murowchick, James B. 33

N

Naldrett, A.J. 76
Nelson, Philip H. 57
Nokleberg, Warren J. 36
Nuelle, L.M. 16
Nuñez, Fernando 69

O

Offield, Terry W. 58
Olmore, S.D. 69, 80

P

Page, N.J 80
Pardiarto, Bambang 82
Perry, E.C., Jr. 1
Peterman, Zell E. 72
Peterson, James A. 63
Pickthorn, W.J. 32
Pierce, Frances Wahl 59
Piper, David Z. 38
Pitkin, James A. 6, 60
Popenoe, Peter 61
Poppe, L.J. 63
Potter, Christopher J. 63
Prieto, Freddy 69

Q

Quispesivana, Luis 21

R

Raines, G.L. 67
Rajamani, V. 76
Raymond, William H. 16
Richmond, B.A. 78
Riehle, J.R. 65
Rodriguez, Jaime 21
Root, David H. 6
Rowan, L.C. 21
Rubin, D.M. 78
Rye, R.O. 16

S

Sanford, Ward E. 79
Sanzolone, Richard F. 74
Sawatzky, D.L. 67
Scanlon, Kathryn M. 4
Schmidt, Jeanine M. 6
Scholl, D.W. 78
Schulz, Marjorie S. 37

Schweickert, R.A. 67
Senterfit, R.M. 68
Shanks, Wayne C., III 13, 46
Shawe, D.R. 20
Sheppard, Richard A. 38
Shubat, Michael A. 10
Sidder, Gary B. 16, 69, 80
Silberling, N.J. 67
Silberman, Miles L. 70
Sims, P.K. 72
Slaughter, K.E. 34, 39
Smith, Brian M. 70
Smith, Bruce D. 40, 41
Smith, David B. 74
Smith, Steven M. 18
Smith, Virginia K. 37
Snee, L.W. 74
Spirakis, Charles S. 38
Stanley, W.D. 6
Stewart, J.H. 67
Sutphin, D.M. 45
Swayze, Gregg A. 8

T

Taranik, James V. 56
Tejada, Rubén 21
Theobald, P.K. 18, 22
Theodorakos, P.M. 18
Thorman, Charles H. 63
Tingley, Joseph V. 20
Tosdal, R.M. 69
Turner, Robert L. 20, 67

V

Valley, John W. 13
Vedder, J.G. 78
Vilca, César 21

W

Walker, R.J. 76
Williams-Stroud, Sherilyn 38
Winkler, G.R. 50
Wojniak, Wayne S. 34, 77
Wong, Florence L. 78
Wood, Warren W. 79
Woodruff, Laurel G. 26
Wrucke, Chester T. 52
Wynn, J.C. 80

Y

Yoon, Suk-Hoon 37

Z

Zientek, Michael L. 82
Zierenberg, Robert A. 46